ENGINEERING OF RECOMBINANT WHOLE-CELL BIOCATALYSTS FOR GREEN AND EFFICIENT PRODUCTION OF CHIRAL CHEMICALS

WU SHUKE

(B.S. Peking University)

A THESIS SUBMITTED

FOR THE DEGREE OF DOCTOR OF PHILOSOPHY

IN CHEMICAL AND PHARMACEUTICAL ENGINEERING (CPE)

SINGAPORE-MIT ALLIANCE

NATIONAL UNIVERSITY OF SINGAPORE

2015

DECLARATION

I hereby declare that this thesis is my original work and it has been written by me in its entirety. I have duly acknowledged all the sources of information which have been used in the thesis.

This thesis has also not been submitted for any degree in any university previously.

_____

Wu Shuke

13 Oct 2015

ACKNOWLEDGEMENT

At this moment of completing the thesis, I would like to thank many people for their kind support, encouragement, guidance, and motivation to me during the long PhD journey.

First of all, I would like to express my sincere gratitude and appreciation to my main thesis supervisor, Prof. Li Zhi (NUS), for his patient and constant guidance to bring me into an interesting world of enzymes and chiral chemicals. His insightful and inspiring thinking influenced and benefited my current research and future career development. Importantly, I highly appreciate Prof. Li for trusting in my person and supporting me to explore many of my ideas.

I also would like to thank my co-supervisor, Prof. Daniel I. C. Wang (MIT), for bringing me into a broad field of bioengineering and biotechnology. His critical thinking, independence, hardworking, and generousness impressed me, and I am trying to learn these from him. Furthermore, Prof. Wang kindly provided many opportunities for me to meet many great people and smart minds.

Another key person to thank is Prof. Too Heng-Phon, co-chair of SMA CPE program. As my thesis committee member, he gave me some helpful suggestions. More importantly, he generously provided me with a great help during a period of very hard time. Without the help, this thesis could not be completed in time.

Sincere thanks go to all the SMA CPE faculty members, Prof. Raj Rajagopalan, Prof. Saif Khan, and Prof. Mark Saeys, for many enjoyable discussions and talks.

I am deeply grateful to Dr. Li Aitao, Dr. Liu Ji, and Dr. Wang Wen. Dr. Li unselfishly taught me many experimental skills and shared with me his hands-on experience in biotransformation and organic synthesis. Dr. Liu provided a great assist

in both research and many miscellaneous tasks. Dr. Wang is like a big sister to me, and always provided kind support.

I cannot forget the friendship and help from my other colleagues in Prof. Li's group: Dr. Wang Zunsheng, Dr. Wang Tianwen, Dr. Yan Jinyong, Dr. Zhang Dongxu, Dr. Ye Lidan, Dr. Huang Renliang, Dr. Zhang Jiandong, Dr. Ye Lijuan, Dr. Tang Wenglin, Dr. Pham Quang Son, Dr. Ngo Nguyen Phuong Thao, Zillillah, Gao Pengfei, Priscilia Adrian Limadinata, Yang Yi, Zeng Shichao, Akbar Vahidi Khalfekandi, and Tian Kaiyuan. And also thank two helpful SMA colleagues: Dr. Chen Xixian, and Dr. Zhang Congqiang.

My PhD research has benefited from many other people's efforts as well. I appreciate the helps from Mdm. Li Fengmei, Mdm. Li Xiang, Dr. Yang Liming, Mr. Lim Hao Hiang, Mr. Tan Evan, Seow Vui Yin, and Mdm. Chan Xuan Zhen.

Lastly but not least, all these things will not be possible without the encouragement, support, understanding, and love from my parents and wife. Especially, I am greatly indebted to my wife for all of my night and weekend works. Let me express my sincere gratitude and deepest appreciation to them.

TABLE OF CONTENTS

SUMMARY

Biocatalysis is a green and useful tool for chemical production, especially for the production of enantiopure fine chemicals and pharmaceutical intermediates, with wide industrial application and huge market. Nevertheless, many biocatalytic reactions are still not efficient for practical application, and most of industrial biotransformations are mainly based on one-step biocatalysis. To address some of these problems in this Ph. D. thesis, I aim 1) to engineer a recombinant whole-cell biocatalyst expressing an epoxide hydrolase for green and efficient production of enantiopure epoxides and vicinal diols, 2) to develop novel whole-cell based cascade biocatalysis for asymmetric dihydroxylation of alkenes to practically prepare both enantiomers of the corresponding vicinal diols in high *ee* and yield, and 3) to develop novel and efficient one-pot multi-step cascade biocatalysis to prepare enantiopure hydroxy acid, amino alcohol, and amino acid from styrene or bio-based L-phenylalanine.

Firstly, a unique epoxide hydrolase (SpEH) from *Sphingomonas* sp. HXN-200 was successfully identified and cloned based on genome sequencing for enantioselective hydrolysis of racemic and *meso*-epoxides to prepare the corresponding (*S*)-epoxides and (*R*, *R*)-vicinal diols, respectively. The engineered *E. coli* (SpEH) highly expressed SpEH and gave 172 times higher cell-based activity for the hydrolysis of styrene oxide than that of *Sphingomonas* sp. HXN-200. Kinetic resolution of several selected racemic styrene oxides with the rest cells of *E. coli* (SpEH) produced the corresponding (*S*)-styrene oxides in 98.0-99.5% *ee* and 35.1-46.5% yield. Hydrolysis of three cyclic *meso*-epoxides afforded the corresponding (*R*, *R*)-vicinal diols in 86-93% *ee* and 90-99% yield. Biotransformation at higher substrate concentration produced (*S*)-styrene oxide in 430 mM (51 g/L$_{org}$) and (1*R*, 2*R*)-cyclohexene diol in 500 mM (58 g/L). The *E. coli* (SpEH) cells are highly active and easily available biocatalysts for the practical production of these useful and valuable enantiopure epoxides and vicinal diols.

Next, an intracellular epoxidation-hydrolysis cascade was developed for efficient asymmetric *trans*-dihydroxylation of aryl olefins to produce chiral vicinal diols by combining styrene monooxygenase (SMO) and epoxide hydrolase. *E. coli* (SSP1) was engineered to coexpress SMO and SpEH for efficient *S*-enantioselective dihydroxylation. On the other hand, for *R*-enantioselective dihydroxylation, *E. coli* (SST1) was engineered to coexpress SMO and the epoxide hydrolase from *Solanum tuberosum* (StEH), which has a complementary regioselectivity to SpEH. Biotransformation of 15 terminal aryl olefins with *E. coli* (SSP1) and *E. coli* (SST1), respectively, produced the corresponding 15 (*S*)-vicinal diols and 15 (*R*)-vicinal diols in high *ee* (99-84%) and high yield (>65%), respectively. The *trans*-dihydroxylation was also demonstrated on several non-terminal and cyclic aryl olefins to give diols in high *ee* and *de*, and the process was easily scaled up by using growing cells in a bioreactor. The cascade biocatalysis provides a green and useful synthetic tool to produce chiral vicinal diols, complementary to Sharpless *cis*-dihydroxylation.

Finally, a modular approach was applied for one-pot multi-step cascade biocatalysis to achieve asymmetric oxy- and amino-functionalization of terminal alkene to produce chiral hydroxy acid, amino alcohol, and amino acid. The following enzyme modules were designed, constructed, and tested: (1) SMO-SpEH for converting alkene to 1,2-diol; (2) alcohol dehydrogenase-aldehyde dehydrogenase for converting 1,2-diol to α-hydroxy acid; (3) alcohol dehydrogenase-ω-transaminase for converting 1,2-diol to 1,2-amino alcohol; (4) hydroxy acid oxidase-α-transaminase for converting α-hydroxy acid to α-amino acid. Assembly of different modules in *E. coli* provided several whole-cell biocatalysts to convert styrene to (*S*)-mandelic acid, (*S*)-phenylethanolamine, and (*S*)-phenylglycine in high *ee* and yield, respectively. In this work, cascade biocatalysis was harnessed to achieve asymmetric one-pot multi-step oxy- and amino-functionalization of hydrocarbons, which is useful but challenging in chemistry. The cascade transformation represents a novel artificial pathway, with no

natural counterparts. Furthermore, with one additional enzyme module (ammonia lyase-decarboxylase), enantiopure (*S*)-mandelic acid, (*S*)-phenylethanolamine, and (*S*)-phenylglycine were also directly produced from bio-based L-phenylalanine. This provides the opportunity to produce these useful and valuable enantiopure chemicals from renewable feedstock.

LIST OF TABLES

LIST OF FIGURES

LIST OF SCHEMES

LIST OF SYMBOLS

3D	Three Dimensional
ADH	Alcohol Dehydrogenase
AlaDH	Alanine Dehydrogenase
ALDH	Aldehyde Dehydrogenase
ATP	Adenosine Triphosphate
CAT	Catalase
CFE	Cell Free Extract
cdw	Cell Dry Weight
de	Diastereomeric Excess
E	Enantioselectivity Factor
E. coli	*Escherichia coli*
ee	Enantiomeric Excess
EH	Epoxide Hydrolase
ER	Enoate Reductase
FAD (FADH$_2$)	Flavin Adenine Dinucleotide (Reduced Form)
FMN	Flavin Mononucleotide
GC	Gas Chromatography
GluDH	Glutamate Dehydrogenase
HHDH	Halohydrin Dehalogenase
HMO	Hydroxy Mandelate Oxidase
HPLC	High-Performance Liquid Chromatography
IPA	Isopropyl alcohol
IPTG	Isopropyl β-D-1-Thiogalactopyranoside
KERD	Ketone Reductase
KP	Potassium Phosphate
LB	Luria-Bertani

m-CPBA	*meta*-Chloroperoxybenzoic Acid
MA	Mandelic Acid
Mald	Mandelaldehyde
NAD$^+$ (NADH)	Nicotinamide Adenine Dinucleotide (Reduced Form)
NADP$^+$ (NADPH)	Nicotinamide Adenine Dinucleotide Phosphate (Reduced)
n-Hex	*n*-Hexane
NMR	Nuclear Magnetic Resonance
PAD	Phenylacrylic Acid Decarboxylase
PAL	Phenylalanine Lyase
PCR	Polymerase Chain Reaction
PEA	Phenylethanol Amine
PED	Phenylethane Diol
PG	Phenylglycine
PGA	Phenylglyoxylic Acid
SDS-PAGE	Sodium Dodecyl Sulfate-Polyacrylamide Gel Electrophoresis
SMO	Styrene Monooxygenase
Sty	Styrene
TB	Terrific broth
TFA	Trifluoroacetic Acid
THF	Tetrahydrofuran
TLC	Thin Layer Chromatography
α-TA	α-Transaminase
ω-TA	ω-Transaminase

Chapter 1. Introduction

This chapter provides the background, objectives, and organization of this thesis.

1.1 Chiral Chemicals

The word "Chirality" was derived from the Greek word meaning handedness. In chemistry, chiral chemicals are a huge group of asymmetric molecules with non-superposable mirror image, which are similar to the left and right hands.[1] In biology, chirality is the key intrinsic feature of many macromolecules (*e.g.* proteins, DNAs), which serve as basis of life. The asymmetric molecular recognition and interaction between small chiral molecules and complex macromolecules in living organisms is the scientific base for the increasing industrial demand of enantiopure chiral chemicals.[1-3] For example, increasing numbers of active pharmaceutical ingredients were manufactured as single enantiomer forms, because different enantiomers of the drug have different interactions with the targeted receptor site in human body, resulting in different biological activities.[4, 5] 4 out of 5 best-selling drugs in US 2012 are enantiopure chiral drugs (Figure 1.1).[6] In addition, many agrochemicals and fragrance are also produced in enantiopure forms, due to the different effects on plants and phytopathogens and different odors of different enantiomers.[7-9] Therefore, it is gaining importance to develop technologies to produce chiral chemicals in high enantiopurities in an efficient, environmentally friendly, and sustainable way.
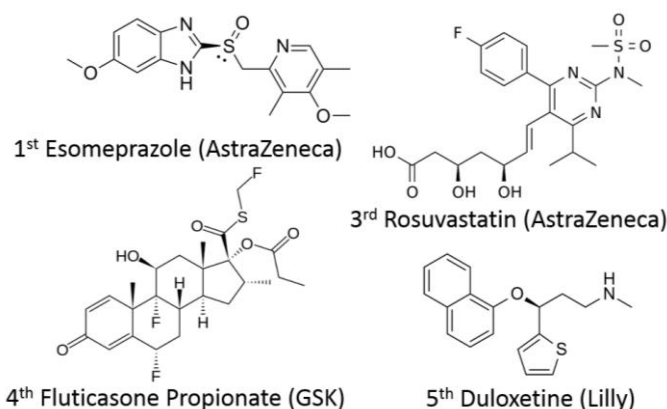
Figure 1.1. Enantiopure chiral drugs in top 5 best-selling drugs in US 2012 (Adapted with permission, Copyright © American Chemical Society and Njardarson Group).[6]

1.2 Production of Chiral Chemicals

Except for some naturally occurring chiral compounds (*e.g.* amino acids, carbohydrates) which were isolated directly, the majority of non-natural chiral chemicals were obtained by costly and cumbersome traditional technologies, such as physical separation (chiral chromatography, diastereomeric crystallization) from racemic compounds and chemical derivation (chiral pool synthesis) from enantiopure natural chemicals before early 1990s.[2-4] Recently, due to the rapid progress in stereoselective chemical transformation, more enantiopure chiral compounds were produced by kinetic resolution of racemic substrates and asymmetric synthesis from achiral substrates via chemocatalysis (organometallic catalysis and organocatalysis) and biocatalysis.[10-14] An example for production of chiral epoxide is shown Figure 1.2.
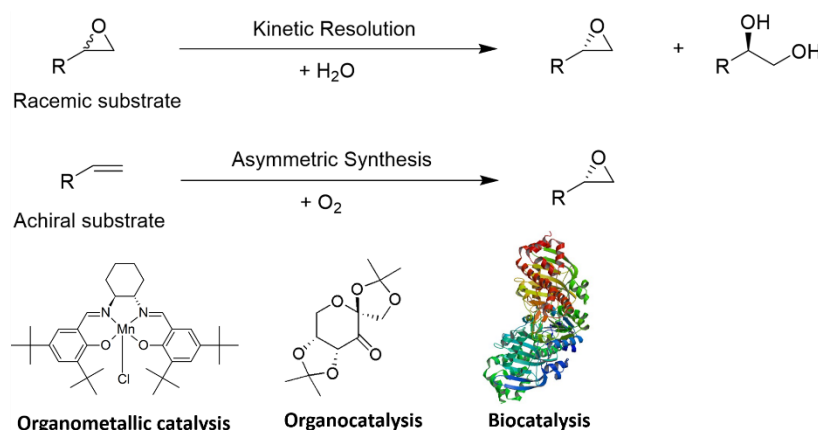
Figure 1.2. Production of chiral epoxides by kinetic resolution (hydrolysis of racemic epoxide) or asymmetric synthesis (epoxidation of achiral alkene) *via* organometallic catalysis, organocatalysis, or biocatalysis.

1.3 Biocatalysis

Biocatalysis is the use of natural catalysts, enzymes, to catalyze chemical transformation.[15] The most remarkable feature of biocatalysis is often high to excellent selectivity (chemoselectivity, regioselectivity, and enantioselectivity), which is prerequisite to produce chiral chemicals in high enantiopurities.[16-27] Besides the high selectivity, biocatalysis also provides two important advantages comparing to

chemocatalysis in asymmetric organic synthesis. Biocatalysis is environmentally benign and less hazardous, because it usually occurs in aqueous buffer (less organic solvent used) at moderate temperature and pressure (less energy input), and enzyme is generally biodegradable without involving toxic heavy metals (common in organometallic catalysis).[16-27] The other advantage is that enzymes are generally cheaper than some precious metal catalysts. Thanks to the advance of recombinant DNA technology, most of enzymes were available by facile fermentation of recombinant microbes growing on inexpensive and renewable resources. Thus, biocatalysis is becoming a green and efficient synthetic tool for chiral chemical production.[16-27] Although various types of enzymes and biocatalytic processes have been explored in laboratory nowadays, many of them are still suffering from low efficiency (productivity and product concentration) and limited substrate and product scope. Robust enzymes and efficient biocatalytic processes are highly demanded to facilitate the translation of academic research into industrial implementations.

Advantages:
❖ High Selectivity: Chemo-, Regio-, Stereo-
❖ Non-Toxicity: Mild Conditions, Biodegradable,
❖ Low Cost: Available by Fermentation

Biocatalysis

Disadvantages:
❖ Low Efficiency: Productivity, Product Titer
❖ Limited Scope: Substrate, Both Enantiomers
❖ Relatively Low Stability for Long Time
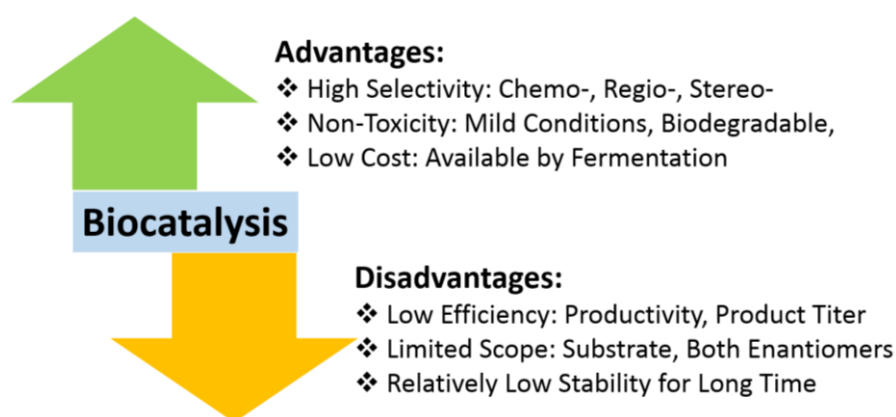
Figure 1.3. Advantages and disadvantages of biocatalysis in general.

1.4 Whole-Cell Biocatalysis

Biocatalysis could be performed with different forms of biocatalyst, such as purified or immobilized enzymes (*in vitro*) and enzymes inside whole cells. The choice of forms often depends on a case-by-case basis. Whole cell is a popular choice because of its several advantages over *in vitro* biocatalysis (Figure 1.4).[28-32] Firstly, enzymes in whole cell are readily available from fermentation directly without further

downstream processes, *e.g.* disruption of cells and purification of enzymes. Secondly, enzymes would be more active in their natural environment (inside cell, for most enzymes), and possibly be more stable due to the protection of the membrane and cell walls. In addition, naturally existing cofactors (*e.g.* NAD(P)H, ATP) could be easily regenerated in whole cells, and this is particularly important for enzyme-catalyzed oxidoreductions.[28-32] Last but not the least, whole cells provide the context for co-localization of multiple enzymes and enzyme components, which will increase the local concentration of enzymes and reduce the diffusion of intermediates in multistep catalysis.[33]
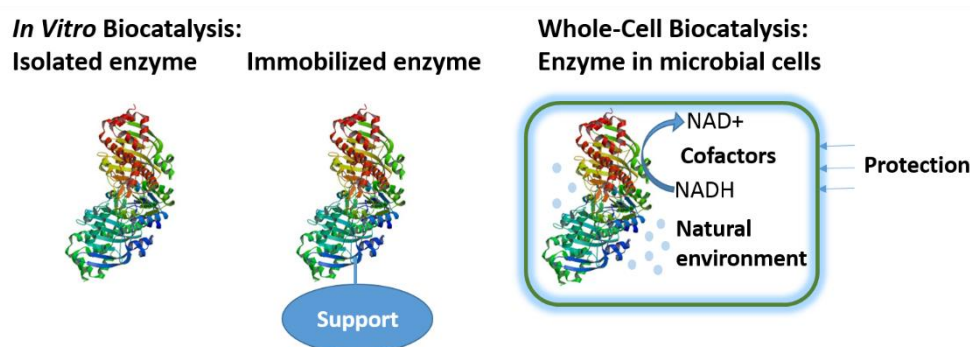
Figure 1.4. Types of biocatalysis: *in vitro* biocatalysis and whole-cell biocatalysis.

1.5 Cascade Biocatalysis

Enzymes are especially suitable for multistep catalysis in one pot or one cell (cascade/tandem biocatalysis), because most of enzymes catalyze reactions in similar conditions as they occur in cellular metabolism naturally. Thus, performing cascade biocatalysis is attractive to circumvent the time-consuming, yield-decreasing, waste-producing, and labor-demanding intermediate recovery and purification steps in traditional multistep synthesis.[34-40] Distinctive from metabolic engineering, cascade biocatalysis is designed and engineered in a bottom-up way and largely unlinked to the metabolism (except for cofactors).[34-40] It could be performed with different forms of biocatalysts, such as *in vitro*, whole cell, or mixture of *in vitro* and whole cell. By supplying different starting substrates, multistep biocatalysis could generate diverse

non-natural chemicals, especially chiral compounds in high enantiopurity (Figure 1.5).[34-40] Although several interesting prototypes of cascade biocatalysis have been developed recently, the majority of them are with low efficiency, limited substrate scope, and only one enantiomer produced. Furthermore, novel types of biocatalytic cascades are still limited in academia but they are highly demanded for pharmaceutical and other chemical industries.
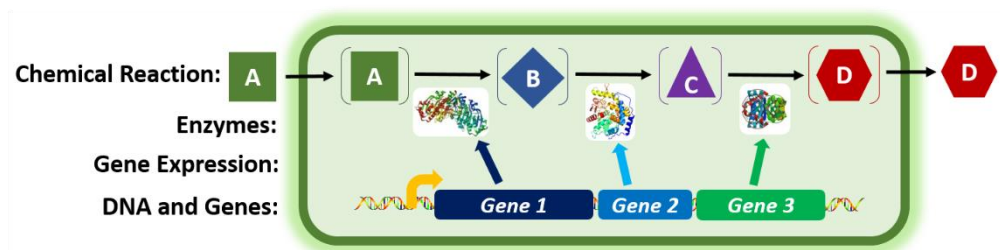
Figure 1.5. Whole-cell based cascade biocatalysis.

1.6 Thesis Objectives

i) As mentioned above, many biocatalytic reactions are still not efficient for practical application, due to the low activity of biocatalysts and poor performance of processes. This problem persists in enantioselective hydrolysis of epoxides to produce enantiopure epoxides and vicinal diols. To address this gap, we aim to identify and clone a unique epoxide hydrolase (SpEH) from *Sphingomonas* sp. HXN-200, and develop a robust recombinant whole-cell biocatalyst and an efficient process for enantioselective hydrolysis of racemic and *meso*-epoxides to practically produce chiral epoxides and diols in high *ee* and high concentration.

ii) Another current limitation in biocatalysis is that most of industrial biotransformations are mainly based on one-step biocatalysis. Although several types of cascade biocatalysis have been recently reported, most of them are still suffering from low productivity, limited substrate scope, and no access to multiple enantiomers. Thus, we aim to develop a whole-cell based epoxidation-hydrolysis cascade for efficient asymmetric *trans*-dihydroxylation of a range of aryl alkenes to access to both

enantiomers of the corresponding vicinal diols in high enantiopurity. The cascade biocatalysis process should be robust, scalable, and comparable to chemical asymmetric dihydroxylation.

iii) To further address the gap of multistep biocatalysis and provide very novel cascade transformations with no natural or chemical counterparts, we propose to develop modular cascade biocatalysis for achieving asymmetric oxy- and amino-functionalization of easily available alkenes to produce valuable chiral α-hydroxy acids, 1,2-amino alcohols, and α-amino acids in high enantiopurity. To utilize renewable feedstock as starting material, we also aim to extend the cascade reactions to start from bio-based phenylalanine. These will serve as potential prototypes for future industrial implementation.
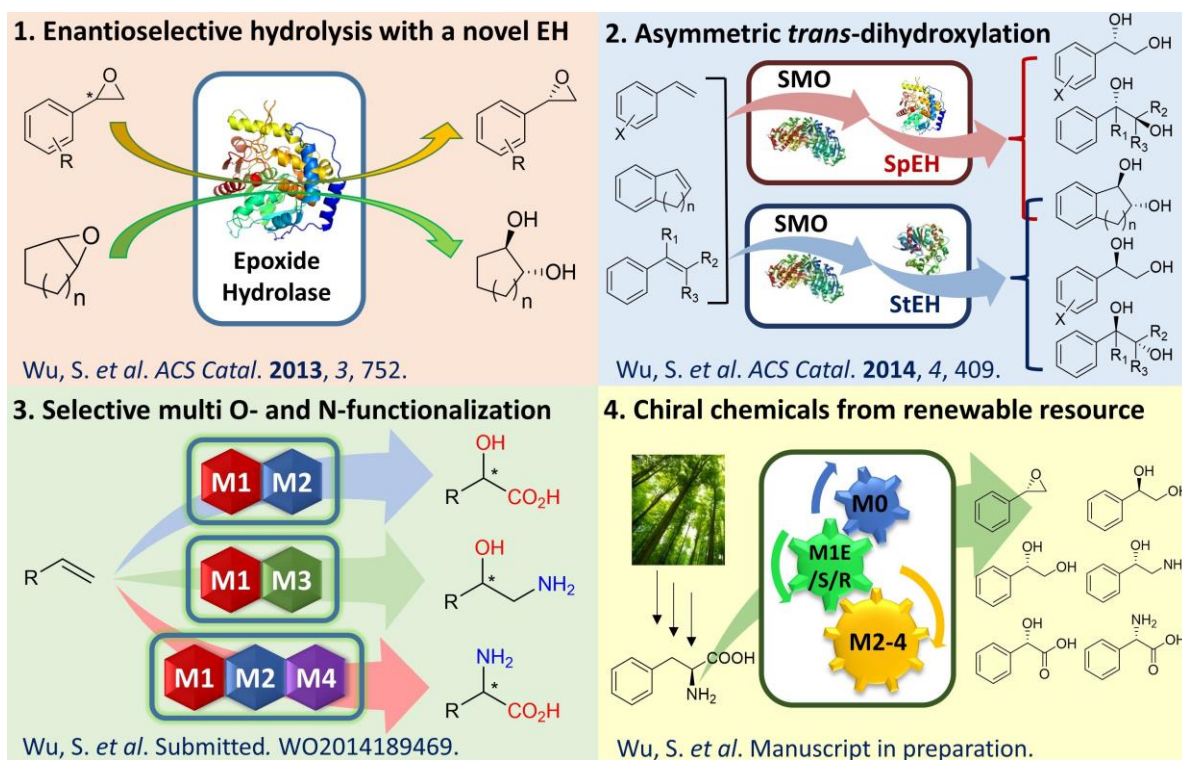
Figure 1.6. Overall diagram summarizing the current works in the PhD thesis.

1.7 Novelty and Significance of the Thesis

i) The newly cloned SpEH is highly active and showing the highest *S*-enantioselectivity for several epoxides, and thus enables the development of efficient biotransformation process to practically produce chiral epoxides and vicinal diols.

ii) The novel intracellular epoxidation-hydrolysis cascade provides access to both enantiomers of many aromatic vicinal diols in high *ee*, which is challenging in biocatalysis, and the method is much greener than Sharpless dihydroxylation.

iii) The one-pot functionalization of terminal alkenes to chiral α-hydroxy acids and α-amino acids is unique, with no chemical or natural counterpart. The one-pot functionalization of terminal alkenes to 1,2-amino alcohols represents the first biocatalytic aminohydroxylation, being greener than existing chemical methods.

iv) The cascade biocatalysis for converting L-phenylalanine to several types of chiral chemicals provides new opportunities for production of non-natural chemicals from renewable bioresource.

1.8 Thesis Organization

Chapter 1 briefly describes the introduction, objectives, and organization of this thesis.

Chapter 2 gives an intensive literature review of biocatalysis for chiral chemical synthesis, with highlights on enzyme discovery and engineering, several classes of enzymes, and cascade biocatalysis.

Chapter 3 presents the project of cloning a novel epoxide hydrolase and applying it for enantioselective hydrolysis of epoxides.

Chapter 4 describes the work of cascade biocatalysis for asymmetric *trans*-dihydroxylation of aryl olefins to vicinal diols.

Chapter 5 describes the topic of a novel modular cascade biocatalysis to achieve asymmetric oxy- and amino-functionalization of aryl alkenes.

Chapter 6 summarizes the finding and conclusion of this thesis, and gives recommendations for future directions.

Chapter 2 Literature Review

This chapter provides a comprehensive review of the biocatalysis field with a particular focus on the enzyme discovery, whole-cell biocatalysis, and cascade biocatalysis.

2.1 Biocatalysis in the Context of Biotechnology

Biotechnology is a broad discipline of application of advances in life science for development of commercial products, distinguished from fundamental research. According to the application areas, modern biotechnology is divided into three main branches (Figure 2.1).[41]

i) Green biotechnology for application in agriculture. One of the major fields is the development of genetic modified crops for better pathogen resistance (*e.g.* transgenic plants expressing insecticidal proteins),[42] better nutrition (*e.g.* golden rice with increased pro-vitamin A content),[43] and other purposes.

ii) Red biotechnology for application in medicine. A great breakthrough is the development of therapeutic monoclonal antibodies (US sale ~$25 billion in 2012)[44] produced by cell culture technology. And a recent "hot spot" is regenerative medicine by induced pluripotent stem cells.[45]

iii) White biotechnology (industrial biotechnology) for industrial purposes, *e.g.* production of chemicals, materials, and fuels. Although mankind has used bioprocessing such as brewing for thousands of years, it is not until recently that white biotechnology starts to attract great interests from both academia and industry, because it often utilizes renewable bioresource instead of dwindling fossil feedstock and provides green and non-toxic processes with reduced energy consumption and greenhouse gas emissions.[46-48]

2.1.1 Enzymatic Catalysis in White Biotechnology

Enzymatic catalysis (as a broad definition of biocatalysis) is central in white biotechnology (Figure 2.1). In some industries, enzymes produced by fermentation of microbes are directly used for numerous applications, *e.g.* for detergent application and for processing of food and animal feed.[49] In fermentation process, bio-based feedstock is converted to cell mass and metabolites through multiple enzymatic reactions (metabolism) of living microorganisms.[50, 51] In biological wastewater treatment, various organic pollutants and some inorganic nitrogen and phosphate are degraded to CO_2 and converted to cell mass with microorganisms through enzyme catalyzed metabolism.[52] In biological fuel cell, electrical energy is generated from chemical energy via redox reactions catalyzed by enzymes *in vitro* or *in vivo*.[53] In this thesis, we particularly focus on industrial biotechnology for production of organic chemicals.
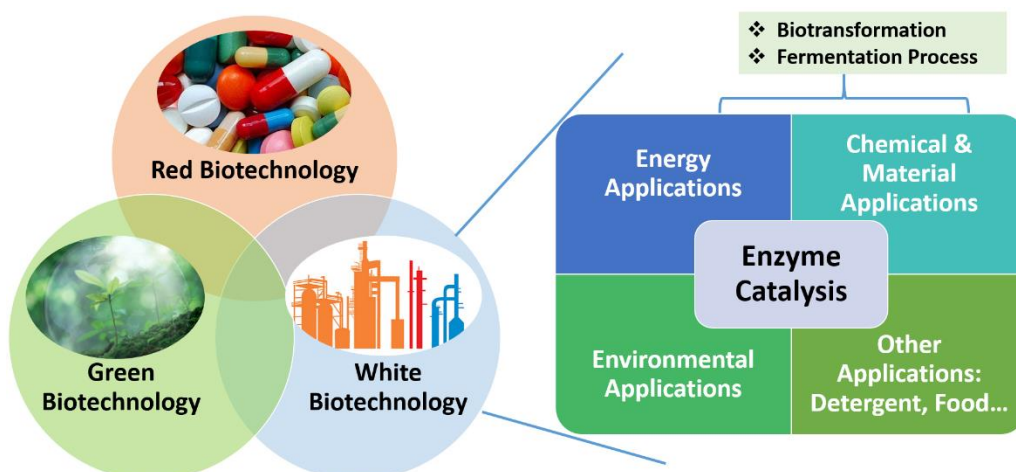
Figure 2.1. Three main parts of Biotechnology, key position of enzymatic catalysis in white biotechnology, and biotransformation and fermentation for production of organic chemicals.

2.1.2 Biotechnology for Production of Organic Chemicals

Organic chemicals were firstly discovered and extracted from living organisms, and had been believed to be a privilege of living organisms. After Wöhler's synthesis of urea from the inorganic substrates in 1828, [54] researchers started to develop theories and methodologies to synthesis various organic compounds (natural or non-natural), which have profound impact on human life and the whole world. However, many natural organic chemicals are still produced by fermentation of microorganisms, as

primary and secondary metabolites, because they are difficult or uneconomical to produce by organic synthesis.

Recently, with the advance in recombinant DNA technology, biotechnological production of small organic chemicals has been significantly improved both in efficiency and chemical complexity. Two different approaches were actively pursued:

i) Biotransformation process (narrow meaning of biocatalysis): employ enzymes and microbial cells for transformation of natural or non-natural substrates to various products with one or several-step conversions.[16-27] This direction is greatly enhanced by genetic engineering and protein engineering recently.

ii) Fermentation process: utilize cellular metabolism to produce organic metabolites from simple growth carbon sources (*e.g.* bio-based glucose). The fermentative production is boosted by recent breakthrough in metabolic engineering and synthetic biology.[55-58]

The key difference between the two approaches is the independence/dependence of internal metabolism. Yet, in some cases, part of the product is from glucose (fermentation) while other part of product is directly provided as substrates.[59, 60] We believe that fermentative process is important for production of many biofuel, bulk chemicals and certain natural products (*e.g.* isoprenoids),[55-58] and biotransformation (biocatalysis) has great potential in production of many diverse fine chemicals and certain biofuels (*e.g.* biodiesel from oil).[16-27]

Since the targeted products in this thesis are several groups of non-natural chiral chemicals, the following sections will concentrate on enzymes and biocatalysis.

2.2 Enzyme Discovery, Engineering, and Design

Because enzymatic catalysis is the center of biocatalysis and white biotechnology, it is particularly important to discover and engineer new enzymes and

novel enzymatic activities. Theoretically, this will extend the boundary of enzymatic catalysis in the chemical space. From a practical point of view, it is the foundation of many applications in biocatalysis, metabolic engineering, and some other fields in biotechnology. Here, traditional strategies and three modern strategies in enzyme discovery and engineering will be briefly reviewed with recent excellent examples. The *de novo* design of enzyme will be concisely discussed as well.

2.2.1 Traditional Enzyme Discovery
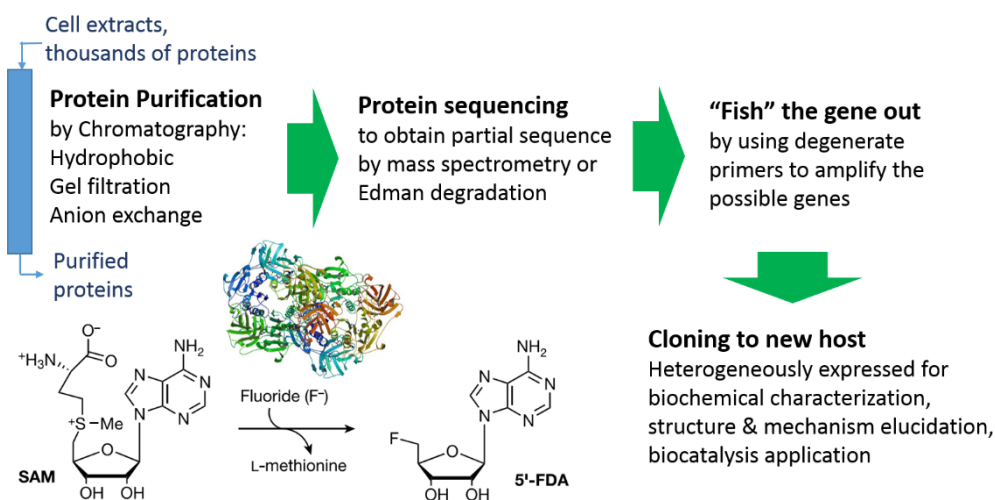
Figure 2.2. An example of traditional protein purification approach for enzyme discovery. Summary of identification of the first fluorination enzyme (Adapted by permission from Macmillan Publishers Ltd: Nature,[61] copyright © 2004).

Traditionally, most of enzymes were discovered by either biochemical purification approaches or genetic complementation approaches (disrupt and reconstitute the phenotype). In one of the biochemical purification approaches, the target enzyme is first purified from a mixture of thousands of intrinsic proteins of the microorganism. Some information of the enzyme (*e.g.* amino acid sequence) could be obtained, and then utilized to identify the corresponding gene. This method was clearly demonstrated in the identification of the first fluorination enzyme (Figure 2.2).[61] In one of the genetic complementation approaches, the genome of the microorganism is broken into small pieces of DNAs to construct a genetic library. Next, the library is introduced to another microorganism (which cannot catalyze the reaction originally), and test the recombinant microbes for the reaction. If one clone of new microbe

catalyzes the reaction, the heterogenous DNA fragment will be isolated to identify the corresponding gene. These traditional approaches are tedious, troublesome, and with serious drawbacks, *e.g.* protein purification is difficult for enzymes in low abundance, and gene expression is unpredictable in heterogenous hosts.

2.2.2 Sequence-Based Enzyme Discovery
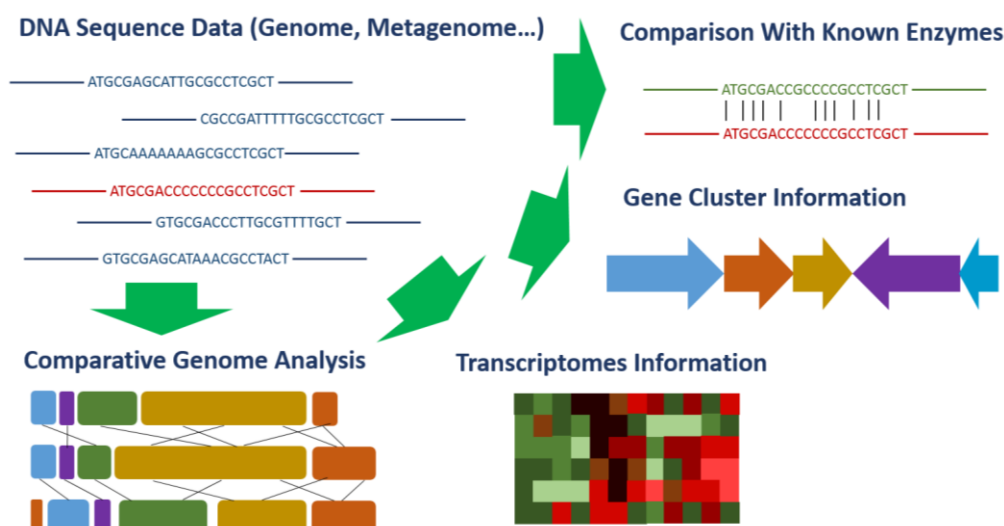
Figure 2.3. Sequence-based enzyme discovery using homology method (comparison with known enzymes), gene clustering, transcriptomes, comparative genome analysis, *etc*.

The situation was drastically changed during the 2000s, due to the great advance of DNA sequencing technology. From 1990 to 2003, the human genome project cost about US$ 3 billion to complete.[62] But recently, many next-generation DNA sequencing technologies could sequence the entire human genome within hours at a low cost of several thousand dollars.[63, 64] Nowadays, DNA sequences of genomes from various organisms and metagenomes from different environments (containing numerous unculturable microbes) are easily available from online database, and these will be an excellent source to discover new enzymes and pathways.[65, 66] When a microorganism is found for some new enzymatic transformation, it is now a common technique to sequence the whole genome to identify the new enzymes and pathways. The most straightforward genome mining method to identify putative enzymes is comparing putative proteins to the known enzymes for similar chemical reactions. This

homology-driven method can be used to identify hundreds of enzymes easily (if the enzymes are ubiquitous), but it often gives "me too" or "me better" enzymes.

To discover unprecedented novel enzymes, besides the genome sequence itself, other information such as gene clustering, transcription profile, and genome of other similar organisms could provide great assistance (Figure 2.3). In bacteria and fungi, the enzymes for biodegradation or biosynthetic pathways are usually encode by genes clustered together on genome, thus the neighborhood of the gene will provide rich information about the function. This is particularly useful to identify biosynthetic pathways and elucidate the novel enzymatic reactions in natural product research. For instance, Prof. Liu's group recently use this approach to identify the first standalone enzyme solely committed to the catalysis of a Diels-Alder reaction ([4+2] cycloaddition) in spinosyn A biosynthesis from *Saccharopolyspora spinosa*.[67] In higher organisms (*e.g.* plant), biochemically related genes are not necessarily clustered together, but they are usually co-regulated in transcription. Thus, the transcription profile (many cDNA sequences) is the key to identify novel enzymes from higher organisms. A recent example is the discovery of a novel iridoid synthase for a new route to cyclize a terpene via dialdehyde instead of diphosphates from *Catharanthus roseus* by Prof. O'Connor's group using feeding studies and transcriptomic data.[68] Another great strategy is comparative genome analysis, which was employed to discover the alkane synthesis pathway from cyanobacteria.[69] Researchers from LS9 Company firstly compared and analyzed the genomes of 9 alkane-producing cyanobacteria and 1 related non-producing cyanobacterium. And the putative pathway was identified and heterogeneously expressed in recombinant *E. coli* to validate the function. To sum up, the fast-growing DNA sequence of various genomes, metagenomes, and transcriptomes, together with bioinformatics analysis (*e.g.* gene clustering, comparative genomics) provide precious information for enzyme discovery.

2.2.3 Structure-Based Enzyme Discovery and Engineering

Protein engineering is a very powerful tool to improve enzyme with better properties in activity, selectivity (chemo-, region- and enantio-selectivity), thermo stability, substrate/product inhibition *etc*.[70-75] It is an enabling technology for many industrial application of biocatalysis, because many natural enzymes are not evolved for performing the desired reactions under the industrial conditions. Enzyme engineering could be traditionally achieved with two approaches. Rational design approach highly depends on the well understanding of the complex structure-function relationship, which is difficult for many enzymes. Directed evolution approach utilizing random mutagenesis (*e.g.* error-prone PCR) could achieve moderate success, but it usually gives huge size of libraries which are difficult for screening and selection. With a rapidly increasing number of 3D protein structure in the RCDB Protein Data Bank, a new semi-rational approach guided by protein structure allows fast engineering of enzymes with relatively small libraries. [70-75] For engineering of substrate scope, selectivity, and activity, the 3D structure of the enzyme would be used to identify the amino acid residues around the catalytic center or substrate binding site, and then a random mutagenesis will focus on these hot spots to create small but smart enzyme libraries to screen (Figure 2.4). These structure-guided methods, *e.g.* CASTing,[76] ISM,[77, 78] have achieved great success in engineering various types of enzymes for biocatalysis applications in the last few years.
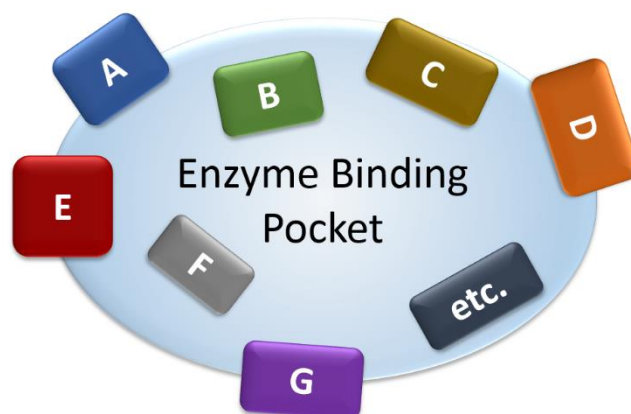
Figure 2.4. A semi-rational approach to engineer enzymes: CASTing method to focus engineering of sites around the substrate binding pocket (Adapted with permission, copyright © 2011 WILEY-VCH).[73]

A famous case is the engineering of a transaminase for manufacture of the chiral drug Sitagliptin by researchers from Codexis (Figure 2.5).[79] The initial transaminase was limited to simple ketones with no detectable acitivity on very bulky prositagliptin. The engineering was started with expending the active site by mutagenesis and screening with increasing bulky substrates, and finally gave an engineered transaminase with 27 mutated sites. This engineered transaminase was applied to convert 200 g/L prositagliptin to sitagliptin with 99.95% *ee* and 92% yield. In comparison with chemo-catalyzed process, the biocatalysis process clearly demonstrates both economic advantage of higher yield, higher enantiopurity, higher productivity, and lower cost, and environmental advantage of less waste and no toxic heavy metals. It is an excellent example of biocatalysis for production of chiral chemicals.
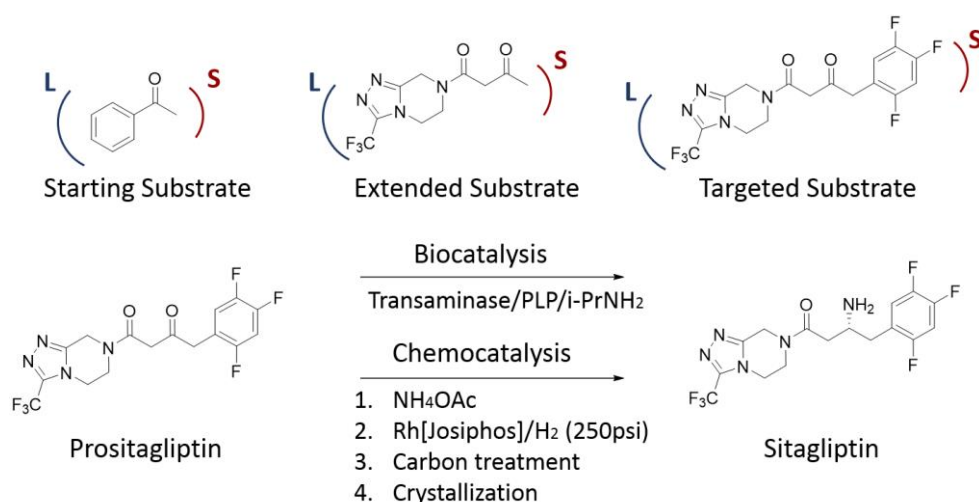
Figure 2.5. Engineering of transaminase for Sitagliptin manufacture: focus engineering of the large and small binding pockets (L, S) for accepting very bulky prositagliptin (Adapted with permission, copyright © 2010 The American Association for the Advancement of Science).[79]

2.2.4 Mechanism-Based Enzyme Discovery and Engineering

Enzyme promiscuity is the ability of an enzyme to transform different non-natural substrates (substrate promiscuity), and to catalyze distinctively different chemical transformations with different transition states (catalytic promiscuity).[81-83] The promiscuity is especially important for evolution of organisms. For biocatalysis,

while substrate promiscuity is well conceptually accepted and usually experimentally explored, catalytic promiscuity is still rather unexplored though it is more important to discover new types of enzymatic transformations. Catalytic promiscuity involves breaking/forming different types of chemical bonds with similar or altered catalytic mechanism. Thus, the understanding of catalytic mechanism would significantly contribute to the discovery and engineering of new enzyme-catalyzed transformations.

One of the well-known examples of enzyme catalytic promiscuity is the C-C bond formation reaction (aldol addition and Michael addition) catalyzed by versatile lipases, which naturally catalyze the hydrolysis of esters.[84, 85] In its native reaction mechanism of lipase, an oxyanion hole is formed in the catalytic center to polarize the carbonyl bond (C=O) in the ester substrate and assists the nucleophilic attack by a serine residue at the active site. In the proposed mechanism for aldol addition, the oxyanion hole still functions to polarize the carbonyl group (C=O) of ketone, but a histidine residue acts as base to abstract an α-proton to facilitate C-C bond formation with a second substrate.[86]
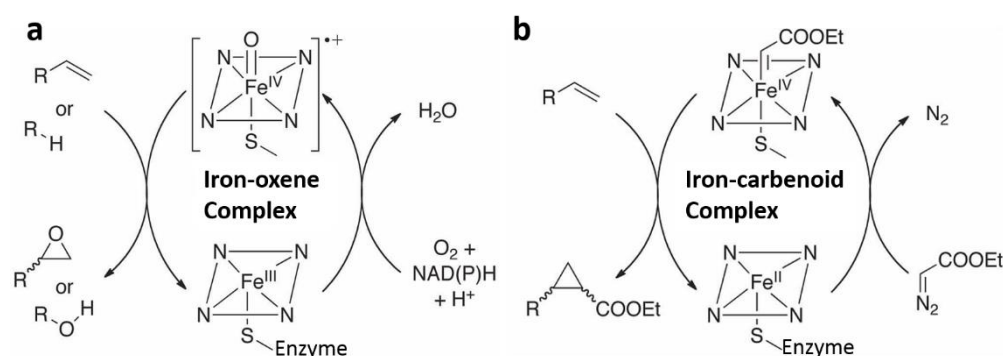
Figure 2.6. Engineering of P450 monooxygenase for carbene transfer. **a)** Natural epoxidation/hydroxylation reactions *via* iron-oxene intermediate; **b)** engineered cyclopropanation reaction *via* iron-carbenoid intermediate (Adapted with permission, copyright © 2013 The American Association for the Advancement of Science).[87]

More recently, Prof. Arnold group provided an excellent example of catalytic promiscuity of P450 monooxygenase.[87] P450 monooxygenases are versatile enzymes for various oxidative transformations, such as hydroxylation, epoxidation, oxidative coupling, and heteroatom oxygenation, and mostly via the reactive high-valent iron-oxene intermediate (Figure 2.6a). The transferring of oxene to olefins through this

intermediate gives epoxides (epoxidation). They proposed to achieve distinctive carbene transferring via a similar high-valent iron-carbenoid species (Figure 2.6b). Transferring carbene to olefins is a widely used reaction in organic chemistry (cyclopropanation), which was unknown in enzyme catalysis before. In their study, several P450BM3 variants were tested for cyclopropanation of styrene with diazoester carbene precursors, and further mutagenesis of P450BM3 led to good activity (TTN up to 300), diastereoselectivity (up to 92:8) and enantioselectivity (up to 97% *ee*). In a follow-up study, rational engineering of P450BM3 gave a new P411BM3, and then a very efficient whole-cell biocatalysis process was developed to produce cyclopropanes in high enantioselectivity (99% *ee*), high product titer (27 g/L), and good yield (78%, 48,800 TTN).[88] These impressive studies not only provided a novel enzymatic approach for many carbene transfer reactions, but also demonstrated that the enzyme mechanism can be purposely designed and altered for unnatural enzymatic transformations.

2.2.5 Computation-Based *de novo* Enzyme Design
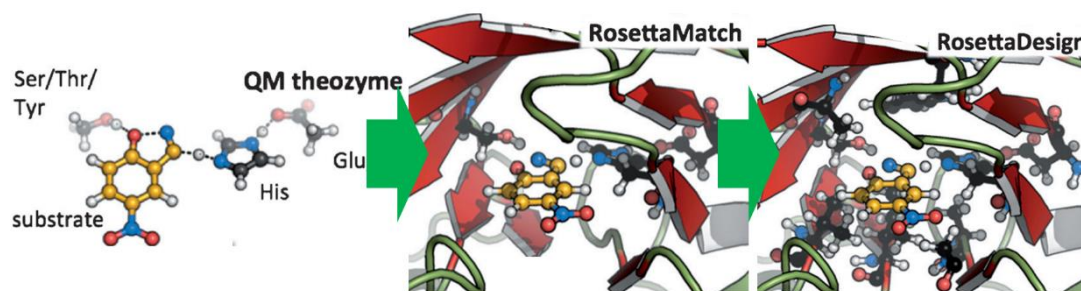
Figure 2.7. Key steps of computational *de novo* enzyme design (Adapted with permission, copyright © 2013 WILEY-VCH).[90]

When discussing about enzyme discovery and engineering, it is impossible not to mention computation-based *de novo* enzyme design.[89, 90] In this approach, quantum mechanical calculations are firstly used to generate the three dimensional arrangements (theozymes) of amino acid residues to stabilize the transition state of the target reaction. Then the theozymes are incorporated into possible protein scaffolds by matching to existing protein 3D structures in database with efficient algorithms. The active site residues and other residues were further optimized with computational programs, and

usually several possible amino acid sequences were generated at the last of the computational design. Experiments are carried out to further validate and test these possible *in silico* designed enzymes. Initial successful examples include the design of enzymes for Kemp elimination and Diels-Alder cycloaddition by Prof. Baker's group.[91, 92] The work represents a great success of computation-based *de novo* enzyme design for expanding the scope of enzymatic catalysis. Extensive protein engineering (directed evolution) was applied to improve the efficiency of the designed enzyme for Kemp elimination, resulting in a highly active artificial enzyme with a k_{cat} of 700 s^{-1} and a k_{cat}/K_m of 230,000 M^{-1} s^{-1}, which is comparable with the high rates of many natural enzymes.[93]

As a conclusion of this part, discovery of new enzymes and novel enzymatic activities are fundamentally important for biocatalysis. Information from DNA sequence, protein structure, and enzyme mechanism is often the basis of enzyme discovery and engineering. By combination of knowledge from sequence, structure, mechanism, and tools from bioinformatics and computation, we can envision that more and more powerful enzymes will be discovered, engineered, and designed for various applications in the near future—a booming age of biocatalysis.

2.3 Enzymes for Biocatalysis

Enzymes are typically classified into different categories and subcategories according to the types of reaction catalyzed.[94, 95] A numerical classification scheme for enzymes is the EC number. Table 2.1 shows the six categories of enzymes with the key enzymes in this thesis highlighted in **bold**.

Table 2.1. Classification of enzymes.[94]

Enzyme Group	Reaction Catalyzed	Examples
EC 1: Oxidoreductases	Oxidation or reduction reactions: transfer of electrons, and H, O atoms	**monooxygenase, oxidase, dehydrogenase**

EC 2: Transferases	Transfer of a functional group, such as NH_2-, CH_3-, RCO-, and -H_2PO_4	kinase, **transaminase**
EC 3: Hydrolases	Hydrolysis, use water to cleave chemical bonds	lipase, peptidase, **epoxide hydrolase**
EC 4: Lyases	Non-hydrolytic addition or removal of groups	**decarboxylase**, aldolase, **lyase**
EC 5: Isomerases	Intramolecule rearrangement	mutase, **isomerase**
EC6: Ligases	Utilize ATP to join two molecules by forming new C-O, C-S, C-N or C-C bonds	synthetase

In biocatalysis for production of organic chemicals, traditionally most useful enzymes are the hydrolytical enzymes (EC 3). More recently, there is a fast progress in application of oxidoreductases (EC 1) for more challenging but useful redox reactions. And some other subgroups of enzyme such as transaminase (EC 2), and aldolase (EC 4) are drawing attentions from academia and industry as well.[16-27] Several groups of enzymes used in this thesis and their biocatalysis applications are individually reviewed in the following sections.

2.3.1 Epoxide Hydrolases for Enantioselective Hydrolysis

a) Kinetic resolution of racemic epoxides
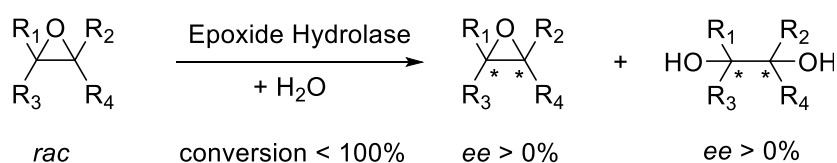
b) Desymmetrization of *meso*-epoxides
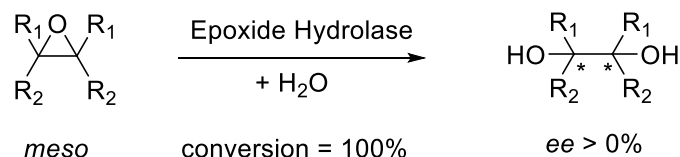
Scheme 2.1. Enantioselective hydrolysis of epoxides by epoxide hydrolase: **a)** kinetic resolution of racemic epoxides to produce chiral epoxides and diols; **b)** desymmetrization of *meso*-epoxides to produce chiral vicinal diols.

Epoxide hydrolase (EH, EC 3.3.2.x) is a ubiquitously found enzyme in living organisms responsible for the hydrolysis of epoxides. Because of the toxicity of

epoxides, the major physiological role of EH is detoxification, though it has other roles in catabolism and regulation of signaling molecules in certain organisms.[96] EH is one of the most useful enzymes for production of chiral chemicals, since it often exhibits stereoselectivity in hydrolysis of racemic epoxides (kinetic resolution) and *meso*-epoxides (desymmetrization) to prepare chiral epoxides and vicinal diols (Scheme 2.1).[97-104] Chiral epoxides are very useful synthetic synthons, because they could easily react with different nucleophiles to offer various other chiral compounds (Scheme 2.2).[105] EH also has other advantages for industrial application: only use water as co-substrates; independent from cofactors; relatively stable; and often with broad substrate scope (this feature is important for a detoxification enzyme).
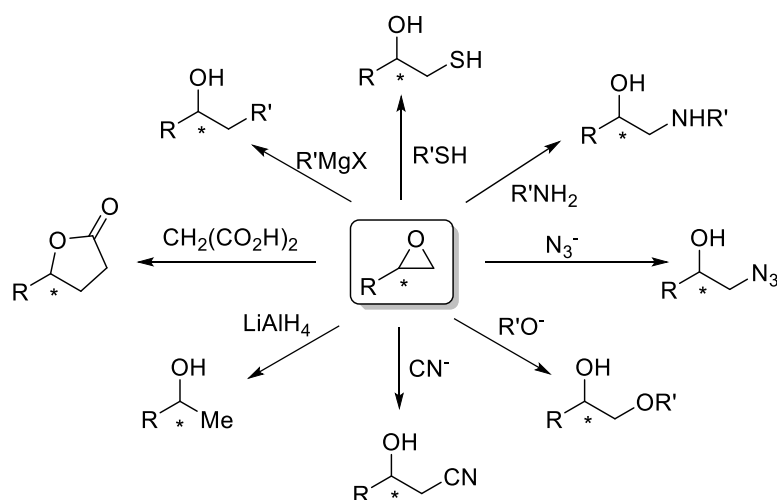
Scheme 2.2. Various chiral compounds could be derived from chiral epoxides.[105]

2.3.1.1 Structure and Mechanism of Epoxide Hydrolase

The majority of EHs (except for several EHs, such as limonene EH) belong to the α/β-hydrolase fold proteins. The 3D structure of EH has a relatively conserved core domain containing eight stranded β-sheets surrounded by α-helices, a less conserved lid domain, and a flexible loop connecting both domains (Figure 2.8).[102]
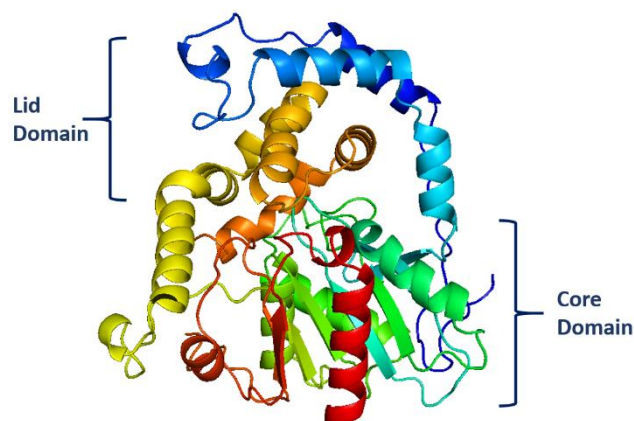
Figure 2.8. 3D structure of α/β-hydrolase fold EH from *Aspergillus niger* (PDB 1QO7).

The reaction mechanism of EH resembles to that of other hydrolases in the α/β-hydrolase fold family (Figure 2.9). The first step of mechanism involves a nucleophilic attack of an Asp residue on the carbon of epoxide ring, giving a covalently bound ester intermediate. In the second step, the intermediate is hydrolyzed by an activated water molecule in which proton is abstracted by a charge relay system (His-Asp/Glu). The catalytic trial (Asp-His-Asp/Glu) is on the core domain. Other key residues are two Tyr groups from lid domain, which provide hydrogen bonding and protonating of the oxygen of epoxide. These two Tyr residues in the catalytic center also distinguish EH from other members of the α/β-hydrolase fold family.
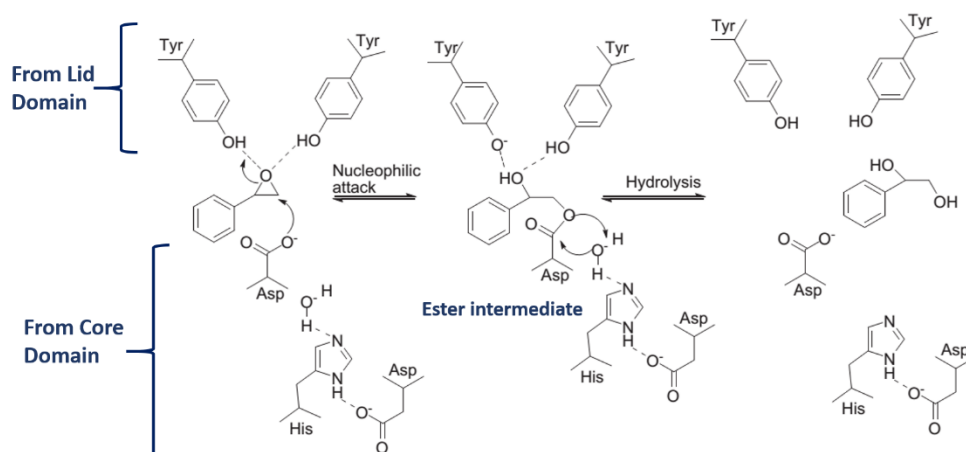
Figure 2.9. Mechanism of α/β-hydrolase fold EH (Adapted with permission, copyright © 2010 Elsevier).[103]

2.3.1.2 Well-Studied Epoxide Hydrolases

Prof. Furstoss' group initiated the study of EH from fungus *Aspergillus niger* (AnEH) for kinetic resolution of racemic epoxides to prepare enantiopure epoxides in early 1990s.[106,107] AnEH was found to exhibit high *R*-enantioselectivity ($E > 30$) for kinetic resolution of *para*-substituted styrene oxides,[108] but it showed low to moderate *R*-enantioselectivity ($E < 30$) for other substituted styrene oxides.[109] High concentration biotransformation (substrate concentration > 50 g/L) was achieved with AnEH for hydrolysis of *para*-chlorostyrene oxide,[110] and several other useful epoxides.[111-113] The 3D structure of AnEH was determined in 2000,[114] and Prof. Reetz group performed protein engineering to improve the enantioselectivity for hydrolysis of phenyl glycidyl ethers.[115, 116]

Another famous EH, ArEH was initially purified from epichlorohydrin degrading bacterium *Agrobacterium radiobacter* AD1 by Prof. Janssen's group in early 1990s.[117] Then the cloning and heterogeneous expression of ArEH facilitated the detailed biochemical characterization and elucidation of the reaction mechanism.[118] The native ArEH showed a moderate *R*-enantioselectivity ($E = 10$-20) for kinetic resolution of racemic styrene oxides and derivatives,[119] but a good selectivity in desymmetrization of *meso*-cyclohexene oxide to give (1*R*, 2*R*)-cyclohexane-diol.[120] The elucidation of 3D structure of ArEH in 1999[121] significantly contributed to the further protein engineering to improve activity and selectivity.[122-124] However, there is no report of application of ArEH for biotransformation in high concentration (possibly due to substrate/product inhibition).

2.3.1.3 Epoxide Hydrolase from *Sphingomonas* sp. HXN-200

Previously, our group has discovered that an alkane degrading bacterial strain *Sphingomonas* sp. HXN-200 catalyzed the enantioselective hydrolysis of *meso-N*-protected-3, 4-epoxy-pyrrolidine and *meso*-cyclohexene oxide to give corresponding (*R*, *R*)-vicinal diols in high *ee* (desymmetrization, Scheme 2.3).[125] Another study showed that it hydrolyzed racemic *N*-protected-3,4-epoxy-piperidine to yield

corresponding enantiopure (−)-epoxide via kinetic resolution.[126] The cell and CFE (cell free extract) of *Sphingomonas* sp. HXN-200 were also found to have moderate to high *R*-enantioselectivity towards styrene oxide and chlorostyrene oxides.[127, 128] Especially for *meta*-chlorostyrene oxide, the *R*-selectivity ($E = 41$) is the highest among all of the EHs. And for styrene oxide, the *R*-selectivity ($E = 26\text{-}29$) is the highest among all of the native EHs at that time. The high *R*-selectivity enables the production of valuable (*S*)-styrene oxides via kinetic resolution (Scheme 2.3). Starting from 320 mM racemic styrene oxide, 129 mM (15 g/L$_{org}$) enantiopure (*S*)-styrene oxide was produced with 60 g/L CFE of *Sphingomonas* sp. HXN-200.[127] Obviously, the loading of biocatalyst is too high and the product concentration is still low for practical application.
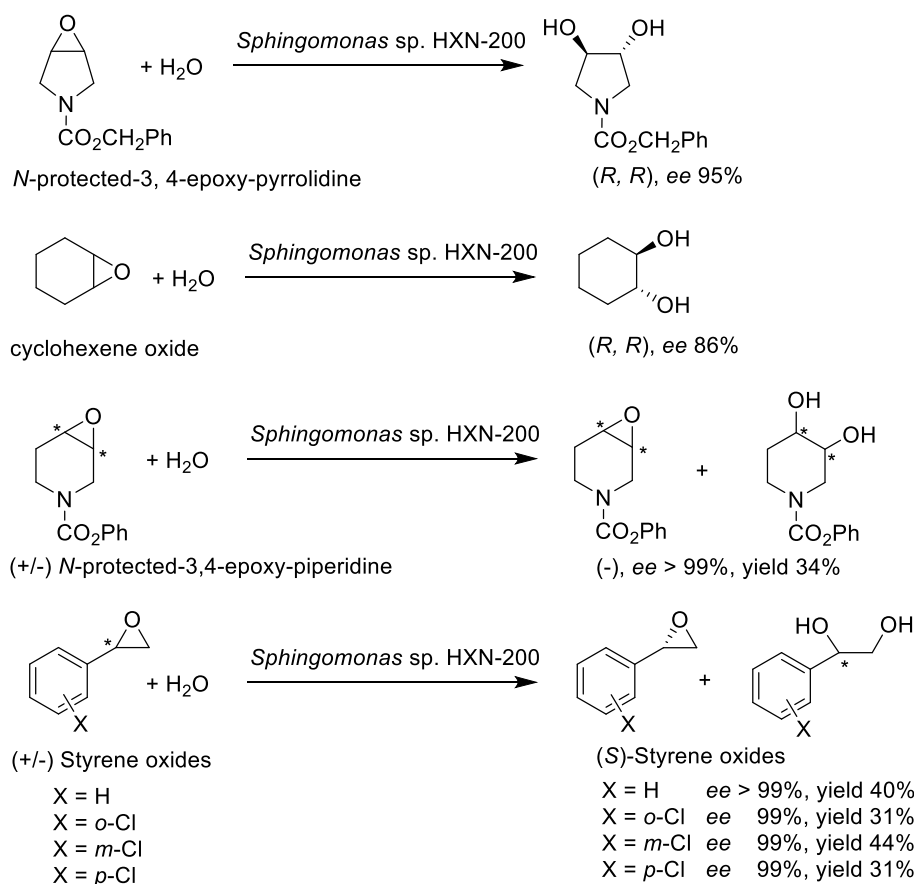
Scheme 2.3. Enantioselective hydrolysis of *meso* and racemic epoxides with *Sphingomonas* sp. HXN-200.[125-128]

However, the EH form *Sphingomonas* sp. HXN-200 has not been identified yet. The identification and cloning of the EH will contribute to 1) much more efficient biocatalysis by highly heterogeneously expressing the EH in *E. coli*; 2) biochemical

characterization of the enzyme; 3) further 3D structure elucidation and protein engineering; 4) other biocatalytic applications, such as enzyme immobilization and cascade biocatalysis. It was unsuccessful to identify the EH using a biochemical purification method (unpublished results from previous group members), probably due to the very low abundance ($< 1\%$) of the EH in the native *Sphingomonas* sp. HXN-200.

2.3.2 Monooxygenases for Asymmetric Epoxidation

Although EH is a facile biocatalyst to produce valuable chiral epoxides, the drawback is the maximum 50% yield in kinetic resolution. Another potential approach is direct asymmetric epoxidation of prochiral alkene to give chiral epoxide in maximum 100% yield (Scheme 2.4).[105, 129] In the early studies, chloroperoxidase (EC 1.11.1.10) was found to be a great biocatalyst for highly enantioselective epoxidation of aliphatic *cis*-alkenes and 1,1-disubstituted terminal alkenes.[130, 131] However, it only showed low to moderate selectivity for mono-substituted terminal alkenes and styrene derivatives.[132] Recently, there is a growing interest to use ubiquitous O_2 instead of H_2O_2 as a green and cheap oxidant.[133] And monooxygenases (EC 1.13.x.x and EC 1.14.x.x) are the enzymes catalyzing the insertion of one oxygen atom of O_2 into organic substrates (hydroxylation: insert O into C-H bond; epoxidation: insert O into C=C bond).[134]

a) Kinetic resolution of racemic epoxides
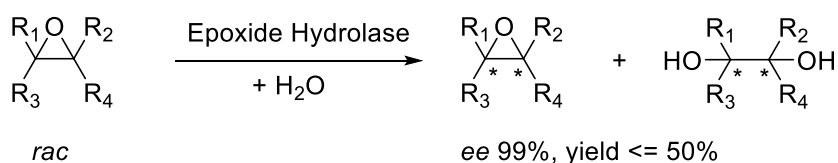
b) Asymmetric epoxidation of prochiral alkenes
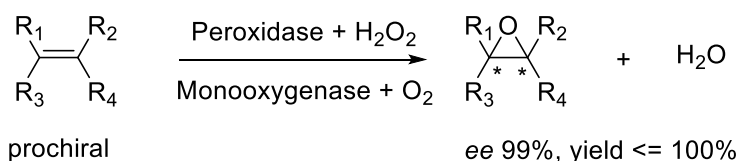
Scheme 2.4. Two approaches to produce chiral enantiopure epoxides **a)** kinetic resolution of racemic epoxides by EH, maximum yield: 50%; **b)** Asymmetric epoxidation of alkenes by peroxidation or monooxygenase, maximum yield: 100%.

2.3.2.1 Styrene Monooxygenase
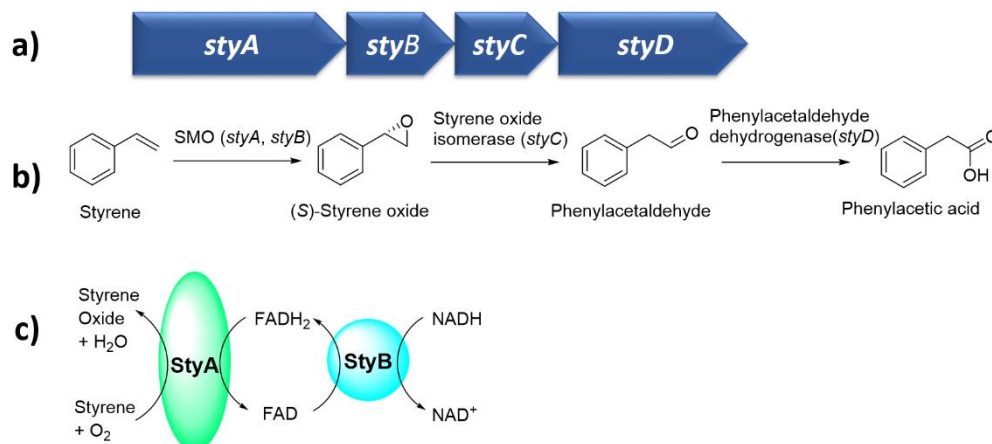
Figure 2.10. a) Genetic organization of styrene degradation pathway in *Pseudomonas*; **b)** styrene degradation pathway in *Pseudomonas*; **c)** function and electron transfer of the two component SMO.

One of the most famous monooxygenases for enantioselective epoxidation is the styrene monooxygenase (SMO, EC 1.14.14.11), a two component flavin-dependent monooxygenase.[135,136] The SMO was first discovered in the styrene degrading pathway from several *Pseudomonas* species (Figure 2.10).[137-140] It comprises two components: StyA consumes O_2 and $FADH_2$ for epoxidation of styrene, and StyB utilizes NADH to reduce FAD to $FADH_2$.[141] One component SMO (fused StyA and StyB) was later discovered from a *Rhodococcus* species.[142]

All the discovered SMOs catalyze highly enantioselective epoxidation of styrene to produce enantiopure (*S*)-styrene oxide (*ee* > 99%). Further exploration of the substrate scope found that SMO accepts various styrene analogues to give *S*-epoxides in very high enantiopurity (most *ee* > 95%) and relatively good product concentration (Scheme 2.5).[143-145] Because SMO consumes stoichiometric cofactor $FADH_2$ or NADH for the epoxidation, various methods have been developed to regenerate the cofactors for the epoxidation *in vitro*, including: enzyme method using a formate dehydrogenase,[146] chemical method using a transition metal complex,[147] and electrochemical method directly using cathode.[148] However, using recombinant whole cells with cofactor regenerated by cell metabolism seems a more efficient and

economical option for SMO-catalyzed epoxidation. After about one decade's development from Prof. Witholt's and Prof. Schmid's groups,[149-152] the epoxidation of styrene by recombinant whole cells expressing SMO was improved to be one of most productive biocatalytic oxyfunctionalization processes: (*S*)-styrene oxide was produced at 72.6 g/L_{org} from styrene and glucose in 8 h.[152] In a detailed environmental and economic assessment, the biocatalytic process is comparable or better than other chemical processes, demonstrating the great potential of biocatalysis in epoxidation and other oxyfunctionalization.
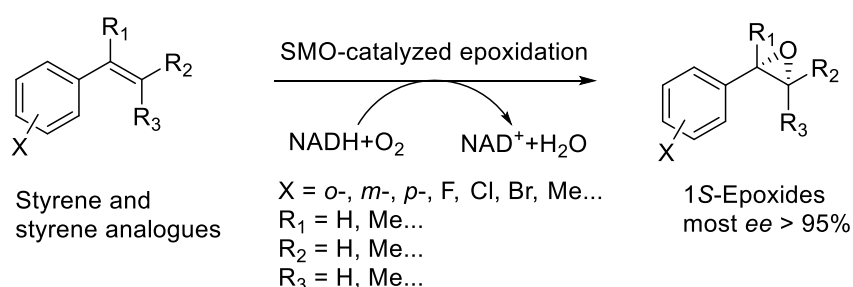
Scheme 2.5. SMO-catalyzed highly selective epoxidation of styrene and analogues.

Recently, the 3D structures of StyA and StyB were reported,[153, 154] which enable detailed characterization of reaction mechanism and structure-guided protein engineering of SMO. Initial attempt to change the enantioselectivity of SMO was rather unsuccessful.[155] This led to a hypothesis that enantioselectivity of SMO is controlled by the overall shape of the binding site, and thus simply mutating one or two residues could not alter the selectivity. It will be interesting to engineer existing SMOs or to bioprospect new enzymes for epoxidation with a reversed *R*-selectivity.

2.3.2.2 P450 Monooxygenases

Cytochrome P450 monooxygenases (EC 1.14.13.x, EC 1.14.14.x and EC 1.14.15.x) are heme-dependent enzymes that are ubiquitously found. They are versatile biocatalysts for a variety of chemical transformations, such as hydroxylation, epoxidation, dealkylation, and heteroatom oxygenation.[156-159] The monooxygenation reactions (*e.g.* hydroxylation and epoxidation) utilize O_2 and depend on the electron transfer between heme and NAD(P)H via electron partner proteins.

Many native P450 monooxygenases are responsible for epoxidation in some natural product biosynthesis.[160] Importantly, because of the promiscuous nature of P450 enzymes, P450s responsible for hydroxylation are usually also capable of performing epoxidation, and some P450 variants (mutants) could have altered selectivity for epoxidation.[161] One of the most famous P450s is P450BM3, a native fatty acid hydrolase from *Bacillus megaterium*.[162] For epoxidation of styrenes, P450BM3 is not a good choice: native P450BM3 gave (*R*)-styrene oxide in low *ee* of 20%,[163] and several mutants produced the reverse enantiomer (*S*)-styrene oxide but in low *ee*.[164]
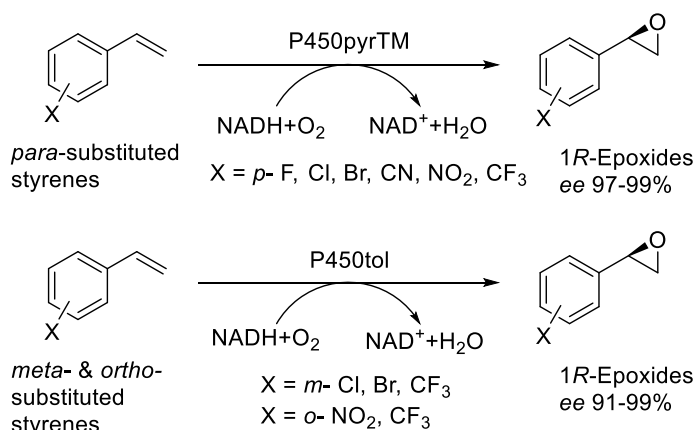
Scheme 2.6. Highly *R*-selective epoxidation of substituted styrenes with P450pyrTM and P450tol.

In search of new enzymes for epoxidation with high *R*-selectivity, the P450pyr from *Sphingomonas* sp. HXN-200, which has been investigated for selective hydroxylation in our group previously,[165-168] was found to catalyze epoxidation of styrenes.[169] More importantly, a triple mutant, P450pyrTM showed significant improvement in *R*-selectivity for epoxidation of *para-* substituted styrenes, giving the corresponding (*R*)-styrene oxides in 97-99% *ee* (Scheme 2.6).[169] A novel P450tol responsible for toluene hydroxylation in *Rhodococcus coprophilus* TC-2, was recently discovered in our lab for epoxidation of *meta-* and *ortho-* substituted styrenes to produce the corresponding (*R*)-styrene oxides in 91-99% *ee*.[170] The high *R*-selectivity of P450pyrTM and P450tol makes them special, and complementary to the *S*-selective

SMO. However, the activity and efficiency of epoxidation by P450 monooxygenase are rather low, which require intensive development for future application.

2.3.3 Dehydrogenases and Oxidases for Selective Alcohol Oxidation

Oxidation of alcohols to produce carbonyl compounds (ketones, aldehydes, acids) is an important and useful oxidative chemical transformation. However, traditional chemocatalysis approaches often involve toxic metal agents and/or problematic oxidants with low regioselectivity. Alternatively, several types of enzymes, such as dehydrogenase and oxidase, have been developed as a green method for alcohol oxidation with appropriate selectivity.[171-174] Depending on enzymes and substrates, the oxidation could convert secondary alcohols to ketones or convert primary alcohols to aldehydes and acids. In this thesis, we are particularly interested in regioselective oxidation of the primary alcohol group in diols to produce α-hydroxy acids, and oxidation of α-hydroxy acids to α-keto acids (Scheme 2.7).

a) Oxidation of secondary alcohol to ketone
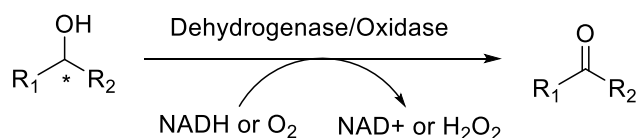
b) Terminal oxidation of diol to hydroxy acid
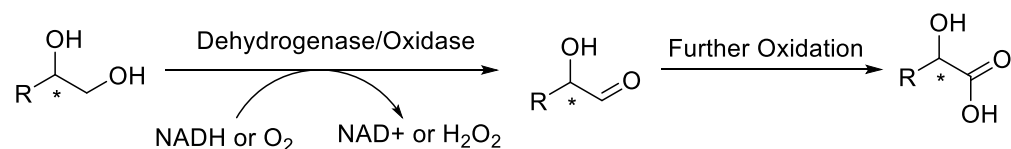
c) Oxidation of hydroxy acid to keto acid
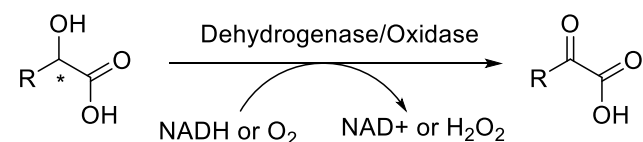
Scheme 2.7. Alcohol oxidation by dehydrogenase or oxidase **a)** oxidation of secondary alcohol to ketone; **b)** terminal oxidation of diol to hydroxy acid; **c)** oxidation of α-hydroxy acid to α-keto acids.

2.3.3.1 Alcohol Dehydrogenases

Alcohol dehydrogenases (ADHs, mainly EC 1.1.1.x) are distributed in a wide range of organisms and responsible for reversible oxidation of alcohols mainly using nicotinamide cofactors NAD(P)$^+$.[175] Although the majority of ADHs show preference for oxidation of secondary alcohols, there are several exceptions which prefer oxidizing primary alcohols to aldehydes and acids.[176, 177] ADH from horse liver (HLADH) was reported to oxidize several small aliphatic 1,2-diols and amino alcohols to hydroxy aldehydes and amino aldehydes.[178] But transformation of bulky diols (such as aromatic diols) has not been reported. Similar to HLADH, a thermophilic ADH from *Bacillus stearothermophilus* also oxidizes primary alcohols, but with rather unexplored substrate scope.[179, 180]

Some non-canonical ADHs are independent of nicotinamide cofactors. The membrane-bound ADH (mADH, EC 1.1.5.x) using pyrroquinoline quinone cofactor is the key enzyme for terminal oxidation in acetic bacteria (*Acetobacter* or *Gluconobacter* species).[181-183] Acetic bacteria could catalyze the incomplete oxidation of carbohydrates and alcohols to organic acids, which is distinguished from the complete oxidation to carbon dioxide and water by other aerobic microorganisms.[184, 185] However, because of the nature of mADH (membrane-bounded, using pyrroquinoline quinone cofactor), heterogenous expression of functional mADH has not been reported and further application is rather limited. Another non-canonical ADH is FAD dependent AlkJ, which is responsible for aliphatic alcohol oxidation in the well-studied alkane-metabolizing *Pseudomonas putida* GPo1.[186, 187] The alkane degradation pathway involves hydroxylation of alkane to alcohol by AlkBGT, oxidation of alcohol to aldehyde by AlkJ, oxidation of aldehyde to acid by AlkH, and activation of acid to acyl-CoA by AlkK (Scheme 2.8). AlkJ is initially classified as a member of glucose-methanol-choline (GMC) oxidoreductase family according to its sequence.[188] Recently, the detailed biochemical characterization of AlkJ evidenced that it is an FAD-dependent membrane-associated dehydrogenase coupling to the bacterial

respiratory chain.[189] However, only several *n*-alkanol and derivatives were tested as substrates of AlkJ, leaving other potential substrates unexplored. It will be interesting to further explore these ADHs for terminal oxidation of diols.
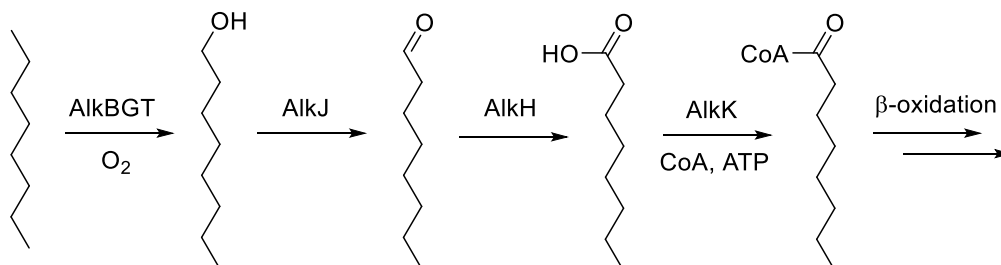
Scheme 2.8. Alkane (*n*-octane) degradation pathway in *Pseudomonas putida* GPo1. AlkJ is the key enzyme in oxidation of terminal alcohol to aldehyde.

2.3.3.2 Alcohol Oxidases

Alcohol oxidases (EC 1.1.3.x) provide a facile tool for alcohol oxidation, because they directly utilize the most economical and greenest oxidant, O_2, and give nontoxic H_2O_2 or H_2O as byproduct.[171-174] These oxidases employ tightly bound redox-active prostetic groups (*e.g.* FAD) instead of diffusible and sensitive nicotinamide cofactor, which makes them suitable for many *in vitro* applications. The majority of alcohol oxidases contain a flavin cofactor (FAD or FMN), thus they are often referred as flavoprotein oxidases.[190, 191] In comparison with reversible oxidation/reduction by most of dehydrogenases, oxidation by oxidases is irreversible, which provides strength in certain biocatalysis applications.

We are interested in oxidation of α-hydroxy acids to α-keto acids, which is catalyzed by FMN-dependent 2-hydroxyacid oxidase family. Two well-known enzymes in this family are lactate oxidase[192] and glycolate oxidase.[193] However, their good substrates are short- and medium-chain 2-hydroxy acids, but not more bulky aromatic acids. On the other hand, a hydroxymandelate oxidase (HMO) was identified in the biosynthesis pathway of vancomycin group of antibiotics.[194, 195] The enantioselectivity of HMO was found to be highly *S*-selective, leaving (*R*)-mandelic acid unreacted. HMO could be a very efficient enzyme in oxidation of (*S*)-mandelic acid and its analogues to the corresponding α-keto acids.

2.3.4 Amino Transferases for Reductive Amination

Amino group is one of most important functional groups in bioactive compounds, due to its distinct electrostatic and hydrogen bonding interactions with other molecules. The formation of amino group was usually achieved via amination of carbonyl group (ketones and aldehydes) by chemical catalysts or enzymes, mainly transaminases (EC 2.6.1.x).[196, 197] In fact, transaminases are the key enzymes for nitrogen metabolism in living organisms, maintaining the synthesis/degradation of amino acids. In biocatalysis, two types of transaminases have been applied for synthesis of chiral amino acids and amines.

2.3.4.1 α-Transaminases

α-Transaminases (α-TAs) catalyze the reversible transferring of amino groups between α-amino acids (amine donor) and α-keto acids (amine acceptor) using pyridoxal 5'-phosphate as a prosthetic group (Scheme 2.9a). L-selective α-TAs are ubiquitously found for the synthesis of proteinogenic amino acids, and D-selective α-TAs were discovered in many bacterial species (*e.g. Bacilli*) to produce D-amino acids for peptidoglycan and secondary metabolite biosynthesis.[198] Many of these α-TAs accept a range of α-keto acids, thus they are valuable for production of various natural and unnatural amino acids, especially D-amino acids.[199, 200]
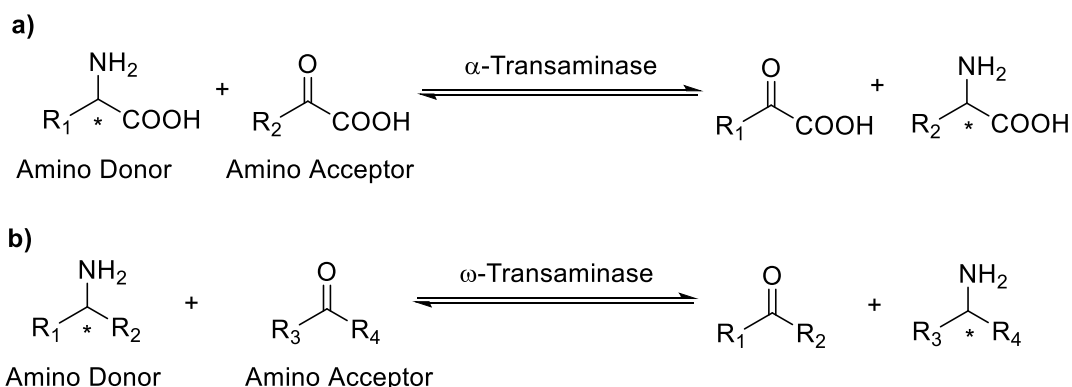
Scheme 2.9. Transferring of amino group catalyzed by **a)** α-transaminase and **b)** ω-transaminase.

2.3.4.2 ω-Transaminases

Chiral amines are indispensable structure components in many chiral pharmaceuticals,[201] but they are inaccessible with native α-TAs, which require acid groups in substrates. To achieve green and efficient production of these chiral amines, ω-transaminases (ω-TAs) were recently discovered and developed as promising enzymes, and plenty of papers were published during the last few years.[202-206] Distinguished from the limited scope of α-TAs, ω-TAs could use amines (without acid group) as donor and ketones/aldehydes (without acid group) as acceptor for transamination (Scheme 2.9b), and thus with great potential for synthetic application. The ω-TA from *Vibrio fluvialis* is the first reported enzyme for asymmetric reductive amination (*S*-selective) with relatively broad substrate scope.[207] Another similar ω-TA from *Chromobacterium violaceum* catalyzes *S*-selective amination of even more diverse substrates, including aliphatic and aromatic keto acids, aldehydes, and ketones.[208] On the other hand, a group of useful *R*-selective ω-TAs were discovered by Prof. Bornscheuer's group via structure-guided *in silico* enzyme mining.[80] Further study of these enzymes provides a versatile toolbox for *R*-amine synthesis, and two representative examples are from *Aspergillus terreus* and *Aspergillus fumigatus*.[209]
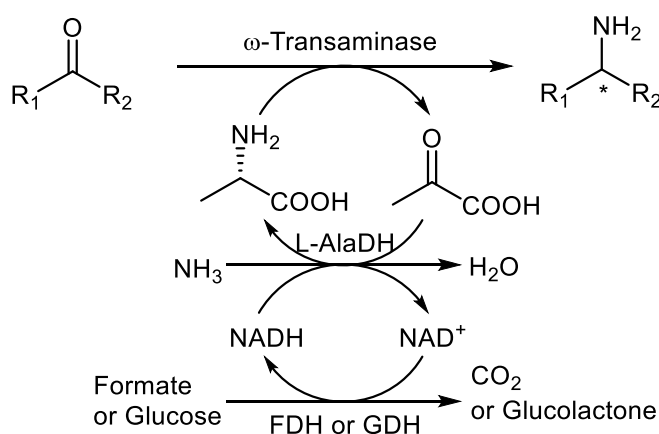
Scheme 2.10. An elegant strategy to overcome equilibrant problem in transamination.[210]

One common problem of using ω-TAs is the equilibrant reaction, which often requires a large excess of amine donor to achieve high yield of amine products.[202-206] Many strategies have been developed to overcome this issue, mainly through removing of the co-product (ketone/aldehyde/keto acid). The most elegant strategy is using L-

alanine dehydrogenase (L-AlaDH) to regenerate L-alanine (amine donor) from pyruvate (co-product) and ammonia (Scheme 2.10).[210] The resulting net reaction is reductive amination of ketones with stoichiometric consumption of ammonia and easily available reducing agents (glucose or formate). This regeneration strategy is generally applicable in other systems, *e.g.* cascade biocatalysis containing ω-TAs.

2.4 Whole-Cell Biocatalysis and its Applications

Enzymes in purified form are suitable for accurate scientific characterization and medical application. For synthesis application, it depends on many factors to choose the forms of biocatalyst. Relatively simple and stable enzymes in the class of hydrolases (*e.g.* lipase) and in the class of transferases (*e.g.* transaminase) are usually applied in isolated or immobilized forms, because those could offer clean reaction system without cell mass, give few byproducts produced by other enzymes in cells, and eliminate the potential diffusion limit of cell membranes. Nevertheless, as for many complex or unstable redox enzymes, it is generally better to apply microbial cells containing the enzymes as biocatalysts.

2.4.1 Advantages of Whole-Cell Biocatalysis

Whole-cell biocatalysis offers several advantages over *in vitro* biocatalysis (Figure 2.11).[28-33]

i) Many oxidoreductases, such as alcohol dehydrogenase, ene-reductase, monooxygenase, consume stoichiometric cofactors, such as NAD(P)H. The regeneration of these cofactors by another enzyme or cell metabolism inside the microbial cell is an efficient and economical way,[211-213] whereas *in vitro* regeneration of the cofactors is less efficient and more expensive. An excellent example is the biocatalytic epoxidation of styrene by SMO: the recombinant whole-cell process[149-152] is more efficient than several other processes with cell-free systems.[146-148]

ii) Whole cells provide a natural environment for enzymes. For example, many membrane-bound enzymes are inactive without the membrane environment of cells, and some complex enzymes involve electrons transfer in several components (*e.g.* P450 monooxygenase) which is easy to achieve within cell as it does naturally, but it is difficult or inefficient to reconstitute *in vitro*. A number of synthetically useful enzymes are membrane bounded or integrated, such as alkane monooxygenase AlkB[214] and xylene monooxygenase XylM.[215]

iii) The cell membrane, though poses some diffusion limitations, could protect fragile enzymes from harsh conditions of the process, such as organic solvents[216, 217] or ionic liquids.[218, 219] These water immiscible solvents are sometimes applied in biocatalytic processes to increase substrate solubility, reduce substrate/product inhibition, and facilitate product recovery.

iv) Because most enzymes are initially produced in recombinant microbial cells through fermentation, enzyme in the microbial cells is the most inexpensive form of biocatalysts without further processing, such as breaking cells by homogenization and purifying enzyme by chromatography.
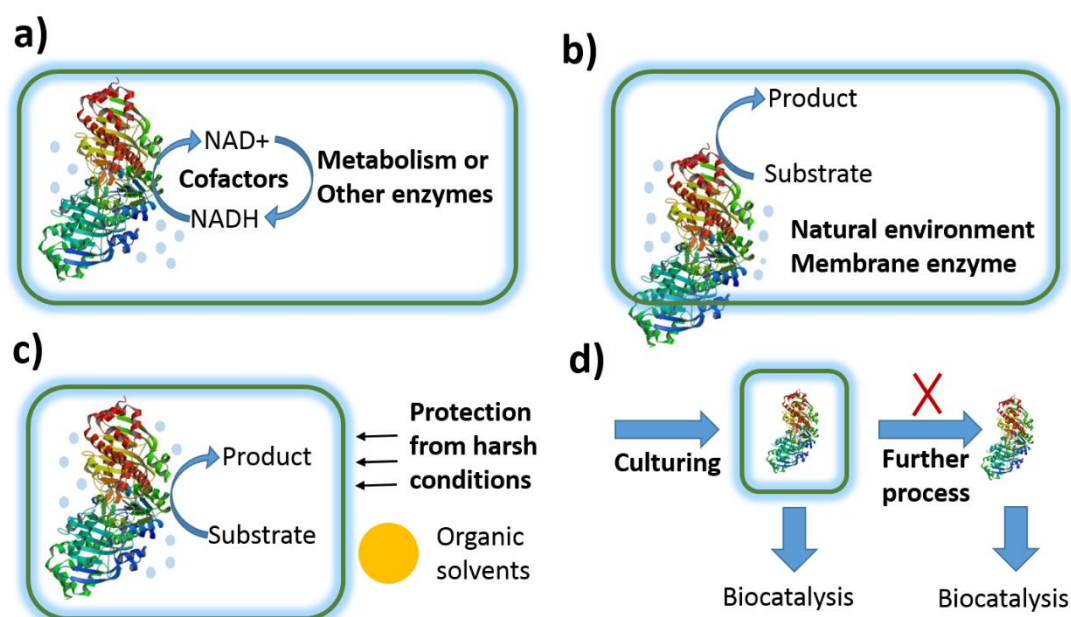
Figure 2.11. Four advantages of whole-cell biocatalysis: **a)** easy cofactor regeneration in cells; **b)** cells provide the natural environment for enzymes; **c)** cell membrane protect enzymes; **d)** cells are cheap without further processing.

Therefore, whole-cell biocatalysis is a common choice of many biocatalysis laboratories in both academia and industry.

2.4.2 Categories of Whole-Cell Biocatalysts

Depending on the status of cells performing reactions, whole-cell biocatalysts can be grouped into growing cells, resting cells, or dead cells.

i) Applying growing cells allows continuous generating enzymes when performing reactions, and this is particularly suitable for less stable enzymes. The use of growing cells has other advantages. For instance, growing cells could adapt for chemical reactions and manage the related stress (*e.g.* from organic solvents and reactive oxygen species). Cells cultured by high density cultivation techniques[220-222] could be directly employed for biotransformations in the same bioreactor without isolating the cell mass by centrifugation or filtration. But growing cells will generate extra cell mass as waste, and sometimes trend to degrade the substrates and products to something else during the reaction.

ii) Resting cells are not active in dividing themselves (increasing cell mass), but still metabolically active (still live). They are usually obtained by limitation of the certain nutrition, such as nitrogen or phosphate. Resting cells could be able to provide higher efficiency than growing cells during the reaction in terms of energy sources, since energy is not used for growth in resting cells theoretically. The maximum NADH regeneration rate of 367 U/g cdw was estimated for resting *E. coli* cells metabolizing glucose based on a flux balance analysis of the metabolic network.[223] A recent investigation of epoxidation by recombinant *E. coli* expressing SMO found that resting cells have higher specific activity (U/g cdw) and product yield on glucose (mol product/mol glucose) than growing cells in a similar setup, however, resting cells are prone to product inhibition/toxicity and enzyme loss.[224]

iii) Another type of whole-cell catalyst is dead cells, which are usually obtained by freeze and thaw or lyophilization. Frozen or lyophilized cells prepared previously could be easily stored and transported to other places, avoiding the trouble to prepare the biocatalysts each time before performing reactions. This feature is especially welcome by organic laboratories without biological settings. Since they are metabolically inactive, additional enzymes should be co-produced for cofactor regeneration. An excellent example was reported by Prof. Xu's group: lyophilized *E.coli* coexpressing a reductase and glucose dehydrogenase was used for asymmetric reduction of ethyl 2-oxo-4-phenylbutyrate at an unprecedented high concentration of 620 g/L.[225] The enzymes used in lyophilized cells must be stable and robust to work independent of cell physiological status.

2.4.3 Limitations of Whole-Cell Biocatalysis

Whole-cell biocatalysis suffers from two common problems: side reactions catalyzed by other enzymes in cells and limited mass transfer over cell membranes/walls.

Microbial cells contain hundreds of enzymes which might transform the substrates or products to other undesired byproducts. The likelihood of side reactions depends on substrates, intermediate, and products. For instance, aldehydes are vulnerable to be reduced to alcohols or oxidized to acids by many dehydrogenases inside cells. Over expression of desired enzymes will increase the formation of targeted products, and knock-down or knock-out of problem-causing native enzymes would reduce the byproduct formation.

Cell membranes and walls often act as possible barriers for the entry of substrates into cells and the exit of products from cells, which might compromise the productivity of whole-cell biocatalysis.[226] Although small hydrophobic compounds could easily diffuse through cytoplasmic membranes (phospholipid bilayers), outer

membrane/cell wall (lipopolysaccharides) is the possible barrier. Many methodologies have been developed to reduce the mass transfer limitation. Cell permeabilization by chemical treatment is a simple technique,[227, 228] but the method is often destructive to cell metabolism and leads to cofactor leakage and enzyme destabilization. Another interesting method is genetic engineering of *E. coli* host to produce less lipopolysaccharide, and thus increase the general permeability of cell walls.[229] More specific but powerful approach is engineering of transporter proteins. Recently, expression of outer membrane protein AlkL in *E. coli* was found to boost the oxyfunctionalization of fatty acid esters and the hydroxylation of limonene.[230, 231] This type of membrane transporters will provide an elegant solution to mass transfer issues of whole-cell biocatalysis.

2.5 Cascade Biocatalysis
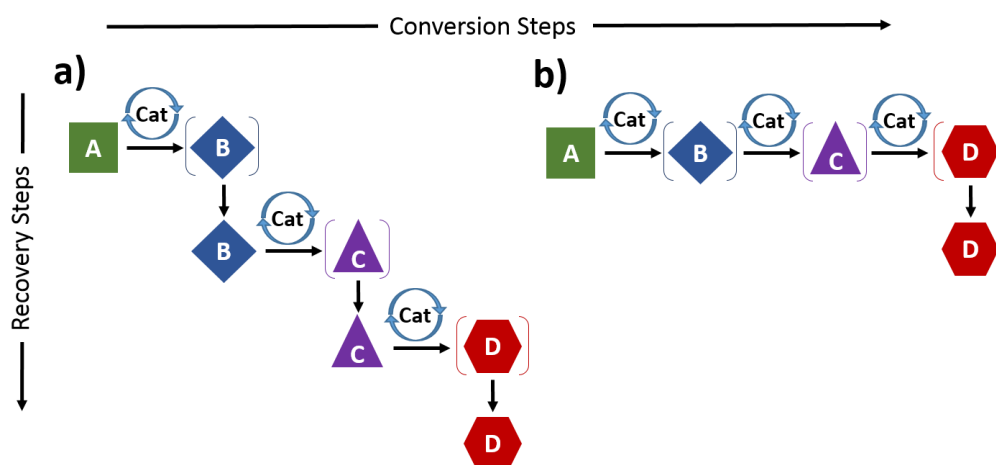
Figure 2.12. Comparison of traditional multi-step synthesis and cascade/tandem catalysis in one pot: **a)** traditional multi-step synthesis requires a recovery step after each conversion step; **b)** cascade/tandem catalysis avoids intermediate recovery steps.

Performing multiple catalyzed reactions in one pot is an important technology for chemical production, since it circumvents the tedious isolation and purification of intermediates which are usually time-consuming, labor-demanding, yield-decreasing, and waste-producing in traditional multi-step synthesis (Figure 2.12).[232-234] Furthermore, cascade/tandem catalysis also offers additional advantages, such as overcoming thermodynamic hurdles to drive the reversible reactions to complete and reducing accumulation of unstable or toxic intermediates. Enzymes, as they catalyze a

variety of reactions in living organisms naturally, are intrinsically compatible catalysts to perform the cascade/tandem catalysis in mild conditions.[34-40] Here, we would like to refer cascade biocatalysis as performing two or more enzyme-catalyzed chemical transformations in the same reaction vessel in a sequential or simultaneous manner. During the past decades, a variety of biocatalytic cascades have been developed, ranging from simple redox independent cascades to complex cascades with multiple interconnected redox reactions. The following review of biocatalytic cascades is subdivided into four sections according to the types of chemical transformation involved: i) cascades without oxidoreduction, ii) cascades with oxidation, iii) cascades with reduction, and iv) cascades with both oxidation and reduction. The multiple enzymatic reactions in cell metabolism are under the scope of metabolic engineering[55-58] and will not be discussed here. And multiple enzymatic reactions only linked by cofactors have been developed as a matured technique (cofactor recycling/regeneration)[211-213] and will not be discussed neither.

2.5.1 Cascades without Oxidoreduction

Biocatalytic non-oxidoreductions are usually facile, robust and efficient transformations without involving redox agents such as $NAD(P)^+/NAD(P)H$. The enzymes are often more stable and active than redox enzymes. Therefore, many non-redox cascades were first developed as early examples in cascade biocatalysis, and some of these processes have been implemented in industry.
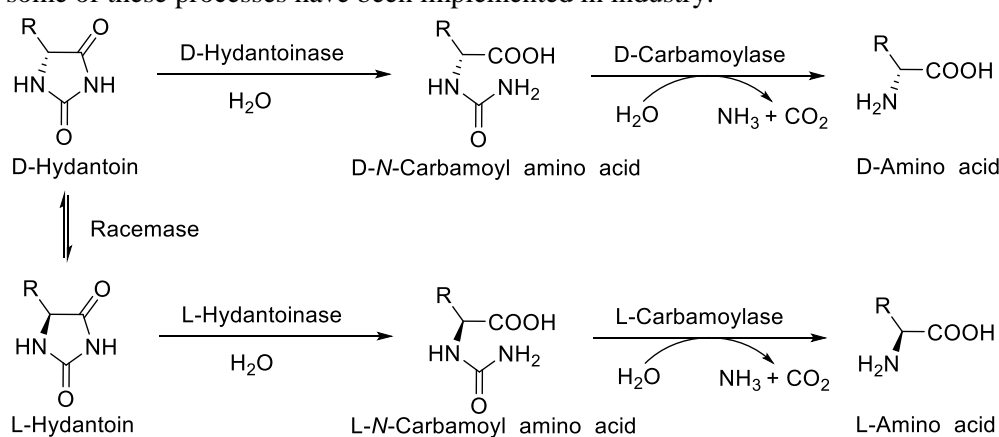
Scheme 2.11. Hydantoinase process for α-amino acids production.

An outstanding example is the racemase-hydantoinase-carbamoylase system (hydantoinase process) for production of optically pure α-amino acids (Scheme 2.11).[235-237] The hydantoin were first selectively hydrolyzed to D- or L-*N*-carbamoyl amino acids by hydantoinases, and then the following hydrolysis by *N*-carbamoylases gives rise to free D- or L-amino acids. Sometimes, hydantoin racemases are involved as a third enzyme for kinetic dynamic resolution. The cascade was firstly discovered from some hydantoin-utilized microorganisms, thus it is a natural cascade similar to the degradation pathway of hydantoin. This method is particularly important to produce many useful D-amino acids, such as D-phenylglycine and D-hydroxy-phenylglycine for the side chains of β-lactam antibiotics.[238] Recently, an efficient *in vivo* cascade biocatalytic system was developed with recombinant *E. coli* cells coexpressing the three enzymes by engineering of the corresponding genes in a polycistronic structure.[239]
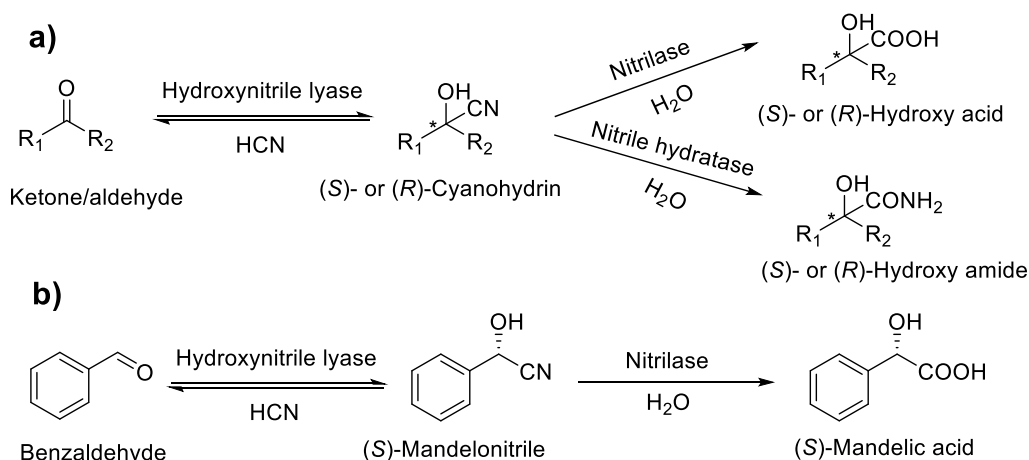
Scheme 2.12. Non-redox bienzymatic cascade to produce for α-hydroxy acids/amides: **a)** a general scheme; b) a representative example of producing (*S*)-mandelic acid.[240]

In addition to natural cascades, enzymes from different sources can be combined to form artificial cascades, a series of chemical transformations without any known natural counterparts (pathways). An interesting example of non-redox artificial cascade is transformation of aldehydes and ketones to α-hydroxyl amides/acids by several nitrile-related enzymes (Scheme 2.12a). Prof. Sheldon's group first reported the bienzymatic cascade to convert cheap benzaldehyde to enantiopure (*S*)-mandelic acid by using cross-linked aggregate of plant-originated *S*-selective hydroxynitrile

lyase (oxynitrilase) and bacterial non-selective nitrilase (Scheme 2.12b).[240] Subsequently, similar bienzymatic cascade comprised of hydroxynitrile lyase and nitrile hydratase was developed to convert aldehydes to (S)-α-hydroxycarboxylic amides.[241] Recently, the *in vivo* version of this bienzymatic cascade was successfully demonstrated with recombinant *E. coli* coexpressing the enzymes,[242] and further development using ionic liquids improved the process efficiency to give synthetically relevant amounts of products.[243] A common problem of this cascade is the involvement of highly toxic HCN in the synthesis.

2.5.2 Cascades with Oxidation

Biocatalytic oxidoreductions are generally more challenging than non-oxidoreductions because of involvement of redox reagents. But oxidations are very important transformations since the major feedstock for organic synthesis are highly reduced hydrocarbons while functional organic chemicals are usually at higher oxidized states. Thus, many biocatalytic cascades involving at least one oxidation step were reported recently.

a)

b)

c)
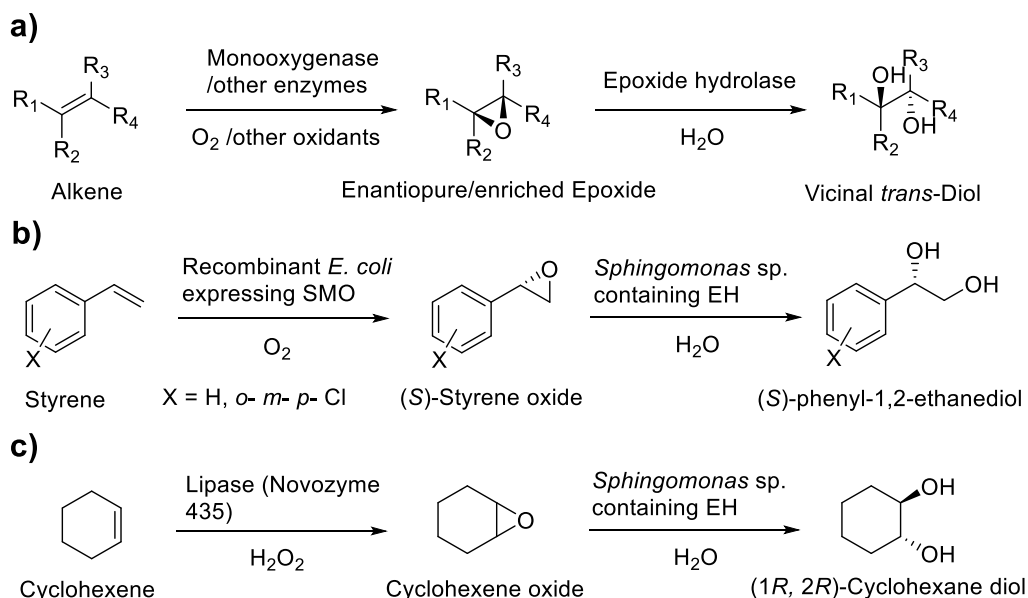
Scheme 2.13. Epoxidation-hydrolysis cascade to convert alkenes to vicinal *trans*-diols: **a)** a general scheme; **b)** a representative example of converting styrene;[247] **c)** a representative example of converting cyclic olefins.[248]

One useful oxidative cascade is epoxidation-hydrolysis to convert C=C double bond to two vicinal alcohol groups by a monooxygenase and an epoxide hydrolase (Scheme 2.13a). The overall transformation is a formal *trans*-dihydroxylation. The cascade is not involved in the major pathways of microbial alkene degradation, but it was discovered in fungal transformation of some terpenes (*e.g.* limonene).[244-246] Previously, our lab discovered that the alkane-degrading bacterium *Sphingomonas* sp. HXN-200 could convert *N*-substituted tetrahydropyridines and pyrrolines to the corresponding *trans*-diols in high enantioselectivity via the epoxidation-hydrolysis cascade.[126] However, these wild type strains containing appropriate monooxygenases and epoxide hydrolases are rare and with very limited potential. As a solution, enzymes from different origins can be purposely combined in one pot to convert cheap alkenes to more useful *trans*-diols. To demonstrate the concept, we combined recombinant *E. coli* cells expressing SMO and cells of *Sphingomonas* sp. HXN-200 containing EH to convert styrene and chlorostyrenes to the corresponding (*S*)-phenyl-1,2-ethanediols in high *ee* (Scheme 2.13b).[247] This is a significant progress in epoxidation-hydrolysis cascade. However, two different strains need to be cultured separately, and impractical high loading of *Sphingomonas* sp. HXN-200 (up to 65 g/L) was used because of the low EH activity in the wild type strain. Furthermore, the substrate scope of the cascade was rather unexplored, considering the broad scope of SMO. Last, only *S*-enantiomers of diols were produced in the study, with *R*-enantiomers inaccessible. Recently, the cascade was applied to convert several cyclic olefins with lipase-mediated epoxidation and hydrolysis by *Sphingomonas* sp. HXN-200.[248] However, the lipase-mediated epoxidation used reactive H_2O_2 as oxidant which was incompatible with EH-catalyzed hydrolysis. The relatively incompatible conditions led to a sequential cascade in a highly diluted solution. Obviously, an efficient and facile system for epoxidation-hydrolysis cascade is yet to be demonstrated.

a)

b)

c)
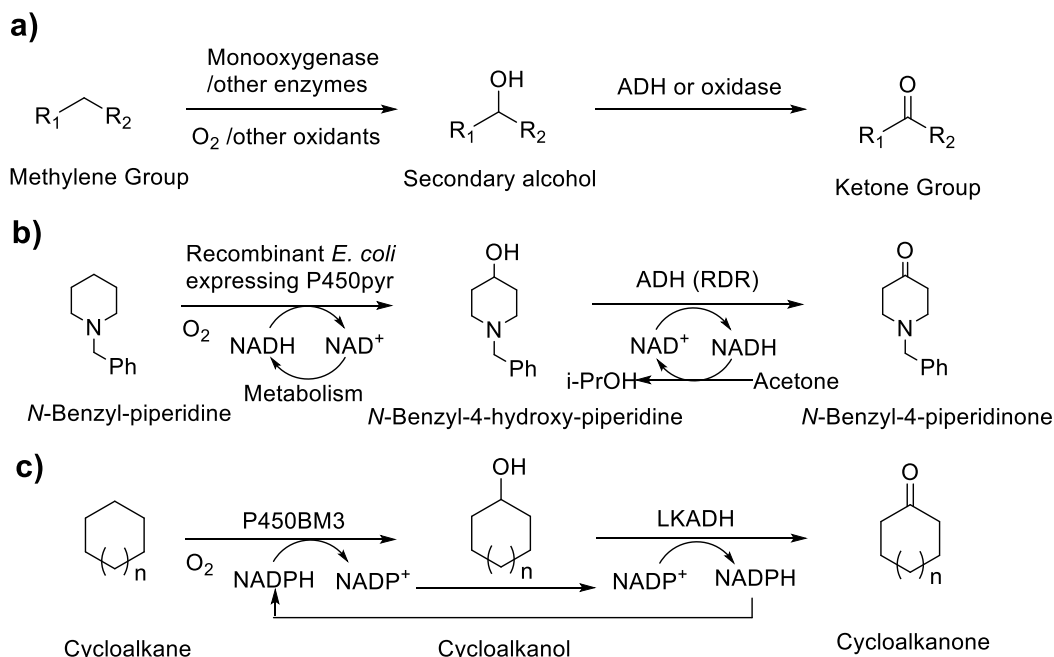
Scheme 2.14. Hydroxylation-oxidation cascade to convert methylene groups to ketone groups: **a)** a general scheme; **b)** a representative example of converting non-activated methylene groups;[251] **c)** a representative example with internal cofactor recycling.[252]

The hydroxylation-oxidation cascade converting the methylene group ($-CH_2-$) to carbonyl group (C=O) is a useful but challenging reaction (Scheme 2.14a), because it involves activation of C-H bonds which is difficult to achieve by chemocatalysis under mild conditions. Naturally, some bacteria use monooxygenases and dehydrogenases for the two steps (hydroxylation and oxidation) in alkane degradation.[249, 250] To produce more synthetic relevant products, the cascade could combine monooxygenases and ADHs from different sources for the two individual reactions, respectively. Previously, our lab developed a system comprised of a monooxygenase-containing microorganism (*in vivo*) and a commercially purified ADH (*in vitro*) to convert benzylic or non-activated methylene groups to ketone groups with excellent regioselectivity (Scheme 2.14b).[251] However, the required cofactors were individually regenerated in the system: NADH for the P450 monooxygenase was regenerated via cell metabolism of glucose, and NAD(P)$^+$ for the ADH was regenerated by adding co-substrate acetone to ADH. Recently, Prof. Gröger's group demonstrated the cascade on cyclohexene and *n*-heptane using P450BM3 monooxygenase and ADH *in vitro* with internal recycling of cofactors (Scheme 2.14c).[252, 253] And the same

system was further demonstrated and optimized in recombinant *E. coli* to improve the efficiency and product concentration.[254]

2.5.3 Cascades with Reduction

a)

b)
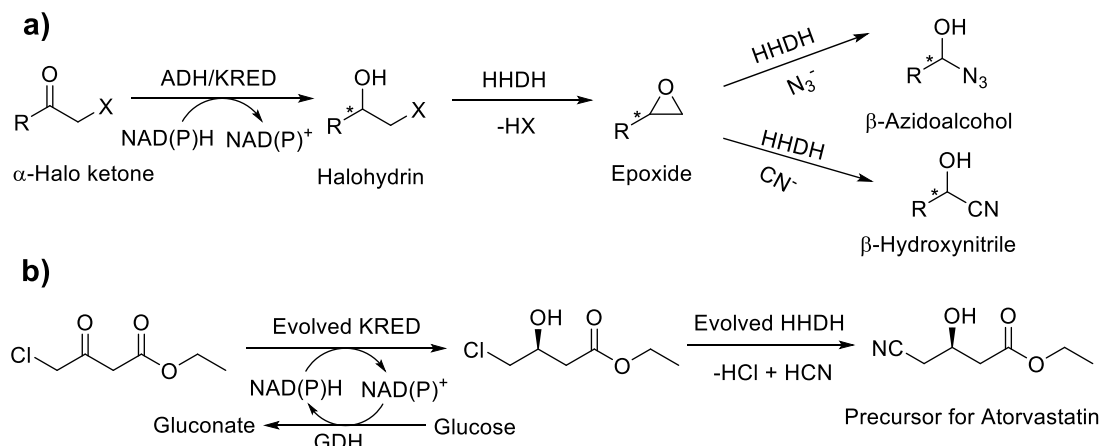
Scheme 2.15. Reduction-dehalogenation cascade to convert α-halo ketones to various non-halogenated compounds: **a)** a general scheme; **b)** a representative example of production of an atorvastatin precursor.[260]

Asymmetric reductions by alcohol dehydrogenases (ADHs), ketone reductases (KERDs), enoate reductases (ERs), and ω-transaminases (ω-TAs) can be combined with other non-redox reactions to form useful reductive cascades. Two types of reductive cascades are reviewed here.

The reduction-dehalogenation cascade converts achiral α-halo ketones to various chiral non-halogenated compounds by ADHs/KERDs and halohydrin dehalogenases (HHDHs) (Scheme 2.15a). Prof. Kroutil's group firstly developed the one-pot process to produce both enantiomers of epoxides from α-chloro ketones by combining a Prelog- or anti-Prelog ADH with a non-selective HHDH.[255] Because HHDH also exhibits catalytic promiscuity for ring opening of epoxides by various nucleophiles (*e.g.* N_3^-, CN^-),[256, 257] they further extended the cascade to produce enantiopure β-azidoalcohols and β-hydroxynitriles.[258] Recently, a *in vivo* version of this cascade was developed to have higher efficiency.[259] To efficiently produce useful pharmaceutical intermediates, Codexis applied protein engineering of KERD and HHDH to achieved a practical two-step synthesis of chiral hydroxynitrile precursor for the blockbuster drug Lipitor® (Atorvastatin, Scheme 2.15b).[260]
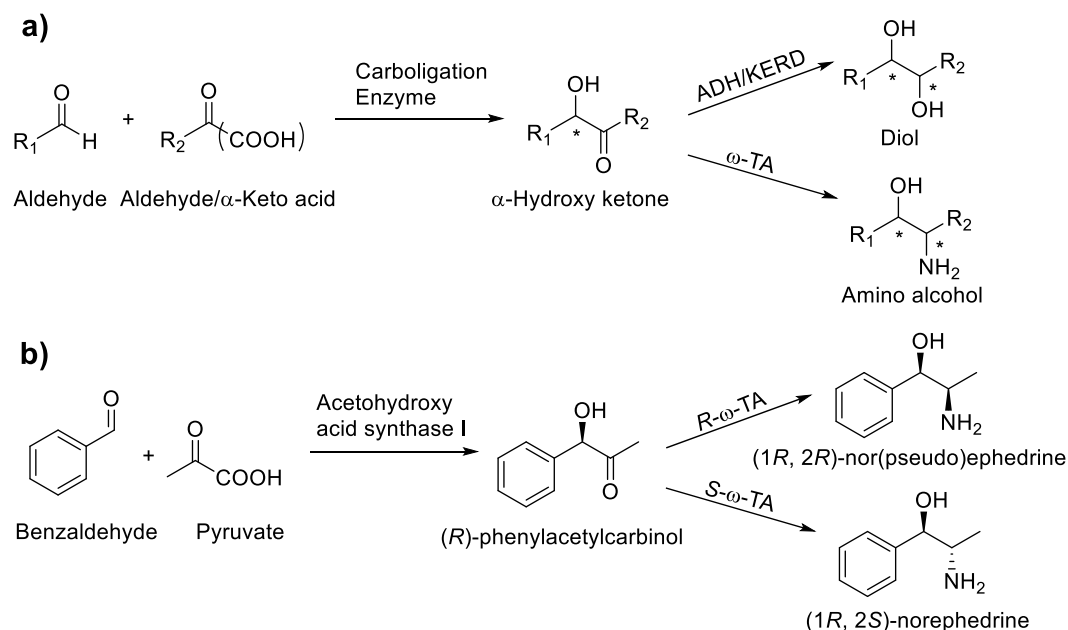
Scheme 2.16. Carboligation-reduction cascade to convert aldehyde and α-keto acid to diol and amino alcohol: **a)** a general scheme; **b)** a representative example of production of nor(pseudo)ephedrine.[266]

Another interesting reductive cascade combines carboligation by decarboxylases or other C-C bond forming enzymes[261, 262] and ketone reduction/amination by ADHs (KERDs)/ω-TAs (Scheme 2.16a). The cascade was first reported in an early study of two-step enzymatic synthesis of all stereoisomers of 1-phenylpropane-1,2-diol starting from benzaldehyde and acetaldehyde using lyase/decarboxylase and ADHs.[263] Prof. Rother's group successfully further developed the two-step biocatalytic cascade to produce (1*R*, 2*R*)-phenylpropane-1,2-diol in high concentration with combination of resting or lyophilized whole cells.[264, 265] In comparison with chiral diols, chiral amino alcohols are more useful and could be achieved with similar cascade by ω-TAs instead of ADHs. The same group recently reported a significant progress to produce very useful alkaloids (1*R*, 2*S*)-norephedrine and (1*R*, 2*R*)-nor(pseudo)ephedrine from benzaldehyde and pyruvate using acetohydroxyacid synthase I and *S*-ω-TA or *R*-ω-TA (Scheme 2.19b).[266] The process was further optimized and other two stereoisomers of nor(pseudo)ephedrine were also produced in a following study.[267]

2.5.4 Cascades with Both Oxidation and Reduction

Because of the divergent reaction conditions of oxidation and reduction, these two types of reaction are generally challenging in chemistry to be performed simultaneously in one reaction vessel. However, enzymes are suitable to perform multiple independent redox reactions due to their high substrate and cofactor specificity, and cellular and subcellular compartment. Recent development of cascades containing both oxidation and reduction is reviewed here.
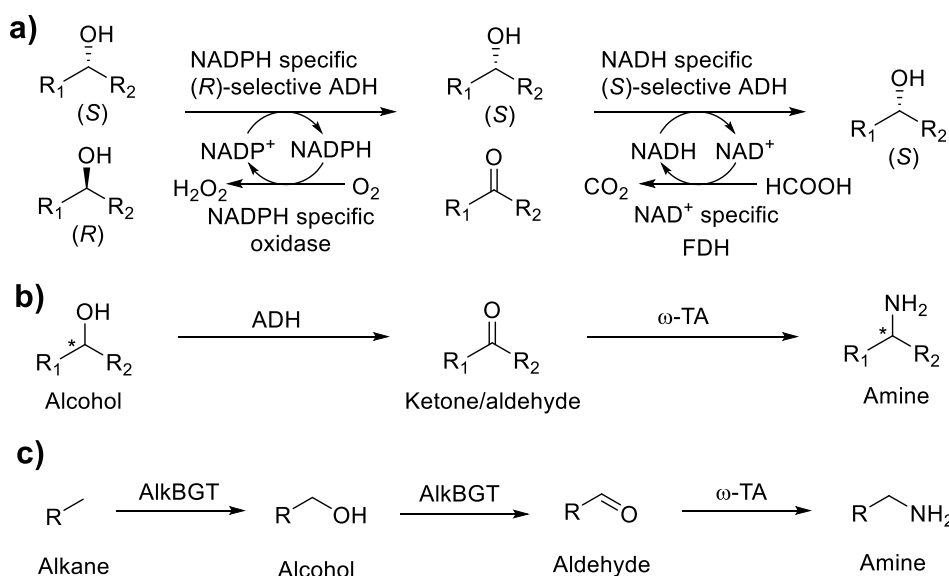
Scheme 2.17. Three redox cascades containing oxidation and reduction: **a)** an elegant design for deracemization of secondary alcohols;[269] **b)** a cascade to convert alcohol group to amine group;[271-273] **c)** a cascade for direct terminal amino-functionalization.[274]

One of the best early examples of redox cascade is deracemization of secondary alcohols to enantiopure form reported by Prof. Kroutil's group in 2008 (Scheme 2.17a). The concept was first proved by using *in vivo R*-selective oxidation with wild type strains, *in vitro S*-selective reduction with ADHs, and cofactor recycling.[268] In the following study, the authors designed an elegant *in vitro* system comprised of selective oxidation with NADPH specific ADH, selective reduction with NADH specific ADH, and recycling of both cofactor $NADP^+$ and NADH (Scheme 2.17a).[269] The same cascade was also employed for deracemization of α-hydroxy acids.[270] In addition, the second step in the cascade could be replaced with ω-TA-catalyzed reductive amination to achieve conversion of hydroxy group to amine group

(Scheme 2.17b). This concept was first proved for amination of aliphatic and aromatic primary alcohols[271, 272] and then demonstrated for enantioselective amination of secondary alcohols.[273] Adding one hydroxylation step to the cascade could achieve formal amino-functionalization of C-H bond (Scheme 2.17c), which was recently achieved using one recombinant whole-cell catalyst coexpressing the necessary enzymes.[274]
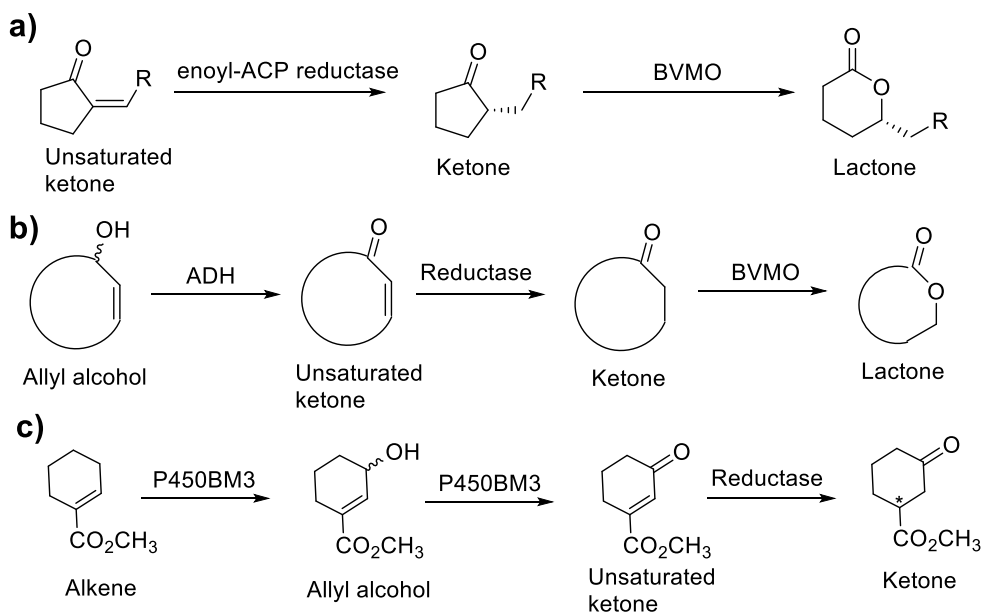
Scheme 2.18. Three redox cascades containing Baeyer-Villiger oxidation and/or C-C double bond reduction: **a)** a cascade to convert unsaturated ketone to lactone;[275] **b)** a cascade to convert allyl alcohol to lactone;[277] **c)** a cascade to convert alkene to ketone.[278]

Other interesting redox cascades contain C=C double bond reduction and/or Baeyer-Villiger oxidation. Recently, our group developed a cascade to convert cyclopentanones (unsaturated ketones) to (*R*)-δ-lactones using a wild type strain containing C=C double bond reaction enzyme and a recombinant *E. coli* strain expressing cyclohexanone monooxygenase (Scheme 2.18a).[275] An enoyl-ACP reductase was later identified from the wild type strain for the reation, and further selective Baeyer-Villiger oxidation polished the *ee* of (*R*)-2-alkylcyclopentanones up to 99%.[276] Prof. Bornscheuer's group added one more ADH-catalyzed oxidation step to the cascade to convert allyl alcohols to chiral lactones (Scheme 2.18b).[277] And prof. Reetz's group utilized P450BM3 for hydroxylation and oxidation of 1-cyclohexene carboxylic acid methyl ester and a reductase for the following C=C double bond

reduction (Scheme 2.18c).[278] Other useful cascades involving Baeyer-Villiger monooxygenase were reported to break unsaturated long-chain fatty acids or cyclohexanol into medium-chain α,ω-dicarboxylic acids, ω-hydroxycarboxylic acids, and ω-aminocarboxylic acids. [279-281]

2.5.5 Challenges in Cascade Biocatalysis

As mentioned above, various types of biocatalytic cascades have been demonstrated in academic research, but many of them are still suffering from limitations, and development of novel and useful cascade biocatalysis is facing several challenges. The following part discusses five issues in cascade biocatalysis, and the opportunities to overcome these problems as well.
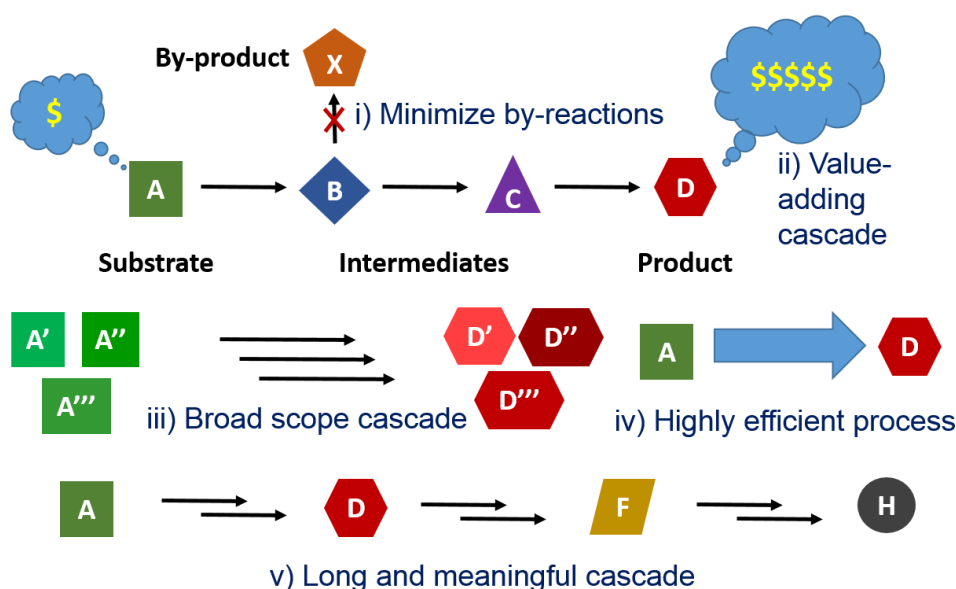
Figure 2.13. Illustration of five challenges in cascade biocatalysis.

i) Multiple-step conversion without significant side reactions. When multiple chemicals are exposed to multiple catalysts in one reaction vessel, the system will be vulnerable to catalytic crosstalk, namely, undesired reactions from unintended precursors catalyzed by enzymes in the cascade. This is not uncommon phenomenon when using enzymes with catalytic promiscuity or broad substrate scope. As a solution, the cascade can be performed sequentially instead of simultaneously. Another possible solution is to use more specific enzymes by discovery or protein engineering.

ii) Synthetically useful cascades. From synthetic point of view, the unit price of initial substrates should be lower than those of final products and intermediates. However, in some of recent reported cascades, substrates seem more expensive and difficult to synthesize than intermediates and final products. In general, value-adding transformations increase molecular complexity, such as extension of carbon chain (carboligation), addition of functional groups (oxy- amino- functionalization), and generation of chiral center (asymmetric reaction). Through multiple value-adding reactions, cascade biocatalysis would possibly directly convert very cheap substrates, *e.g.* alkanes/alkenes, to generate useful and chiral products. Yet, this type of cascades are rare, especially for enantioselective functionalization of hydrocarbons.

iii) Broad scope cascades. Cascades accepting various substrates to produce various products could be particularly useful for synthesis of fine chemicals. Since many fine chemicals are with very limited market individually, a one-for-many approach is always welcome. In general, enzymes have relatively narrow scope compared to chemical catalysts, though some enzymes could accept substrates with similar structure. Thus, cascades with relatively broad scope are seldom reported, because they require multiple enzymes with broad substrate scopes, which are not easy to be satisfied simultaneously.

iv) Efficiency of cascade biocatalysis. Efficiency of biocatalytic process (*e.g.* activity, productivity, product concentration) is often the key performance index for industrial application. As for cascade biocatalysis, it is more challenging because it requires high efficiency of each step of the reactions involved. As far as we know, most of the reported redox cascade biocatalysis produced products in low concentration of 0.1-100 mM (about 0.01-10 g/L). To achieve highly efficient cascade biocatalysis, efficient enzymes for each step should be discovered or engineered, and the catalytic systems and conditions need to be optimized (*e.g.* balance the amount of each enzyme,

and search for the best compromised reaction conditions). Therefore, only a small number of cascade biocatalysis were applied in industry hitherto.
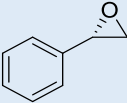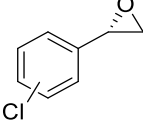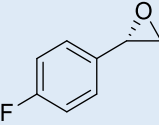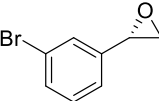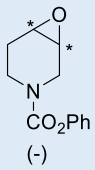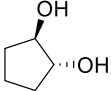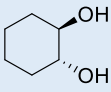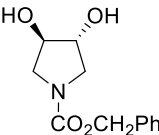
v) Design, construct, and optimize cascade with >3 steps. The majority of cascades developed contain only 2 or 3 steps, but further extending them to multiple >3 steps could face several significant challenges in design, construction, and optimization. For the design of long cascades, the retrosynthetic analysis in organic chemistry could assist design of meaningful cascades.[365] For construction and optimization of cascade, modularization of a serial of transformation into several modular transformations is a potential strategy to ease the construction and to reduce the number of variables in optimization. Such a modular approach has been successfully applied in synthetic biology[366-368] and metabolic engineering,[369-371] but it is still seldom used in cascade biocatalysis.

3 ENANTIOSELECTIVE HYDROLYSIS OF EPOXIDES WITH RECOMBINANT WHOLE CELLS EXPRESSING A NOVEL EPOXIDE HYDROALSE

Figure 3.1. Enantioselective hydrolysis racemic and *meso*-epoxides with recombinant *E. coli* (SpEH) to prepare epoxides and diols in high enantiopurity.

3.1 Introduction
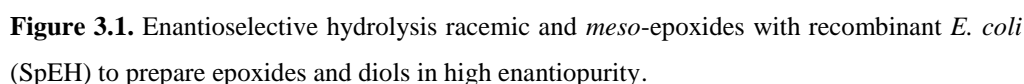
Enantiopure epoxides are versatile chiral building blocks in organic chemistry (refer to Scheme 2.2), and they are mainly produced via hydrolytic kinetic resolutions with Co(salen) catalysts developed by Prof. Jacobsen's group in late 1990s to early 2000s.[282, 283] However, chiral salen ligands are still expensive and cobalt is toxic to environment. On the other hand, nature provides epoxide hydrolase (EH) for the same epoxide hydrolysis reaction, representing a simple and green alternative method for the syntheses of enantiopure epoxides and vicinal diols.[97-104] Although many EHs have been discovered, cloned, and engineered recently, it is still challenging to develop easily available, highly active, and enantioselective EH for efficient production of desired epoxides and vicinal diols in a practical way, *e.g.* giving high product concentration and enantiopurity, with low catalyst loading, and in a short reaction time.

We are interested in developing a novel EH and engineering a powerful biocatalyst for the efficient production of valuable chiral epoxides (*S*)-**1**−**7**, (−)-**8**, and vicinal diols (*R*, *R*)-**12**−**14**. The following Table 3.1 gives a brief summary of these desired products and their potential synthetic applications (final products can be synthesized from them).

Table 3.1. Desired chiral epoxides and diols and their synthetic application.

Structure	Name	Synthetic Applications
	(*S*)-Styrene oxide (*S*)-**1**	Levamisole (nematocide, anticancer),[284, 285] (−)-hyperolactone C (anti-HIV)[286]
	(*S*)-2-, 3-, and 4-Chlorostyrene oxides (*S*)-**2**–**4**	EMI39.3, EMI40.1, and EMI37.1 (antiviral),[287] BMS-536924 (IGF-1R kinase inhibitor)[288]
	(*S*)-4-Fluorostyrene oxide (*S*)-**6**	Inhibitors to monoamine transporters[289]
	(S)-3-Bromostyrene oxide (*S*)-**7**	Agents to treat ophthalmic diseases[290]
	(−)-*N*-Phenoxycarbonyl-3,4-epoxypiperidine (−)-**8**	Single enantiomer of Ifoxetine sulfate (antidepressant),[291] Cisapride hydrate (prokinetic agent)[292]
	(1*R*, 2*R*)-Cyclopentane diol (1*R*, 2*R*)-**12**	Hepatitis C virus protease inhibitors,[293] chiral ligands[294]
	(1*R*, 2*R*)-Cyclohexane diol (1*R*, 2*R*)-**13**	Potential anticancer compounds,[295, 296] chiral auxiliary[297]
	(3*R*, 4*R*)-3,4-dihydroxypyrrolidine (3*R*, 4*R*)-**14**	Sialyl Lewis X mimetics,[298] aza-sugars,[299] antibiotics[300]

51

Several EHs have been reported to produce some of these target compounds. AnEH from fungus *Aspergillus niger* showed a low to moderate enantioselectivity factor (*E*) of 2-16 for the hydrolysis of racemic epoxides to produce (*S*)-**1**−**3**, **6**, and **7**, and an exceptional high *E* of 80 for hydrolysis to give (*S*)-**4**;[108-110, 116] ArEH from bacterium *Agrobacterium radiobacter* exhibited an moderate *E* of 10-16 for the hydrolysis to give (*S*)-**1**−**4**;[119] and RgEH from yeast *Rhodotorula glutinis* provided an *E* of 15 for the hydrolysis of racemic **1** to give (*S*)-**1**.[301] The majority of enantioselectivities of these EHs are not satisfactory. We recently discovered that an alkane-degrading strain *Sphingomonas* sp. HXN-200 showed a relatively high *E* of 29, 12, 41, and 11 for the hydrolysis of racemic epoxide **1**−**4** to produce (*S*)-**1**−**4**, respectively.[127, 128] The enantioselectivity is higher than those of other known EHs for producing (*S*)-**1** and (*S*)-**3**. It is also the only known biocatalyst for the hydrolysis of racemic **8** to afford (−)-**8**.[126] On the other hand, for the enantioselective hydrolysis of *meso*-epoxides **9**–**11**, RgEH gave vicinal diols (1*R*, 2*R*)-**12** in 98% *ee* and (1*R*, 2*R*)-**13** in 90% *ee*, respectively;[302] ArEH afforded (1*R*, 2*R*)-**13** in 99% *ee*;[120] and engineered EHs BD10721, BD9883, and BD9884 produced (1*R*, 2*R*)-**12** in 90% *ee*, (1*R*, 2*R*)-**13** in 96% *ee*, and (3*R*, 4*R*)-**14** in 93% *ee*, respectively.[303] The *Sphingomonas* sp. HXN-200 was also found to catalyze the enantioselective hydrolysis of *meso*-epoxides, giving (1*R*, 2*R*)-**13** in 86% *ee* and (3*R*, 4*R*)-**14** in 95% *ee*.[125, 126] However, the EH from *Sphingomonas* sp. HXN-200 has not been identified and cloned yet.

Besides the issue with selectivity, many reported EH processes were only demonstrated to produce chiral epoxides and diols in low concentration (*e.g.* <30 g/L). There are only a few examples with high product concentration: immobilized AnEH (20 g/L) was used to prepare 500 mM (*S*)-**1** in 99% *ee* and 50% yield,[304] and crude extract of AnEH (256 g/L) was applied to produce 940 mM (*S*)-**4** in 99% *ee* and 47% yield.[110] From a practical point of view, the use of easily available and low-cost whole cell biocatalysts is a much more economical alternative. In one example, 92 g cdw/L

recombinant yeast cells expressing RgEH were applied for the hydrolysis of racemic **1** for 24 h to give 719 mM (*S*)-**1** in 98% *ee* and 41% yield.[305] Obviously, the activity of the cells is too low, and the required cell density is too high for practical application. Moreover, the presence of surfactant (40% Tween 20) seriously hinders downstream processing. For *Sphingomonas* sp. HXN-200, the whole-cell activity for hydrolysis was also too low.[125-128] Furthermore, the growth of *Sphingomonas* sp. HXN-200 on *n*-octane is troublesome and problematic.

Herein, we report our progress in:

i) Identification, cloning, and characterization of a novel SpEH from *Sphingomonas* sp. HXN-200;

ii) Engineering of recombinant *E. coli* cells expressing the SpEH as easily available and highly active catalysts for the enantioselective hydrolysis of racemic and *meso*-epoxides (Scheme 3.1);

iii) Development of an efficient biotransformation process to produce epoxides (*S*)-**1**−**7**, (−)-**8** and vicinal *trans*-diols (*R*, *R*)-**12**−**14** in high *ee* and high concentration at low catalyst loading within a short reaction time.
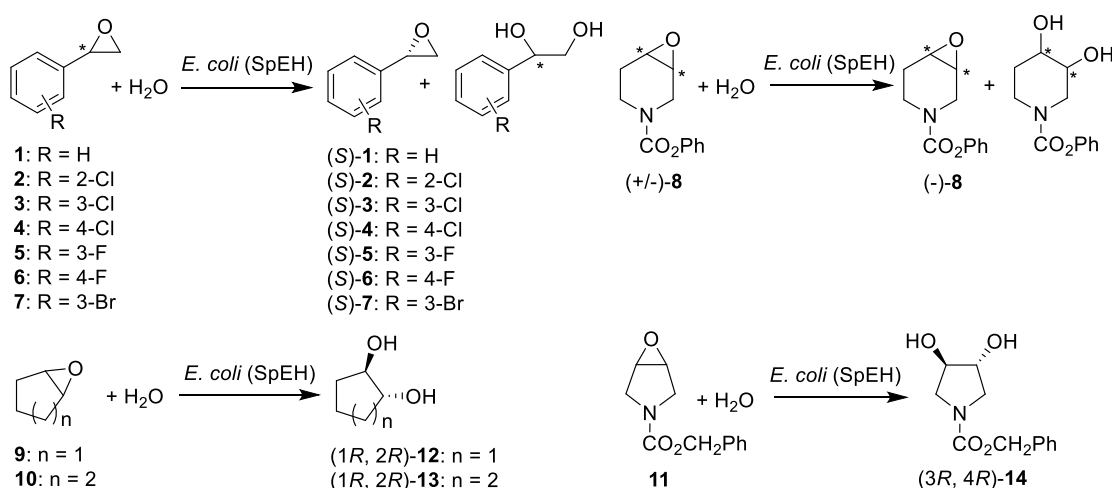
Scheme 3.1. Enantioselective hydrolysis of racemic and *meso*-epoxides with recombinant *E. coli* expressing EH from *Sphingomonas* sp. HXN-200.

3.2 Experimental Section

3.2.1 Chemicals, Strains, and Materials

Most of chemicals and solvents were directly purchased from the following suppliers and used without further purification. Styrene oxide **1** (97%), (*S*)-**1** (98%), (*R*)-**1** (98%), 2-(4-chlorophenyl)oxirane **4** (96%), 2-(4-fluoro-phenyl)oxirane **6** (95%), cyclopentene oxide **9** (98%), cyclohexene oxide **10** (98%), (1*R*, 2*R*)-1,2-cyclopentanediol **12** (98%), (±)-*trans*-1,2-cyclopentanediol **12** (97%), (1*R*, 2*R*)-1,2-cyclo-hexanediol **13** (99%), (1*S*, 2*S*)-1,2-cyclohexane-diol **13** (99%), THF (99.9%), phenyl chloroformate (99%), benzyl chloroformate (99%), 1,2,5,6-tetrahydropyridine (97%), benzyl 3-pyrroline-1-carboxylate (90%), and *m*-CPBA (77%) were from Sigma-Aldrich. 2-(2-chlorophenyl)oxirane **2** (97%) and 2-(3-chlorophenyl)oxirane **3** (97%) were from Amatek Chemical. 3-fluorostyrene (97%) and 3-bromostyrene (97%) were from Alfa Aesar. Dichloromethane (HPLC), ethyl acetate (HPLC), chloroform (HPLC), and isopropanol (HPLC) were from Fisher. Acetonitrile (HPLC) and *n*-hexane (HPLC) were from TEDIA. Silica gel 60 (0.040–0.063 mm) was from Merck. 2-(3-Fluorophenyl)oxirane **5** and 2-(3-Bromophenyl)oxirane **7**, were synthesized according to a published method.[108] *N*-phenoxycarbonyl-3,4-epoxy-piperidine **8** and *N*-benzyloxycarbonyl-3,4-epoxy-pyrrolidine **11** were synthesized according to published procedures.[126] All the synthesized chemicals were purified by flash chromatography on silica gel columns, and confirmed by ^{1}H NMR analysis.

T7 Express Competent *Escherichia coli*, restriction enzymes, and Quick DNA Ligase were from New England Biolabs. DNA oligos, Tris buffer (1 M) and IPTG (>99%) were purchased from first BASE. Phusion DNA polymerase was purchased from Thermo Scientific. Medium components (LB, tryptone, and yeast extract) were from Biomed Diagnostics. Antibiotics kanamycin (>99%) and NaCl (>99%) were bought from Sigma-Aldrich.

3.2.2 Analytical Methods

The concentrations of epoxides **1**–**7** and their corresponding diols were determined using a Shimadzu prominence HPLC system (reverse phase) with UV detection at 210 nm (Column: Agilent Poroshell 120 EC-C18 150×4.6 mm, 2.7 µm). Condition: 40% water: 60% acetonitrile. Flow rate: 0.5 mL min^{-1}. Retention times (min): **1** (6.4) and its diol (3.6); **2** (8.8) and its diol (3.9); **3** (8.3) and its diol (3.9); **4** (8.2) and its diol (3.9); **5** (6.9) and its diol (3.9); **6** (6.6) and its diol (3.6); **7** (9.3) and its diol (4.2).

The *ee* values and concentrations of **1**–**8** and **14** were measured using a Shimadzu prominence HPLC system (normal phase) and UV detection at 210 nm with a Daicel AS-H or OB-H chiral column (250×4.6 mm, 5µm) (Table 3.2).

Table 3.2. Chiral HPLC methods for separate different enantiomers of **1**–**8** and **14**.

Sub.	Column	Conditions	Retention time (min)	
1	AS-H	10% IPA: 90% *n*-Hex, 0.5 mL min^{-1}	10.9 (*R*)	11.9 (*S*)
2	AS-H	0% IPA: 100% *n*-Hex, 0.5 mL min^{-1}	22.5 (*R*)	23.2 (*S*)
3	AS-H	10% IPA: 90% *n*-Hex, 0.5 mL min^{-1}	11.1 (*R*)	11.9 (*S*)
4	AS-H	10% IPA: 90% *n*-Hex, 0.5 mL min^{-1}	11.9 (*R*)	14.0 (*S*)
5	AS-H	10% IPA: 90% *n*-Hex, 0.5 mL min^{-1}	10.2 (*R*)	11.0 (*S*)
6	AS-H	10% IPA: 90% *n*-Hex, 0.5 mL min^{-1}	13.5 (*R*)	14.0 (*S*)
7	AS-H	10% IPA: 90% *n*-Hex, 0.5 mL min^{-1}	11.4 (*R*)	12.0 (*S*)
8	OB-H	40% IPA: 60% *n*-Hex, 0.5 mL min^{-1}	56.2 (+)	64.7 (−)
14	AS-H	5% IPA: 95% *n*-Hex, 1.0 mL min^{-1}	46.3 (3*R*, 4*R*)	56.1 (3*S*, 4*S*)

The concentrations of **9**–**11** were determined by using an Agilent 7890A GC system with an HP-5 column (30 m × 0.32 mm × 0.25 mm). Temperature program for

9 and **10**: 45 °C for 1 min, increase to 140 °C at 15 °C min^{-1} and to 280 °C at 49 °C min^{-1}. Retention times (min): **9** (5.6) and **10** (6.7). Temperature program for **11**: 100 °C for 1 min, increase to 280 °C at 10 °C min^{-1}. Retention time (min): **11** (14.6).

The *ee* values of diols **12** and **13** were determined using an Agilent 7890A GC system with Macherey-Nagel Lipodex-E chiral column (25 m × 0.25 mm) at 100 °C constant. Retention times (min): (1*S*, 2*S*)-**12** (31.3), (1*R*, 2*R*)-**12** (34.1), (1*R*, 2*R*)-**13** (32.7), and (1*S*, 2*S*)-**13** (33.9).

The configurations of **1**, **12** and **13** were assigned by using authentic samples of (*S*)-**1** and (1*R*, 2*R*)-**12** and (1*R*, 2*R*)-**13**. And the configurations of **2**, **3**, **4**, **8**, and **14** were established by comparison with our previous published HPLC data of (*S*)-**2**, (*S*)-**3**, (*S*)-**4**, (−)-**8** and (3*R*, 4*R*)-**14**.[126, 128, 248] The other bioproducts **5**, **6**, and **7** were assigned by comparison with the epoxidation products by a well-known *S* selective styrene monooxygenase.[138-152]

3.2.3 Identification of SpEH and Genetic Engineering of *E. coli* (SpEH)

The strain *Sphingomonas* sp. HXN-200 was grown in E2 medium with *n*-octane vapor as reported previously.[127] The genomic DNA of *Sphingomonas* sp. HXN-200 was extracted by using Blood and Tissue Kit (Qiagen), and then sent to Beijing Genome Institute for *de novo* bacterial genome sequencing with Illumina Highseq2000. The whole genome of *Sphingomonas* sp. HXN-200 was about 4.75 Mb with 4,544 open reading frames (genes) predicted by Glimmer 3.0 software and functional annotated by searching against the KEGG, COG, SwissProt, TrEMBL, NR databases. There are four possible EHs in the genome: Sp154 (SpEH), Sp990, Sp3688, and Sp4354. All of these putative EHs were amplified by PCR using the genome as template with appropriate primers (Table 3.3). PCR procedures were according to the instruction of Phusion DNA polymerase. The PCR product was subjected to double digestion with appropriate restriction enzymes (NdeI/XhoI) and ligated to pRSFduet

plasmid (Novagen). The ligation products were transformed into T7 Express competent *E. coli* cells to give *E. coli* strains for recombinant protein expression and activity test.

Table 3.3. Primers (DNA oligos) used in the study of SpEH.

Name	Sequence
Sp154-NdeI-F	ATCGCATATGATGAACGTCGAACATATCCGCCC
Sp154-XhoI-R	ATCGCTCGAGTCAAAGATCCATCTGTGCAAAGGCC
Sp990-NdeI-F	ATCGCATATGTCTCGCTACACCCATGTCATCT
Sp990-XhoI-R	ATCGCTCGAGTCAGCCTAGCGGCATCTCAAGCACC
Sp3688-NdeI-F	ATCGCATATGACGGCCGGTCCGGTCGCGGCG
Sp3688-XhoI-R	ATCGCTCGAGTCAGGGCATCGCGCGTTCGAGTTCG
Sp4354-NdeI-F	ATCGCATATGCAGGAAGCGATGAGCGCATATC
Sp4354-XhoI-R	ATCGCTCGAGCTAGCCGGCGAAAAAGGCGTCCAGT
Sp154-BspHI-F	ACTGTCATGATGAACGTCGAACATATCCGCCC
Sp154-His-KpnI-R	ATGGTACCTAGTGGTGATGATGGTGATG AAGATCCATCTGTGCAAAGGCC

3.2.4 Cell Growth and Specific Activity of *E. coli* (SpEH)

The *E. coli* (SpEH) was grown in 2 mL LB medium containing kanamycin (50 mg/L) at 37°C for 7−10 h and then inoculated into 50 mL TB (terrific broth) medium containing kanamycin (50 mg/L). When OD_{600} reached 0.6 (about 2 h), IPTG (Isopropyl β-D-1-Thiogalactopyranoside, 0.5 mM) was added to induce the expression of protein. The cells continued to grow for 10−12 h at 25°C 250rpm, and the cell density reached > 4 g cdw/L. Then the cells were harvested by centrifugation (5000 g, 5 min) and resuspended in Tris buffer (50 mM, pH 7.5) for activity testing and asymmetric hydrolysis. Activity test: freshly prepared *E. coli* (SpEH) cells were diluted by Tris buffer (50 mM, pH 7.5) to 2 mL with 0.5 g cdw/L cell density. And then 2 mL of *n*-hexane containing styrene oxide **1** (200 mM) was added to the reaction system in the

flask. The reaction mixture was shaken (250 rpm) in an incubator at 30°C for the 30 min. 300μL aliquots were taken out at 0, 10, 20, and 30 min for HPLC analysis.

3.2.5 His-tagged SpEH Cloning and Purification for Kinetic Data Determination

For engineering of His-tagged SpEH, the similar cloning protocol applied with slightly different primers (Sp154-BspHI-F, Sp154-His-KpnI-R) and different restriction sites (NcoI/KpnI) on pRSFduet. The *E. coli* (His-tagged SpEH) was grown and expressed the His-tagged SpEH in the same condition of *E. coli* (SpEH). Then the cells were broken by cell homogeniser (Stansted fluid power LTD), and then subjected to centrifugation (15000 rpm, 20 min, 4 °C). The His-tagged SpEH was purified from the supernatant (cell free extract) by using Ni-NTA agarose (Qiagen) according to the standard protocol. A SDS-PAGE (12% resolving gel and 4% stacking gel) was applied to check the purity of the protein.

To determine the kinetics data, 1 μg of the purified SpEH was incubated with (*S*)-**1** (0.5–8 mM) or (*R*)-**1** (0.2–4 mM) in 1 mL of Tris buffer (50 mM, pH 7.5). The mixtures were shaken at 30 °C. 300 μL aliquots were taken out at different time points (0, 2, 4 and 8 min) and immediately mixed with 300 μL cold acetonitrile to quench the reaction. The samples were analyzed by HPLC to quantify the diol formation immediately. The initial velocities were calculated and used to give a Lineweaker-Burk plot (1/v *vs.* 1/[S]) to determine K_m, V_{max} and k_{cat}.

3.2.6 General Procedure for Enantioselective Hydrolysis of Racemic Epoxides with Resting Cells of *E. coli* (SpEH)

Freshly prepared *E. coli* (SpEH) cells were diluted by Tris buffer (50 mM, pH 7.5) to a 5 mL system with required cell density (Table 3.4) in a 100 mL flask. And then 5 mL of *n*-hexane containing appropriate amount of epoxides (Table 3.4) was added to the reaction system in the flask. The reaction mixture was shaken (250 rpm) in an incubator (New Brunswick Scientific) at 30°C for the appropriate time. 200 μL

aliquots were taken out at different time points for HPLC analysis. Analytic samples were prepared by centrifugation, and then organic phases (50μL) were separated and diluted with *n*-hexane (containing 2 mM ethyl benzene as internal standard) before HPLC analysis for quantification of *ee* and concentration of the epoxides.

3.2.7 General Procedure for Enantioselective Hydrolysis of *Meso*-epoxides with Resting Cells of *E. coli* (SpEH)

Freshly prepared *E. coli* (SpEH) cells were diluted by Tris buffer (50 mM, pH 7.5) to multiple 1 mL systems with required cell density (Table 3.5) in 50 mL flasks. Next, an appropriate amount of epoxides (Table 3.5) was directly added to the reaction systems in the flasks. The reaction mixture was shaken (250 rpm) in an incubator at 30°C for the appropriate time. One flask was taken out at different time points and totally extracted by adding 2 mL ethyl acetate. Analytic samples were prepared by centrifugation, and then 300μL of organic phases were separated, diluted with ethyl acetate (containing 2 mM *n*-dodecane as internal standard), and dried over Na_2SO_4 before GC quantification of *ee* and concentration of the epoxides.

3.2.8 Procedure for Preparation of (*S*)-1, (*S*)-3, and (*S*)-6 by Enantioselective Hydrolysis of the Corresponding Racemic Epoxides with Resting Cells of *E. coli* (SpEH)

Freshly prepared *E. coli* (SpEH) cells were diluted by Tris buffer (50 mM, pH 7.5) to a 20−110 mL system with required cell density (Table 3.6) in a 250−1000 mL flask. And then 20−100 mL *n*-hexane containing appropriate amount of epoxides (Table 3.6) was added to the reaction system in the flask. The reaction mixture was shaken (250 rpm) in an incubator at 30 °C for the appropriate time. The reaction was monitored by HPLC, and terminated by cooling down on ice once the *ee* value of residual epoxide reached 99%. The reaction system was then immediately extracted three more times by 3×20−100 mL *n*-hexane, and all the organic phases were combined.

After drying over Na_2SO_4, the solvents were removed by evaporation. The crude product was then purified by flash chromatography on a silica gel column with *n*-hexane: ethyl acetate = 50: 1 ($R_f = 0.3$ for all the three products).

3.2.9 Procedure for Preparation of (1*R*, 2*R*)-12, (1*R*, 2*R*)-13, and (3*R*, 4*R*)-14 by Enantioselective Hydrolysis of the Corresponding *Meso*-epoxides with Resting Cells of *E. coli* (SpEH)

Freshly prepared *E. coli* (SpEH) cells were diluted by Tris buffer (50 mM, pH 7.5) to a 5−200 mL system with required cell density (Table 3.7) in a 100−1000 mL flask. And appropriate amount of epoxides (Table 3.7) was added to the reaction system in the flask. The reaction mixture was shaken (250 rpm) in an incubator at 30 °C for the appropriate time. The reaction was monitored by GC, and terminated by cooling down on ice once the conversion of *meso*-epoxides reached 99%. The reaction system was immediately saturated with NaCl and extracted four times by 4×5−200 mL ethyl acetate, and then all the organic phases were combined. After drying over Na_2SO_4, the solvents were removed by evaporation. The crude product of (3*R*, 4*R*)-**14** was then purified by flash chromatography on a silica gel column with ethyl acetate ($R_f = 0.3$). The crude product of (1*R*, 2*R*)-**13** was purified by crystallization in ethyl acetate (first dissolved at 60°C and slowly cooling down to 4°C).

3.3 Results and Discussion

3.3.1 Identification of SpEH, Genetic Engineering of Recombinant *E. coli* Expressing SpEH

Genome information is a valuable source to identify powerful enzymes from microbes.[65, 66] To identify and clone the EH, the whole genome of *Sphingomonas* sp. HXN-200 was sequenced. Bioinformatic analysis suggested four putative EH genes from a total of 4544 possible open reading frames (genes) in the genome. All four putative EHs were successfully cloned and heterologously expressed in *E. coli*. However, only one EH (SpEH) was found to show significant activity for the hydrolysis of racemic styrene oxide **1** to give the corresponding diol.

The gene of SpEH consists of 1146 bp encoding a 381 amino acids polypeptide with a calculated molecular weight of 43.04 kDa (Sequence see Appendix I). A BLASTP search against the NCBI protein database reveals that the most related protein is a putative EH from marine gamma *proteobacterium* HTCC2148, which shares 54% amino acid identity. The low identity suggests that SpEH is unique. Multiple alignments of SpEH and other well-studied EHs (Figure 3.2) showed that SpEH shares the conserve motifs (H-G-X-P and G-X-Sm-X-S/T), the catalytic trial (D-H-D/E), and two conserve Y229 and Y294 with other known EHs, such as AnEH[114] and ArEH.[118] This indicates a similar reaction mechanism of SpEH to these EHs: i) epoxide substrate is stabilized at the catalytic center by forming two hydrogen bonds between epoxide oxygen with two Tyr residues (Y229, Y294); ii) the epoxide carbon is under nucleophilic attack by Asp residue (D171) to form a ester intermediate; iii) the ester intermediate is hydrolyzed by an activated water to give diol product.

```
SpEH    ------------------------------VMNVEHIRPFRVEVPQDALDDLRDRLART 29
MgEH    -MLQTYVEKHDISTRVPHLVSSFTHPMILRDIAMTASIRPFQIAIEDTALEDLHKRISST 59
AnEH    --------------------MSAPFAKFPSSASISPNPFTVSIPDEQLDDLKTLVRLS 38
ArEH    ---------------------------------------------------------
StEH    ---------------------------------------------------------
HsEH    ILTNTWLDDRAERDGLAQLMCELKMHFDFLIESCQVGMVKPEPQIYKFLLDTLKASPSEV 180


SpEH    RWPE---KETVDDWDQGIPLAYARELAIYWRDEYDWR----------RIEARLNTWPNF 75
MgEH    RWPD---SETCKGWDQGMPLEYSRELAQYWVKDYDWR----------RCETMLNNWPNY 105
AnEH    KIAPPTYESLQADGRFGITSEWLTTMREKWLSEFDWR----------PFEARLNSFPQF 87
ArEH    ------------------------------------------MTIRRPEDFKHY 12
StEH    -------------------------------------------------MEKIEHK 7
HsEH    VFLDDIGANLKPARDLGMVTILVQDTDTALKELEKVTGIQLLNTPAPLPTSCNPSDMSHG 240
                                                              .   :


SpEH    LATVD-GLDIHFLHIRSDNPAARPLVLTHGWPGSVLEFLDVIEPLS----------ADYH 124
MgEH    MASID-GQDIHFIHRTSTHANALPLIISHGWPGSVIEFHKIIDALAQPEQYGGDPADAFH 164
AnEH    TTEIE-GLTIHFAALFSEREDAVPIALLHGWPGSFVEFYPILQLFREEYTP---ETLPFH 143
ArEH    EVQLP-DVKIHYVREG----AGPTLLLLHGWPGFWWEWSKVIGPLA----------EHYD 57
StEH    MVAVN-GLNMHLAELG----EGPTILFIHGFPELWYSWRHQMVYLAER---------GYR 53
HsEH    YVTVKPRVRLHFVELG----SGPAVCLCHGFPESWYSWRYQIPALAQA---------GYR 287
             .  :       :*      . .: : **:*    .:  :  :        :


SpEH    LVIPSLPGFGFS-GKPTRPG--WDVEHIAAAWDALMRALGYDR---YFAQGGDWGSAVTS 178
MgEH    VVAPSLPGFGFS-SKPTTTG--TKVEKIGAMWGKLMAELGYDS---YVAQGGDWGSMVTQ 218
AnEH    LVVPSLPGYTFSSGPPLDKD--FGLMDNARVVDQLMKDLGFGSG--YIIQGGDIGSFVGR 199
ArEH    VIVPDLRGFGDSEKPDLNDLSKYSLDKAADDQAALLDALGIEKA--YVVGHDFAAIVLHK 115
StEH    AVAPDLRGYGDTTGAPLNDPSKFSILHLVGDVVALLEAIAPNEEKVFVVAHDWGALIAWH 113
HsEH    VLAMDMKGYGESSAPPEIEE--YCMEVLCKEMVTFLDKLGLSQA--VFIGHDWGGMLVWY 343
             :  .: *: :            :          ::  :.     .   . .


SpEH    AIGMHHAGHCAGIHVNMVVGAPPPE--LMNDLTDEE--KLYLARFGWYQAKDNGYS--TQ 232
MgEH    SMGQTETKHCAGIHINMPIVAPDPE--TMNDLTPLE--QSALEGMAFYNDHDSGYS--KQ 272
AnEH    LLGVGFD-ACKAVHLNLCAMRAPPEGPSIESLSAAE--KEGIARMEKFMTDGLAYA--ME 254
ArEH    FIRKYSDRVIKAAIFDPIQPDFGPV---YFGLGHVH--ESWYSQFHQLDMAVEVVG--SS 168
StEH    LCLFRPDKVKALVNLSVHFSKRNPKMNVVEGLKAIYGEDHYISRFQVPGEIEAEFAPIGA 173
HsEH    MALFYPERVRAVASLNTPFIPANPNMSPLESIKANP-VFDYQLYFQEPGVAEAELEQNLS 402
                           ..       *     .:                *


SpEH    QATRPQTIGY--------------ALTDSP--AGQMAWIAEKFHGWTDCGHQPGGQSVG 275
MgEH    QSTRPQTISY--------------GLADSP--VGQMAWIVEKFYAWTDCEKN----GVK 311
AnEH    HSTRPSTIGH--------------VLSSSP--IALLAWIGEKYLQWVDKPLP------- 290
ArEH    REVCKKYFKH--------------FFDHWS--YRDELLTEEELEVHVDNCMK------- 204
StEH    KSVLKKILTYRDPAPFYFPKGKGLEAIPDAP--VALSSWLSEEELDYYANKFE------ 224
HsEH    RTFKSLFRASDESVLSMHKVCEAGGLFVNSPEEPSLSRMVTEEEIQFYVQQFK------ 455
             :                     :  .        *:


SpEH    GHPEQAVSKDAMLDTISLYWLTASAASSARLYWHSFRQFAAGE----------IDVPTGC 325
MgEH    -HPENVLSKDELLDNVMLYWLNNCAGSSARLYWESFNQPNLAP----------IDMPVGC 360
AnEH    --------SETILEMVSLYWLTESFPRAIHTYRETTPTASAPNGATMLQKELYIHKPFGF 342
ArEH    --------PDNIHGGFNYYRANIRPDAALWTDLDHTMS-------------DLPVTMIW 242
StEH    --------QTGFTGAVNYYRALPINWELTAPWTGAQVKVPTKF---------IVGEFDLV 267
HsEH    --------KSGFRGPLNWYRNMERNWKWACKSLGRKILIP---------------ALMV 491
             :    .   *


SpEH    SLFPNEIMRLSRRWAERRYRNIVYWSEAARGGHFAAWEQPELFAAEVRAAFAQMDL---- 381
MgEH    SIFPCEIFRSSRRWAAKRFSNIVHWNELEKGGHFAAFEQPQIFIKEVSDCFRKLR----- 415
AnEH    SFFPKDLCPVPRSWIATTG-NLVFFRDHAEGGHFAALERPRELKTDLTAFVEQVWQK--- 398
ArEH    GLGDTCVPYAPLIEFVPKYYSNYTMETIEDCGHFLMVEKPEIAIDRIKTAFR-------- 294
StEH    YHIPGAKEYIHNGGFKKDVPLLEEVVVLEGAAHFVSQERPHEISKHIYDFIQKF------ 321
HsEH    TAEKDFVLVPQMSQHMEDWIPHLKRGHIEDCGHWTQMDKPTEVNQILIKWLDSDARNPPV 551
                                 .*:  ::*      :  .
```

Figure 3.2. Sequence alignment of SpEH with several known EHs (by ClustalW2). SpEH, EH from *Sphingomonas* sp. HXN-200 (this study); MgEH, putative EH from marine *gamma proteobacterium* HTCC2148 (EEB77043.1); AnEH, EH from *Aspergillus niger* (Q9UR30); ArEH, EH from *Agrobacterium radiobacter* AD1 (O31243); StEH, EH from *Solanum tuberosum* (Q41415); HsEH, EH from *Homo sapiens* (P34913). Yellow: conserve motifs, H-G-X-P and G-X-Sm-X-S/T; Green: catalytic trial, D-H-D/E; Cyan: two conserve tyrosine residues, Y. "*": the identical residues; ".": similar residues; ":": highly similar residues.

The recombinant *E. coli* (SpEH) grown easily in TB medium, and the expression of SpEH was induced by adding IPTG. As shown in Figure 3.3, a cell density of 4.0−4.5 g cdw/L was achieved at 12−15 h. Cells taken at different time points showed different whole-cell activity toward the hydrolysis of racemic styrene oxide **1**. The highest cell-based specific activity was observed for the cells grown at 11−14 h at the late exponential growing phase. The expressing of SpEH was clearly shown in the SDS-PAGE of the cell-free extracts (CFE) of the *E. coli* cells taken at 14 h (Figure 3.4, Lane 3). The specific activity of the *E. coli* cells reached 1.6 U/mg cdw (cell dry weight) which is 172 times higher than that of the cells of the wild-type strain *Sphingomonas* sp. HXN-200 (9.3U/g cdw).[127] These results demonstrated clearly that *E. coli* (SpEH) cells are highly active and easily available biocatalyst for epoxide hydrolysis. The use of the *E. coli* cells as catalyst is of economic advantage over the use of CFE or purified enzyme. In addition to the higher specific activity, recombinant *E. coli* cells gave also cleaner reaction than the wild-type cells which contain the EH at low level and also other enzymes for side reactions.
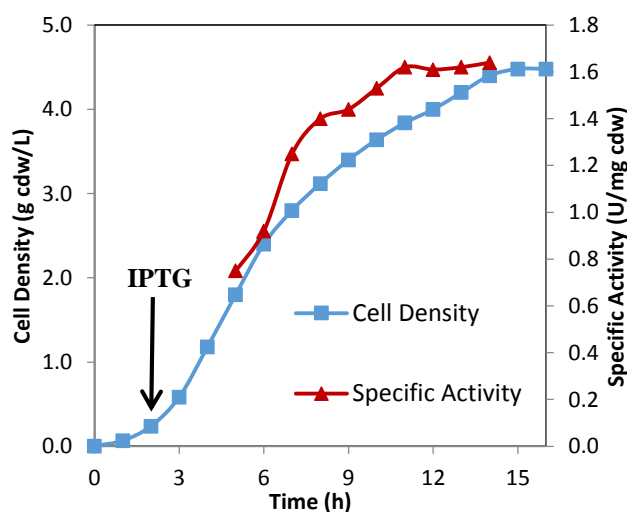
Figure 3.3. Cell growth and cell-based specific activity for the hydrolysis of styrene oxide of *E. coli* (SpEH). Initially, cells were grown at 37 ºC, induced at 2 h by IPTG (0.5 mM), and then grown at 25 ºC.
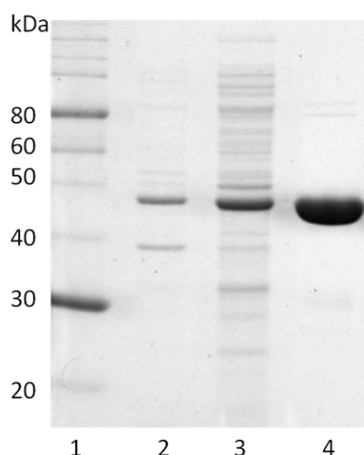
Figure 3.4. SDS-PAGE of SpEH in different forms. Lane 1: protein marker; Lane 2: cell debris of *E. coli* (SpEH); Lane 3: cell free extract of *E. coli* (SpEH); Lane 4: purified His-tagged SpEH.

3.3.2 Kinetic Characterization of Purified SpEH

An *E. coli* strain expressing SpEH with His-tagged at the C-terminal was genetically engineered to facilitate the purification of SpEH. Cells were grown and homogenized, and the CFE was subjected to affinity chromatography with a Ni-NTA column. His-tagged SpEH was purified to apparent homogeneity as indicated in SDS-PAGE (Figure 3.4, Lane 4), with the molecular weight of 46 kDa. This value is very close to the calculated one of 43.9 kDa. The specific activity for the hydrolysis of styrene oxide **1** was determined to be 16 U/mg protein for His-tagged SpEH. A set of hydrolysis reactions were performed with SpEH (1μg/mL) at various concentrations (0.2−8 mM) of (*S*)-**1** and (*R*)-**1**, respectively, to determine the kinetic data. The initial velocities at different substrate concentrations were used for a Lineweaker−Burk plot (Figure 3.5). The kinetic data were obtained from the plot (Table 3.4). The enantioselectivity factor *E* was calculated from $(k^R_{cat}/K^R_m)/(k^S_{cat}/K^S_m)$ as 16 for the hydrolysis of racemic styrene oxide **1**. This value is slightly lower than the *E* value of 21−23 established previously by the kinetic resolution of **1** with resting cells of *Sphingomonas* sp. HXN-200 in the same single aqueous phase system.[127]

Table 3.4. Kinetic data of hydrolysis of (*S*)-**1** and (*R*)-**1** with SpEH.

Substrate	K_m (mM)	V_{max} (µmol min^{-1} mg^{-1})	k_{cat} (s^{-1})	k_{cat}/K_m (mM^{-1} s^{-1})
(*S*)-**1**	1.24	10.3	7.4	6.0
(*R*)-**1**	0.15	19.8	14.2	97.3
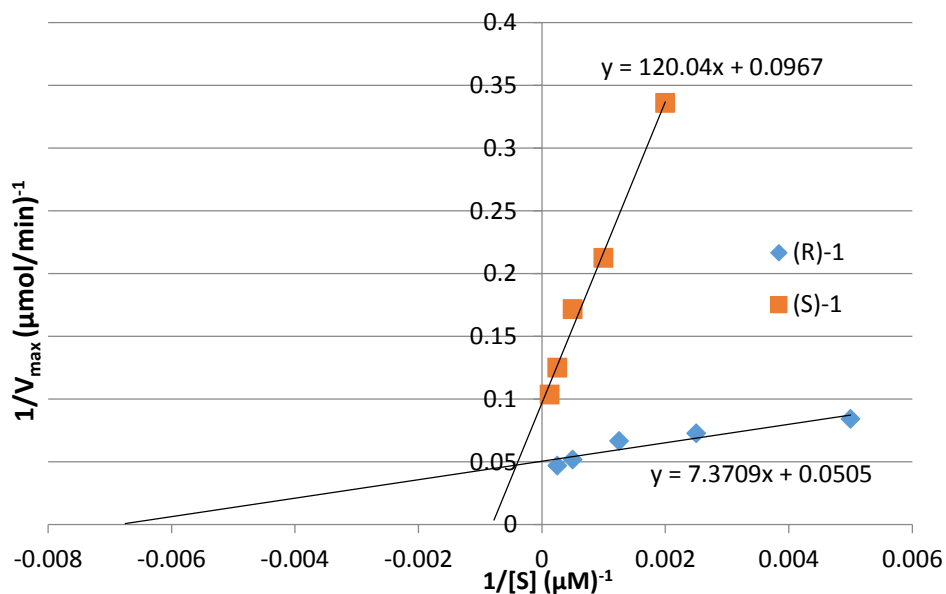
Figure 3.5. Lineweaver-Burk Plot of SpEH for (*R*)-**1** and (*S*)-**1**.

3.3.3 Enantioselective Hydrolysis of Racemic Epoxides with Resting Cells of *E. coli* (SpEH)

Resting cells of *E. coli* (SpEH) were explored for the enantioselective hydrolysis of racemic epoxides **1−8** in a two-phase system consisting of *n*-hexane/aqueous buffer (1:1). In such a system, *n*-hexane acts as a reservoir of the substrate, which reduces the nonenzymatic hydrolysis as well as the toxic effect of the epoxide on cells; the maintaining of diol products in aqueous phase allows for easy separation of epoxides and diols.[306] Substrate concentration of 200−100 mM and cell density of 0.5−1.0 g cdw/L were used (Table 3.5). (*S*)-**1** was produced in 99.1% *ee* and 41.6% yield after 2.5 h reaction, with a specific activity of 1.4 U/mg cdw. The enantioselectivity factor *E* reached 30, similar to that obtained with the cells of the wild-type stain *Sphingomonas* sp. HXN-200 in the same two-liquid phase system.[127]

Furthermore, hydrolysis of epoxide **3**, **5−7** gave (*S*)-**3**, (*S*)-**5−7** in 98.0−99.4% *ee* and 42.3−46.5% yield within 1.5−5.5 h. The *E* values of 36, 35, 28, and 57 represent the highest enantioselectivities among all the known EHs for the preparation of (*S*)-**3**,[109, 307] (*S*)-**5**, (*S*)-**6**,[108, 109] and (*S*)-**7**,[109] respectively. The specific activities of 2.9−0.88 U/mg cdw of the *E. coli* cells were also very high. Compared to the epoxides with a substitution at the *para* or *ortho* position (**2**, **4**, **6**), the epoxides with a substitution at the *meta* position (**3**, **5**, **7**) were hydrolyzed faster (higher specific activity) and more selectively (higher *E*). This preference is significantly different from other well-known EHs (such as AnEH),[108, 109] indicating the unique substrate specificity and special synthetic application of SpEH.

Table 3.5. Enantioselective hydrolysis of racemic epoxides **1**–**8** with *E. coli* (SpEH)[a]

1: R = H **2**: R = 2-Cl **3**: R = 3-Cl **4**: R = 4-Cl
5: R = 3-F **6**: R = 4-F **7**: R = 3-Br
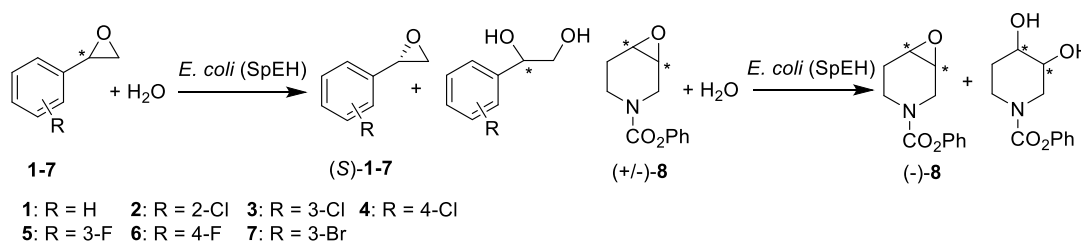
Sub.	Conc. (mM)[b]	Cell density (g cdw/L)[c]	Time (min)	Activity (U/mg cdw)[d]	Prod.	*ee* (%)[e]	Yield (%)[e]	*E*[f]
1	200	0.5	150	1.4	(*S*)-**1**	99.1	41.6	30
2	200	1.0	420	0.28	(*S*)-**2**	99.3	19.9	7
3	200	0.5	330	2.2	(*S*)-**3**	98.0	44.3	36
4	200	0.5	480	0.92	(*S*)-**4**	98.1	35.1	14
5	200	0.5	90	2.5	(*S*)-**5**	99.4	42.3	35
6	200	0.5	280	0.88	(*S*)-**6**	98.3	42.3	28
7	150	0.5	180	2.9	(*S*)-**7**	98.0	46.5	57
8	100	1.0	25	4.3	(−)-**8**	99.5	37.6	22

[a]The reaction was performed in a two-phase system consisting of Tris–HCl buffer (50 mM, pH 7.5) and *n*-hexane (1:1). [b]Concentration was based on the volume of organic phase. [b]Cell density was based on the volume of aqueous phase. [d]Specific activity was determined at 30 min. [e]*ee* value and yield were determined by chiral HPLC analysis (chromatograms see Appendix I). [f]*E* value was calculated by $E = \ln[(1\text{-}c)(1\text{-}ee_s)]/\ln[(1\text{-}c)(1+ee_s)]$.
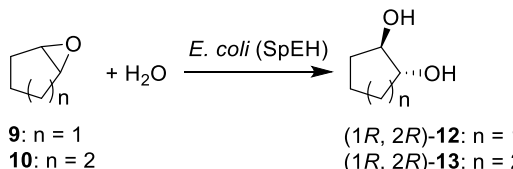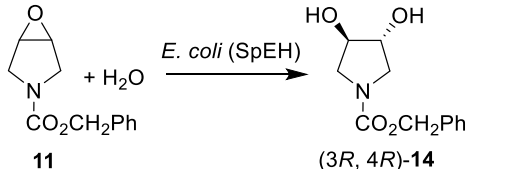
In addition, *E. coli* (SpEH) cells showed an *E* value of 22 for the hydrolysis of 100 mM *N*-phenoxycarbonyl epoxypiperidine **8** to give (−)-**8** in 99.5% *ee* and 37.6% yield. The specific activity reached 4.3 U/g cdw, and the resolution was completed within only 25 min.

In the view of even more practical applications, the enantioselectivity of SpEH could be further improved. Currently, we are working on elucidation of the 3D structure of SpEH and directed evolution of this EH to enhance its enantioselectivity toward the hydrolysis of racemic epoxides **1−8**.

3.3.4 Enantioselective Hydrolysis of *meso*-Epoxides with Resting Cells of *E. coli* (SpEH)

Biotransformation of *meso*-epoxides **9−11** at 100 mM was carried out with resting cells of *E. coli* (SpEH) at a cell density of 1.0 g cdw/L. Aqueous buffer was used as a single phase for the reaction, since the nonenzymatic hydrolysis rates were low for these cyclic epoxides. As shown in Table 3.6, the corresponding (*R*, *R*)-vicinal *trans*-diols **12−14** were produced in 86−93% *ee* and 90−99% yield, respectively. Although the *ee* of (1*R*, 2*R*)-**12** is lower than that obtained with RgEH, the specific activity of 0.34 U/mg cdw is much higher than that of the *R. glutinis* cells.[302] The *ee* of (1*R*, 2*R*)-**13** is also lower than that obtained with ArEH;[120] however, a simple crystallization in ethyl acetate improved the *ee* to 99%. The high specific activity of 0.81 U/mg cdw makes the application of the *E. coli* (SpEH) cells for the preparation of (1*R*, 2*R*)-**13** practical. The *E. coli* (SpEH) cells showed also very high activity (2.3 U/mg cdw) for the hydrolysis of *meso*-epoxide **11** to (3*R*, 4*R*)-**14**, allowing for the completion of the reaction within 1 h. The enantioselectivity for this substrate is the best among known examples.[303]

Table 3.6. Enantioselective hydrolysis of *meso*-epoxides **9–11** with *E. coli* (SpEH)[a]

9: n = 1
10: n = 2

(1*R*, 2*R*)-**12**: n = 1
(1*R*, 2*R*)-**13**: n = 2

11

(3*R*, 4*R*)-**14**

Sub.	Conc. (mM)	Cell density (g cdw/L)	Time (min)	Activity (U/mg cdw)[b]	Prod.	*ee* (%)[c]	Yield (%)[d]	*E*[e]
9	100	1.0	360	0.34	(1*R*, 2*R*)-**12**	88	99	16
10	100	1.0	120	0.81	(1*R*, 2*R*)-**13**	86	99	13
11	100	1.0	60	2.3	(3*R*, 4*R*)-**14**	93	90	28

[a]The reaction was performed in Tris–HCl buffer (50 mM, pH 7.5). [b]Specific activity was determined at 30 min. [c]*ee* value was determined by chiral GC or HPLC analysis (chromatograms see Appendix I). [d]Yield was determined by GC analysis. [e]*E* value was calculated by $E = (1+ee_p)/(1-ee_p)$.

3.3.5 Synthesis of (*S*)-Styrene Oxide in High Concentration with Resting Cells of *E. coli* (SpEH)

The easily available and highly active *E. coli* (SpEH) cells were examined for the hydrolysis at even higher substrate concentration. For demonstration, styrene oxide **1** was chosen as a model substrate. 1 M (120 g/L$_{org}$) racemic **1** was hydrolyzed in a simple two-phase system consisting of *n*-hexane: aqueous buffer (1:1) at a density of *E. coli* (SpEH) cells of 5.0 g cdw/L$_{aq}$. As shown in the time course of the biotransformation (Figure 3.6), the decrease of (*R*)-**1** is linear during the first 40 min, and the reaction finished within 1 h to give (*S*)-**1** >99% *ee* and 43% yield. The *E* value at this high substrate concentration was 39, which is the highest among all EHs in the form of free enzyme, cell extracts, or whole cells.[116, 119, 127, 305, 308, 309] The product concentration reached 430 mM in organic phase (51 g/L$_{org}$), and the overall space-time-yield amounted to 26 g/L/h. The cell-based specific productivity reached 10.3 g/h/g cdw. This value is 542 times higher than that (0.019 g/h/g dry weight of cell-free extracts) with *Sphingomonas* sp. HXN-200.[127] It is also 264 times higher than that

(0.039 g/h/g cdw) achieved in recombinant RgEH-catalyzed kinetic resolution of 1.8 M **1** at a cell density of 92 g cdw/L for 24 h.[305] Obviously, *E. coli* (SpEH) cells are highly productive catalysts for the resolution of styrene oxide **1** to prepare (*S*)-**1**.
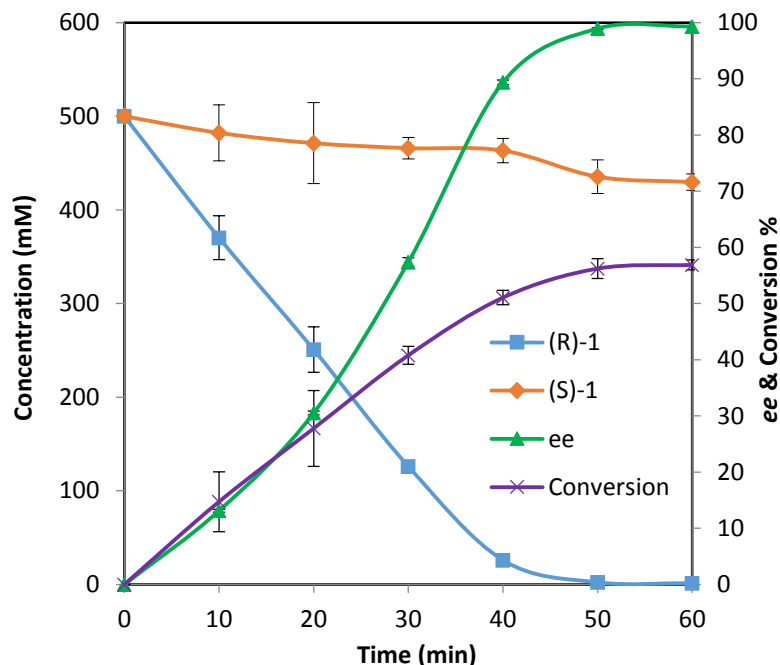
Figure 3.6. Time course of the enantioselective hydrolysis of 1 M racemic styrene oxide **1** with resting cells of *E. coli* (SpEH) (5 g cdw/L) in a two-phase system consisting of Tris–HCl buffer (50 mM, pH 7.5) and *n*-hexane (1:1). The error bar represents standard deviation of three independent experiments.

3.3.6 Synthesis of (1*R*, 2*R*)-Cyclohexane 1,2-Diol in High Concentration with Resting Cells of *E. coli* (SpEH)

There is no report on EH-catalyzed enantioselective hydrolysis of *meso* epoxides in high concentration (*e.g.* > 30 g/L). The *E. coli* (SpEH) cells were thus examined for the hydrolysis of cyclohexene oxide **10**, as a mode *meso*-epoxide, in high concentration. The reaction was carried out in aqueous buffer. Because of the limited solubility of **10**, a second phase was formed initially at high substrate concentration, and it was emulsified into aqueous buffer during the course of biotransformation. Various substrate concentrations and cell densities were tested, while their ratio was fixed at 100 mM: 1 g cdw/L. As shown in Figure 3.7, the higher substrate concentration,

the lower the conversion. While 200 mM and 400 mM **10** were fully converted to (1*R*, 2*R*)-diol **13** in 86% *ee* in 2 and 3 h, respectively, 600 mM, 800 mM, and 1 M substrate were transformed to (1*R*, 2*R*)-**13** in only 70%, 45%, and 17%, respectively, after 3 h reactions. Obviously, substrate at these concentrations can become toxic to the cells and inhibit the catalytic activity. To achieve high conversion at higher substrate concentration, higher cell density was applied. For instance, at the cell density of 10 g cdw/L, 500 mM **10** was transformed to diol **13** in >99% yield (58 g/L) in 1 h. To our knowledge, this is the first example of EH-catalyzed enantioselective hydrolysis of *meso*-epoxide to give high product concentration (>30 g/L).
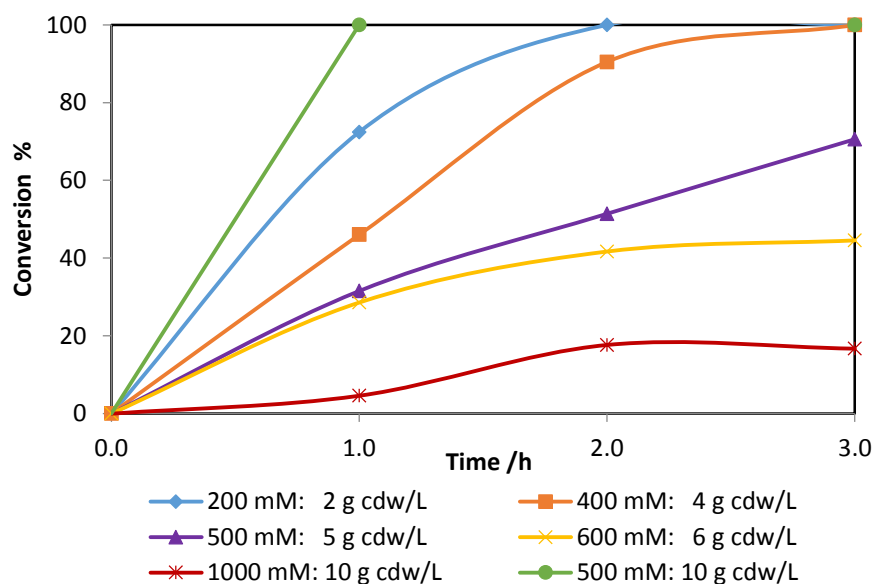
Figure 3.7. Time course of enantioselective hydrolysis of cyclohexene oxide **10** with resting cells of *E. coli* (SpEH) in Tris–HCl buffer (50 mM, pH 7.5) with various substrate concentrations (mM): cell densities (g cdw/L).

3.3.7 Preparation of (*S*)-Epoxides with Resting Cells of *E. coli* (SpEH)

Enantioselective hydrolysis of styrene oxide **1** was performed on a 10-g scale. Biotransformation was carried out in 200 mL mixture of Tris−HCl buffer and *n*-hexane (1:1) containing 1 M (120 g/L$_{org}$) styrene oxide **1** in the organic phase and 5.0 g cdw/L$_{aq}$ of *E. coli* (SpEH) cells. Additional ten milliliters of cell suspension (5 g cdw/L) was added at 1 h, and the reaction was stopped at 70 min. (*S*)-**1** remained in 42% with >99%

ee. The space-time yield reached 18 g/L/h, which is higher than those of known bioprocesses for the preparation of (*S*)-**1**, including the asymmetric epoxidation of styrene.[152] Workup and flash chromatography gave 4.338 g of enantiopure (*S*)-**1** in 36.4% isolated yield (Table 3.7). Gram scale resolution of **3** (200 mM, 30 g/L$_{org}$) and **6** (500 mM, 69 g/L$_{org}$) was also achieved with the resting cells of *E. coli* (SpEH) under non-optimized conditions within 80−90 min. Enantiopure epoxides (*S*)-**3** and (*S*)-**6** were obtained in 37.9% and 31.3% isolated yields, respectively (Table 3.7). In addition to the high product concentrations, the product/cells ratios (7.9−11.7 g/g cdw) as well as cell-based specific productivities (5.7−8.8 g/h/g cdw) of these three preparative biotransformations are also high. These results suggested that *E. coli* (SpEH) is a powerful catalyst for the practical preparation of these useful and valuable (*S*)-epoxides. When *E. coli* (SpEH) was compared with the industrial standard, Jacobsen's Co(salen) catalyst, for the preparation of (S)-styrene oxide **1**,[283] the product/catalyst ratio is similar; but *E. coli* (SpEH) showed higher catalyst-based specific productivity (6.8 g product/h/g cells) than Co(salen) catalyst (0.2 g product/h/g cat); moreover, *E. coli* (SpEH) cells are greener and cheaper than Co(salen) catalyst.

Table 3.7. Preparation of (*S*)-**1**, (*S*)-**3**, and (*S*)-**6** with resting cells of *E. coli* (SpEH).

Sub.	Scale (mL)[a]	Sub. conc. (mM)[b]	Cell density (g cdw /L)[c]	Time (min)	Prod.	Prod. conc. (g/L)[d]	*ee* (%)[e]	Isolated yield (g)	(%)	Prod. / cells (g/g cdw)	Produc-tivity (g/h/g cdw)
1	210	1000	5.0	70	(*S*)-**1**	50.4	>99	4.338	36.4	7.9	6.8
3	80	200	1.0	80	(*S*)-**3**	12.7	>99	0.468	37.9	11.7	8.8
6	40	500	2.5	90	(*S*)-**6**	26.1	>99	0.432	31.3	8.6	5.7

[a]The reaction was performed in a two-phase system consisting of Tris–HCl buffer (50 mM, pH 7.5) and *n*-hexane (1:1), and the scale was referred to the total volume. [b]Concentration was based on the volume of the organic phase. [c]Cell density was based on the volume of the aqueous phase. [d]Product concentration was determined by chiral HPLC analysis and based on the volume of the organic phase. [e]*ee* was determined by chiral HPLC analysis.

3.3.8 Preparation of (*R*, *R*)-Vicinal Diols with Resting Cells of *E. coli* (SpEH)

Practical syntheses of vicinal *trans*-diols from *meso*-epoxides were also demonstrated. Preparation of (1*R*, 2*R*)-1, 2-cyclohexanediol **13** was performed in 200 mL of aqueous buffer containing 500 mM (49.1 g/L) cyclohexene oxide **10** and 10 g cdw/L of resting cells of *E. coli* (SpEH). A conversion of >99% was achieved at 2 h. The space time yield reached 26 g/L/h, which is attractive for industrial application and also the highest one reported for the biocatalytic synthesis of (1*R*, 2*R*)-**13**. Simple workup afforded 10.284 g (89% isolated yield) (1*R*, 2*R*)-**13** in 86% *ee* (Table 3.8). Very importantly, the *ee* value was improved to 99% by simple crystallization in ethyl acetate, with an overall isolated yield of 68.5% starting from substrate **10**. Other two useful vicinal *trans*-diols (1*R*, 2*R*)-**12** and (3*R*, 4*R*)-**14** were also synthesized by the enantioselective hydrolysis of *meso*-epoxides **9** (200 mM, 17 g/L) and **11** (200 mM, 44 g/L) with resting cells of *E. coli* (SpEH) (4.0 g cdw/L), respectively (Table 3.8). After >99% conversion was reached at 3 and 2 h, respectively, simple workup afforded (1*R*, 2*R*)-**12** in 87% *ee* and 70.4% isolated yield and (3*R*, 4*R*)-**14** in 93% *ee* and 94.1% isolated yield, respectively. Moreover, the product/cells ratios (3.6−11.1 g/g cdw) and the cell-based specific productivities (1.2−5.6 g/h/g cdw) of these three preparations are also attractive for practical syntheses. The facile preparation of these useful vicinal *trans*-diols in high *ee*, high concentration, and high yield demonstrated the great application potential of the *E. coli* (SpEH).

Table 3.8. Preparation of (*R*, *R*) vicinal *trans*-diols **12**, **13**, and **14** with *E. coli* (SpEH).

Sub.	Scale (mL) [a]	Sub. conc. (mM)	Cell density (g cdw/L)	Time (min)	Prod.	Prod. conc. (g/L) [b]	*ee* (%) [c]	Isolated yield (g)	(%)	Prod./ cells (g/g cdw)	Productivity (g/h/g cdw)
9	100	200	4.0	180	(1*R*,2*R*)-**12**	20.4	87	1.436	70.4	3.6	1.2
10	200	500	10.0	120	(1*R*,2*R*)-**13**	58.1	86 99[d]	10.28	88.6 68.5[d]	5.1	2.6
11	5	200	4.0	120	(3*R*,4*R*)-**14**	47.4	93	0.223	94.1	11.1	5.6

[a]The reaction was performed in Tris–HCl buffer (50 mM, pH 7.5). [b]Product concentration was determined by GC analysis. [c]Product *ee* value was determined by chiral GC analysis. [d]Product *ee* value and yield were obtained after crystallization in ethyl acetate.

Table 3.9. Physical properties, ^{1}H NMR analysis, and optical rotations of chiral epoxides and diols prepared by using *E. coli* (SpEH).

Prod.	Appearance	^{1}H NMR chemical shift [a]	$[\alpha]_D^{28}$ [b]	Lit. $[\alpha]_D$
(*S*)-1	colourless liquid	7.26–7.38 (m, 5H, ArH), 3.85–3.88 (dd, J = 4.0, 2.8 Hz, 1H), 3.14–3.16 (dd, J = 5.2, 4.0 Hz, 1H), 2.79–2.82 (dd, J = 5.6, 2.8 Hz, 1H)	+25.0º (*c* 1.00, CHCl$_3$)	$[\alpha]_D^{21}$ = +24º (*c* 1.00, CHCl$_3$)[310]
(*S*)-3	light yellow liquid	7.26–7.28 (m, 3H, ArH), 7.16–7.18 (m, 1H, ArH), 3.82–3.84 (dd, J = 4.0, 2.4 Hz, 1H), 3.13–3.16 (dd, J = 5.6, 4.0 Hz, 1H), 2.75–2.77 (dd, J = 5.6, 2.4 Hz, 1H)	+12.1º (*c* 1.00, CHCl$_3$)	$[\alpha]_D^{23}$ = +11.2º (*c* 1.39, CHCl$_3$)[311]
(*S*)-6	colourless liquid	7.22–7.27 (m, 2H, ArH), 7.00–7.06 (m, 2H, ArH), 3.83–3.85 (dd, J = 4.0, 2.4 Hz, 1H), 3.12–3.15 (dd, J = 5.6, 4.0 Hz, 1H), 2.75–2.77 (dd, J = 5.2, 2.4 Hz, 1H)	+17.2º (*c* 1.00, CHCl$_3$)	$[\alpha]_D^{20}$ = +15.6º (*c* 0.97, CHCl$_3$)[108]
(**1R,2R**)-12	light yellow oil	3.93–3.98 (m, 2H), 3.18 (s, 2H, OH), 1.94–2.04 (m, 2H), 1.67–1.74 (m, 2H), 1.47–1.56 (m, 2H)	–28.8º (*c* 1.00, H$_2$O)	$[\alpha]_D^{25}$ = –24º (MeOH)[312]
(**1R,2R**)-13	white crystal	3.32–3.34 (m, 2H), 3.08 (br s, 2H, OH), 1.95–1.96 (m, 2H), 1.68–1.69 (m, 2H), 1.24–1.30 (m, 4H)	–39.0º (*c* 1.00, H$_2$O)	$[\alpha]_D^{20}$ = –38.4º (*c* 0.17, H$_2$O)[313]
(**3R,4R**)-14	light yellow syrup	7.24–7.36 (m, 5H, ArH), 5.07 (s, 2H), 4.08–4.09 (m, 2H), 3.62–3.66 (m, 2H), 3.62–3.66 (m, 2H), 3.25 (s, 2H)	+7.4º (*c* 1.00, CHCl$_3$)	$[\alpha]_D^{25}$ = +7.56 (*c* 1.80, CHCl$_3$)[126]

[a]^{1}H NMR was determined in CDCl$_3$ with TMS as internal standard using a 400 MHz Bruker NMR system (spectral see Appendix I). [b]Optical rotation was determined using a Jasco polarimeter DIP-1000.

3.4 Conclusion

A unique epoxide hydrolase (SpEH) from *Sphingomonas* sp. HXN-200 was successfully identified and cloned based on genome sequencing and bioinformatics analysis. The engineered *E. coli* (SpEH) highly expressed SpEH and gave 172 times higher cell-based activity for the hydrolysis of styrene oxide **1** than that of *Sphingomonas* sp. HXN-200. Hydrolysis of racemic styrene oxide **1**, substituted styrene oxides **3**, **5–7**, and *N*-phenoxycarbonyl-3,4-epoxypiperidine **8** (200–100 mM) with resting cells of *E. coli* (SpEH) provided (*S*)-epoxides **1**, **3**, **5–7** and (–)-**8** in 98.0–99.5% *ee* and 37.6–46.5% yield. Hydrolysis of *meso-* cyclopentene oxide **9**, cyclohexene oxide **10**, and *N*-benzyloxycarbonyl-3,4-epoxypyrrolidine **11** (100 mM) afforded the corresponding (*R*, *R*)-vicinal *trans*-diols **12–14** in 86–93% *ee* and 90–99% yield. The *ee* of (1*R*, 2*R*)-cyclohexane-1,2-diol **13** was improved to 99% by simple crystallization. These biotransformations showed high cell-based specific activities (0.28–4.3 U/mg cdw), product concentration, product/cells ratio, and cell-based productivity. Hydrolysis at even higher substrate concentrations was also achieved: (*S*)-**1** was produced in 430 mM (51 g/L$_{org}$) and 43% yield; (1*R*, 2*R*)-**13** was produced in 500 mM (60 g/L) and >99% yield. Gram-scale preparation of epoxides (*S*)-**1**, (*S*)-**3**, (*S*)-**6** and diols (1*R*, 2*R*)-**12**, (1*R*, 2*R*)-**13**, (3*R*, 4*R*)-**14** were also demonstrated. *E. coli* (SpEH) cells showed the highest selectivity to produce (*S*)-**1** (*E* of 39) among all known EHs in the form of whole cells or free enzymes and the highest enantioselectivities to produce (*S*)-**3**, **5**, **6**, **7** and (–)-**8** (*E* of 36, 35, 28, 57 and 22, respectively) and (*R*, *R*)-**14** among all known EHs. The easily available and highly active *E. coli* (SpEH) cells are the best biocatalysts known thus far for the practical preparation of these useful and valuable enantiopure epoxides and vicinal diols via hydrolysis. In addition, the SpEH could be applied in other applications, such as in multistep cascade biocatalysis to produce chiral diols or other α-hydroxy compounds.

4 ENANTIOSELECTIVE CASCADE BIOCATALYSIS: AYMMETRIC TRANS-DIHYDROXYLATION OF ARYL OLEFINS WITH RECOMBINANT BIOCATALYSTS
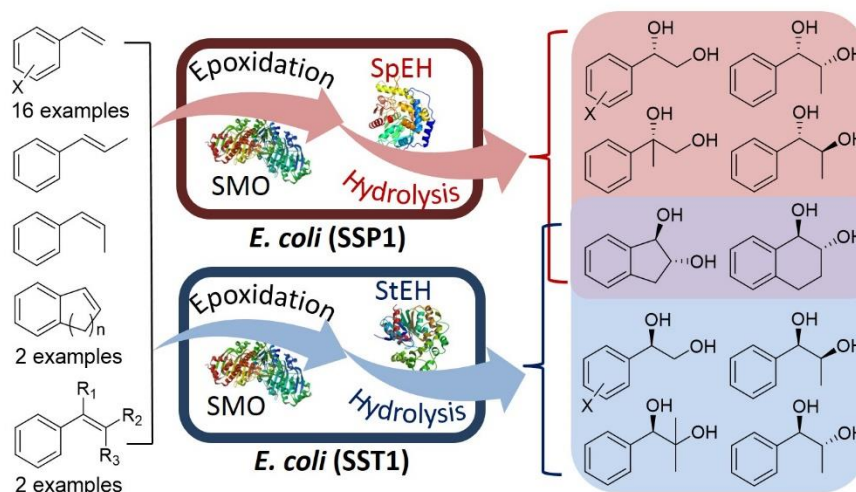
Figure 4.1. Asymmetric *trans*-dihydroxylation of aryl olefins with recombinant *E. coli* coexpressing styrene monooxygenase and different epoxide hydrolases.

4.1 Introduction

In comparison with hydrolysis and reduction, enantioselective oxidation is more challenging in chemistry because it is difficult to fully control selectivity in a system with highly reactive oxidants. Nevertheless, several types of asymmetric oxidations have been developed. One of the most elegant asymmetric oxidations is Sharpless dihydroxylation, which together with Sharpless epoxidation and Sharpless aminohydroxylation was recognized by winning Nobel Prize in 2001.[314] In Sharpless asymmetric dihydroxylation, C=C double bond is stereoselectively oxidized to two *cis*-hydroxyl groups with osmium tetroxide and chiral cinchona alkaloid ligands (Figure 4.2).[315] Although it is a powerful reaction with broad substrate scope and high site selectivity, it suffers from several drawbacks: the osmium is highly toxic; cinchona ligands are expensive; and ferricyanide oxidants are inefficient. On the other hand,

nature provides dioxygenases for dihydroxylation with oxygen, however, they are usually limited to low regioselectivity and moderate enantioselectivity.[316, 317]
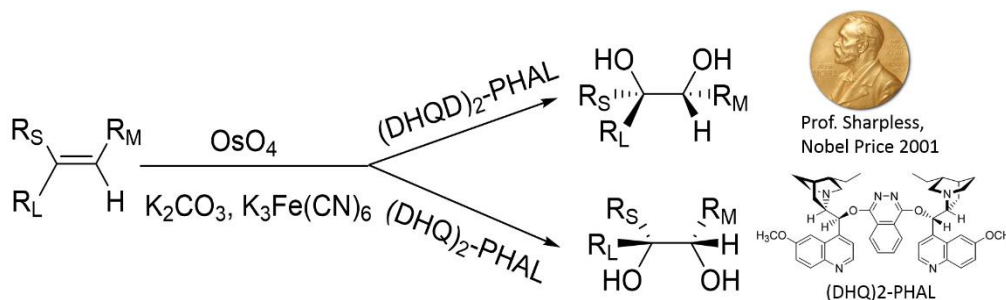
Figure 4.2. Sharpless asymmetric dihydroxylation of olefins to chiral vicinal *cis*-diols with osmium tetroxide catalyst, chiral cinchona alkaloid ligands, and ferricyanide oxidants.

To provide a highly selective and green alternative method for asymmetric dihydroxylation of olefins, we recently developed a novel type of cascade biocatalysis, one-pot cascade epoxidation-hydrolysis, to achieve formal *trans*-dihydroxylation. Cells of *Sphingomonas* sp. HXN-200 containing a P450 monooxygenase and epoxide hydrolase (EH) were used to catalyze the enantioselective *trans*-dihydroxylation of several cyclic olefins.[126] A tandem biocatalysts system consisting of the *Escherichia coli* cells expressing styrene monooxygenase (SMO)[138-152] and the cell-free extract of *Sphingomonas* sp. HXN-200 containing the EH (SpEH)[125-128] was engineered for one-pot (*S*)-enantioselective dihydroxylation of aryl olefins;[247] lipase-mediated epoxidation and EH-catalysed epoxide hydrolysis were combined for the enantioselective *trans*-dihydroxylation of cyclic olefins via one-pot sequential epoxidation and hydrolysis.[248] While asymmetric *cis*-dihydroxylation of olefins can be achieved in one step by Sharpless dihydroxylation,[315] chemical *trans*-dihydroxylation of olefins requires two reaction steps: epoxidation of olefins[318] and subsequent hydrolysis of epoxides,[282] which needs the separation of toxic and unstable epoxide intermediates and also utilizes toxic metals (*e.g.* Osmium, Cobalt). Thus, one-pot cascade biocatalysis for *trans*-dihydroxylation of alkenes provide a greener and more efficient synthetic method for the preparation of enantiopure vicinal diols than the corresponding two-step chemical catalysis. It is a complementary tool to Sharpless dihydroxylation.

We are interested in further developing this type of cascade biocatalysis as a practical method for the preparation of enantiopure vicinal diols that are useful and valuable synthetic intermediates for many pharmaceuticals, bioactive compounds, and chiral reagents.[319-328] A group of enantiopure vicinal diols are selected as target compounds (Scheme 4.1). For example, (S)-1-phenyl-1,2-ethanediol **1c** is a crucial synthetic precursor for pharmaceutical (R)-fluoxetine,[320] chiral phosphoramidite ligand,[321] and auxiliary for stereoselective glycosylation;[322] (R)-1-(4-fluorophenyl)-1,2-ethanediol **2c** is an intermediate for preparing cholesterol-lowering medicine Ezetimibe;[323] (R)-1-(3-chlorophenyl)-1,2-ethanediol **9c** is a key chiral synthon for β_3-adrenergic agonists;[324] (S)-1-(3-methoxyphenyl)-1,2-ethanediol **12c** is a chiral ligand for chromium complexes catalysts;[325] (1R,2S)-phenylpropanediol **16c** and (1S,2S)-**16c** are useful for the synthesis of muscle relaxant phenylcarbanate[326] and selegiline,[327] respectively; (1R, 2R)-indanediol **18c** can be easily converted to (1S)-amino-(2R)-indanol for the synthesis of anti-HIV drug Indinavir.[328] Thus far, the reported cascade biocatalysis system for the dihydroxylation of olefins is relatively complicated, its efficiency needs to be further improved for practical application, the substrate scope is not fully explored, and the dihydroxylation is only S-selective.
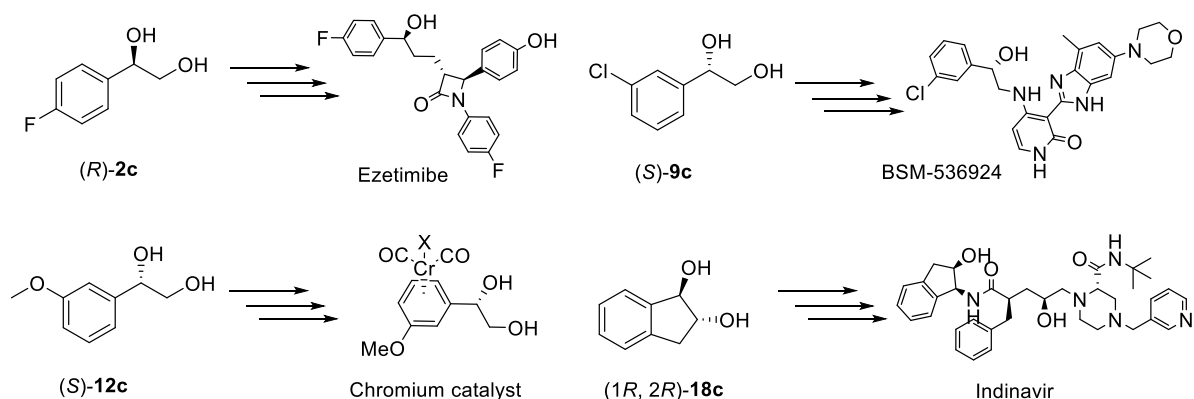
Scheme 4.1. Some important applications of chiral aryl vicinal diols.

Here, we report our progress in:

i) Development of *E. coli* (SSP1) cells coexpressing SMO and SpEH as a simpler and more efficient biocatalyst for *S*-enantioselective dihydroxylation of 15 terminal aryl olefins **1a–15a** to produce the corresponding (*S*)-vicinal diols **1c–15c** in high *ee* and good yield (Scheme 4.2).

ii) Engineering of *E. coli* (SST1) cells coexpressing SMO and another EH (StEH, with the complementary regioselectivity of SpEH) as a simple and efficient biocatalyst for *R*-enantioselective dihydroxylation of 15 terminal aryl olefins **1a–15a** to produce the corresponding (*R*)-vicinal diols **1c–15c** in high *ee* and good yield (Scheme 4.2).

iii) Further exploration of *E. coli* (SSP1) and *E. coli* (SST1) cells for the highly enantioselective *trans*-dihydroxylation of non-terminal aryl olefins **16a–17a** to synthesize all four enantiomers of 1-phenyl-1,2-propanediol **16c** and conversion of aryl cyclic olefins **18a–19a** to prepare (1*R*, 2*R*)-*trans*-diols **18c–19c**.

iv) Scaling up the cascade biocatalysis process in a bioreactor and preparation of 10 useful chiral vicinal diols.

1a-c: X = H	**4a-c**: X = *p*-Br	**7a-c**: X = *p*-CF₃	**10a-c**: X = *m*-Br	**13a-c**: X = *o*-F
2a-c: X = *p*-F	**5a-c**: X = *p*-Me	**8a-c**: X = *m*-F	**11a-c**: X = *m*-Me	**14a-c**: X = *o*-Cl
3a-c: X = *p*-Cl	**6a-c**: X = *p*-OMe	**9a-c**: X = *m*-Cl	**12a-c**: X = *m*-OMe	**15a-c**: X = *o*-Me
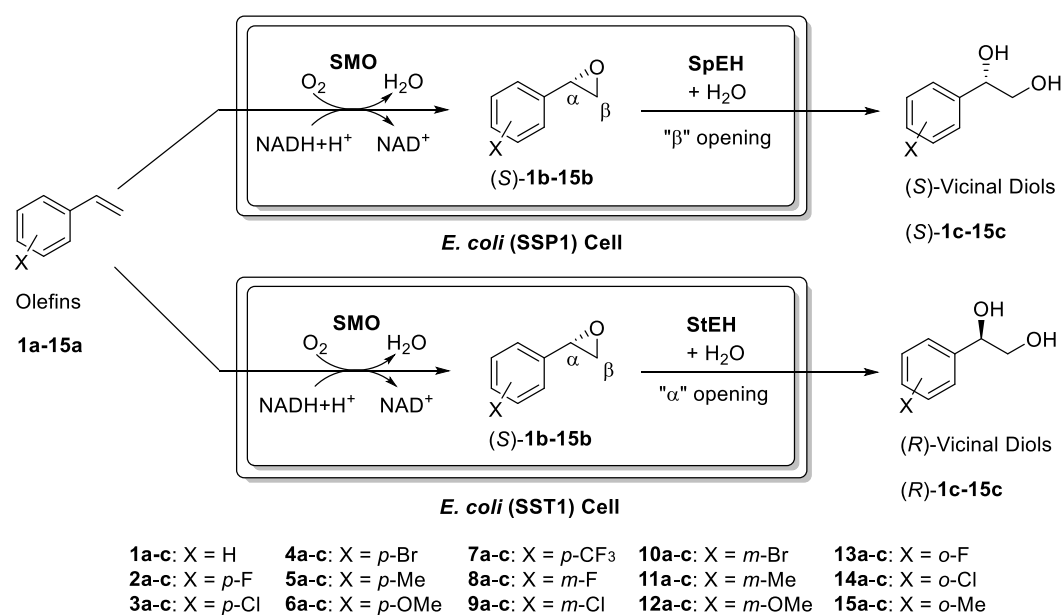
Scheme 4.2. Enantioselective dihydroxylation of aryl olefins **1a–15a** with *E. coli* (SSP1) to produce (*S*)-vicinal diols (*S*)-**1c–15c**, and with *E. coli* (SST1) to produce (*R*)-vicinal diols (*R*)-**1c–15c**, respectively.

4.2 Experimental Section

4.2.1 Chemicals, Strains, and Materials

The chemicals, strains, and materials which have been used in Chapter 3 were not listed here. Please refer to section 3.2.1 for detail.

Many chemicals and solvents were directly purchased from the commercial suppliers and used without further purification. Chemicals from Sigma-Aldrich: styrene **1a** (≥99%), 4-fluorostyrene **2a** (99%), 4-chlorostyrene **3a** (97%), 4-bromostyrene **4a** (97%), 4-methylstyrene **5a** (≥99%), 3-chlorostyrene **9a** (98%), 3-bromostyrene **10a** (97%), 3-methylstyrene **11a** (99%), 3-methoxystyrene **12a** (97%), 2-fluorostyrene **13a** (98%), 2-methylstyrene **15a** (≥95%), *trans-β*-methylstyrene **16a** (99%), 2-methyl-1-phenyl-1-propene **20a** (99%), *α*-methylstyrene **21a** (99%), 3-trifluoromethylstyrene **22a** (99%), 1-phenyl-1,2-ethanediol **1c** (97%), 2-phenyl-1,2-propanediol **21c** (97%), (*R*)-1-phenyl-1,2-ethanediol (*R*)-**1c** (99%), (*S*)-1-phenyl-1,2-ethanediol (*S*)-**1c** (99%), (*S*)-1-(2-chlorophenyl)-1,2-ethanediol (*S*)-**14c** (96%), (1*R*, 2*R*)-*trans*-1,2,3,4-tetrahydro-1,2-naphthalenediol (1*R*, 2*R*)-**19c** (≥96%), (1*S*, 2*S*)-*trans*-1,2,3,4-tetrahydro-1,2-naphthalenediol (1*S*, 2*S*)-**19c** (≥96%), H_2SO_4 (98%), NaOH (pellets), AD-mix-α, AD-mix-β, Hexadecane (99%), Na_2SO_4 (anhydrous, ≥99%), $Na_2CO_3•H_2O$ (puriss), $NaHCO_3$ (ACS reagent), *tert*-Butyl alcohol (≥99%). Chemicals from Alfa Aesar: 4-methoxystyrene **6a** (98%), 4-trifluoromethylstyrene **7a** (98%), 3-fluorostyrene **8a** (97%), 2-chlorostyrene **14a** (98%), 1,2-dihydronaphthalene **19a** (96%). Chemical from Merck: Indene **18a** (≥95%). Chemicals from TCI: *cis-β*-methylstyrene **17a** (≥98%), 1,2-dihydroxyindan **18c** (≥98%, mixture of *cis* and *trans*). Chemicals from Enamine: 2-(4-trifluoromethylphenyl)oxirane **7b** (95%), 2-(3-trifluoromethylphenyl)oxirane **22b** (95%). Chemicals from Spectra Group: 1-(4-methylphenyl)-1,2-ethandediol **5c**, 1-(3-chlorophenyl)-1,2-ethandediol **9c**. Chemical from Maybridge: (1*R*, 2*R*)-indan-1,2-diol (1*R*, 2*R*)-**18c** (97%). Solvent from Fisher:

dichloromethane (HPLC). *trans*-1,2-Dihydroxyindan *trans*-**18c** (>95%) was from previous synthesis.[329]

Many racemic diols were synthesized and purified as analytical standards with the following three methods:

i) Chemical synthesis method A: direct acid hydrolysis of racemic epoxide. According to a previous publication:[108] 200 mg epoxides were dissolved in the mixture of 10 mL THF and 5 mL water. Then 100 μL concentrated H_2SO_4 (98%) was added into the system. The reaction was magnetically stirred at room temperature and TLC was performed to check the conversion of epoxide and formation of diol. When the majority of epoxide was hydrolyzed (usually take 12–36 h), the reaction system was neutralized by adding saturated $NaHCO_3$ solution, saturated with solid NaCl, followed by extraction by ethyl acetate three times (3×10 mL). The combined organic phase was washed with saturated NaCl solution and dried over Na_2SO_4 overnight. The solvent was then removed by evaporation. The crude product was purified by flash chromatography on a silica gel column (n-hexane: ethyl acetate = 2:1 to 1:1, $R_f \approx 0.3$). The racemic diols produced by method A including: 1-(4-fluorophenyl)-1,2-ethanediol **2c**, 1-(4-chlorophenyl)-1,2-ethanediol **3c**, 1-(4-bromophenyl)-1,2-ethanediol **4c**, 1-(4-trifluoromethyl)-1,2-ethanediol **7c**, 1-(3-fluorophenyl)-1,2-ethanediol **8c**, 1-(3-bromophenyl)-1,2-ethanediol **10c**, 1-(2-chlorophenyl)-1,2-ethanediol **14c**, and 1-(3-trifluoromethyl)-1,2-ethanediol **22c**. All the racemic diols were obtained in 40–80% yield. Only **8c** is colorless oil, and others are white to light yellow solids under 4 °C storage.

ii) Chemical synthesis method B: *m*-CPBA epoxidation of olefins and followed by acid hydrolysis. According to a previous report:[126] *m*-CPBA (2 mmol) was stepwise added to a stirred solution of olefin (2 mmol) in a CH_2Cl_2: water system (20 mL, 1:1) on ice, and the mixture was stirred at room temperature for 3–12 h. If needed, a second equivalent of *m*-CPBA (2 mmol) was then added to the mixture and stirred for longer

time (additional 12 h) to complete the reaction. Na_2CO_3 (10%) was added to adjust pH to 8, and then the mixture was extracted with CH_2Cl_2 three times (3×20 mL). The organic phase was separated, washed with saturated NaCl solution, and dried using Na_2SO_4, and the solvent was removed by evaporation. The crude epoxide intermediate was directly used for acid hydrolysis without purification. A mixture of 10 mL THF and 5 mL water was added to the system, followed by addition of 100 μL concentrated H_2SO_4 (98%) to start hydrolysis at room temperature. When the hydrolysis completed (12–36 h), the reaction system was neutralized by $NaHCO_3$ solution, saturated with solid NaCl and then extracted by ethyl acetate three times (3×10 mL). The combined organic phase was washed with saturated NaCl solution and dried over Na_2SO_4 overnight. The solvent was then removed by evaporation. The crude product was purified by flash chromatography on a silica gel column (*n*-hexane: ethyl acetate = 2:1 to 1:1, $R_f \approx 0.3$). The racemic diols produced by method B including: 1-(4-methoxyphenyl)-1,2-ethanediol **6c**, 1-(3-methylphenyl)-1,2-ethanediol **11c**, 1-(3-methoxyphenyl)-1,2-ethanediol **12c**, 1-(2-fluorophenyl)-1,2-ethanediol **13c**, 1-(2-methylphenyl)-1,2-ethanediol **15c**, 1,2,3,4-tetrahydro-1,2-naphthalenediol (*trans*: *cis* ≈ 5: 1) **19c**. Except **6c** was obtained in 10% yield, all the other racemic diols were obtained in 30–70% yield. While **11c** is colorless oil, others are white to light yellow solid under 4 ºC storage.

iii) Chemical synthesis method C: *m*-CPBA epoxidation of olefins and base hydrolysis in one pot. According to a previous study[330]: *m*-CPBA (2 mmol) was stepwise added to a stirred solution of olefin (2 mmol) in CH_2Cl_2 (15 mL) on ice, and the mixture was stirred at room temperature for 3–12 h. If needed, a second equivalent of *m*-CPBA (2 mmol) was then added to the mixture and stirred for longer time (additional 12 h) to complete the reaction. Once the epoxidation finished, high concentrated NaOH (10 M, 100 μL) was added, and the mixture was reflux at 80 ºC. The reaction was monitored by TLC, and once completed, extracted with CH_2Cl_2 three

times (3×20 mL). The organic phase was separated, washed with saturated NaCl solution, and dried using Na_2SO_4, and the solvent was removed by evaporation. The crude product was purified by flash chromatography on a silica gel column (*n*-hexane: ethyl acetate = 2:1 to 1:1, $R_f \approx 0.3$). The racemic diols produced by method C including: 1-phenyl-1,2-propanediol **16c** (as mixture of four enantiomers), 2-methyl-1-phenyl-1,2-propanediol **20c**, which were obtained in 40–60% yield, and become white solid under 4 ºC storage.

Many enantiopure/enriched diols were synthesized in 10 mg-scale as chiral standards using Sharpless dihydroxylation method. The asymmetric synthesis was performed as reported[331]: 0.1 mmol olefin was added to 1 mL mixture of *tert*-BuOH and water (1:1) with 0.15g AD-mix-α (or AD-mix-β for another enantiomer). The reaction was shaken on a mixing block at room temperature for 3 h, and then 50 mg Na_2SO_3 was added to quench the dihydroxylation. The *tert*-BuOH was removed by evaporation, and the remaining aqueous phase was saturated with NaCl and extracted with ethyl acetate (2 mL). The organic layer was dried by Na_2SO_4 for 5 h, and then the clear upper layer was separated and evaporated. The enantiopure/enriched diols were obtained and directly used in chiral HPLC analysis without further purification. The enantiopure/enriched diols prepared including: (*S*)-**2c**, (*S*)-**3c**, (*S*)-**4c**, (*S*)-**5c**, (*S*)-**6c**, (*S*)-**7c**, (*S*)-**8c**, (*S*)-**9c**, (*S*)-**10c**, (*S*)-**11c**, (*S*)-**12c**, (*S*)-**13c**, (*S*)-**15c**, (1*S,* 2*S*)-**16c**, (1*S,* 2*R*)-**16c**, (*S*)-**20c**, (*S*)-**21c**, (*S*)-**22c**, (*R*)-**2c**, (*R*)-**3c**, (*R*)-**4c**, (*R*)-**5c**, (*R*)-**6c**, (*R*)-**7c**, (*R*)-**8c**, (*R*)-**9c**, (*R*)-**10c**, (*R*)-**11c**, (*R*)-**12c**, (*R*)-**13c**, (*R*)-**15c**, (1*R,* 2*S*)-**16c**, (1*R,* 2*R*)-**16c**, (*R*)-**20c**, (*R*)-**21c**, (*R*)-**22c**.

Glucose, and other salts in culture medium were from Sigma Aldrich or Merck. IPTG from Gold Biotechnology. Other biochemicals and strains are the same to Chapter 3.

The following two culture media were used:

1 L M9 medium containing: 8.5 g $Na_2HPO_4 \cdot 2H_2O$, 3.0 g KH_2PO_4, 0.5 g NaCl, 1.0 g NH_4Cl, 2 mL $MgSO_4$ solution (1M), 0.1 mL $CaCl_2$ solution, 1 mL 1000X MT solution (8.3 g/L $FeCl_3 \cdot 6H_2O$, 0.84 g/L $ZnCl_2$, 0.13 g/L $CuCl_2 \cdot 2H_2O$, 0.1 g/L $CoCl_2 \cdot 2H_2O$, 0.1 g/L H_3BO_3, 0.016 g/L $MnCl_2 \cdot 4H_2O$, 1 M HCl), 30 g/L glucose, and 5 g/L yeast extract.

1 L modified Riesenberg medium[332] containing: 13.3 g KH_2PO_4, 4.0 g $(NH_4)_2HPO_4$, 1.7 g Citric acid, 1.2 g $MgSO_4 \cdot 7H2O$, 4.5 mg Thiamin HCl, 15 g Glucose, 10 mL trace metal solution (6 g/L Fe(III) citrate, 1.5 g/L $MnCl_2 \cdot 4H_2O$, 0.8 g/L $Zn(CH_3COO)_2 \cdot 2H_2O$, 0.3 g/L H_3BO_3, 0.25 g/L $Na_2MoO_4 \cdot 2H_2O$, 0.25 g/L $CoCl_2 \cdot 6H_2O$, 0.15 g/L $CuCl_2 \cdot 2H_2O$, 0.84 g/L EDTA, 0.1 M HCl).

4.2.2 Analytical Methods

The concentrations of diol products (**1c–22c**) from biotransformations were determined using a Shimadzu prominence reverse phase HPLC system with an Agilent Poroshell 120 EC-C18 column (150 × 4.6 mm, 2.7 μm) and UV detection at 210 nm. Conditions: 40% water: 60% acetonitrile, flow rate: 0.4 mL min^{-1}. The retention times for most of the diols (**1c–22c**) are from 4 to 5 min. The concentrations of alkene substrates (**1a–22a**) were quantified using a Shimadzu prominence normal phase HPLC system with an Agilent Zorbax Rx-SIL column (150 × 4.6 mm, 5 μm) and UV detection at 210 nm. Condition: 10% IPA: 90% *n*-hexane, flow rate: 1.0 mL min^{-1}. The retention times for most of the alkenes (**1a–22a**) are from 1 to 2 min.

The *ee* and *de* values of diol products (**1c–22c**) were determined by chiral HPLC using a Shimadzu prominence HPLC system (normal phase) and UV detection at 210 nm with a Daicel AS-H, OB-H, or IA-3 chiral column (250 × 4.6 mm, 5μm) (Table 4.1).

Table 4.1. Chiral HPLC methods and retention times for all diols (**1c–22c**).

Prod.	Column	Conditions	Retention time (min)	
1c	AS-H	10% IPA: 90% *n*-Hex, 1.0 mL min^{-1}	10.9 (*S*)	11.6 (*R*)
2c	AS-H	10% IPA: 90% *n*-Hex, 1.0 mL min^{-1}	11.6 (*S*)	12.7 (*R*)
3c	AS-H	10% IPA: 90% *n*-Hex, 1.0 mL min^{-1}	10.9 (*S*)	12.4 (*R*)
4c	AS-H	10% IPA: 90% *n*-Hex, 1.0 mL min^{-1}	10.9 (*S*)	12.5 (*R*)
5c	AS-H	10% IPA: 90% *n*-Hex, 1.0 mL min^{-1}	9.9 (*S*)	11.1 (*R*)
6c	AS-H	10% IPA: 90% *n*-Hex, 1.0 mL min^{-1}	18.3 (*S*)	19.7 (*R*)
7c	AS-H	10% IPA: 90% *n*-Hex, 1.0 mL min^{-1}	7.3 (*S*)	8.7 (*R*)
8c	AS-H	10% IPA: 90% *n*-Hex, 1.0 mL min^{-1}	9.9 (*S*)	10.6 (*R*)
9c	AS-H	10% IPA: 90% *n*-Hex, 1.0 mL min^{-1}	10.3 (*S*)	10.7 (*R*)
10c	AS-H	10% IPA: 90% *n*-Hex, 1.0 mL min^{-1}	10.7 (*S*)	11.0 (*R*)
11c	AS-H	10% IPA: 90% *n*-Hex, 1.0 mL min^{-1}	9.3 (*S*)	9.8 (*R*)
12c	IA-3	10% IPA: 90% *n*-Hex, 1.0 mL min^{-1}	12.8 (*S*)	13.8 (*R*)
13c	AS-H	10% IPA: 90% *n*-Hex, 1.0 mL min^{-1}	10.9 (*S*)	9.7 (*R*)
14c	AS-H	10% IPA: 90% *n*-Hex, 1.0 mL min^{-1}	11.5 (*S*)	9.5 (*R*)
15c	AS-H	10% IPA: 90% *n*-Hex, 1.0 mL min^{-1}	9.3 (*S*)	8.9 (*R*)
16c	IA-3	5% IPA: 95% *n*-Hex, 1.0 mL min^{-1}	16.8 (1*S*, 2*S*); 18.2 (1*S*, 2*R*)	18.7 (1*R*, 2*S*); 20.5 (1*R*, 2*R*)
18c	OB-H	10% IPA: 90% *n*-Hex, 1.0 mL min^{-1}	11.9 (1*S*, 2*S*); 16.0&17.2 (*cis*)	13.4 (1*R*, 2*R*); 16.0&17.2 (*cis*)
19c	OB-H	10% IPA: 90% *n*-Hex, 1.0 mL min^{-1}	12.5 (1*S*, 2*S*); 15.2&16.6 (*cis*)	13.7 (1*R*, 2*R*); 15.2&16.6 (*cis*)
20c	IA-3	10% IPA: 90% *n*-Hex, 1.0 mL min^{-1}	8.6 (*S*)	10.6 (*R*)
21c	AS-H	10% IPA: 90% *n*-Hex, 1.0 mL min^{-1}	8.6 (*S*)	10.2 (*R*)
22c	AS-H	10% IPA: 90% *n*-Hex, 1.0 mL min^{-1}	6.9 (*S*)	7.4 (*R*)

4.2.3 Genetic Engineering of Recombinant *E. coli* Strains Coexpressing SMO and SpEH or StEH

Construction of plasmid SSP1: primers StyA-BspHI-F and StyA-EcoRI-R (see Table 4.2 for a full list of primers) were used to amplify the *styA* from pSPZ10,[149] and primers StyB-EcoRI-RBS-F and StyB-KpnI-R were used to amplify the *styB* from pSPZ10, and primers SpEH-KpnI-RBS-F and SpEH-XhoI-R were used to amplify the *spEH* from the genome of *Sphingomonas* sp. HXN-200. Phusion DNA polymerase was used for all the PCRs according to the instruction. The PCR products were subjected to double digestion with appropriate restriction enzymes (New England Biolabs), and the parental plasmid pRSFduet (Novagen) was also subjected to digestion. Then ligation of digested PCR product and plasmid was performed, and then the ligation products were used for chemical transformation of competent T7 Express Competent *E. coli* cell (New England Biolabs). The three genes (*styA*, *styB*, and *spEH*) were inserted to pRSFduet one by one (first *styA*, then *styB*, last *spEH*). The final successful construction is SSP1 which was transformed to *E. coli* to give *E. coli* (SSP1).

Similarly, the construction of plasmid SSP2-1 used primers StyA-BspHI-F, StyA-EcoRI-R, StyB-EcoRI-RBS-F, StyB-HindIII-R, SpEH-NdeI-F, and SpEH-XhoI-R. The genetic construction is on the same parental plasmid pRSFduet but using different cloning sites. The transformation of SSP2-1 gave *E. coli* (SSP2-1).

Similarly, the construction of plasmid SSP2-2 used primers StyA-BspHI-F, StyA-EcoRI-R, StyB-NdeI-F, StyB-KpnI-R, SpEH-KpnI-RBS-F, and SpEH-XhoI-R. The genetic construction is on the same parental plasmid pRSFduet but using different cloning sites. The transformation of SSP2-2 gave *E. coli* (SSP2-2).

Construction of plasmid SST1 is similar to SSP1, but *stEH* was amplified from the synthesized *stEH* gene (codon optimized for *E. coli*, See appendix II for the DNA sequence) from Genscript according to the sequence Genbank U02497 using primers

StEH-KpnI-RBS-F and StEH-XhoI-R. Other *styA* and *styB* construction is the same to SSP1 by using the intermediate genetic construct in the last step engineering of SSP1. The transformation of SST1 gave *E. coli* (SST1).

Table 4.2. Primers (DNA oligos) used for cloning of SMO, SpEH, and StEH.

Name	Sequence
StyA-BspHI-F	ACTGTCATGAAAAAGCGTATCGGTATTGTTGG
StyA-EcoRI-R	ACTGGAATTCTCATGCTGCGATAGTTGGTGCGAACTG
StyB-EcoRI-RBS-F	ACTGGAATTCTAAGGAGATTTCAAATGACGCTGAAAAAAGATATGGC
StyB-NdeI-F	ACTGCATATGACGCTGAAAAAAGATATGGC
StyB-HindIII-R	ACTGAAGCTTTCAATTCAGTGGCAACGGGTTGC
StyB-KpnI-R	ACTGGGTACCTCAATTCAGTGGCAACGGGTTGC
SpEH-NdeI-F	ATCGCATATGATGAACGTCGAACATATCCGCCC
SpEH-KpnI-RBS-F	ACTGGGTACCTAAGGAGATATATCATGATGAACGTCGAACATATCCGCC
SpEH-XhoI-R	ATCGCTCGAGTCAAAGATCCATCTGTGCAAAGGCC
StEH-NdeI-F	ACTGCATATGGAGAAAATCGAACACAAGATG
StEH-KpnI-RBS-F	ACTGGGTACCTAAGGAGATATATCATGGAGAAAATCGAACACAAGATG
StEH-XhoI-R	ACTGCTCGAGTTAGAATTTTTGAATAAAATC

Construction of plasmid SST2-1 is similar to SSP2-1, but just the gene of last enzyme *stEH* was amplified using StEH-NdeI-F, and StEH-XhoI-R. And the construction intermediate in the last step of SSP2-1 was used for SST2-1. The transformation of SST2-1 gave *E. coli* (SST2-1).

Construction of plasmid SST2-2 is similar to SSP2-2, but just the gene of last enzyme *stEH* was amplified using StEH-KpnI-RBS-F, and StEH-XhoI-R. And the

construction intermediate in the last step of SSP2-2 was used for SST2-2. The transformation of SST2-2 gave *E. coli* (SST2-2).

4.2.4 Cell Growth and Dihydroxylation Activity of *E. coli* (SSP1) or *E. coli* (SST1)

E. coli strain, *E. coli* (SSP1) or *E. coli* (SST1), was cultured in 2mL LB medium containing kanamycin (50 mg/L) at 37 °C for 7–10 h, and then inoculated into 50 mL M9 medium containing glucose (30 g/L), yeast extract (5 g/L), and kanamycin (50 mg/L). The cells were grown at 37 °C for 2 h to reach an OD_{600} of 0.6, and then IPTG (0.5 mM) was added to induce the expression of enzymes. The cells continued to grow for 10–12 h at 25 °C to reach a cell density of 5–6 g cdw/L. The cells were harvested by centrifugation (5000g, 5 min), and the cell pallets were used as catalysts for the activity test or biotransformation.

Activity test: freshly prepared *E. coli* (SSP1) or *E. coli* (SST1) cells were suspended to a cell density of 1.0 g cdw/L in KP (potassium phosphate) buffer (200 mM, pH 8.0) containing glucose (2%, w/v) and 40 μL styrene **1a** stock solution (0.5 M in ethanol) to 2 mL system. The reaction mixture was shaken at 250 rpm and 30 °C for 30 min. 1 mL aliquots were taken out and mixed with 1 mL acetonitrile to stop reaction. After centrifugation, the supernatant was used for HPLC analysis of the diol product.

4.2.5 General Procedure for Enantioselective Dihydroxylation of Aryl Olefins 1a–22a with Resting Cells of *E. coli* (SSP1) or *E. coli* (SST1)

Freshly prepared *E. coli* (SSP1) or *E. coli* (SST1) cells were resuspended to a cell density of 10 g cdw/L in KP buffer (200 mM, pH 8.0) containing glucose (2%, w/v) to 2 mL system in a shaking flask (100 mL). 2 mL *n*-hexadecane containing 20 mM aryl olefins **1a–22a** was added to the reaction system to form a second phase. The reaction mixture was shaken at 250 rpm and 30 °C for 8 h. 200 μL aliquots of each phase were taken out at 0 h, 0.5 h, 2 h, and 8 h for following the reaction. For organic phase, *n*-hexadecane (100 μL) were separated after centrifugation, diluted with 900 μL

n-hexane (containing 2 mM benzyl alcohol as internal standard), and subjected to normal phase HPLC analysis for quantifying the olefin substrates **1a–22a** and possible epoxide intermediate. For aqueous phase, supernatants (100 µL) were separated after centrifugation, diluted with 400 µL water and 500 µL acetonitrile (containing 2 mM benzyl alcohol as internal standard), and then used for reverse phase HPLC analysis of the diol products **1c–22c**. The remaining aqueous phase (about 1 mL) after 8 h in the flask was subjected to centrifugation to remove the cells, followed by extraction with ethyl acetate and dry over Na_2SO_4. After evaporation, the residue was dissolved in 2 mL solvent (hexane: IPA = 9:1) for chiral HPLC analysis of the *ee* and/or *de* of the diol products **1c–22c**.

4.2.6 General Procedure for Preparation of (1*S*)-Vicinal Diols by Enantioselective Dihydroxylation of Aryl Olefins with Resting Cells of *E. coli* (SSP1)

Freshly prepared *E. coli* (SSP1) cells were resuspended to a cell density of 20 g cdw/L in KP buffer (200 mM, pH 8.0) containing glucose (2%, w/v) to 45 mL system in a shaking flask (250 mL with tri-baffle). 5 mL *n*-hexadecane containing 2.50 mmol substrate (0.260 g **1a**, 0.305 g **2a**, 0.295 g **5a**, 0.346 g **9a**, and 0.335 g **12a**) was added to the reaction system to form a second phase (50 mM substrate concentration based on total reaction volume). The reaction mixture was shaken at 250 rpm and 30 ºC, and the reaction was monitored by TLC. After 5–8 h, the substrate disappeared totally, and the reaction mixture was then saturated with NaCl. After centrifugation, the aqueous phase was collected and washed with 10 mL *n*-hexane. The aqueous phase was then extracted with ethyl acetate three times (3 × 50 mL), and all the organic phase were combined. After drying over Na_2SO_4, the solvents were removed by evaporation. The crude diol products were purified by flash chromatography on a silica gel column with *n*-hexane: ethyl acetate (2–1:1) as eluent ($R_f ≈ 0.3$ for all diol products).

4.2.7 General Procedure for Preparation of (1*R*)-Vicinal Diols by Enantioselective Dihydroxylation with Resting Cells of *E. coli* (SST1)

Freshly prepared *E. coli* (SST1) cells were resuspended to a cell density of 20 g cdw/L in KP buffer (200 mM, pH 8.0) containing glucose (2%, w/v) to 45 mL system in a shaking flask (250 mL with tri-baffle). 5 mL *n*-hexadecane containing 2.50 mmol substrate (0.260 g **1a**, 0.305 g **2a**, 0.346 g **9a**, 0.295 g **16a**, and 0.295 g **17a**) was added to the reaction system in the flask. The reaction mixture was shaken at 250 rpm and 30 ℃. The reaction was monitored by TLC. After 5–8 h, the substrate disappeared totally. The reaction mixture was then saturated with NaCl. After centrifugation, the aqueous phase was collected and then washed with 10 mL *n*-hexane. The aqueous phase was extracted with ethyl acetate three times (3×50 mL), and all the organic phase were combined. After drying over Na_2SO_4, the solvents were removed by evaporation. The crude diol products were then purified by flash chromatography on a silica gel column with *n*-hexane: ethyl acetate (2–1:1) ($R_f \approx 0.3$ for all diol products).

4.2.8 Enantioselective Dihydroxylation of Styrene 1a with Growing Cells of *E. coli* (SST1) in a Bioreactor

E. coli (SST1) was cultured in 2 mL LB medium containing kanamycin (50 mg/L) at 37 ℃ for 7–10 h, and then inoculated into 100 mL M9 medium containing glucose (30 g/L), yeast extract (5 g/L), and kanamycin (50 mg/L). The cells were grown at 30 ℃ for 12 h to reach an OD_{600} of 15. All culture was transferred into 900 mL sterilized modified Riesenberg medium with 15 g/L glucose as carbon source in a 3 L fermentor (Sartorius). The cells were grown in the fermentor at 30 ℃ for 12 h to reach an OD_{600} of 15–18. During the batch growth, the pH value was maintained at 7.0 by adding 30% phosphoric acid or 25% ammonia solution based on pH sensing, and the stirring rate was kept constant at 1000 rpm, and aeration rate was kept constant at 1 L/min. At the end of batch growth (12 h), P_{O2} started to increase, indicating glucose depletion. Fed-batch growth was started by feeding a solution containing 730 g/L glucose and 19.6 g/L $MgSO_4 \cdot 7H_2O$. The feeding rate was stepwise increased: 6.5 mL/h for 1 h, 8 mL/h for 1 h, 10 mL/h for 1h, 13 mL/h for 1 h, then kept at 16 mL/h until the

end of reaction. Stirring rate was stepwise increased: 1200 rpm for 2 h, 1500 rpm for 2h, then kept at 2000 rpm until the end of reaction. Aeration rate was stepwise increased: 1.2 L/min for 2 h, 1.5 L/min for 2h, then kept at 2.0 L/min until the end of reaction. Antifoam PEG2000 (Fluka) was added when necessary. After fed-batch growth for 2 h, IPTG (0.5 mM) was added to induce the expression of protein. After fed-batch growth for 5 h, the cell density reached 20 g cdw/L, and the biotransformation started by dropwise adding styrene **1a** at the rate of 6 mL/h for 4 h, and then 3 mL/h for additional 1 h. The reaction was monitored by taking sample every hour for analyzing the formation of diol **1c** by reverse phase HPLC. After 5 h reaction, 120 mM (*R*)-1-phenyl-1,2-ethanediol was produced in 96.2% *ee*.

4.3 Results and Discussion

4.3.1 Genetic Engineering of *E. coli* Coexpressing of SMO and SpEH for *S*-Selective Dihydroxylation of Styrenes

SMO was chosen as the enzyme for epoxidation of olefins in the first step of the cascade, since it is a well-known enzyme for the epoxidation of styrenes to give (*S*)-epoxides in high *ee*.[138-152] In addition, the epoxidation of styrenes with recombinant *E. coli* expressing SMO has been developed as one of the most productive biocatalytic oxyfunctionalization processes.[152] EH from *Sphingomonas* sp. HXN-200 (SpEH) was used as the enzyme for the hydrolysis of the epoxides in the second step of the cascade, because this EH is known to hydrolyze (*S*)-styrene oxides at the *β* position to give (*S*)-diols in high *ee* with the retention of configuration. [127, 128] The *E. coli* strain expressing SpEH was also developed as an efficient catalyst for the preparation of enantiopure epoxides by kinetic resolution (see Chapter 3).
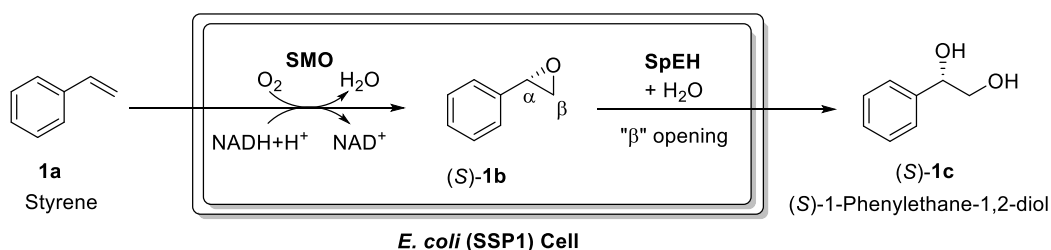
Scheme 4.3. Enantioselective dihydroxylation of styrene **1a** with *E. coli* (SSP1) coexpressing SMO and SpEH to produce (*S*)-**1c**.

To develop recombinant *E. coli* containing both SMO and SpEH as a simple and efficient catalyst system for the dihydroxylation of olefins (Scheme 4.3), the two coding sequences of SMO (*styA* and *styB*) were amplified from pSPZ10 plasmid,[149] and the gene of SpEH was amplified from the genome of the *Sphingomonas* sp. HXN-200. To optimize the expression level of the three genes, we engineered three different expression cassettes on the commercially available plasmid pRSFduet (Figure 4.3a): SSP1, an artificial operon of *styA*, *styB*, and *spEH* controlled by one T7 promoter;

91

SSP2-1 and SSP2-2, where *styA*, *styB*, and *spEH* are under the control of two T7 promoters. These plasmids were transformed into *E. coli* T7 expression cell to give *E. coli* (SSP1), *E. coli* (SSP2-1), and *E. coli* (SSP2-2), respectively. These strains were grown in TB medium, and IPTG was added to induce protein expression. As a result, all three strains were able to coexpress SMO (StyA and StyB) and SpEH, but at different levels. The strains were examined for biotransformation of 100 mM styrene **1a** in a two-liquid phase system consisting of potassium phosphate (KP) buffer and *n*-hexadecane (1:1). *E. coli* (SSP1) showed the best results, producing 65 mM (*S*)-1-phenylethane-1,2-diol **1c** in 99% *ee* at 5 h (Figure 4.3a). Other two strains also gave (*S*)-**1c**, but in lower concentration. In comparison of other two strains, *E. coli* (SSP1) has higher ratio of SMO/SpEH, which is desirable for the cascade dihydroxylation, since the catalytic efficiency of SpEH ($k_{cat}/K_m = 6.0$ mM^{-1} s^{-1}, Chapter 3) is higher than that of SMO ($k_{cat}/K_m = 4.2$ mM^{-1} s^{-1}).[141] The superior of *E. coli* (SSP1) is also probably due to the more homogeneous expression of several genes in one operon. *E. coli* (SSP1) was selected for further development.

Figure 4.3. a) Genetic constructions of and dihydroxylation with three different *E. coli* strains coexpressing SMO (StyA and StyB) and SpEH; **b)** Genetic constructions of and dihydroxylation with three different *E. coli* strains coexpressing SMO (StyA and StyB) and StEH. The dihydroxylation of 100 mM styrene **1a** to diol **1c** was performed with resting cells (10 g cdw/L) of the corresponding *E. coli* strain at 30 °C in a two-liquid phase system (*n*-hexadecane: KP buffer = 1:1).

4.3.2 Genetic Engineering of *E. coli* Coexpressing of SMO and StEH for *R*-Selective Dihydroxylation of Styrenes
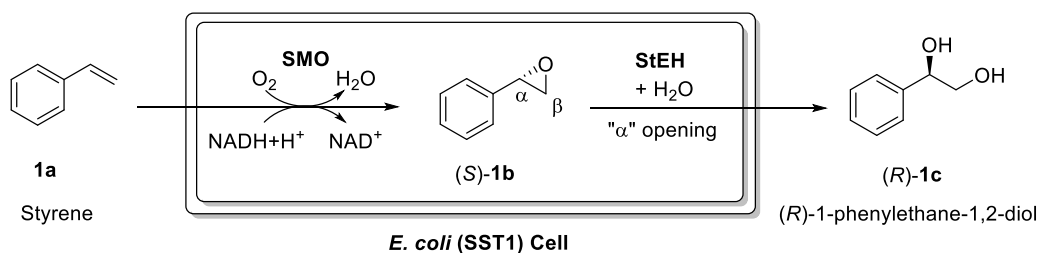
Scheme 4.4. Enantioselective dihydroxylation of styrene **1a** with *E. coli* (SST1) coexpressing SMO and StEH to produce (*R*)-**1c**.

To develop a cascade biocatalysis for *R*-selective dihydroxylation of styrenes, the EH from *Solanum tuberosum* (StEH) was selected as the enzyme for the hydrolysis step, because StEH is known to hydrolyze (*S*)-styrene oxides to offer (*R*)-diols by opening at the *α* position (inversion of configuration).[333–336] The regioselectivity for the hydrolysis with StEH is complementary to that with SpEH. The gene of StEH was synthesized according to the reported potato cDNA sequence[334] with codon optimization for the expression in *E. coli*. Similar to the engineering of SMO and SpEH, three different expression cassettes of SMO and StEH were constructed, and three strains *E. coli* (SST1), *E. coli* (SST2-1), and *E. coli* (SST2-2) were obtained and evaluated for the dihydroxylation (Figure 4.3b). *E. coli* (SST1) gave a specific activity of 40 U/g cdw and produced 82 mM (*R*)-1-phenylethane-1,2-diol **1c** in 96% *ee* at 5 h in the dihydroxylation of 100 mM styrene **1a** at a cell density of 10 g cdw/L in the two-liquid phase system. It is the best among the three strains. Thus, *E. coli* (SST1) was chosen for further development as a powerful catalyst for *R*-enantioselective dihydroxylation of styrenes, being complementary to *E. coli* (SSP1) for the cascade biocatalysis.

4.3.3 Cell Growth and Activity of *E. coli* (SSP1) and *E. coli* (SST1)

E. coli (SSP1) strain was grown easily in M9 medium with glucose as carbon source in a shaking flask, and SMO and SpEH were coexpressed by adding IPTG as inducer. The growth and activity of the cells were monitored by taking samples at different time points for measuring the optical density and dihydroxylation activity. As shown in Figure 4.4a, the cells reached a high density (5–6 g cdw/L; cdw: cell dry weight) at 13–16 h. High specific activities (70–80 U/g cdw) toward (*S*)-dihydroxylation of styrene **1a** were achieved at the late exponential growing phase (11–13 h). In the SDS-PAGE of the cell free extract of the *E. coli* (SSP1) taken at 12 h (Figure 4.4c, lane 3), StyA, StyB, and SpEH are clearly visible.
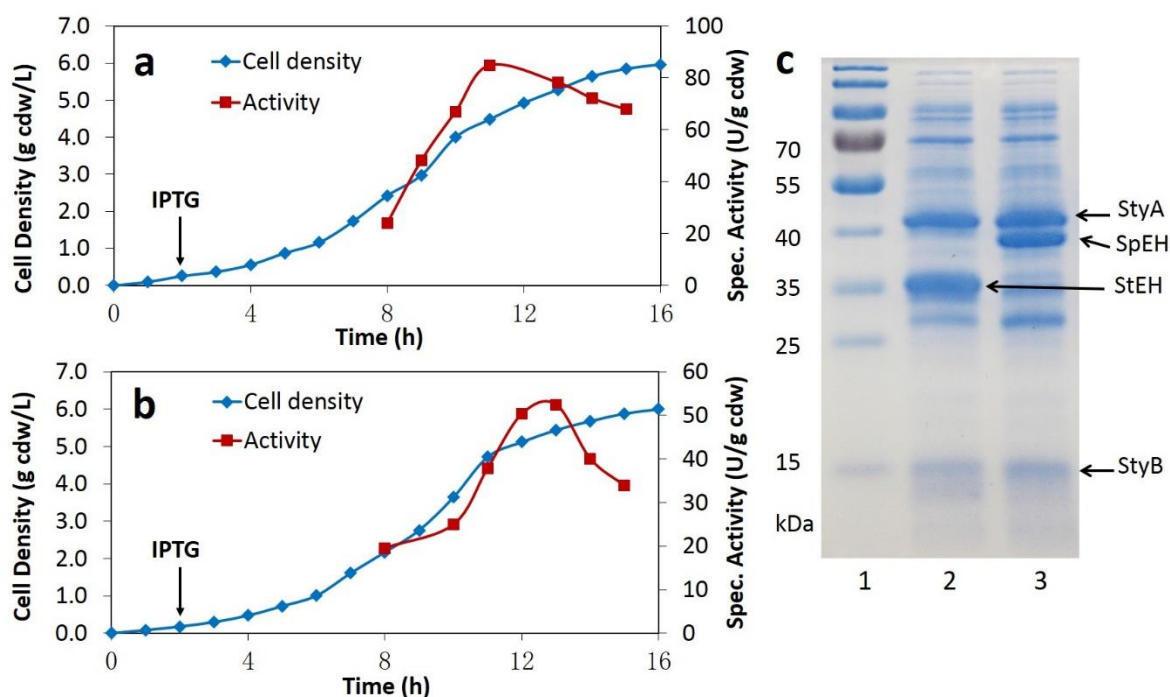
Figure 4.4. a-b) Cell growth and specific activity for dihydroxylation of the recombinant strains. **a)** *E. coli* (SSP1); **b)** *E. coli* (SST1). Cells were initially cultured at 37 °C, induced at 2 h by the addition of IPTG (0.5 mM), and then grown at 25 °C. The activities were based on 30 min dihydroxylation of 10 mM styrene **1a** with resting cells (1 g cdw/L) in aqueous buffer. **c)** SDS-PAGE, Lane 1: Protein Marker; Lane 2: Cell-free extract of *E. coli* (SST1) coexpressing SMO and StEH taken at 12 h; Lane 3: Cell-free extract of *E. coli* (SSP1) coexpressing SMO and SpEH taken at 12 h.

E. coli (SST1) showed a similar cell growth curve and reached high cell density (5–6 g cdw/L) at 13–16 h (Figure 4.4b). Good specific activities (40–50 U/g cdw) for

R-dihydroxylation of styrene **1a** were also achieved at the late exponential growing phase (12–14 h). The SDS-PAGE of the cell free extract of the *E. coli* (SST1) taken at 12 h (Figure 4.4c, lane 2) also clearly demonstrated the expressing of StyA, StyB, and StEH in *E. coli* (SST1).

4.3.4 *S*-selective *trans*-Dihydroxylation of Terminal Aryl Olefins with Resting Cells of *E. coli* (SSP1)

1a-c: X = H	**4a-c**: X = *p*-Br	**7a-c**: X = *p*-CF₃	**10a-c**: X = *m*-Br	**13a-c**: X = *o*-F
2a-c: X = *p*-F	**5a-c**: X = *p*-Me	**8a-c**: X = *m*-F	**11a-c**: X = *m*-Me	**14a-c**: X = *o*-Cl
3a-c: X = *p*-Cl	**6a-c**: X = *p*-OMe	**9a-c**: X = *m*-Cl	**12a-c**: X = *m*-OMe	**15a-c**: X = *o*-Me
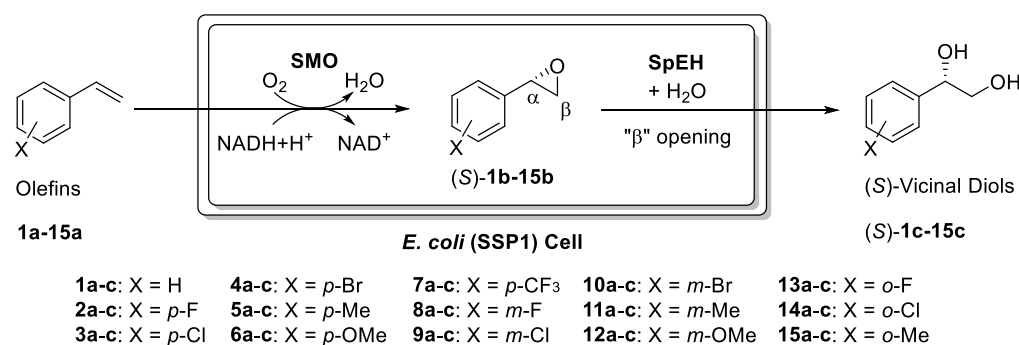
Scheme 4.5. Enantioselective dihydroxylation of aryl olefins **1a–15a** with *E. coli* (SSP1) coexpressing SMO and SpEH to produce (*S*)-vicinal diols (*S*)-**1c–15c**.
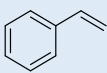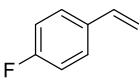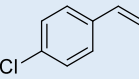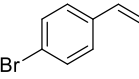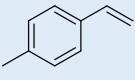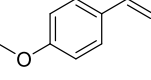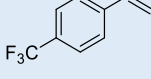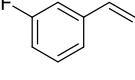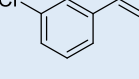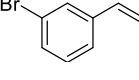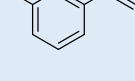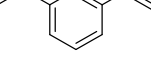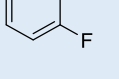
To explore the synthetic potential of *E. coli* (SSP1), the resting cells of the strain were employed for the dihydroxylation of 20 mM styrene **1a** and substituted styrenes **2a–15a** (Scheme 4.5) in a two-liquid phase system containing KP buffer and *n*-hexadecane (1:1). The *n*-hexadecane phase acts as a reservoir of the substrate and possible epoxide intermediate to reduce their inhibition effect on the enzymes. As listed in Table 4.3, (*S*)-vicinal diols **1c–15c** were produced in high *ee* from **1a–15a** by the one-pot cascade epoxidation and hydrolysis with resting cells of *E. coli* (SSP1). Importantly, many vicinal diols, such as (*S*)-**1c–4c**, (*S*)-**7c–10c**, (*S*)-**12c**, and (*S*)-**13c**, were produced in excellent *ee* (>97.5%). Other vicinal diols, including (*S*)-**5c**, (*S*)-**11c**, and (*S*)-**14c**, were obtained in high *ee* (92.2–93.9%). The configurations of **1c–15c** were established by comparing bioproducts with the standard diols that were either commercially available or prepared via Sharpless asymmetric dihydroxylation (Figure S2.1-S2.15, Appendix II). The high *S*-enantioselectivity of dihydroxylation is due to the high *S*-enantioselectivity of SMO-catalyzed epoxidation of styrenes and the high
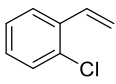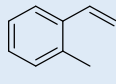
regioselectivity of SpEH-catalyzed hydrolysis of (*S*)-epoxides at the *β* position. Only two diols, (*S*)-**6c** and (*S*)-**15c,** were produced in moderate *ee* (83.2% and 65.7%), possibly due to the autohydrolysis of unstable epoxide **6b** or the reduced regioselectivity of SpEH in hydrolysis of epoxide **15b**.

Most of the dihydroxylations gave high conversion and high yield. (*S*)-Vicinal diols **1c**, **8c**, **9c**, **11c**, **12c**, and **13c** were obtained in 91–>99% yields, (*S*)-**2c** and (*S*)-**5c** were formed in 86–88% yields, and (*S*)-**3c**, (*S*)-**6c**, and (*S*)-**10c** were produced in 67–73% yields. This confirmed that SMO and SpEH coexpressed in the *E. coli* cells are very active for the cascade biocatalysis. The specific activity for these *S*-dihydroxylations is 11–55 U/g cdw, with the exception for the *S*-dihydroxylation of **10a** (8 U/g cdw). In the previous reported tandem biocatalysts system, (*S*)-epoxide **1b** accumulated as the intermediate in the early stage of the biotransformation.[247] Due to the high activity of SpEH in *E. coli* (SSP1), there was no epoxide accumulated during the cascade biocatalysis with resting cells of *E. coli* (SSP1). The time curve of dihydroxylation of **9a** was a representative example (Figure 4.5), which clearly evidenced this point. In comparison with the previous reported tandem biocatalysts (20 mM **1a** was converted in 21 h with 2.5 g cdw/L of *E. coli* cells expressing SMO and 20 g protein/L of cell free extract containing SpEH),[247] the use of resting cells of *E. coli* (SSP1) coexpressing SMO and SpEH provides a much simpler catalyst and much higher catalytic efficiency: 20 mM **1a** was converted to (*S*)-**1c** in only 2 h with 10 g cdw/L of *E. coli* (SSP1) cells.

The *S*-dihydroxylations of **4a**, **7a**, **14a**, and **15a** with resting cells of *E. coli* (SSP1) gave lower yields (25–34%). This is mainly due to the low epoxidation activity of SMO towards these substrates, which have either a strong electron-withdrawing group or an *ortho*-substitution.[143-145]

Table 4.3. Enantioselective dihydroxylation of aryl olefins **1a–15a** with resting cells of *E. coli* (SSP1) and *E. coli* (SST1), respectively.

Substrate[a]		Catalyst	Act. (U/g cdw)[b]	Conv. (%)[c]	Prod.	Yield (%)[d]	ee (%)[e]
1a		*E. coli* (SSP1)	46	>99	(S)-**1c**	92	98.1
		E. coli (SST1)	39	>99	(R)-**1c**	93	95.5
2a		*E. coli* (SSP1)	33	>99	(S)-**2c**	88	97.9
		E. coli (SST1)	41	>99	(R)-**2c**	90	95.2
3a		*E. coli* (SSP1)	20	67	(S)-**3c**	67	97.8
		E. coli (SST1)	22	90	(R)-**3c**	89	95.6
4a		*E. coli* (SSP1)	7	40	(S)-**4c**	34	97.7
		E. coli (SST1)	7	92	(R)-**4c**	86	94.4
5a		*E. coli* (SSP1)	12	98	(S)-**5c**	86	93.9
		E. coli (SST1)	15	>99	(R)-**5c**	85	87.7
6a		*E. coli* (SSP1)	26	>99	(S)-**6c**	67	83.2
		E. coli (SST1)	20	>99	(R)-**6c**	65	85.4
7a		*E. coli* (SSP1)	2	31	(S)-**7c**	25	97.5
		E. coli (SST1)	2	18	(R)-**7c**	19[f]	87.7
8a		*E. coli* (SSP1)	41	>99	(S)-**8c**	>99	98.4
		E. coli (SST1)	43	>99	(R)-**8c**	>99	94.2
9a		*E. coli* (SSP1)	22	96	(S)-**9c**	95	97.5
		E. coli (SST1)	15	97	(R)-**9c**	95	95.8
10a		*E. coli* (SSP1)	8	80	(S)-**10c**	67	97.5
		E. coli (SST1)	6	98	(R)-**10c**	86	84.2
11a		*E. coli* (SSP1)	11	97	(S)-**11c**	91	93.1
		E. coli (SST1)	9	98	(R)-**11c**	92	98.2
12a		*E. coli* (SSP1)	55	>99	(S)-**12c**	96	97.6
		E. coli (SST1)	40	>99	(R)-**12c**	>99	87.3
13a		*E. coli* (SSP1)	11	94	(S)-**13c**	94	98.6
		E. coli (SST1)	17	98	(R)-**13c**	89	68.1

14a	(2-chlorostyrene structure)	*E. coli* (SSP1)	4	31	(*S*)-**14c**	34[f]	92.2
		E. coli (SST1)	2	26	(*R*)-**14c**	10	36.9
15a	(2-methylstyrene structure)	*E. coli* (SSP1)	5	36	(*S*)-**15c**	34	65.7
		E. coli (SST1)	5	34	(*R*)-**15c**	15	89.9

[a] The reactions were performed with substrates **1a–15a** (20 mM in organic phase) and resting cells (10 g cdw/L) in a two-liquid phase system consisting of KP buffer (200 mM, pH 8.0, 2% glucose) and *n*-hexadecane (1:1) at 30 °C for 8 h. [b] Activity is the specific activity determined for initial 30 min. [c] Conversion is the consumption of starting substrate, determined by normal phase HPLC analysis of the remaining substrate in the *n*-hexadecane phase. Error limit: 3% of the state values. [d] Yield is the analytical yield of the formation of diol product, determined by reverse phase HPLC analysis of the product in the aqueous phase. Error limit: 3% of the state values. [e] *ee* value was determined by chiral HPLC analysis. Error limit: 0.2% of the state values. [f] Yield is slightly higher than conversion due to the error limit in the measurement of yield and conversion.
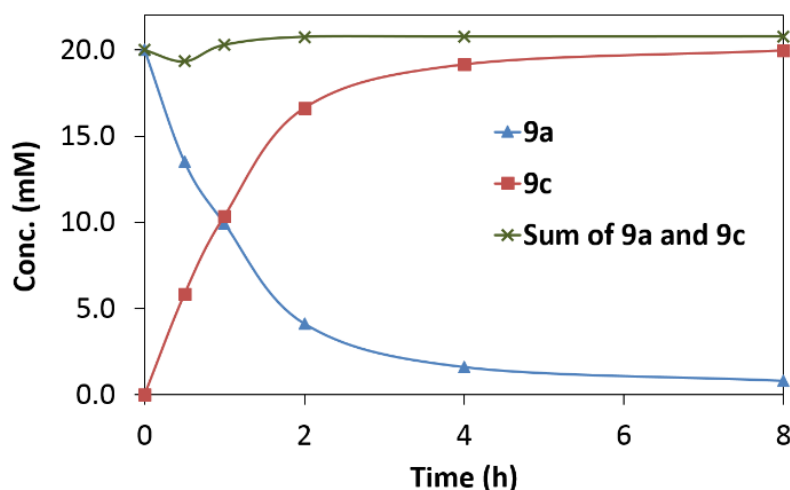
Figure 4.5. Typical time course of enantioselective dihydroxylation of 3-chlorostyrene **9a** to (*S*)-1-(3-chlorophenyl)-1,2-ethanediol **9c** with resting cells of *E. coli* (SSP1). The dihydroxylation was performed with resting cells (10 g cdw/L) in a two-liquid phase system (*n*-hexadecane: KP buffer = 1:1).

4.3.5 *R*-selective *trans*-Dihydroxylation of Terminal Aryl Olefins with Resting Cells of *E. coli* (SST1)

To explore the synthetic potential of another strain, *E. coli* (SST1), the resting cells of the strain were used for the *R*-dihydroxylation of 20 mM olefins **1a–15a** (Scheme 4.6) in the same two-liquid phase system as described above. The results are listed in Table 4.3, and (*R*)-vicinal diols (*R*)-**1c–15c** were produced from **1a–15a** by the one-pot cascade epoxidation and hydrolysis with resting cells of *E. coli* (SST1).

Many (*R*)-vicinal diols, such as (*R*)-**1c–4c**, (*R*)-**8c**, (*R*)-**9c**, and (*R*)-**11c**, were produced in excellent *ee* (94.2–98.2%). The diols (*R*)-**5c–7c**, (*R*)-**10c**, (*R*)-**12c**, and (*R*)-**15c** were also formed in high *ee* (84.2–89.9%). The high *R*-enantioselectivity of dihydroxylation is the combined result of high *S*-enantioselectivity of SMO-catalyzed epoxidation of styrenes and the high regioselectivity of StEH-catalyzed hydrolysis of (*S*)-epoxides at the *α* position. Only (*R*)-**13c** and (*R*)-**14c** were obtained in low *ee* (68.1% and 36.9%). The low enantioselectivity was probably caused by the hindrance of the *ortho*-substitution in epoxides **13b–14b** for the hydrolysis at the *α* position with StEH.

1a-c: X = H	**4a-c**: X = *p*-Br	**7a-c**: X = *p*-CF$_3$	**10a-c**: X = *m*-Br	**13a-c**: X = *o*-F
2a-c: X = *p*-F	**5a-c**: X = *p*-Me	**8a-c**: X = *m*-F	**11a-c**: X = *m*-Me	**14a-c**: X = *o*-Cl
3a-c: X = *p*-Cl	**6a-c**: X = *p*-OMe	**9a-c**: X = *m*-Cl	**12a-c**: X = *m*-OMe	**15a-c**: X = *o*-Me
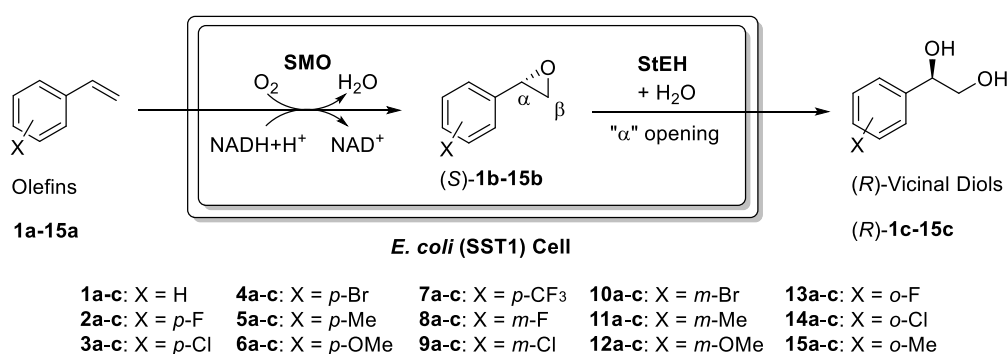
Scheme 4.6. Enantioselective dihydroxylation of aryl olefins **1a–15a** with *E. coli* (SST1) coexpressing SMO and StEH to produce (*R*)-vicinal diols (*R*)-**1c–15c**.

Most of the *R*-dihydroxylations with the resting cells of *E. coli* (SST1) also gave high conversion and high yield. (*R*)-Vicinal diols **1c**, **2c**, **3c**, **8c**, **9c**, **11c**, and **12c** were obtained in 90–>99% yields, (*R*)-**4c**, (*R*)-**5c,** (*R*)-**10c** and (*R*)-**13c** were formed in 85-89% yields, and (*R*)-**6c** was produced in 65% yield. This confirmed also that SMO and StEH coexpressed in the *E. coli* cells are very active for the cascade biocatalysis. The specific activity for these *R*-dihydroxylations is 15–43 U/g cdw, with the exception for the *R*-dihydroxylations of **4a**, **10a**, and **11a** (6–9 U/g cdw). Due to the high activity of StEH in *E. coli* (SST1), no epoxide was accumulated in the dihydroxylations of **1a-12a**. Accumulation of epoxide was observed only in the dihydroxylation of *ortho*-substituted olefins **13a–15a**. Here, the resting cells of *E. coli* (SST1) coexpressing SMO and StEH were developed as a simple and efficient catalyst for the synthesis of these (*R*)-vicinal diols via dihydroxylation, being the first biocatalytic system for the

R-enantioselective dihydroxylations of styrenes. Clearly, *E. coli* (SSP1) and *E. coli* (SST1) are excellent cascade biocatalysts with complementary enantioselectivity for the dihydroxylation of styrene and its derivatives. It is the first example to achieve the reversal of overall enantioselectivity of cascade biocatalysis by changing the regioselectivity in an individual reaction step. The concept can be applied to solve the problem of lacking mirror-image enzymes in biocatalysis, in addition to the discovery and development of enantiocomplementary enzymes.[337]

The *R*-dihydroxylations of **7a**, **14a**, and **15a** with resting cells of *E. coli* (SST1) gave lower yields (10–19%). This is similar to the cases with *E. coli* (SSP1) and due to the low activity of SMO.

4.3.6 Asymmetric *trans*-Dihydroxylation of Nonterminal Aryl Olefins with Resting Cells of *E. coli* (SSP1) and *E. coli* (SST1)
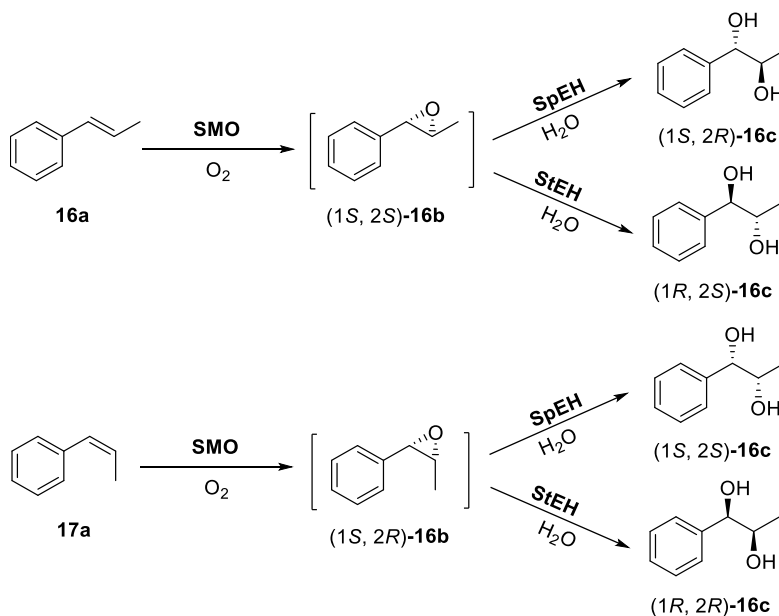
Scheme 4.7. Enantioselective *trans*-dihydroxylation of nonterminal aryl olefins **16a** and **17a** with *E. coli* (SSP1) (SMO & SpEH) to produce vicinal diols (1*S*, 2*R*)-**16c** and (1*S*, 2*S*)-**16c**, and with *E. coli* (SST1) (SMO & StEH) to produce vicinal diols (1*R*, 2*S*)-**16c** and (1*R*, 2*R*)-**16c**, respectively.

To prepare vicinal diols with two chiral centres and evidently distinguish our *trans*-dihydroxylation with Sharpless *cis*-dihydroxylation, we tested the dihydroxylation of nonterminal olefin substrates **16a** and **17a** with our catalysts (Scheme 4.7). The *trans*-dihydroxylation was also performed in a two-phase system with resting cells as catalysts. As shown in Table 4.4, *trans*-dihydroxylation of **16a** and **17a** with *E. coli* (SST1) gave (1*R*, 2*S*)-**16c** and (1*R*, 2*R*)-**16c** in excellent *ee* (>98%) and *de* (≥98%), respectively. The configuration of **16c** was established by comparing bioproducts with the standard diols that were prepared via Sharpless asymmetric dihydroxylation (Figure S2.16-S2.17, Appendix II). The yields (96% and 89%) and the specific activities (15 and 20 U/g cdw) were also high. On the other hand, *trans*-dihydroxylation of *β*-methyl styrenes **16a** and **17a** with *E. coli* (SSP1) afforded (1*S*, 2*R*)-**16c** in 94.2% *ee* and 91.8% *de* and (1*S*, 2*S*)-**16c** in 85.6% *ee* and >99% *de*, respectively. The regioselectivity and the yield for the hydrolysis were decreased possibly as a result of the steric hindrance of a *β*-methyl group in the epoxide intermediate to the hydrolysis at the *β* position with SpEH. Nevertheless, the product *ee* and *de* were still quite high. The great achievement here was the production of all four stereoisomers of 1-phenyl-1,2-propanediol **16c** in high *ee* and *de* by the *trans*-dihydroxylation of *trans*-alkene **16a** and *cis*-alkene **17a** with the two complementary biocatalysts, respectively. In comparison, the elegant Sharpless dihydroxylation has difficulty in transforming *cis*-alkene such as **17a** with high selectivity.[315]
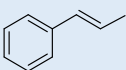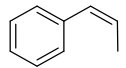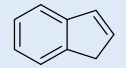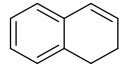
4.3.7 Asymmetric *trans*-Dihydroxylation of Cyclic Aryl Olefins with Resting Cells of *E. coli* (SSP1) and *E. coli* (SST1)

18a-19a   (1*S*, 2*R*)-**18b-19b**   (1*R*, 2*R*)-**18c-19c**

18a-c: n = 1   **19a-c**: n = 2
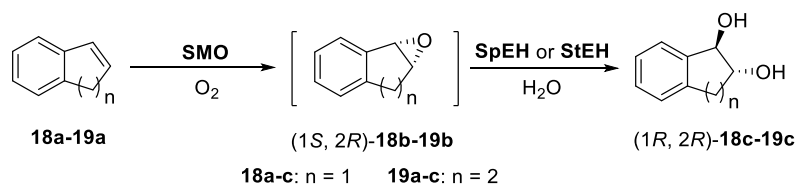
Scheme 4.8. Enantioselective *trans*-dihydroxylation of aryl cyclic olefins **18a** and **19a** with *E. coli* (SSP1) (SMO & SpEH) or *E. coli* (SST1) (SMO & StEH) to produce vicinal diols (1*R*, 2*R*)-**18c** and (1*R*, 2*R*)-**19c**.

101

The *trans*-dihydroxylation of cyclic aryl olefins **18a** and **19a** (Scheme 4.8) was performed with resting cells of *E. coli* (SSP1) and *E. coli* (SST1). As shown in Table 4.4, *E. coli* (SSP1) gave (1*R*, 2*R*)-**18c** and (1*R*, 2*R*)-**19c** in very high *ee* (>96%), *de* (>98%), and yield (73-80%) from **18a** and **19a**, respectively. The configurations of **18c–19c** were established by comparing bioproducts with the standard diols that were commercially available (Figure S2.18-S2.19, Appendix II). The unexpected change of the enantioselectivity of the dihydroxylation was possibly caused by the change of the regioselectivity of SpEH in *E. coli* (SSP1) to the cyclic epoxides **18b** and **19b**. On the other hand, *E. coli* (SST1) also produced (1*R*, 2*R*)-**18c** and (1*R*, 2*R*)-**19c** in very high *ee* (>96%), *de* (>98%), and yield (67-71%) from **18a** and **19a**, respectively. These results demonstrated once again the unique potential of *E. coli* (SSP1) and *E. coli* (SST1) in asymmetric *trans*-dihydroxylation of *cis*-alkenes. In comparison, Sharpless dihydroxylation has difficulty with *cis*-alkenes as starting materials and could not produce *trans*-vicinal diols (1*R*, 2*R*)-**18c** and (1*R*, 2*R*)-**19c** from *cis*-alkenes **18a** and **19a**.[315]

Table 4.4. Enantioselective *trans*-dihydroxylation of nonterminal aryl olefins **16a**, **17a** and aryl cyclic olefins **18a**, **19a** with resting cells of *E. coli* (SSP1) and *E. coli* (SST1), respectively.

Substrate[a]	Catalyst	Act. (U/g cdw)[b]	Conv. (%)[c]	Prod.	Yield (%)[d]	*ee* (%)[e]	*de* (%)[f]
16a	*E. coli* (SSP1)	23	80	(1*S*, 2*R*)-**16c**	22	94[g]	91.8
	E. coli (SST1)	15	>99	(1*R*, 2*S*)-**16c**	96	>98[g]	98.0
17a	*E. coli* (SSP1)	19	94	(1*S*, 2*S*)-**16c**	75	85.6	>99
	E. coli (SST1)	20	97	(1*R*, 2*R*)-**16c**	89	98.8	>99
18a	*E. coli* (SSP1)	28	97	(1*R*, 2*R*)-**18c**	80	98.0	98.8
	E. coli (SST1)	20	98	(1*R*, 2*R*)-**18c**	71	96.1	98.1
19a	*E. coli* (SSP1)	4	75	(1*R*, 2*R*)-**19c**	73	96.8	>99
	E. coli (SST1)	4	69	(1*R*, 2*R*)-**19c**	67	99.6	>99

[a-e] same to table 4.3. [f] *de* value was determined by chiral HPLC analysis. Error limit: 0.2% of the state values. [g] Error limit: 0.5% of the state values.
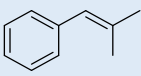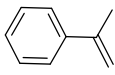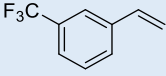
4.3.8 Asymmetric *trans*-Dihydroxylation of Other Aryl Olefins with Resting Cells of *E. coli* (SSP1) and *E. coli* (SST1)

$$21a\text{-}c: R_1 = CH_3, R_2 = H \qquad 22a\text{-}c: R_1 = H, R_2 = CF_3$$
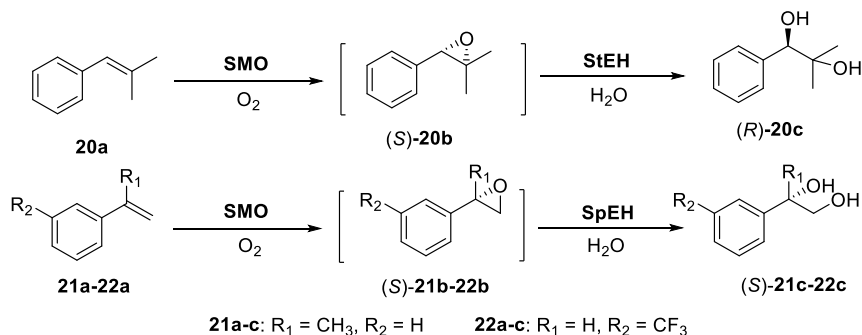
Scheme 4.9. Enantioselective dihydroxylation of aryl olefins **20a–22a** with *E. coli* (SSP1) (expressing SMO and SpEH) or *E. coli* (SST1) (expressing SMO and StEH) to produce vicinal diols (*R*)-**20c**, (*S*)-**21c**, and (*S*)-**22c**.

We further tested *E. coli* (SSP1) and *E. coli* (SST1) for the dihydroxylation of substituted olefins (**20a–22a**) (Scheme 4.9, Table 4.5) in a two-liquid phase system with the resting cells as catalysts. With two methyl groups on the β carbon, **20a** could not be converted to (*S*)-**20c** in high *ee* by *E. coli* (SSP1) due to the huge steric hindrance at the β position for the hydrolysis with SpEH. On the other hand, dihydroxylation of **20a** with *E. coli* (SST1) gave (*R*)-**20c** in 98.2% *ee* and 83% yields. In contrary, dihydroxylation of **21a** and **22a** with *E. coli* (SSP1) afforded (*S*)-**21c** in 94.5% *ee* and (*S*)-**22c** in 97.6% *ee*, respectively. But dihydroxylation of **21a** and **22a** with *E. coli* (SST1) failed to produce (*R*)-**21c** and (*R*)-**22c**, which is probably due to the poor α-regioselectivity of StEH to the corresponding epoxide intermediates. The configurations of **20c–22c** were established by comparing bioproducts with the standard diols that were prepared via Sharpless asymmetric dihydroxylation (Figure S2.20-2.22, Appendix II).

Table 4.5. Enantioselective dihydroxylation of aryl olefins **20a–22a** with resting cells of *E. coli* (SSP1) and *E. coli* (SST1), respectively.

Substrate[a]	Catalyst	Act. (U/g cdw)[b]	Conv. (%)[c]	Prod.	Yield (%)[d]	*ee* (%)[e]
20a	*E. coli* (SSP1)	16	76	(*S*)-**20c**	11	3.4
	E. coli (SST1)	17	80	(*R*)-**20c**	83[f]	98.2
21a	*E. coli* (SSP1)	8	62	(*S*)-**21c**	56	94.5
	E. coli (SST1)	11	68	(*S*)-**21c**	24	46.0
22a	*E. coli* (SSP1)	2	41	(*S*)-**22c**	46[f]	97.6
	E. coli (SST1)	3	22	(*S*)-**22c**	13	74.0

[a-f] same to table 4.3.

4.3.9 Preparation of 10 Vicinal Diols with Resting Cells of *E. coli* (SSP1) or *E. coli* (SST1)

To further demonstrate the synthetic potential of *trans*-dihydroxylation via cascade biocatalysis, we carried out the preparation of 10 valuable vicinal diols from 7 aryl olefins **1a**, **2a**, **5a**, **9a**, **12a**, **16a**, **17a** on 50 mL scale with the resting cells of *E. coli* (SSP1) or *E. coli* (SST1). The syntheses were performed at substrate concentration of 50 mM (based on total reaction volume) in a modified two-phase system containing 45 mL aqueous KP buffer and 5 mL *n*-hexadecane. The reactions were monitored by TLC by checking the disappearance of substrates. After 5–8 h, the reactions were stopped, and the products were separated and purified by flash chromatogram. All 10 useful and valuable vicinal diols (*S*)-**1c**, (*S*)-**2c**, (*S*)-**5c**, (*S*)-**9c**, (*S*)-**12c**, (*R*)-**1c**, (*R*)-**2c**, (*R*)-**9c**, (1*R*,2*S*)-**16c**, and (1*R*,2*R*)-**16c** were obtained in high *ee* (92.4–98.6%), *de* (*de* ≥ 98%, if applicable), and good isolated yield (70.6–85.5%) (Table 4.6). The dihydroxylation via cascade biocatalysis gave around 0.3 g of product/g of cells. In the representative procedure of Sharpless asymmetric dihydroxylation,[315] 1.4 g AD-mix-α was used for the dihydroxylation of 1 mmol of olefin, corresponding to about 0.1 g of product/g of catalyst. In our cascade biocatalysis for *trans*-dihydroxylation of olefins,

whole cells are used as the less expensive and greener catalyst, molecular oxygen is used as the less expensive and green oxidant, and water is used for the epoxide hydrolysis. The green and efficient cascade biocatalysis provides practical syntheses of the useful and valuable vicinal aryl diols in high *ee* and high yield.

Table 4.6. Preparation of (*R*)- or (*S*)- vicinal diols in high *ee* by enantioselective dihydroxylation of aryl alkenes with resting cells of *E. coli* (SSP1) or *E. coli* (SST1).

Sub.[a]	Catalyst	Time (h)	Prod.	Isolated (g)	Yield (%)	*ee* (%)[b]	*de* (%)[c]	Prod./cells (g/g cdw)
1a	*E. coli* (SSP1)	5	(*S*)-**1c**	0.295	85.5	96.3	n.a.[d]	0.30
1a	*E. coli* (SST1)	5	(*R*)-**1c**	0.289	83.8	95.8	n.a.	0.29
2a	*E. coli* (SSP1)	6	(*S*)-**2c**	0.299	76.7	96.7	n.a.	0.30
2a	*E. coli* (SST1)	5	(*R*)-**2c**	0.325	80.7	96.7	n.a.	0.33
5a	*E. coli* (SSP1)	8	(*S*)-**5c**	0.279	73.4	92.4	n.a.	0.28
9a	*E. coli* (SSP1)	8	(*S*)-**9c**	0.326	75.6	96.5	n.a.	0.33
9a	*E. coli* (SST1)	8	(*R*)-**9c**	0.304	70.6	96.3	n.a.	0.30
12a	*E. coli* (SSP1)	6	(*S*)-**12c**	0.358	85.3	96.8	n.a.	0.36
16a	*E. coli* (SST1)	7	(1*R*,2*S*)-**16c**	0.313	82.3	>98[e]	98.2	0.31
17a	*E. coli* (SST1)	8	(1*R*,2*R*)-**16c**	0.300	78.8	98.6	>99	0.30

[a] The reactions were performed with substrates (50 mM based on total volume) and resting cells (20 g cdw/L) in a two-liquid phase system (50 mL) consisting of KP buffer (200 mM, pH 8.0, 2% glucose) and *n*-hexadecane (9:1) at 30 °C. [b] *ee* value was determined by chiral HPLC analysis. Error limit: 0.2% of the state values. [c] *de* value was determined by chiral HPLC analysis. Error limit: 0.2% of the state values. [d] n.a.: not applicable. [e] Error limit: 0.5% of the state values.

Table 4.7. Physical properties, ^{1}H NMR analysis, and optical rotations of chiral vicinal diols prepared by using *E. coli* (SSP1) or *E. coli* (SST1).

Prod.	Appearance	^{1}H NMR chemical shift [a]	$[\alpha]_D$ [b]	Lit. $[\alpha]_D$
(*S*)-1c	White solid	7.23–7.38 (m, 5H, ArH), 4.79–4.82 (m, 1H), 3.62–3.76 (m, 2H), 2.50–2.78 (br, 2H, OH).	$[\alpha]_D^{25}$: +36.8° (*c* 1.0, EtOH)	$[\alpha]_D^{23}$: +38.4° (*c* 4.38, EtOH)[283]
(*R*)-1c	White solid	7.26–7.37 (m, 5H, ArH), 4.76–4.79 (dd, *J* = 8.4, 3.2 Hz, 1H), 3.70–3.74 (dd, *J* = 11.6, 3.2 Hz, 1H), 3.60–3.65 (dd, *J* = 11.6, 8.4 Hz, 1H), 3.05–3.20 (br, 2H, OH).	$[\alpha]_D^{26}$: -38.2° (*c* 1.0, EtOH)	$[\alpha]_D^{25}$: -37.8° (*c* 1.0, EtOH)[338]
(*S*)-2c	White solid	7.26–7.34 (m, 2H, ArH), 7.01–7.06 (t, *J* = 8.8, 2H, ArH), 4.77–4.80 (dd, *J* = 8.4, 3.2 Hz, 1H), 3.70–3.74 (dd, *J* = 11.2, 3.2 Hz, 1H), 3.58–3.63 (dd, *J* = 11.2, 8.4 Hz, 1H), 2.52–2.75 (br, 2H, OH).	$[\alpha]_D^{27}$: +63.6° (*c* 1.0, CHCl$_3$)	$[\alpha]_D^{30}$: +62.8° (*c* 1.0, CHCl$_3$)[339]
(*R*)-2c	White solid	7.26–7.34 (m, 2H, ArH), 7.01–7.06 (t, *J* = 8.4, 2H, ArH), 4.77–4.80 (dd, *J* = 8.4, 3.6 Hz, 1H), 3.70–3.74 (dd, *J* = 11.2, 3.2 Hz, 1H), 3.58–3.63 (dd, *J* = 11.2, 8.4 Hz, 1H), 2.50–2.72 (br, 2H, OH).	$[\alpha]_D^{27}$: -62.8° (*c* 1.0, CHCl$_3$)	$[\alpha]_D^{25}$: -58.2° (*c* 1.0, CHCl$_3$)[338]
(*S*)-5c	White solid	7.14–7.26 (m, 4H, ArH), 4.74–4.77 (dd, *J* = 8.0, 3.2 Hz, 1H), 3.68–3.72 (dd, *J* = 11.2, 3.2 Hz, 1H), 3.61–3.65 (dd, *J* = 11.6, 8.4 Hz, 1H), 2.95–3.08 (br, 2H, OH), 2.34 (s, 3H)	$[\alpha]_D^{27}$: +66.2° (*c* 1.0, CHCl$_3$)	$[\alpha]_D^{30}$: +68.5° (*c* 1.12, CHCl$_3$)[339]
(*S*)-9c	Colorless syrup	7.14–7.22 (m, 4H, ArH), 4.71–4.74 (dd, *J* = 8.0, 3.6 Hz, 1H), 3.67–3.71 (dd, *J* = 11.2, 3.2 Hz, 1H), 3.53–3.58 (dd, *J* = 11.2, 8.0 Hz, 1H), 2.36 (s, 2H, OH)	$[\alpha]_D^{25}$: +21.8° (*c* 1.0, EtOH)	$[\alpha]_D^{26}$: +21.1° (*c* 1.31, EtOH)[283]
(*R*)-9c	Colorless syrup	7.23–7.39 (m, 4H, ArH), 4.79–4.82 (dd, *J* = 8.0, 3.2 Hz, 1H), 3.75–3.79 (dd, *J* = 11.2, 3.2 Hz, 1H), 3.61–3.66 (dd, *J* = 11.2, 8.0 Hz, 1H), 2.67 (s, 2H, OH)	$[\alpha]_D^{26}$: -23.6° (*c* 1.0, EtOH)	$[\alpha]_D^{25}$: -22.5° (*c* 1.1, EtOH)[338]
(*S*)-12c	Colorless syrup	6.84–7.19 (m, 4H, ArH), 4.69–4.73 (dd, *J* = 8.0, 4.0 Hz, 1H), 3.73 (s, 3H), 3.66–3.70 (dd, *J* = 11.6, 3.6 Hz, 1H), 3.56–3.60 (dd, *J* = 11.6, 8.0 Hz, 1H), 2.43 (s, 2H, OH)	$[\alpha]_D^{25}$: +25.6° (*c* 1.0, EtOH)	$[\alpha]_D^{27}$: +26.9° (*c* 1.12, EtOH)[283]

| (**1R,2S**)-**16c** | Color-less syrup | 7.29–7.43 (m, 5H, ArH), 4.69–4.70 (d, J = 4.4 Hz, 1H), 4.01–4.07 (m, 1H), 2.17 (s, 2H, OH), 1.10–1.12 (d, J = 7.2 Hz, 3H) | $[\alpha]_D^{25}$: -16.6° (*c* 1.0, EtOH) | $[\alpha]_D^{20}$: -17.8° (*c* 1.0, EtOH)[340] |
| (**1R,2R**)-**16c** | Color-less syrup | 7.26–7.38 (m, 5H, ArH), 4.35–4.37 (d, J = 7.2 Hz, 1H), 3.82–3.89 (quint, J = 6.4 Hz, 1H), 2.52 (s, 2H, OH), 1.04–1.06 (d, J = 6.4 Hz, 3H). | $[\alpha]_D^{27}$: -51.2° (*c* 1.0, CH_2Cl_2) | $[\alpha]_D^{20}$: -51.3° (*c* 3.5, $CHCl_3$)[263] |

[a]^{1}H NMR was determined in $CDCl_3$ with TMS as internal standard using a 400 MHz Bruker NMR system (spectral see Appendix II). [b]Optical rotation was determined using a Jasco polarimeter DIP-1000.

4.3.10 Synthesis of (*R*)-1-Phenyl-1,2-ethanediol with Growing Cells in Fermentor

We further explored the potential of using growing cells of the recombinant *E. coli* strain for the dihydroxylation of aryl olefins. Dihydroxylation of styrene **1a** with *E. coli* (SST1) was chosen as a model reaction. To avoid the possible environmental concerns and reduce the additional cost, the organic phase (*n*-hexadecane) was not applied in the growing cell experiment. Instead, styrene **1a** was fed directly and slowly to the reaction mixture to alleviate the toxicity of styrene.

E. coli (SST1) was grown in a fermentor overnight to a cell density of 7 g cdw/L, glucose was fed, and IPTG was added to induce the enzyme expression. After 5 h growth, the cell density reached 20 g cdw/L, and styrene **1a** was fed to start the dihydroxylation. After 5 h biotransformation with the growing cells, 120 mM (16.6 g/L) (*R*)-1-phenyl-1,2-ethanediol **1c** was produced in 96.2% *ee* with an average volumetric productivity of 3.3 g/L/h for the reaction period. The enantioselectivity of the dihydroxylation with growing cells was the same as that with resting cells. Thus, the cascade biocatalysis for enantioselective dihydroxylation can be performed with either growing cells or resting cells as catalysts, it can also be carried out in either aqueous phase or a two-phase system, and it can be easily scaled up by using a fermentor. The use of growing cells as the catalyst may further improve the product titer and

107

volumetric productivity. Further optimization of the process could make the cascade biocatalysis even more practical for the enantioselective *trans*-dihydroxylation of aryl olefins.

4.4 Conclusion

E. coli (SSP1) cells coexpressing styrene monooxygenase (SMO) and epoxide hydrolase SpEH were developed as a green and efficient biocatalyst for *S*-enantioselective dihydroxylation of aryl olefins via intracellular cascade epoxidation and hydrolysis. The *S*-enantioselectivity was generated by SMO-catalyzed *S*-selective epoxidation and SpEH-catalyzed regioselective hydrolytic opening of the (*S*)-epoxide at the *β* position. Dihydroxylation of terminal aryl olefins **1a–15a** with resting cells of *E. coli* (SSP1) offered (*S*)-vicinal diols **1c–15c** in high *ee* (97.5-98.6% for 10 diols; 92.2–93.9% for 3 diols) and high yield (91%-99% for 6 diols; 86-88% for 2 diols; 67-73% for 3 diols).

Combining SMO and epoxide hydrolase StEH showing an *α* opening of aryl epoxides for the cascade biocatalysis gave rise to *R*-enantioselective dihydroxylation of aryl olefins. *E. coli* (SST1) coexpressing SMO and StEH was also engineered as a green and efficient biocatalyst for *R*-dihydroxylation of aryl olefins, being complementary to *E. coli* (SSP1). Dihydroxylation of terminal aryl olefins **1a–15a** with resting cells of *E. coli* (SST1) afforded (*R*)-vicinal diols **1c–15c** in high *ee* (94.2–98.2% for 7 diols; 84.2-89.9% for 6 diols) and high yield (90-99% for 7 diols; 85-89% for 4 diols; 65% for 1 diol). To the best of our knowledge, it is the first report of reversing the overall enantioselectivity of cascade biocatalysis by changing the regioselectivity in an individual reaction step, which will help to solve the problem of lacking mirror-image enzymes in biocatalysis.

E. coli (SSP1) and *E. coli* (SST1) catalyzed the *trans*-dihydroxylation of either *trans*-aryl olefin **16a** or *cis*-aryl olefin **17a** with excellent and complementary stereoselectivity, giving each of the four stereoisomers of 1-phenyl-1,2-propanediol **16c** in high *ee* and *de*, respectively. Both strains catalyzed the *trans*-dihydroxylation of aryl cyclic olefins **18a** and **19a** to afford the same *trans*-cyclic diols (1*R*, 2*R*)-**18c** and (1*R*, 2*R*)-**19c**, respectively, in excellent *ee* and *de*. This type of cascade biocatalysis provides a complementary tool to Sharpless dihydroxylation, accepting *cis*-alkene and offering enantioselective *trans*-dihydroxylation.

Preparative dihydroxylations with the resting cells of *E. coli* (SSP1) or *E. coli* (SST1) were successfully demonstrated to prepare five (1*S*)-vicinal diols and five (1*R*)-vicinal diols in high *ee* (92.4–98.6%) with high isolated yield (70.6–85.5%). Growing cells of *E. coli* (SST1) were also proven to be a good catalyst for the enantioselective dihydroxylation of styrene **1a** to produce 120 mM (16.6 g/L) (*R*)-1-phenyl-1,2-ethanediol **1c** (96.2% *ee*) in a bioreactor (1 L).

The cascade biocatalysis for dihydroxylation of olefins reported here utilizes molecular oxygen as an inexpensive and green oxidant and water as a simple reagent, thus being sustainable. The developed catalysts show a relatively broad substrate range for aryl olefins, high and complementary enantioselectivity, high activity and yield, thus being useful for the production of several useful and valuable enantiopure vicinal diols and deserving further development for potential industrial application. The reported concept and methodology on engineering efficient, enantioselective, and enantiocomplementary catalysts could be extended to the development of new biocatalysts for enantioselective *trans*-dihydroxylation of other types of olefins by combining other monooxygenases and EHs. Furthermore, this epoxidation-hydrolysis cascade could be utilized to build more complex biocatalytic cascades to achieve even more challenging transformations (See Chapter 5).

5 MODULAR CASCADE BIOCATALYSIS: ASYMMETRIC OXY- AND AMINO-FUNCTIONALIZATION OF ARYL ALKENES AND UTILIZATION OF BIO-BASED PHENYLALANINE
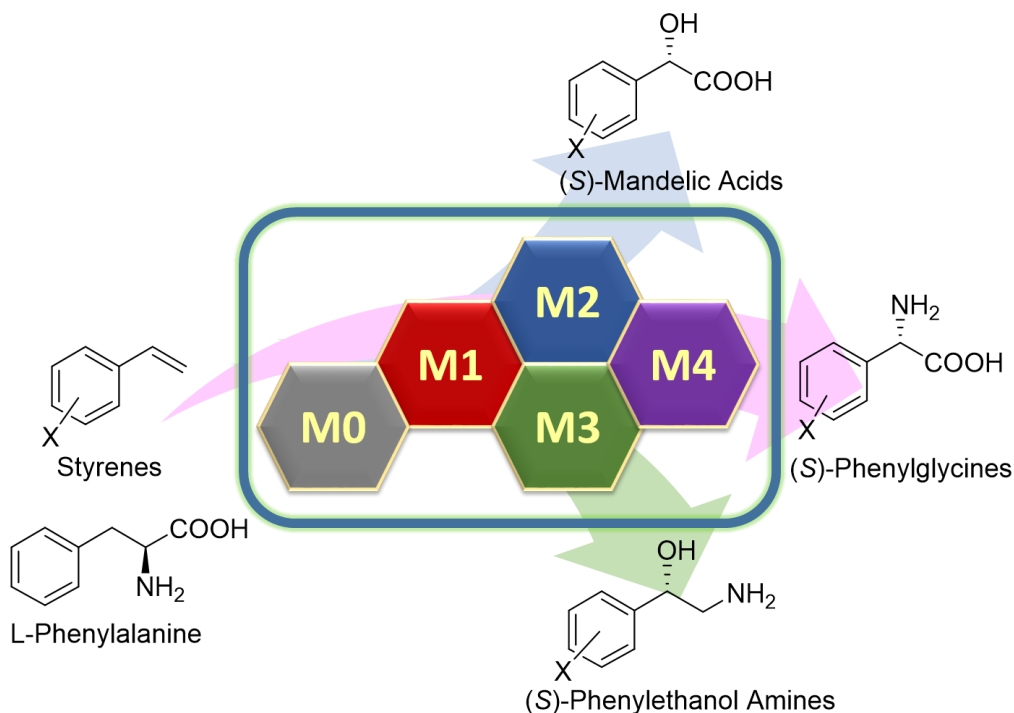
Figure 5.1. Asymmetric oxy- and amino-functionalization of alkenes to chiral hydroxy acids, amino alcohols, and amino acids, with recombinant *E. coli* containing different modules.

5.1 Introduction

Terminal alkenes are ideal starting materials for organic synthesis because they are manufactured on very large scales from petroleum feedstock. Regio- and enantio-selective functionalization of alkenes via various chemicals transformations with appropriate catalysts provides a facile access to a wide range of bulk and specialty chemicals. Many advances of selective alkene functionalization with chemical catalysts were recently reported, such as palladium-catalyzed selective oxidation,[341, 342] iron-catalyzed regioselective hydrosilylation,[343] rhodium-catalyzed stereoselective

aziridination,[344] ruthenium-catalysed alkoxycarbonylation,[345] and photoredox catalyzed regioselective hydrohalogenation.[346] On the other hand, nature provides enzymes as promising alternative catalysts for various types of selective chemical transformations in mild conditions with green and easily available reagents, such as oxygen, ammonia, and glucose.[16-27] Regarding to functionalization of alkenes, a number of enzymatic transformations were reported: epoxidation with monooxygenase or peroxidase,[129, 169, 170, 347] dihydroxylation with dioxygenase,[316, 317] hydration with hydratase or decarboxylase,[348-351] and more recently created cyclopropanation with engineered P450 monooxygenase.[87, 88]

However, one-step transformation with either chemo- or bio-catalysts is limited in accessible chemical space. A possible solution is performing multiple catalyzed reactions in one pot concurrently, namely, cascade/tandem catalysis, which enables facile access to more diverse structures in new ways.[232-234] Recent breakthroughs in cascade selective functionalization of alkenes include anti-Markovnikov hydration via oxidation-hydrolysis-reduction with palladium-acid-ruthenium catalysis,[352] enantioselective diboration-cross-coupling with platinum-palladium catalysis,[353] and selective metathesis-epoxidation with ruthenium-P450 monooxygenase catalysis.[354] In comparison with cascade chemocatalysis or cascade hybrid catalysis,[355, 356] cascade biocatalysis could maintain the green and inexpensive advantages of enzymes (*e.g.* without involving toxic and precious metals) and it is also easy to achieve because of natural compatibility of enzymes.[34-40] Over the years, a variety types of non-natural biocatalytic cascades have been developed.[235-281] Nevertheless, no cascade biocatalysis was reported for enantioselective functionalization of hydrocarbons (alkanes and alkenes), except for the epoxidation-hydrolysis cascade (Chapter 4) we developed for asymmetric *trans*-dihydroxylation of alkenes,[247, 248] which could be achieved via similar one-step *cis*-dihydroxylation with Sharpless method[315] or dioxygenase.[316, 317]
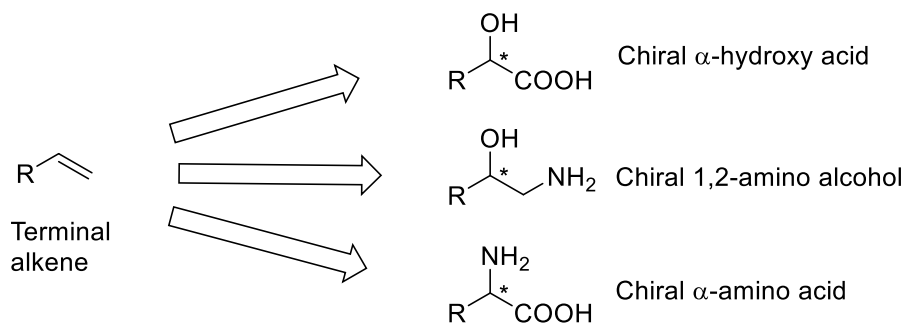
Scheme 5.1. Cascade biocatalysis for one-pot conversion of terminal alkene to chiral α-hydroxyl acid, 1,2-amino alcohol, and α-amino acid.

To address this significant gap, we are interested in developing novel and efficient cascade biocatalysis for oxy- and amino-functionalization of terminal alkene to produce chiral α-hydroxyl acid, 1,2-amino alcohol, and α-amino acid in a highly regio- and enantio-selective manner (Figure 5.1, Scheme 5.1). These three transformations are very useful but significantly challenging in chemistry. Enantiopure α-hydroxyl acid,[357] 1,2-amino alcohol,[358] and α-amino acid[359, 360] are three very important groups of chiral chemicals with broad applications, such as building blocks for bioactive compounds and chiral ligands/auxiliaries for asymmetric synthesis. The transformation of terminal alkene to hydroxyl acid or amino acid represents unequal oxidation of the two alkene carbons to one low (0) and one high (+3) oxidation states, which is very challenging in traditional chemistry, because weak oxidants (*e.g.* OsO_4) oxidize both carbons to low oxidation states (0, +1), while strong oxidants (*e.g.* O_3) usually cleave the double bond and oxidize both carbons to high oxidation states (+2, +3).[361] Further providing enantioselectivity poses additional challenge. On the other hand, the transformation of alkene to 1,2-amino alcohol could be achieved with Sharpless asymmetric aminohydroxylation (oxyamination),[362, 363] but chemical aminohydroxylation methods are still difficult to simultaneously control both regio- and enantio-selectivity excellently, and unable to use inexpensive ammonia as nitrogen source for synthesizing primary amine.[364] Herein, the cascade biocatalysis developed in this thesis represents a novel one-pot synthetic route and provides a unique approach

for green and efficient production of chiral α-hydroxyl acids, 1,2-amino alcohols, and α-amino acids.

5.2 Experimental Section

5.2.1 Chemicals, Strains, and Materials

The chemicals, strains, and materials which have been used in Chapter 3 and Chapter 4 were not listed here. Please refer to section 3.2.1 and 4.2.1 for detail.

All the chemicals and solvents were directly purchased from the commercial suppliers and used without further purification. Chemicals from Sigma-Aldrich: mandelic acid (≥99%), (*R*)-(−)-mandelic acid (≥99%), 3-fluoromandelic acid (98%), (*R*)-4-fluoromandelic acid (98%), 3-chloromandelic acid (98%), (*R*)-3-chloromandelic acid (97%), (*R*)-4-chloromandelic acid (98%), 3-methylmandelic acid (97%), 2-amino-1-phenylethanol (98%), (*R*)-(−)-2-amino-1-phenylethanol (97%), phenylglyoxylic acid (97%), L-phenylglycine (99%), *trans*-cinnamic acid (≥99%), L-alanine (≥99%),L-glutamic acid monosodium salt monohydrate (≥98%). Chemicals from Alfa Aesar: (*S*)-(+)-mandelic acid (≥99%), 4-chloromandelic acid (98%), 4-fluoromandelic acid (98%), (*R*)-(−)-4-methylmandelic acid (98%), D-phenylglycine (99%). Chemicals from TCI: 2-fluoromandelicAcid (>98%).

1 L M9 medium containing: 8.5 g $Na_2HPO_4 \cdot 2H_2O$, 3.0 g KH_2PO_4, 0.5 g NaCl, 1.0 g NH_4Cl, 2 mL $MgSO_4$ solution (1M), 1 mL $CaCl_2$ solution (0.1M), 1 mL 1000X MT solution (8.3 g/L $FeCl_3 \cdot 6H_2O$, 0.84 g/L $ZnCl_2$, 0.13 g/L $CuCl_2 \cdot 2H_2O$, 0.1 g/L $CoCl_2 \cdot 2H_2O$, 0.1 g/L H_3BO_3, 0.016 g/L $MnCl_2 \cdot 4H_2O$, adding EDTA to dissolve), 20 g/L glucose, and 6 g/L yeast extract.

Other biochemicals and strains are the same to Chapter 3 and Chapter 4.

5.2.2 Analytical Methods

The concentration of many substrates, intermediates, and products from biotransformations was determined using a Shimadzu prominence reverse phase HPLC system with an Agilent Poroshell 120 SB-C18 column (150 × 4.6 mm, 2.7 µm) and UV detection at 210 nm. Conditions: 70% water (with 0.1% TFA): 30% acetonitrile, flow rate: 0.5 mL min^{-1}. The following is the retention times: phenylglycine (3.2 min), phenylalanine (3.4 min), phenylethanol amine (3.4 min), phenylethane diol (4.5 min), mandelic acid (4.9 min), hydroxy(phenyl)acetaldehyde (6.0 min), phenylglyoxylic acid (6.2 min), benzyl alcohol (internal standard, 7.3 min). The concentration of styrene substrates was quantified using a Shimadzu prominence normal phase HPLC system with an Agilent Zorbax Rx-SIL column (150 × 4.6 mm, 5 µm) and UV detection at 210 nm. Condition: 10% IPA: 90% *n*-hexane, flow rate: 1.0 mL min^{-1}. The retention times for most of the styrenes are from 1 to 2 min.

The *ee* values of mandelic acids were determined by chiral HPLC using a Shimadzu prominence HPLC system (normal phase) and UV detection at 210 nm with a Daicel AS-H, or IA-3 chiral column (250 × 4.6 mm, 5µm) with 10% IPA: 90% *n*-Hex (containing 0.1% TFA) at 0.5 mL min^{-1}. Retention times for mandelic acid using IA-3 column: (*S*)-mandelic acid (21.5 min), (*R*)-mandelic acid (23.5 min). Retention times for 3-chloromandelic acid using AS-H column: (*S*)-3-chloromandelic acid (21.2 min), (*R*)-3-chloromandelic acid (19.5 min). Retention times for 3-methylmandelic acid using AS-H column: (*S*)-3-methylmandelic acid (20.8 min), (*R*)-3-methylmandelic acid (19.8 min).

5.2.3 Genetic Engineering of Module 1, Module 2, Module 3, Module 4, and Module 0

Construction of Module 1 (*styA-styB-spEH*): Module 1 is the same construct of previous SSP1, an operon of *styA*, *styB*, and *spEH* genes (see Chapter 4). R-M1 represents the recombinant plasmid pRSFduet (Novagen) containing Module 1. To sub-cloning of this operon to other plasmids, primers StyA-BspHI-F and SpEH-XhoI-

R (see Table 5.1 for a full list of primers) were used to amplify the Module 1 from R-M1 with Phusion DNA polymerase according to the instruction. The PCR product was subjected to double digestion with BspHI and XhoI (FastDigest, Thermo Scientific). And the other three vectors, pACYCduet, pCDFduet, and pETduet (Novagen) were also subjected to digestion with NcoI and XhoI. Then ligation of digested PCR product and vectors was performed with T4 DNA ligase (Thermo Scientific), and then the ligation products were used for transformation (heat shock) of chemical competent *E. coli* cells (T7 Express strain, New England Biolabs). The sub-cloning of Module 1 to pACYCduet, pCDFduet, and pETduet gave A-M1, C-M1, and E-M1, respectively.

Construction of Module 2 (*alkJ-aldh*): The *alkJ* gene was amplified from the OCT megaplasmid from *Pseudomonas putida* GPo1[186, 187] using primers AlkJ-BamHI-F and AlkJ-BglII-R (Table 5.1) and Phusion DNA polymerase. The PCR product were double digested with BamHI and BglII, and then ligated to same digested pRSFduet with T4 DNA ligase. The ligation product was transformed (heat shock) into *E. coli* T7 Expression competent cells to give pRSF-AlkJ. On the other hand, the aldh gene was amplified from the genome of *E. coli* K12 MG 1655 using primers EcALDH-BglII-RBS-F and EcALDH-XhoI-R (Table 5.1). The PCR product was double digested with BglII and XhoI, and then ligated to same digested pRSF-AlkJ with T4 DNA ligase. The ligation product was transformed (heat shock) into *E. coli* T7 Expression competent cells to give Module 2 on pRSFduet plasmid, namely R-M2. Similar to Module 1, Module 2 was also sub-cloning to other three vectors by the following procedures. Module 2 operon was amplified with primers AlkJ-BamHI-F and EcALDH-XhoI-R (Table 5.1), digested with BamHI and XhoI, and then ligated to double digested pACYCduet, pCDFduet, and pETduet. The transformation of these products gave A-M2, C-M2, and E-M2, respectively.

Table 5.1. Primers (DNA oligos) used for construction of Module 0-4.

Name	Sequence

StyA-BspHI-F	ACTG<u>TCATGA</u>AAAAGCGTATCGGTATTGTTGG
SpEH-XhoI-R	ATCG<u>CTCGAG</u>TCAAAGATCCATCTGTGCAAAGGCC
AlkJ-BamHI-F	ACTG<u>GGATCC</u>GATGTACGACTATATAATCGTTGGTGCTG
AlkJ-BglII-R	ACTG<u>AGATCT</u>TACATGCAGACAGCTATCATGGCC
EcALDH-BglII-RBS-F	CG<u>AGATCT</u>TAAGGAGATATATA ATGACAGAGCCGCATGTAGCAGTATTA
EcALDH-XhoI-R	ACTG<u>CTCGAG</u>TTAATACCGTACACACACCGACTTAG
CvTA-BglII-RBS-F	CG<u>AGATCT</u>TAAGGAGATATATA ATGCAAAAACAACGCACCACCTCAC
CvTA-XhoI-EcoRI-R	ACTG<u>CTCGAG</u>GAATTC TTACGCCAGGCCACGAGCTTTCAG
AlaDH-EcoRI-RBS-F	ACTG<u>GAATTC</u>TAAGGAGATATATA ATGATCATAGGGGTTCCTAAAGAGAT
AlaDH-XhoI-R	ACTG<u>CTCGAG</u>TTAAGCACCCGCCACAGATGATTCA
HMO-BspHI-F	ACTG<u>TCATGA</u>TGCGTGAACCGCTGACGCTGGATG
HMO-EcoRI-R	ACTG<u>GAATTC</u>TTAGCCGTGAGAACGATCGCGATGC
IlvE-EcoRI-RBS-F	ACTG<u>GAATTC</u>TAAGGAGATATATA ATGACCACGAAGAAAGCTGATTACA
IlvE-BglII-R	ACTG<u>AGATCT</u>TTATTGATTAACTTGATCTAACCAGCCC
GluDH-BglII-RBS-F	ACTG<u>AGATCT</u>TAAGGAGATATATA ATGGATCAGACATATTCTCTGGAGTC
GluDH-KpnI-R	ACTG<u>GGTACC</u>TTAAATCACACCCTGCGCCAGCATC
KatE-KpnI-RBS-F	ACTG<u>GGTACC</u>TAAGGAGATATATA ATGTCGCAACATAACGAAAAGAACC
KatE-XhoI-R	ACTG<u>CTCGAG</u>TCAGGCAGGAATTTTGTCAATCTTAG
AtPAL-NdeI-F	ACTG<u>CATATG</u>GATCAAATCGAAGCAATGTTGTG
AtPAL-XhoI-R	ACTG<u>CTCGAG</u>TTAGCAAATCGGAATCGGAGCTCC
AnOhbA-BspHI-F	ACTG<u>TCATGA</u>GCGCGCAACCTGCGCACCTG
AnOhbA-EcoRI-R	ACTG<u>GAATTC</u>TTAGTTACTGAAGCCCATTTTGGTC
AnPAD-EcoRI-RBS-F	ACTG<u>GAATTC</u>TAAGGAGATATATC ATGTTCAACTCACTTCTGTCCGGC

AnPAD-PstI-R	ACTG<u>CTGCAG</u>TTATTTTTCCCAACCATTCCAACG

Construction of Module 3 (*alkJ-cvωTA-aladh*): The *cvωTA* gene was first synthesized and codon optimized for *E. coli* according to the published gene sequence[208] (see Appendix III for the synthesized DNA sequence, Genscript). Using this synthesized DNA as template, the gene was amplified using primers CvTA-BglII-RBS-F and CvTA-XhoI-EcoRI-R (Table 5.1) and Phusion DNA polymerase. The PCR product was double digested with BglII and XhoI, and then ligated to pRSF-AlkJ (digested with BglII and XhoI) with T4 DNA ligase. The ligation product was transformed (heat shock) into *E. coli* T7 Expression competent cells to give pRSF-AlkJ-CvTA. On the other hand, *aladh* gene was amplified from the genome of *Bacillus subtilis* str.168 using primers AlaDH-EcoRI-RBS-F and AlaDH-XhoI-R (Table 5.1). The PCR product was double digested with EcoRI and XhoI, and then ligated to pRSF-AlkJ-CvTA (digested with EcoRI and XhoI). The ligation product was transformed (heat shock) into *E. coli* T7 Expression competent cells to give Module 3 on pRSFduet plasmid, namely R-M3. Similarly, Module 3 was also sub-cloned to other three vectors by the following procedures. Module 3 operon was amplified with primers AlkJ-BamHI-F and AlaDH-XhoI-R (Table 5.1), digested with BamHI and XhoI, and then ligated to double digested pACYCduet, pCDFduet, and pETduet. The transformation of these products gave A-M3, C-M3, and E-M3, respectively.

Construction of Module 4 (*hmo-ilvE-gludh-katE*): The *hmo* gene was first synthesized and codon optimized for *E. coli* according to the published gene sequence[194] (see Appendix III for the synthesized DNA sequence, Genscript). Using this synthesized DNA as template, the gene was amplified using primers HMO-BspHI-F and HMO-EcoRI-R (Table 5.1). The PCR product was double digested with BspHI and EcoRI, and then ligated to pRSF (digested with NcoI and EcoRI) with T4 DNA ligase. The ligation product was transformed (heat shock) into *E. coli* T7 Expression

117

competent cells to give pRSF-HMO. Next, *ilvE* gene was amplified from the genome of *E. coli* K12 MG 1655 using primers IlvE-EcoRI-RBS-F and IlvE-BglII-R (Table 5.1). The PCR product was digested with EcoRI and BglII, ligated to pRSF-HMO (digested with EcoRI and BglII), and then transformed (heat shock) into *E. coli* T7 Expression competent cells to yield pRSF-HMO-IlvE. Similarly, *gludh* gene was amplified from the genome of *E. coli* K12 MG 1655 using primers GluDH-BglII-RBS-F and GluDH-KpnI-R (Table 5.1). The PCR product was digested with BglII and KpnI, ligated to pRSF-HMO-IlvE (digested with BglII and KpnI), and then transformed into *E. coli* competent cells to offer pRSF-HMO-IlvE-GluDH. In the last step, *ketE* gene was amplified from the genome of *E. coli* K12 MG 1655 using primers KatE-KpnI-RBS-F and KatE-XhoI-R (Table 5.1). The PCR product was digested with KpnI and XhoI, ligated to pRSF-HMO-IlvE-GluDH (digested with KpnI and XhoI), and then transformed into *E. coli* competent cells to offer pRSF-HMO-IlvE-GluDH-KatE (Module 4 on pRSF, R-M4). Similarly, Module 4 was also sub-cloned to other three vectors by first amplified with primers HMO-BspHI-F and KatE-XhoI-R (Table 5.1), digested with BspHI and XhoI, and then ligated to double digested pACYCduet, pCDFduet, and pETduet. The transformation of these products gave A-M4, C-M4, and E-M4, respectively.

Construction of Module 0 (*ohbA-padA-pal*): The *ohbA* and *padA* genes were first synthesized and codon optimized for *E. coli* according to the published gene sequence from *Aspergillus niger*[394, 396] (see Appendix III for the synthesized DNA sequence, Genscript). Using the synthesized DNA as template, the *ohbA* gene was amplified using primers AnOhbA-BspHI-F and AnOhbA-EcoRI-R (Table 5.1). The PCR product was double digested with BspHI and EcoRI, ligated to pRSF (digested with NcoI and EcoRI) with T4 DNA ligase, and then transformed into *E. coli* competent cells to give pRSF-AnOhbA. Next, *padA* gene was amplified using primers AnPAD-EcoRI-RBS-F and AnPAD-PstI-R (Table 5.1). The PCR product was digested with

EcoRI and PstI, ligated to pRSF-OhbA (digested with EcoRI and PstI), and then transformed into *E. coli* T7 Expression competent cells to yield pRSF-AnOhbA-AnPAD. On the other hand, the *pal* gene was amplified from a cDNA library of *Arabidopsis thaliana* (ATCC 77500) using primers AtPAL-NdeI-F and AtPAL-XhoI-R (Table 5.1). The PCR product was double digested with NdeI and XhoI, and then ligated to pRSF-AnOhbA-AnPAD (digested with NdeI and XhoI) with T4 DNA ligase. The ligation product was transformed into *E. coli* competent cells to offer pRSF-AnOhbA-AnPAD-AtPAL (Module 0 on pRSF, R-M0). Module 0 was also sub-cloned to pACYCduet, pCDFduet, and pETduet to give A-M0, C-M0, and E-M0, respectively. For the sub-cloning, Module 0 was first amplified with primers AnOhbA-BspHI-F and AtPAL-XhoI-R (Table 5.1), digested with BspHI and XhoI, ligated to double digested pACYCduet, pCDFduet, and pETduet, and then transformed into *E. coli* competent cells.

5.2.4 Engineering of *E. coli* Strains Containing Multiple Modules

Table 5.2 listed all the 50 *E. coli* strains and the containing modules. These strains were engineered with the following procedures.

Engineering of strains 1-12 containing Module 1 and Module 2: Four *E. coli* strains containing A-M2, C-M2, E-M2, and R-M2 were grown in 1 mL LB media containing appropriate antibiotic (50 mg/L chloramphenicol, 50 mg/L streptomycin, 100 mg/L ampicillin, or 50 mg/L kanamycin) at 37 °C for overnight. Then 100 μL culture was inoculated into 5 mL fresh LB media containing appropriate antibiotic at 37 °C until OD_{600} reached 0.5 (about 2 h). Then the cells were harvested by centrifugation (2500 g, 10 min, 4 °C) and resuspended in 1 mL cold $CaCl_2$ solution (0.1 M) on ice. The cell suspension was kept on ice and shaken at 90 rpm for 2 h, and then harvested by centrifugation (2500 g, 8 min, 4 °C) and resuspended in 0.2-0.5 mL cold $CaCl_2$ solution (0.1 M) to obtain the competent cells of *E. coli* containing A-M2, C-M2, E-M2, and R-M2, respectively. 0.5 μL of plasmid A-M1, C-M1, E-M1, and R-M1

(100-500 ng/µL) was transformed into the competent cells according to standard heat shock procedure (on ice for 30 min, 42 °C for 90 sec, ice for 5 min, recovery at 37 °C for 45 min). The recombinant cells were spread on LB agar plates with two appropriate antibiotics. The 12 combinatorial transformation leaded to strains 1-12.

Engineering of strains 13-24 containing Module 1 and Module 3: Similarly, the competent cells of *E. coli* containing A-M3, C-M3, E-M3, and R-M3 were first prepared according to above procedure, and plasmid A-M1, C-M1, E-M1, and R-M1 were transformed into the competent cells. The 12 combinatorial transformation afforded strains 13-24.

Engineering of strains 25-32 containing Module 1, Module 2, and Module 4: The competent cells of *E. coli* strain 2, 3, 5, 12 were first prepared according to above procedure, and plasmid A-M4, C-M4, E-M4, and R-M4 were transformed into the competent cells. The 8 combinatorial transformation yielded strains 25-32.

Engineering of strains 33-40 containing Module 0, Module 1, and Module 2: The competent cells of *E. coli* strain 2, 3, 5, 12 were used for transformation of plasmid A-M0, C-M0, E-M0, and R-M0. The 8 combinatorial transformation gave strains 33-40.

Engineering of strains 41-46 containing Module 0, Module 1, and Module 3: The competent cells of *E. coli* strain 13, 17, 24 were first prepared according to above procedure, and plasmid A-M0, C-M0, E-M0, and R-M0 were transformed into the competent cells. The 6 combinatorial transformation offered strains 41-46.

Engineering of strains 47-50 containing Module 0, Module 1, Module 2, and Module 4: The competent cells of *E. coli* strain 26, 27 were first prepared according to above procedure, and plasmid C-M0, and E-M0 were transformed into the competent cells to give strain 48, 49, respectively. On the other hand, the competent cells of *E. coli* strains 33, 40 were first prepared according to above procedure, and plasmid R-

M4, and A-M4 were transformed into the competent cells to give strains 47, 50, respectively.

Table 5.2. *E. coli* strains 1-50 and the containing modules.

Strain No.	Module 0	Module 1	Module 2	Module 3	Module 4
1		A-M1	C-M2		
2		A-M1	E-M2		
3		A-M1	R-M2		
4		C-M1	A-M2		
5		C-M1	E-M2		
6		C-M1	R-M2		
7		E-M1	A-M2		
8		E-M1	C-M2		
9		E-M1	R-M2		
10		R-M1	A-M2		
11		R-M1	C-M2		
12		R-M1	E-M2		
13		A-M1		C-M3	
14		A-M1		E-M3	
15		A-M1		R-M3	
16		C-M1		A-M3	
17		C-M1		E-M3	
18		C-M1		R-M3	
19		E-M1		A-M3	
20		E-M1		C-M3	
21		E-M1		R-M3	
22		R-M1		A-M3	
23		R-M1		C-M3	

#					
24		R-M1		E-M3	
25		A-M1	E-M2		C-M4
26		A-M1	E-M2		R-M4
27		A-M1	R-M2		C-M4
28		A-M1	R-M2		E-M4
29		C-M1	E-M2		A-M4
30		C-M1	E-M2		R-M4
31		R-M1	E-M2		A-M4
32		R-M1	E-M2		C-M4
33	A-M0	C-M1	E-M2		
34	A-M0	R-M1	E-M2		
35	C-M0	A-M1	E-M2		
36	C-M0	A-M1	R-M2		
37	C-M0	R-M1	E-M2		
38	E-M0	A-M1	R-M2		
39	R-M0	A-M1	E-M2		
40	R-M0	C-M1	E-M2		
41	A-M0	C-M1		E-M3	
42	A-M0	R-M1		E-M3	
43	C-M0	A-M1		E-M3	
44	C-M0	R-M1		E-M3	
45	R-M0	A-M1		E-M3	
46	R-M0	C-M1		E-M3	
47	A-M0	C-M1	E-M2		R-M4
48	C-M0	A-M1	E-M2		R-M4
49	E-M0	A-M1	R-M2		C-M4
50	R-M0	C-M1	E-M2		A-M4

5.2.5 General Procedure to Culture Recombinant *E. coli* Strains

Recombinant *E. coli* strain was cultured in 1 mL LB medium containing appropriate antibiotic at 37 °C for 7-10 h, and then inoculated into 25 mL M9 medium containing glucose (20 g/L), yeast extract (6 g/L), and appropriate antibiotic in a 125 mL tri-baffled flask. The cells were grown at 37 °C 300 rpm for 1.5-2 h to reach an OD_{600} of 0.6, and then IPTG (0.5 mM) was added to induce the expression of enzymes. The cells continued to grow for 12-13 h at 22 °C to reach late exponential phase. The cells were harvested by centrifugation (2500 g, 10 min), and the cell pellets were resuspended. The resting cells were used as catalysts for biotransformation.

5.2.6 General Procedure for Biotransformation with Resting *E. coli* Cells

Freshly prepared *E. coli* cells were resuspended to a cell density of 10 g cdw/L in KP buffer (200 mM, pH 8.0) containing 0.5-2%, w/v glucose (optional: 50-200 mM NH_3:NH_4Cl 1:10) to 2 mL system in a shaking flask (100 mL). A 2 mL *n*-hexadecane containing 20-100 mM styrene was added to the reaction system to form a second phase. For biotransformation of phenylalanine, the substrate was directly added in the aqueous phase (KP buffer) and a 2 mL pure *n*-hexadecane was added. The reaction mixture was shaken at 300 rpm and 30 °C for 24 h. 150 µL aliquots of each phase were taken out at the specified times (mainly 6 h, 10 h, and 24 h) for the following reaction. For organic phase, *n*-hexadecane (100 µL) were separated after centrifugation, diluted with 900 µL *n*-hexane (containing 2 mM benzyl alcohol as internal standard), and subjected to normal phase HPLC or GC analysis for quantifying styrene and possible epoxide intermediate. For aqueous phase, supernatants (100 µL) were separated after centrifugation, diluted with 400 µL water (containing 0.5% TFA) and 500 µL acetonitrile (containing 2 mM benzyl alcohol as internal standard), and then used for reverse phase HPLC analysis of the hydrophilic products.

5.3 Results and Discussion

5.3.1 Design of Synthetic Routes and Modular Transformations
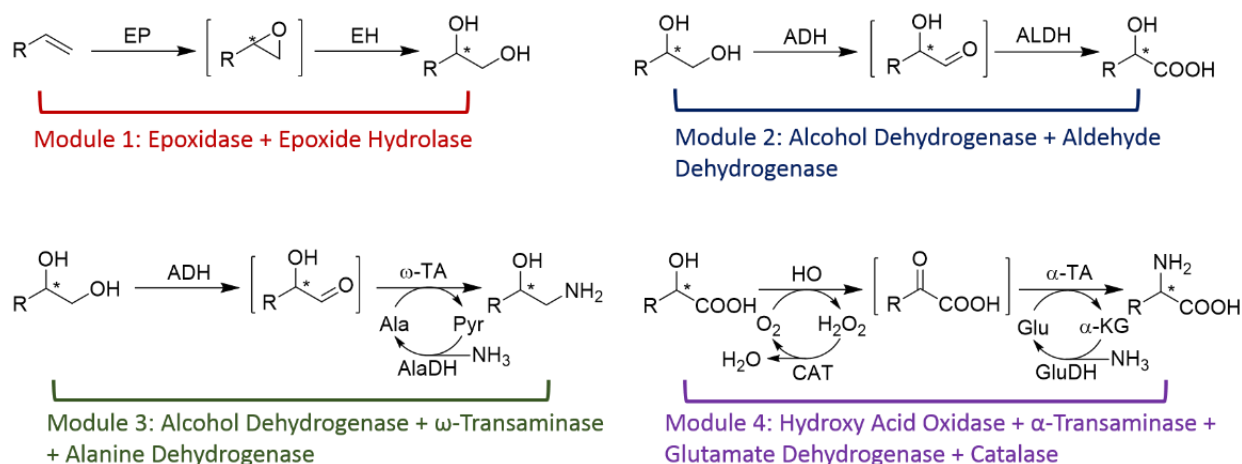
Figure 5.2. Design of four independent modular transformations. Module 1: terminal alkene to 1,2-diol; Module 2: 1,2-diol to α-hydroxy acid; Module 3: 1,2-diol to 1,2-amino alcohol; Module 4: α-hydroxy acid to α-amino acid.

To realize the biocatalytic cascades, we first designed four independent modular transformations (each containing 2-4 reactions) based on biocatalytic retrosynthesis analysis[365] (Figure 5.2). Module 1 is an epoxidation-hydrolysis transformation of terminal alkene to chiral 1,2-diol with epoxidase and epoxide hydrolase (EH). Module 2 is a double terminal oxidation of 1,2-diol to chiral α-hydroxy acid with alcohol dehydrogenase (ADH) and aldehyde dehydrogenase (ALDH). Module 3 is a terminal oxidation-reductive amination of 1,2-diol to chiral 1,2-amino alcohol with ADH, ω-transaminase (ω-TA), and alanine dehydrogenase (AlaDH, to regenerate the direct amine donor). Module 4 is a sub-terminal oxidation-reductive amination of α-hydroxy acid to chiral α-amino acid with hydroxy acid oxidase (HO), α-transaminase (α-TA), glutamate dehydrogenase (GluDH, to regenerate the direct amine donor), and catalase (CAT, to degrade H_2O_2). These modular transformations were designed following some principles of chemistry: a) each module utilizes a stable input (substrate) and gives a stable output (product), because alkene, diol, amino alcohol, hydroxy acid, and amino acid are stable chemicals in general; b) keep the

unstable or toxic intermediate inside the modules to minimize accumulation and side reactions, because epoxide, hydroxy aldehyde, and keto acid are generally reactive and toxic compounds.
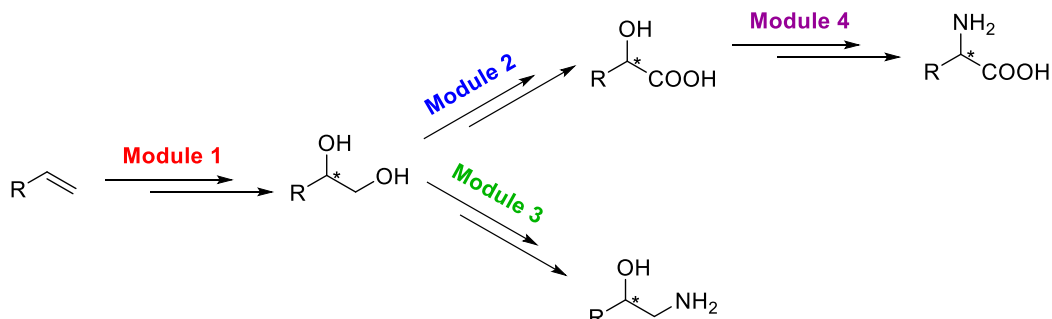
Scheme 5.2. General synthetic routes of terminal alkene to chiral α-hydroxyl acid, 1,2-amino alcohol, and α-amino acids by assembly of different modular transformations.

By assembly of different modules in one cell, terminal alkene can be converted to chiral α-hydroxy acid (Module 1 + Module 2), chiral 1,2-amino alcohol (Module 1 + Module 3), and chiral α-amino acid (Module 1 + Module 2 + Module 4), as draw in Scheme 5.2. In addition, the modular approach provides convenience in adjusting and turning the expression level of multiple proteins, which is a key issue in complex biosystems, such as cascade biocatalysis, synthetic biology,[366-368] and metabolic engineering.[369-371]

To prove the concept, we chose the cascade transformation of styrene and its substituted derivatives to the corresponding chiral (*S*)-mandelic acids, (*S*)-phenylethanol amines, and (*S*)-phenylglycines as the target (Scheme 5.3).
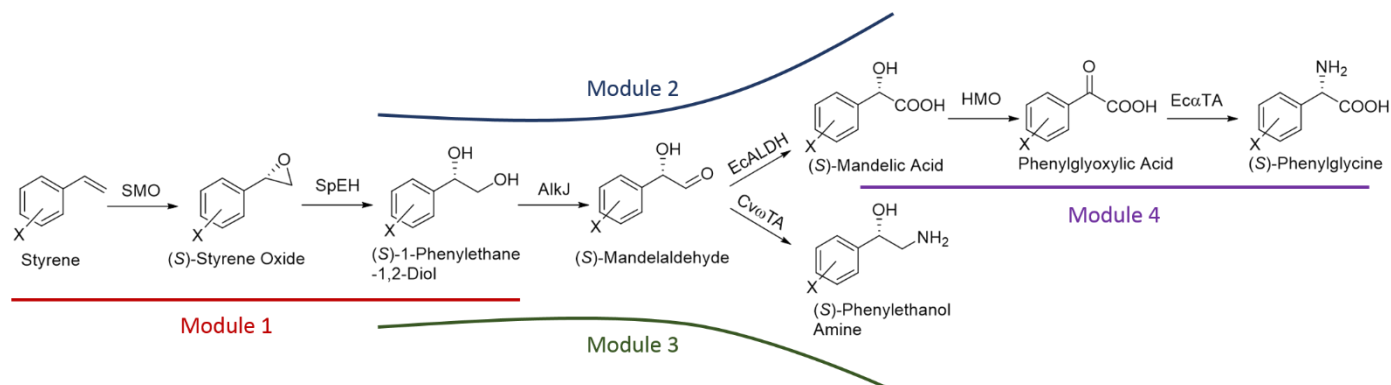
Scheme 5.3. Targeted cascade transformation of styrenes to corresponding chiral (*S*)-mandelic acids, (*S*)-phenylethanol amines, and (*S*)-phenylglycines, with recombinant *E. coli* strains coexpressing multiple enzymes on multiple modules.

5.3.2 Genetic Construction and Functional Test of Module 1

Module 1: SMO (*styA* & *styB*) + SpEH
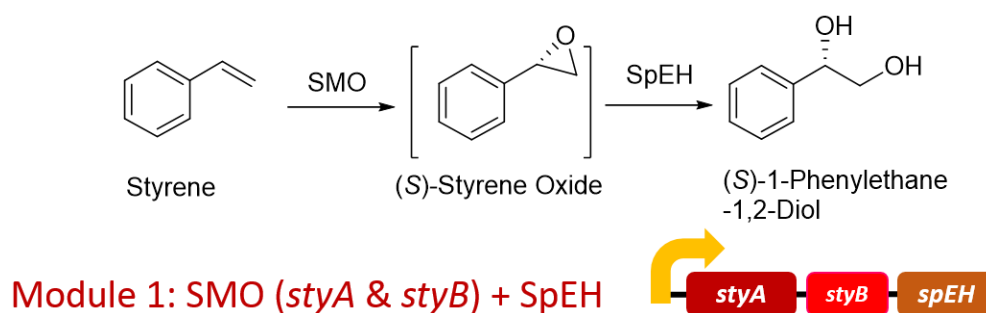
Figure 5.3. Cascade transformation and genetic construction of Module 1.

Module 1 requires the transformation of styrene to (*S*)-phenylethane diol (PED). Previously, we had engineered *E. coli* coexpressing styrene monooxygenase (SMO) and SpEH from *Sphingomonas* sp. HXN-200 to do the same chemistry and produce (*S*)-PEDs in high *ee* and good yield without accumulation of epoxides (Chapter 4). Thus, the genetic construction of an artificial operon containing *styA*, *styB*, and *spEH* was used as Module 1 in this project (Figure 5.3). The expression of two enzymes was examined by a SDS-PAGE analysis, and both StyA and SpEH were clearly visible (Figure 5.4, lane M1), while the size of StyB is too small to show on this gel. To facilitate further assembling multiple modules and optimizing expression, the Module 1 was sub-cloned into four different but compatible plasmids (pACYCduet, pCDFduet, pETduet, and pRSFduet) to give A-M1, C-M1, E-M1, and R-M1.
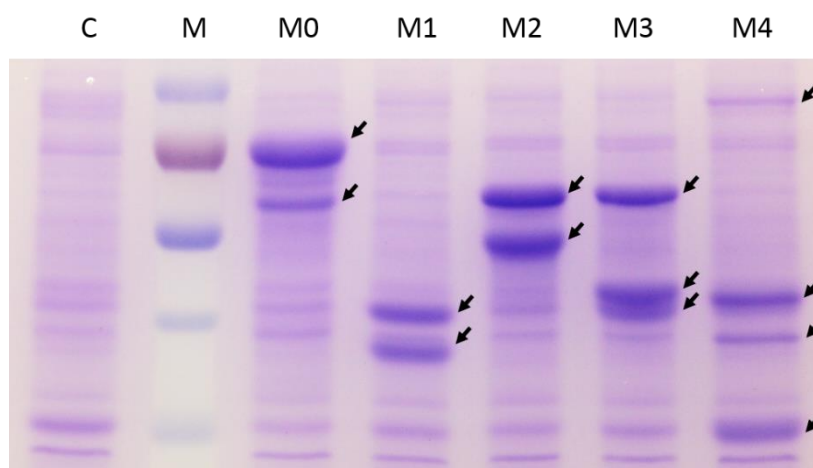
Figure 5.4. SDS-PAGE analysis of whole-cell protein of 5 *E. coli* strains containing Module 1-5, respectively. Arrows indicate the expressed enzymes. C: control; M: Marker; M0: Module 0 (up to down: AtPAL, AnOhbA); M1: Module 1 (StyA, SpEH); M2: (AlkJ, EcALDH); M3: (AlkJ, CvωTA, AlaDH); M4: (CAT, GluDH, HMO, EcαTA).

5.3.3 Genetic Construction and Functional Test of Module 2

Module 2 is a terminal oxidation of (*S*)-phenylethane diol to (*S*)-mandelic acid by ADH and ALDH (Figure 5.5). To find a highly regioselective ADH, we screened many commercial ADHs, cloned ADHs, and wild type strains in our group for oxidation of racemic phenylethane diol. As can be seen in Table 5.3, most enzymes did not show significant activity in oxidation of (*S*)-phenylethane diol, and some enzymes showed sub-terminal oxidation activity or both sub-terminal and terminal oxidation activities. Only three wild type strains, namely *Gluconobacter oxydans* 621H, *Pseudomonas putida* GPo1, and *Sphingomonas* sp. HXN-200, clearly oxidized diol to mandelaldehyde and mandelic acid without forming ketones. Furthermore, *Pseudomonas putida* GPo1 and *Sphingomonas* sp. HXN-200 showed *S*-selective preference in oxidation, producing (*S*)-mandelic acid with (*R*)-diol leftover, while *Gluconobacter oxydans* 621H exhibited *R*-selective preference.

Table 5.3. Summary of screened ADHs and some strains for oxidation of phenylethane diol.

Function	Source	Enzymes/Strains
No activity	Commercial[a]	PpAO, DrADH, TbADH, ScADH,
	Recombinant[b]	ScADH1, ScADH2, ScADH7, EcYdbC, EcYbdR, EcHcaB, PfNahB, BlADH, AcBADH, BsIoIG, BsSCD, BsYueD, BsYugJ, BsYxnA, BsYutJ, BsYusZ, Sp2982, Sp3015, Sp4468
Sub-terminal	Commercial	PlADH, LkADH,
	Recombinant	CpADH,[168] PfADH,[168] RDR[166]
Both sub- and terminal	Commercial	HLADH,
	Recombinant	BsBDHA,[372] BsGubt
Terminal oxidation	Strains	*Gluconobacter oxydans* 621H, *Pseudomonas putida* GPo1, *Sphingomonas* sp. HXN-200

[a]The commercial enzymes are from Sigma-Aldrich in isolated forms (liquid or lyophilized power). [b]The recombinant enzymes were over expressed in *E. coli*: Sc from *Saccharomyces*

cerevisiae, Ec from *Escherichia coli*, Pf from *Pseudomonas fluorescens*, Bl from *Brevibacterium linens*, Ac from *Acinetobacter calcoaceticus*, Bs from *Bacillus subtilis*, Sp from *Sphingomonas* sp. HXN-200.
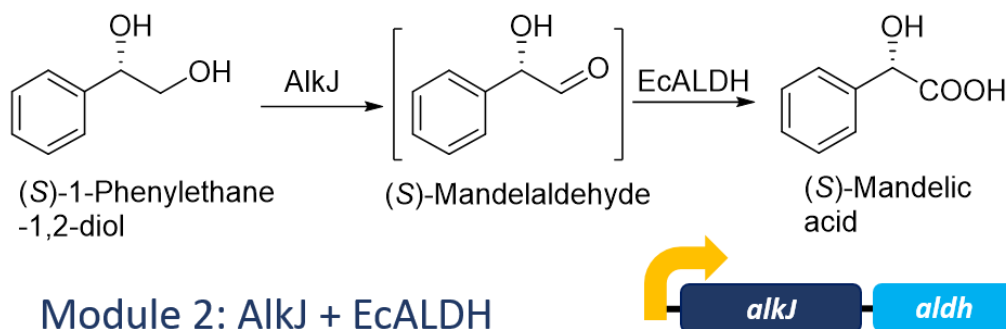
Figure 5.5. Cascade transformation and genetic construction of Module 2.

To identify the responsible ADHs in these wild type strains, we grew the strains with different carbon source and test their oxidation activity. For *Pseudomonas putida* GPo1 and *Sphingomonas* sp. HXN-200, the cells growing on alkane (*n*-octane) showed significant oxidation activity, while the cells growing on glucose or LB media did not give substantial activity. This phenomenon hinted that the diol oxidation is probably related to alkane metabolism. Since the alkane degradation pathway in *Pseudomonas putida* GPo1 has been well studied,[186, 187] the most straightforward hypothesis is that the ADH for oxidation terminal alkanol is responsible for terminal oxidation of diol. We successfully cloned the AlkJ, a membrane-associated non-canonical ADH for terminal alkanol oxidation in *Pseudomonas putida* GPo1.[189] *E. coli* expressing this AlkJ efficiently oxidized phenylethane diol to mandelaldehyde and mandelic acid with the same *S*-selectivity. In order to fully convert mandelaldehyde to mandelic acid, we further cloned an ALDH, phenylacetaldehyde dehydrogenase (*aldh*), from *E. coli* itself.[373] This EcALDH exhibited some substrate promiscuity, accepting α-hydroxy aldehyde (mandelaldehyde). The AlkJ and EcALDH were engineered into one non-natural operon as Module 2 (Figure 5.5). The *E. coli* containing Module 2 coexpressed AlkJ and EcALDH very well (Figure 5.4, lane M2) and catalyzed highly regioselective terminal oxidation of 50 mM racemic phenylethane diol to 26 mM (*S*)-mandelic acid in 18 h without accumulation of mandelaldehyde, leaving 24 mM (*R*)-phenylehtane

diol (Figure 5.6). The high enantioselectivity enables other applications in future, such as oxidative resolution of diols. The Module 2 was also sub-cloned to four plasmids to give A-M2, C-M2, E-M2, and R-M2, similarly.
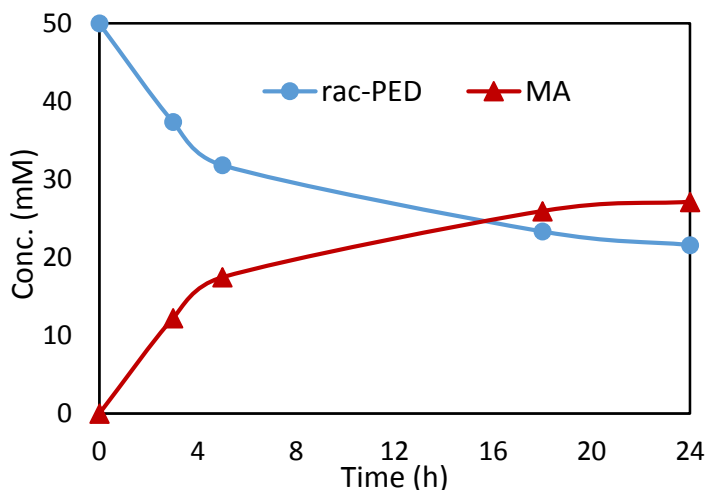
Figure 5.6. Cascade oxidation of 50 mM racemic phenylethane diol (PED) to mandelic acid (MA) with 10 g cdw/L resting cells of *E. coli* expressing AlkJ and EcALDH (Module 2).

5.3.4 Genetic Construction and Functional Test of Module 3
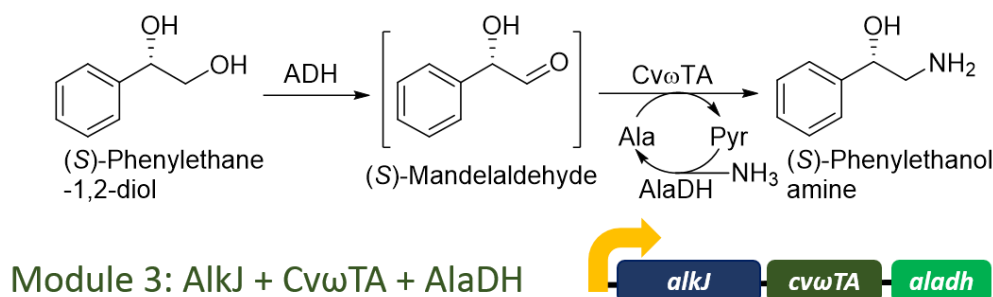
Figure 5.7. Cascade transformation and genetic construction of Module 3.

Module 3 is a cascade transformation including oxidation terminal alcohol to aldehyde and reductive amination of aldehyde to amine. As AlkJ catalyzed the highly regioselective oxidation of (*S*)-phenylehtane diol to (*S*)-mandelaldehyde in Module 2, it is also used as the first enzyme in Module 3. For the second step reductive amination, we cloned and tested the ω-TA from *Chromobacterium violaceum* (CvωTA), which had been reported with very broad substrate scope.[208] An *E. coli* strain was engineered to coexpress AlkJ and CvωTA, and biotransformation of 40 mM (*S*)-phenylehtane diol

using 200 mM L-alanine as amine donor gave 22 mM desired (*S*)-phenylethanol amine (55% yield), with 13 mM (*S*)-mandelaldehyde (intermediate) and 5 mM (*S*)-mandelic acid (byproduct) remained in the system (Figure 5.8a). Clearly, the transamination is a reversible reaction and difficult to fully convert aldehyde to amine. In order to increase the yield of amine and utilize easily available ammonia as amine donor, we employed L-alanine dehydrogenase (AlaDH) from *Bacillus subtilis* to regenerate L-alanine from pyruvate using ammonia, which together with ω-TA have been developed as a formal amination system *in vitro*.[210] An *E. coli* strain was engineered to coexpress AlkJ, CvωTA, and AlaDH by construction of a non-natural operon (Module 3, Figure 5.7, protein expression see Figure 5.4, lane M3). By using this strain, biotransformation of 40 mM (*S*)-phenylehtane diol was significantly improved to afford 32 mM (*S*)-phenylethanol amine (80% yield) with 200 mM ammonia without external L-alanine (Figure 5.8b). This is the first *in vivo* formal amination with coexpressed ω-TA and AlaDH. Similarly, the Module 3 was sub-cloned to four plasmids to give A-M3, C-M3, E-M3, and R-M3.
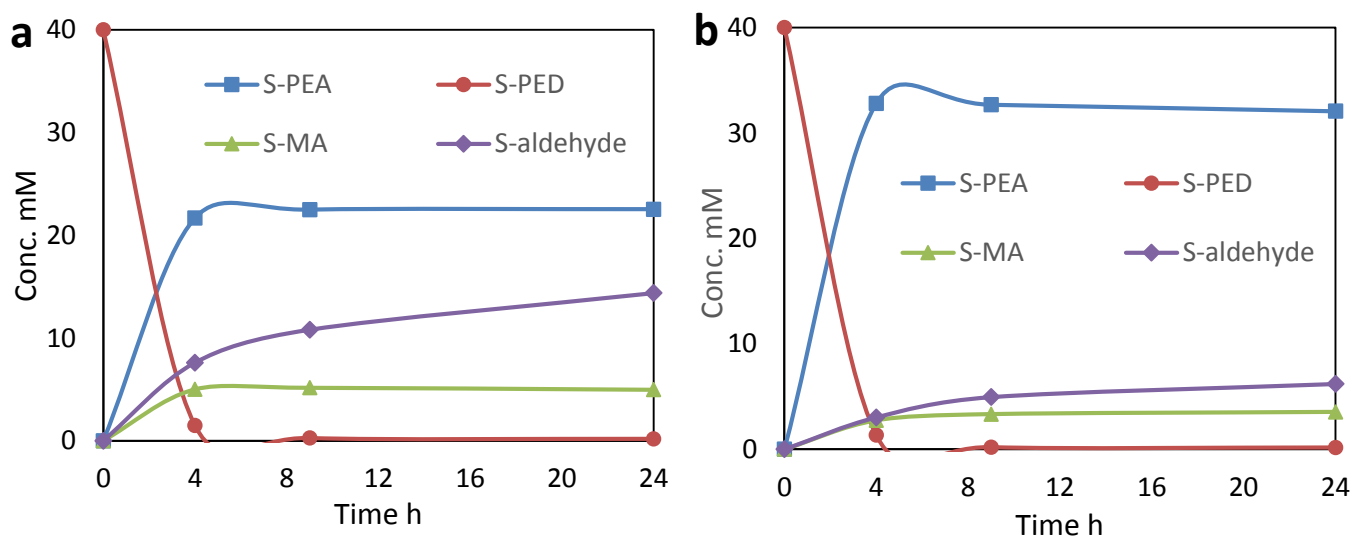
Figure 5.8. Cascade transformation of 40 mM (*S*)-phenylethane diol (PED) to (*S*)-phenylethanol amine (PEA) with **a)** *E. coli* expressing AlkJ and CvωTA and 200 mM L-alanine; **b)** *E. coli* expressing AlkJ, CvωTA, and AlaDH (Module 3) and 200 mM NH₃.

5.3.5 Genetic Construction and Functional Test of Module 4
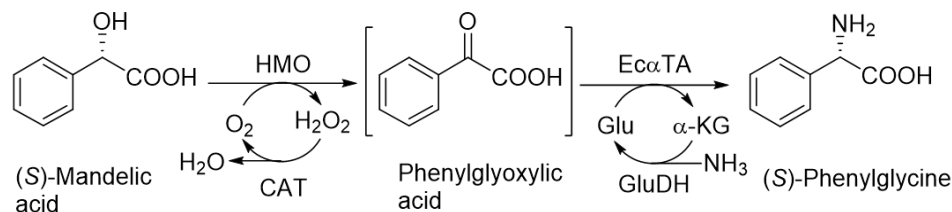
Figure 5.9. Cascade transformation and genetic construction of Module 4.

Module 4 requires a cascade transformation of (*S*)-mandelic acid to (*S*)-phenylglycine via oxidation and reductive amination. Two different enzymes were known to oxidize (*S*)-mandelic acid to phenylglyoxylic acid: (*S*)-mandelate dehydrogenase (MDH) in the mandelic acid degradation pathway of *Pseudomonas putida* ATCC 12633,[374, 375] and hydroxymandelate oxidase (HMO) in the vancomycin biosynthesis pathway of *Streptomyces coelicolor* A3(2).[194, 195] Both enzymes were successfully cloned and over expressed in *E. coli*, and the corresponding whole cells were evaluated for oxidation of 50 mM (*S*)-mandelic acid to phenylglyoxylic acid (Figure 5.10). Clearly, HMO showed higher activity and fully converted 50 mM substrates in 24 h. Thus, HMO was chosen for the Module 4.
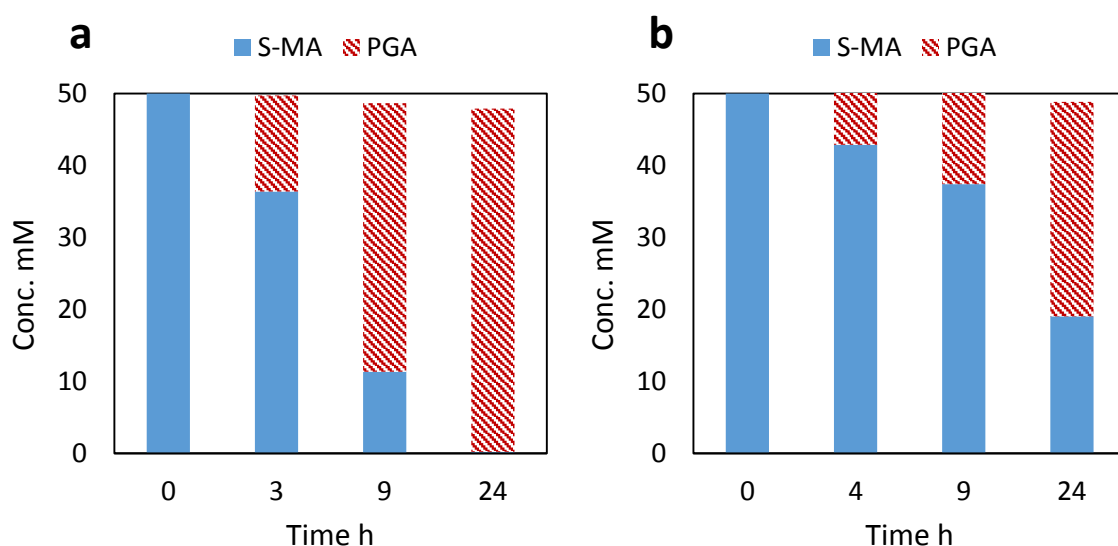
Figure 5.10. Oxidation of 50 mM (*S*)-mandelic acid (MA) to phenylglyoxylic acid (PGA) with
a) *E. coli* expressing HMO, **b)** *E. coli* expressing MDH.

The second reaction in Module 4 is enantioselective amination of phenylglyoxylic acid to L-phenylglycine. Although the transformation has been achieved with some commercial amino acid dehydrogenases in isolated form without sequence information,[376] we cloned and tested the phenylalanine dehydrogenase from *Rhodococcus*[377, 378] but the biotransformation result is not good (data not shown here). Thus, we focused on another type of enzyme, α-transaminase (α-TA), for amination of phenylglyoxylic acid. Four different α-TAs were cloned and tested: L-phenylglycine transaminase (LpgAT) from *Streptomyces pristinaespiralis*,[379] branch chain amino acid transaminase (IlvE) from *E. coli*,[380] aromatic amino acid transaminase (TyrB) from *E. coli*,[381] and aromatic amino acid transaminase (Aro8) from *Saccharomyces cerevisiae*.[382] The *E. coli* cells expressing these α-TAs were examined for amination of 50 mM phenylglyoxylic acid with 200 mM glutamate as amino donor. As can be seen in Figure 5.11a, all the cells converted phenylglyoxylic acid, though incompletely, and the best two are EcIlvE and ScAro8. Obviously, the transamination is a reversible reaction and difficult to complete in this reaction condition. To increase the yield using easily available ammonia as amine donor, we cloned glutamate dehydrogenase (GluDH) from *E. coli* to regenerate glutamate (direct amine donor) using ammonia. GluDH was successfully expressed alone and together with EcIlvE or ScAro8. We evaluated the corresponding *E. coli* strains for amination of 50 mM phenylglyoxylic acid with 200 mM ammonia (Figure 5.11b). *E. coli* coexpressing EcIlvE and GluDH was found to be the best biocatalyst for complete amination of the phenylglyoxylic acid in 9 h.

To construct Module 4, we first combined HMO, EcIlvE, and GluDH together as an operon. Because HMO is a H_2O_2 generating oxidase, we further integrated a catalase, KatE, from *E. coli*,[383] and found that it improved the oxidation of phenylglyoxylic acid of HMO (data not shown here). Thus Module 4 containing four enzymes was constructed (Figure 5.9), and the four enzymes were clearly coexpressed in *E. coli* containing Module 4 (Figure 5.4, lane M4). Cascade transformation was

optimized to convert 45 mM (*S*)-mandelic acid to 42.5 mM (*S*)-phenylglycine (95%
yield) within 32 h (Figure 5.12). Similarly, the Module 4 was also sub-cloned to four
plasmids to give A-M4, C-M4, E-M4, and R-M4, to facilitate further assembly.
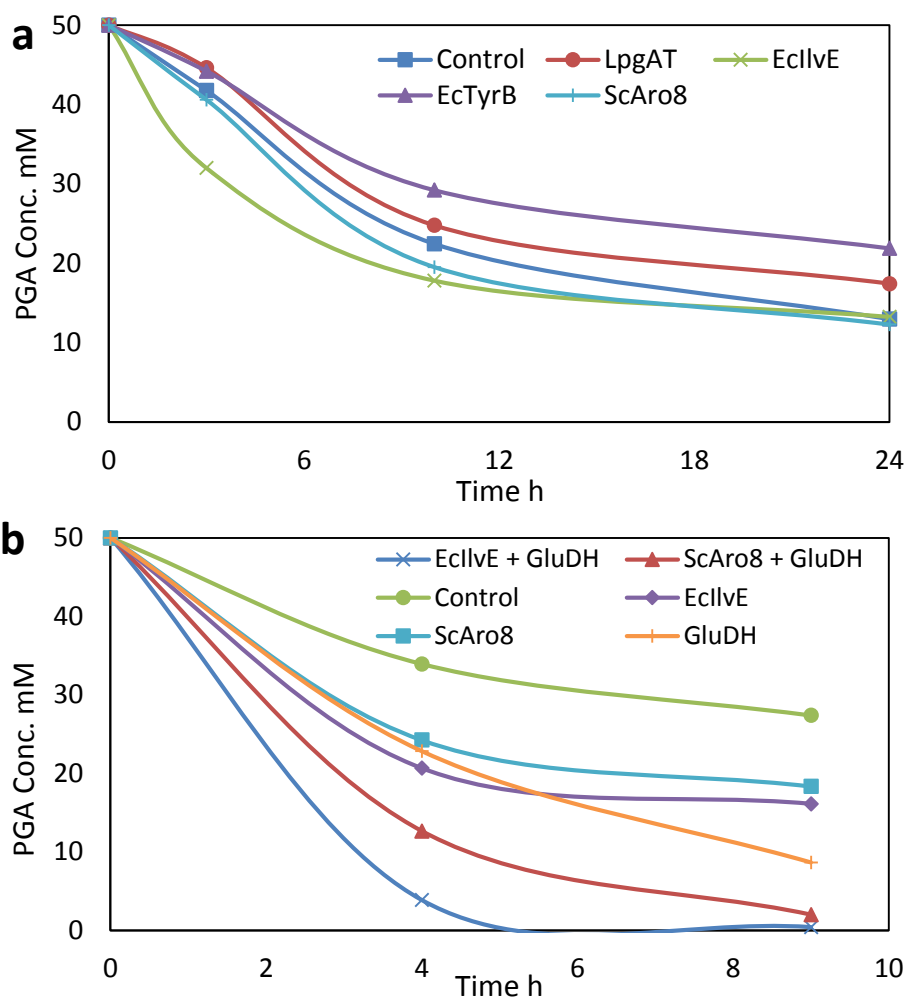
Figure 5.11. Amination of 50 mM phenylglyoxylic acid (PGA) with **a)** *E. coli* expressing α-TA
and 200 mM glutamate, **b)** *E. coli* expressing α-TA and/or GluDH and 200 mM NH_3.
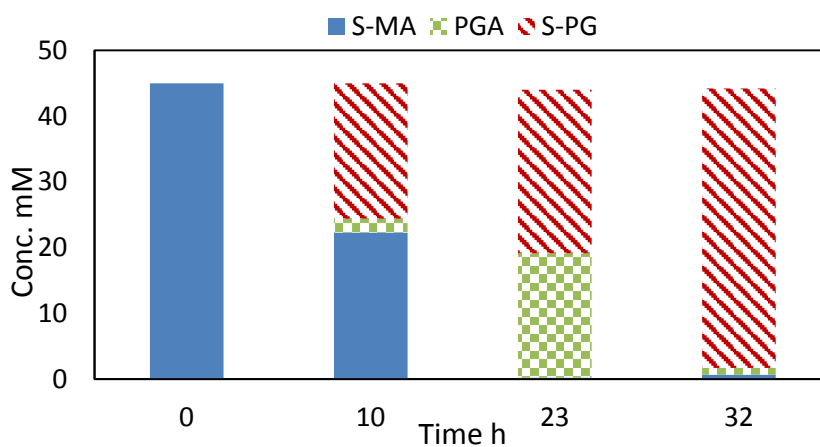
Figure 5.12. Cascade transformation of 45 mM (*S*)-mandelic acid (MA) to (*S*)-phenylglycine
(PG) with *E. coli* coexpressing HMO, EcIlvE, GluDH, KatE (Module 4).

5.3.6 Assembly and Optimization of Module 1 and Module 2 for Cascade Transformation of Styrenes to (*S*)-Mandelic Acids
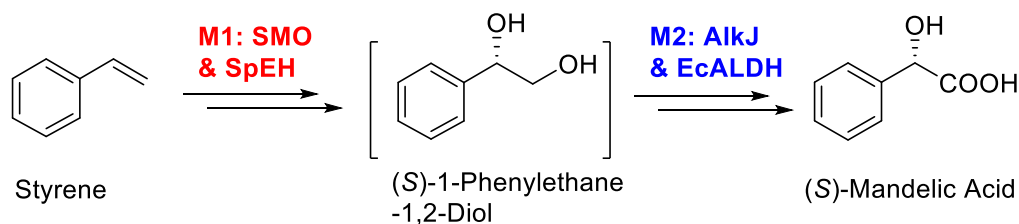
Scheme 5.4. Cascade transformation of styrene to chiral (*S*)-mandelic acid with recombinant *E. coli* coexpressing multiple enzymes on Module 1 and Module 2.

5.3.6.1 Combinatorial Assembly and Cascade Biotransformation with 12 Strains

To achieve efficient cascade transformation of styrene to chiral (*S*)-mandelic acid with one recombinant *E. coli* strain (Scheme 5.4), the Module 1 and Module 2 were assembled together in *E. coli* cells. To explore the optimal combination of Module 1 and 2, four different Module 1 plasmids (A-M1, C-M1, E-M1, & R-M1) and four Module 2 plasmids (A-M2, C-M2, E-M2, & R-M2) were combinatorially transformed into *E. coli* to obtain different *E. coli* strains 1-12, each coexpressing the four enzymes, SMO, SpEH, AlkJ, and EcALDH. The number of strain is 12 not 16, because plasmids with the same backbone (*e.g.* A-M1 and A-M2) are not compatible with each other due to the same *ori* and antibiotic resistance marker. The *E. coli* strains 1-12 were easily grown in M9-glucose medium with the protein expression, and then harvested as resting cells for biotransformation. The strains were individually evaluated for transformation of 100 mM styrene in a two-liquid-phase system (1:1 KP buffer and *n*-hexadecane) containing 0.5% glucose (to regenerate NADH for SMO via cell metabolism). As can be seen in Figure 5.13, all the 12 strains were able to convert styrene to (*S*)-mandelic acid, but in different yields. The best three strains (strains 2, 3, 5) produced 71-83 mM (*S*)-mandelic acid in 24 h with small amount of diol intermediate, while the worst three strains (strains 4, 7, 9) only produced 21-26 mM (*S*)-mandelic acid in 24 h with 59-70 mM diol accumulated. To investigate the possible reasons for the different performance, we conducted a SDS-PAGE analysis of the

whole-cell protein of the 12 strains. As showed in Figure 5.14, the four enzymes were well separated and clearly visible. Good strains (strains 2, 3, 5) exhibited a relatively balanced expression of the four enzymes, whereas bad strains (strains 4, 7, 9) clearly expressed much more SMO and SpEH (Module 1) but much less AlkJ and EcALDH (Module 2), and this also explained the significant accumulation of intermediate diol in these three strains. On the other hand, strains 1 and 12 expressed relatively more AlkJ and EcALDH than SMO and SpEH, which leaded to < 3 mM diol left in 20 h. We demonstrated that the expression level of enzymes significantly influences *in vivo* cascade biocatalysis. Modularization of enzymes provides a basic to optimize cascade biocatalysis via adjusting the expression of modules by using different plasmids (as we have done here), different inducers, or promoters and other sequences.[384-386]
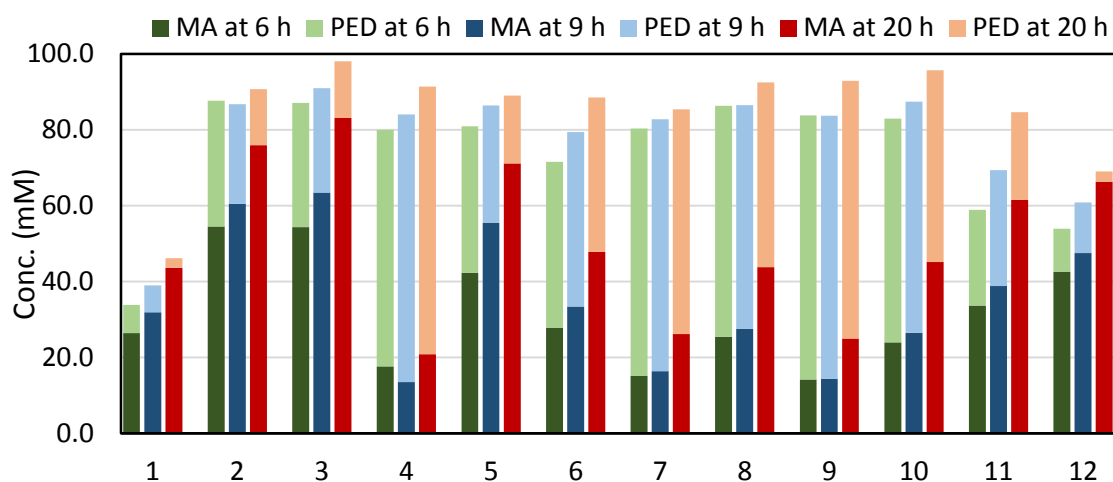
Figure 5.13. Cascade transformation of 100 mM styrene to (*S*)-mandelic acid (MA) via (*S*)-phenylethane diol (PED) with different *E. coli* strains 1-12 containing Module 1 and 2, coexpressing SMO, SpEH, AlkJ, and EcALDH. Values are average of three independent results.

Figure 5.14. SDS-PAGE analysis of whole-cell protein of *E. coli* strains 1-12 containing Module 1 and 2, coexpressing SMO, SpEH, AlkJ, and EcALDH.

5.3.6.2 Biotransformation of Substituted Styrenes with the Best Strain
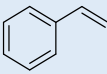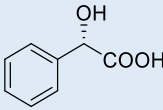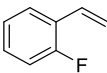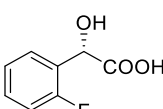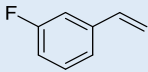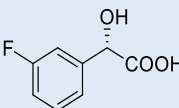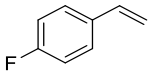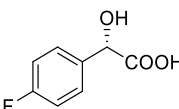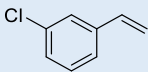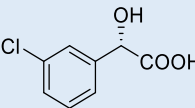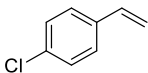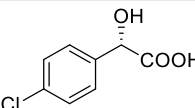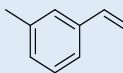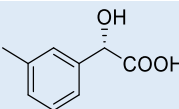
The best *E. coli* strain 3 containing A-M1 and R-M2 was employed to further explore the substrate scope and characterize the cascade transformation. We tested the transformation of a set of substituted styrenes (20 mM) in the same KP buffer: *n*-hexadecane two phase system with resting cells of *E. coli* (strain 3). As listed in Table 5.4, some simple substituted styrenes (fluoro-, chloro-, and methyl-) were also converted to the corresponding substituted (*S*)-mandelic acids in excellent *ee* of ≥97% and high yield of 72-98%, within 12 h. Apparently, all the four enzymes, SMO, SpEH, AlkJ, and EcALDH, exhibited some substrate promiscuity (accept substrate with some variations) and kept the required selectivity (enantioselectivity of SMO, regioselectivity of SpEH and AlkJ). The result demonstrated the synthetic potential of our biocatalytic cascade in multi-step oxyfunctionalization of alkenes to produce various chiral mandelic acids with diverse possible applications. We are currently testing the cascade to convert other alkenes (*e.g.* aliphatic) to other valuable chiral α-hydroxy acids.

5.3.6.3 Cascade Biotransformation at Higher Concentration

To examine the efficiency of the catalysis system, the resting cells of *E. coli* (strain 3) were applied to transform styrene at higher concentration (120 mM) in shaking flasks. As shown in Figure 5.15, 94 mM (14.2 g/L) (*S*)-mandelic acid was produced with 15 g cdw/L *E. coli* (strain 3) in 22 h, which corresponds to 78% yield from styrene. On the other hand, other chemicals, including unreacted substrate styrene, intermediate diol, and byproduct phenylacetic acid, were maintained in low amount (≤ 10 mM). Since the chemical property of (*S*)-mandelic acid is rather different with those of the other chemicals, separation and further purification could be easy to obtain relative pure (*S*)-mandelic acid solid. The cascade biocatalysis converting styrenes to (*S*)-mandelic acids represents a significant advance in biocatalytic asymmetric

oxyfunctionalization, deserving further scaling up in fermentor with growing cells in high density.

Table 5.4. Cascade transformation of (substituted) styrenes to corresponding (*S*)-mandelic acids with *E. coli* (strain 3) coexpressing four enzymes.

Substrate[a]	Conv. STY (%)[b]	Inter. PED (%)[c]	Yield MA (%)[c]	Product	*ee* (%)[d]	Lost (%)[e]
	>98	<1	94		>98	<6
	95	<1	92		N.D.[f]	<3
	>98	<1	95		98	<5
	>98	<1	98		N.D.	<2
	88	<1	83		97	<5
	78	<1	73		N.D.	<5
	97	15	72		98	10

[a] The reactions were performed with substrates (20 mM in organic phase) and resting cells of *E. coli* (strain 3) (10 g cdw/L) in a two-liquid phase system consisting of KP buffer (200 mM, pH 8.0, 0.5% glucose) and *n*-hexadecane (1:1) at 30 °C for 12 h. [b] Consumption of styrene (STY) was determined by normal phase HPLC analysis. [c] Amount of phenylethane diols (PED) and mandelic acids (MA) was determined by reverse phase HPLC analysis. [d] The *ee* value was determined by chiral HPLC analysis. [e] Other lost was calculated from the other values, mainly caused by byproduct formation and substrate evaporation. [f] No determined because of temporary lack of chiral HPLC system.
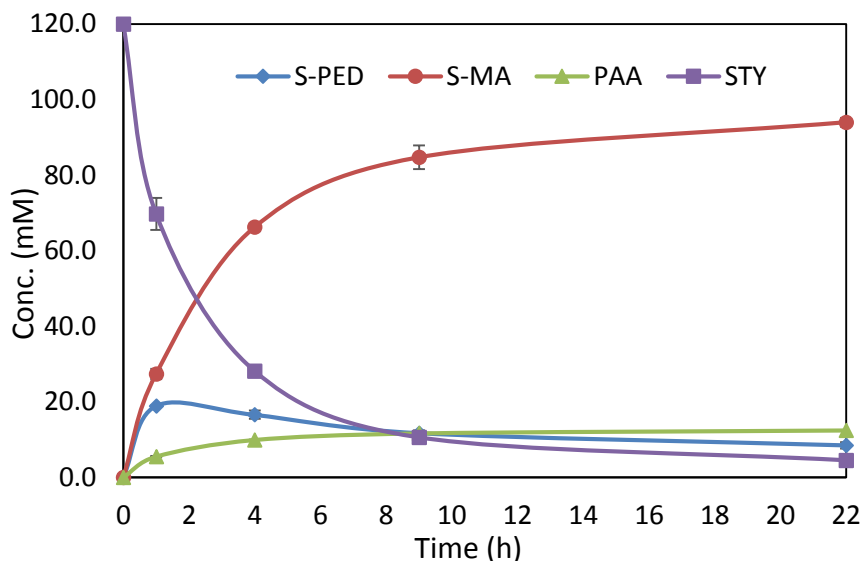
Figure 5.15. Time course of transformation of 120 mM styrene (STY) to (*S*)-mandelic acid (MA) with *E. coli* strain 3 (15 g cdw/L). (*S*)-phenylethane diol (PED) is intermediate and phenylacetic acid (PAA) is byproduct.

5.3.7 Assembly and Optimization of Module 1 and Module 3 for Cascade Transformation of Styrene to (*S*)-Phenylethanol Amine
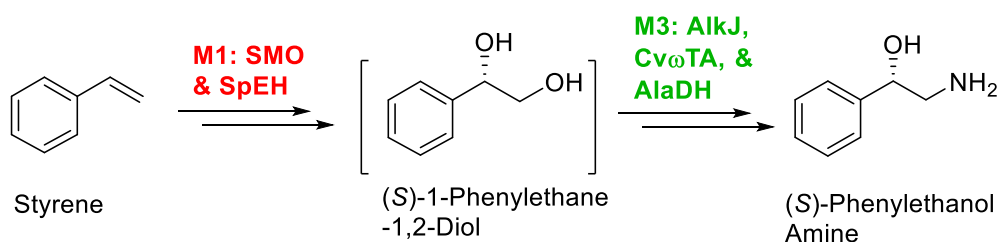
Scheme 5.5. Cascade transformation of styrene to chiral (*S*)-phenylethanol amine with recombinant *E. coli* coexpressing multiple enzymes on Module 1 and Module 3.

5.3.7.1 Optimization of Reaction Conditions for the Cascade Biotransformation

To achieve formal asymmetric aminohydroxylation of styrene to chiral (*S*)-phenylethanol amine (Scheme 5.5), Module 1 (formal dihydroxylation) and Module 3 (alcohol to amine) need to be combined together. Similarly, combinatorial assembly of Module 1 plasmids (A-M1, C-M1, E-M1, & R-M1) and Module 3 plasmids (A-M3, C-M3, E-M3, & R-M3) leaded to *E. coli* strains 13-24, each coexpressing the five enzymes, SMO, SpEH, AlkJ, CvωTA, and AlaDH. Since the reaction is becoming

more complex, we first optimized the cascade reaction by applying different amount of glucose and ammonia. Biotransformation of 50 mM styrene was performed with resting cells of *E. coli* strains 15 and 17 (two representative strains coexpressing five enzymes) with 0.5-2% glucose and 100-400 mM ammonia. The result (Figure 5.16) indicated that the best condition is 2% glucose with 200 mM ammonia for both strains. Too much ammonia might be toxic to the cells and inhibit enzymatic reactions.
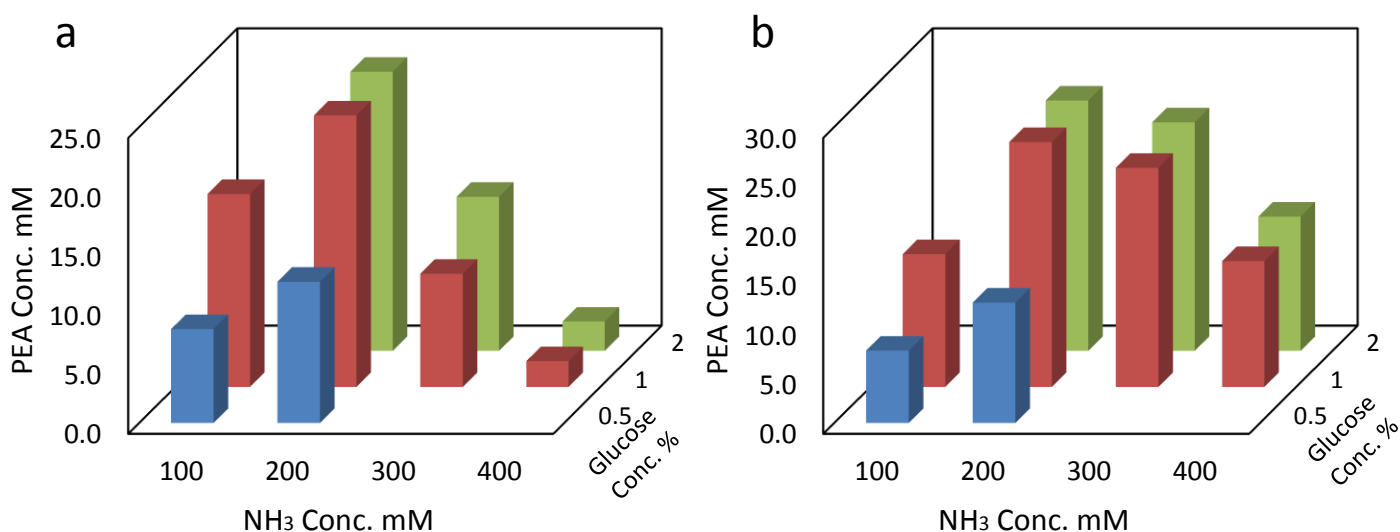
Figure 5.16. Cascade transformation of 50 mM styrene to (*S*)-phenylethanol amine (PEA) with various amount of glucose and ammonia using **a)** *E. coli* strain 15, **b)** *E. coli* strain 17.

5.3.7.2 Cascade Biotransformation with 12 Strains

Using the optimal condition, all the *E. coli* strains 13-24 were individually evaluated for cascade transformation of 50 mM styrene, resulting in very different amount of (*S*)-phenylethanol amine in 10 h (Figure 5.17). The best three *E. coli* strains 14, 17, 24 gave 22-27 mM desired amino alcohol product in 44-54% yield, yet with significant amount of (*S*)-phenylethane diol, (*S*)-mandelaldehyde, and (*S*)-mandelic acid accumulated in the system. We also suspected that styrene was not fully converted in some cases. Nevertheless, chiral (*S*)-phenylethanol amine was still produced in reasonable yield, and more importantly in excellent *ee*, which proved the very high enantioselectivity and regioselectivity of the cascade transformation. To the best of our knowledge, this is the first biocatalytic (formal) asymmetric aminohydroxylation. A

SDS-PAGE analysis was also performed to examine the expression of five enzymes, SMO, SpEH, AlkJ, CvωTA, and AlaDH (Figure 5.18). Strong expression of AlkJ and CvωTA (Module 3) was observed for the best three strains 14, 17, 24, while strong expression of SMO and SpEH (Module 1) often leaded to substantial accumulation of intermediate phenylethane diol (strains 16, 18-22). This suggested that the bottleneck of the cascade is terminal oxidation and amination. The current system would be improved by further optimization of reaction conditions or screening/engineering of better enzymes for terminal oxidation of diol and transamination of α-hydroxy aldehyde.
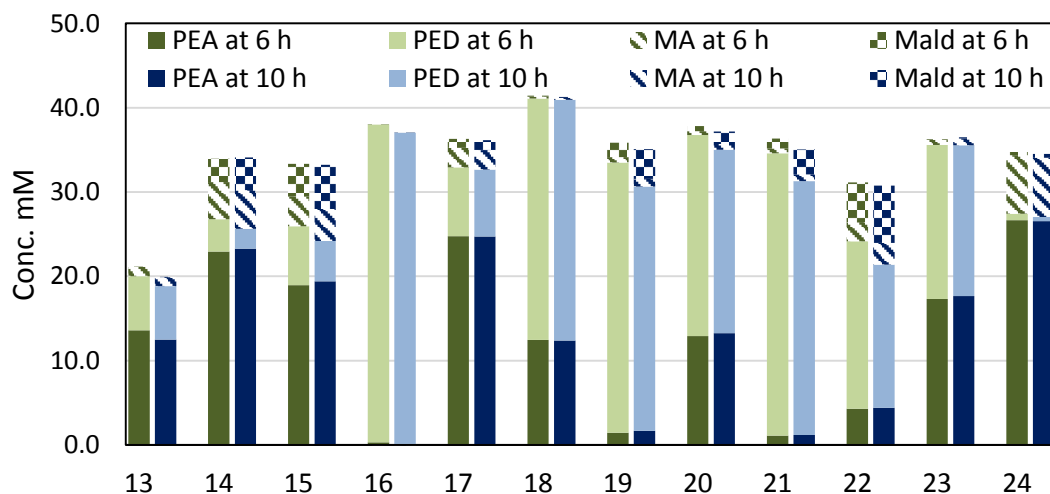
Figure 5.17. Cascade transformation of 50 mM styrene to (*S*)-phenylethanol amine (PEA) with different *E. coli* strains 13-24 containing Module 1 and 3, coexpressing SMO, SpEH, AlkJ, CvωTA, and AlaDH. Values are average of three independent results.
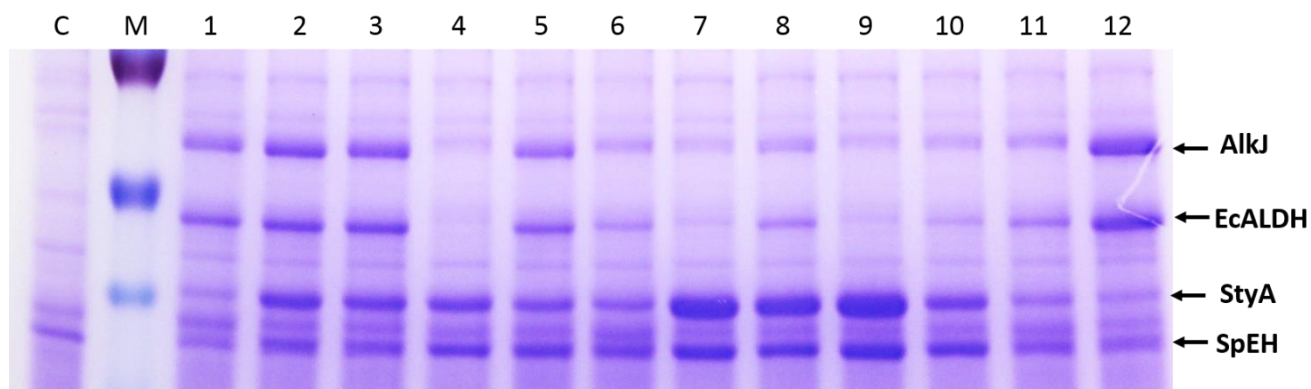

Figure 5.18. SDS-PAGE analysis of whole-cell protein of *E. coli* strains 13-24 containing Module 1 and 3, coexpressing SMO, SpEH, AlkJ, CvωTA, and AlaDH.

5.3.8 Assembly and Optimization of Module 1, Module 2, and Module 4 for Cascade Transformation of Styrene to (*S*)-Phenylglycine
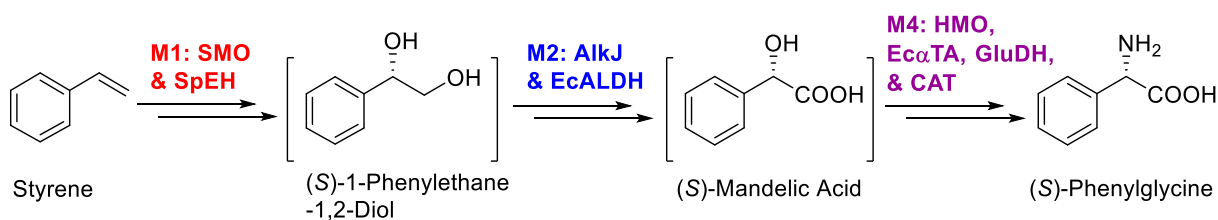
Scheme 5.6. Cascade transformation of styrene to chiral (*S*)-phenylglycine with recombinant *E. coli* coexpressing multiple enzymes on Module 1, Module 2, and Module 4.

To achieve more challenging asymmetric oxy- and amino-functionalization of alkene to chiral α-amino acid, three modular transformations need to be combined together, including Module 1 (dihydroxylation), Module 2 (terminal oxidation), and Module 4 (sub-terminal amination) (Scheme 5.6). Based on the results of styrene to (*S*)-mandelic acid (section 5.3.6), we selected the best four strains, *E. coli* strains 2, 3, 5, 12, containing both Module 1 and Module 2 as parental stains for further assembly with Module 4. Module 4 on four different plasmids (A-M4, C-M4, E-M4, & R-M4) was transformed into *E. coli* strains 2, 3, 5, 12 to give *E. coli* strains 25-32, each containing Module 1, Module 2, and Module 4 on different plasmids. The *E. coli* strains 25-32 were individually evaluated for cascade transformation of 50 mM styrene to (*S*)-phenylglycine. As shown in Figure 5.19, strains 25, 26, 27 successfully produced >40 mM (*S*)-phenylglycine (>80% yield) in 24 h. Other intermediates including phenylethane diol, mandelic acid, and phenylglyoxylic acid, only accounted for <5 mM in total with these three best strains. This is a significant achievement: >80% product yield from initial substrate with six selective enzymatic transformations and two assistant steps. The transformation of styrene to (*S*)-phenylethanol amine and (*S*)-phenylglycine is the first two biocatalytic examples to achieve simultaneously amino- and oxy-functionalization of hydrocarbons. A SDS-PAGE analysis was performed for the whole-cell protein of all the eight strains (data not shown here). However, since the four proteins (GluDH, StyA, HMO, and SpEH) are very close in size, we could not

141

achieve acceptable resolution on normal SDS-PAGE now. Gradient gel may be applied in future.
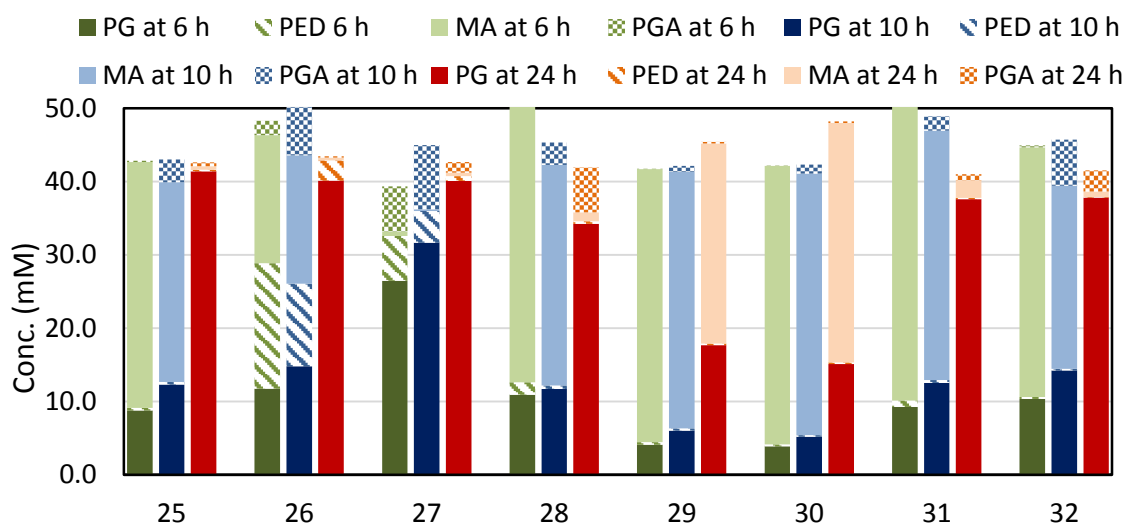
Figure 5.19. Cascade transformation of 50 mM styrene to (*S*)-phenylglycine (PG) with different *E. coli* strains 25-32 containing Module 1, 2, and 4, coexpressing SMO, SpEH, AlkJ, EcALDH, HMO, EcIlvE, GluDH, and CAT. Values are average of three independent results.

5.3.9 Extend the Cascade to Start from Phenylalanine with Module 0

Although terminal alkene is an excellent starting material for organic synthesis, it derives from dwindling petroleum feedstock which is unsustainable from a prospective point of view. Thus, we are interested in extending our biocatalytic cascades to directly using sustainable bioresource as starting material. Recently, progress in metabolic engineering and synthetic biology enables production of more and more basic biochemicals, *e.g.* amino acids, from renewable bioresource via fermentation process.[55-58] Such basic biochemicals will be available in large quantity at low price in the near future, which are similar to basic petrochemicals (*e.g.* alkenes) today, but being greener and more sustainable. To extend the biocatalytic cascades to basic biochemicals, we designed an additional Module 0 to connect styrene to L-phenylalanine (Scheme 5.7).
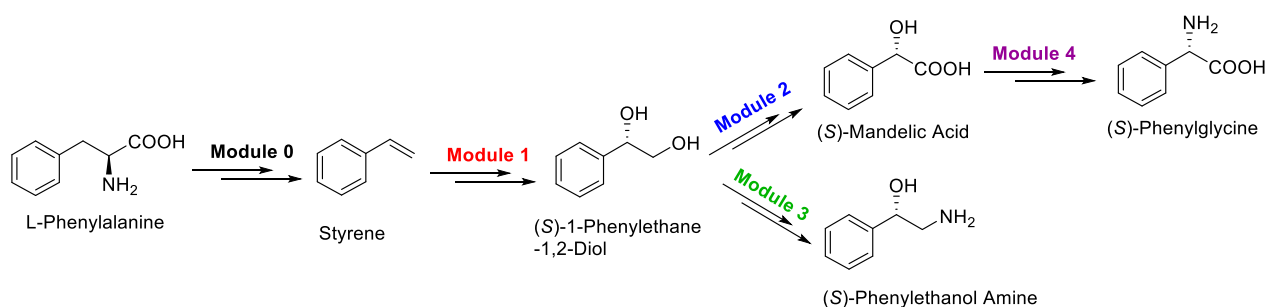
Scheme 5.7. Synthetic routes of L-phenylalanine to chiral mandelic acid, phenylethanol amine, and phenylglycine by assembly of different modular transformations.

Module 0: AtPAL + AnPAD (*ohbA* & *padA*)
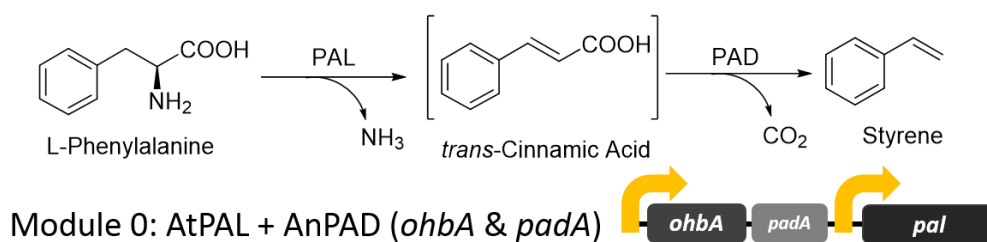
Figure 5.20. Cascade transformation and genetic construction of Module 0.

5.3.9.1 Cloning and Testing PAL and PAD Individually

The transformation of L-phenylalanine to styrene requires removing an amino group and a carboxyl group and forming a C=C double bond (Figure 5.20). Two enzymes were employed for the transformation: phenylalanine lyase (PAL) to convert L-phenylalanine to *trans*-cinnamic acid, and phenylacrylic acid decarboxylase (PAD) to convert cinnamic acid to styrene. PAL belongs to amino acid ammonia lyase which catalyzes reversible hydroamination of unsaturated acid to amino acid,[387, 388] and it is the first committed enzyme for phenylpropanoids biosynthesis in plants.[389] To find an efficient PAL, several PALs were cloned and expressed in *E. coli*, including AtPAL from plant *Arabidopsis thaliana*,[390] AvPAL from cyanobacterium *Anabaena variabilis*,[391] and RtPAL from yeast *Rhodosporidium toruloides*.[392] The corresponding *E. coli* cells expressing these PALs were examined for conversion of 20 mM L-phenylalanine to cinnamic acid. As clearly shown in Figure 5.21a, AtPAL outperformed other two PALs and produced 9 mM cinnamic acid in 5 h. On the other hand, PAD is less studied and only exists in certain yeast and fungus for degradation of some acrylic acids. We initially cloned the *padA* gene from *Saccharomyces*

cerevisiae[393] and *Aspergillus niger*,[394] but both of them did not show decarboxylation activity in recombinant *E. coli*. Two close related genes, *fdc* from *S. cerevisiae*[395] and *ohbA* from *A. niger*,[396] were then cloned but showed a low decarboxylation activity in *E. coli* (Figure 5.21b). Because the *padA* and *fdc*/*ohbA* genes were found to function collaboratively in native organisms,[395, 396] we tested coexpression of *padA* and *ohbA* gene in *E. coli*, and much higher decarboxylation activity was obtained (Figure 5.22b). Thus, AnPadA and AnOhbA are the two components of AnPAD.
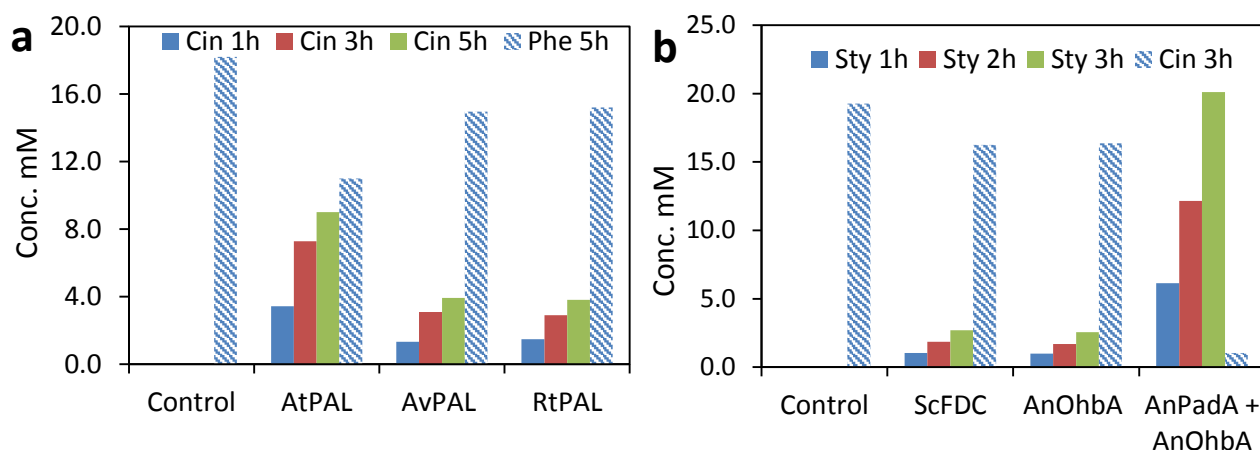
Figure 5.21. a) Conversion of 20 mM L-phenylalanine to cinnamic acid (Cin) with *E. coli* (1 g cdw/L) expressing different PAL; **b)** Conversion of 20 mM cinnamic acid (Cin) into styrene (Sty) with *E. coli* (1 g cdw/L) expressing different PAD component.

5.3.9.2 Genetic Construction and Functional Test of Module 0

To achieve cascade transformation of L-phenylalanine to styrene, the AtPAL and AnPAD were genetically constructed together as an expression cassette (Module 0). *E. coli* cells well-coexpressed these two enzymes (Figure 5.4, lane M0) and efficiently converted 50 mM L-phenylalanine into quantitative amount of styrene in an *n*-hexadecane: KP buffer two-phase system in 5 h (Figure 5.22). Obviously, the irreversible decarboxylation by AnPAD drove the reversible PAL-catalyzed reaction to complete. Although the same reactions have been published for production of styrene from glucose,[397] the decarboxylation was catalyzed by ScFDC, which is much less active than the two component AnPAD (Figure 5.21b). Similarly, the Module 0 was also sub-cloned into four plasmids to give A-M0, C-M0, E-M0, and R-M0.
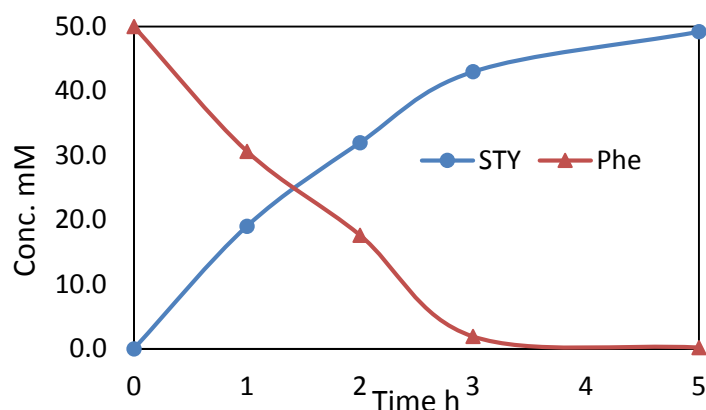
Figure 5.22. Cascade transformation of 50 mM L-phenylalanine to styrene with *E. coli* (5 g cdw/L) coexpressing AtPAL and AnPAD (Module 0).

5.3.10 Assembly and Optimization of Module 0, Module 1, and Module 2 for Cascade Transformation of L-Phenylalanine to (*S*)-Mandelic Acid
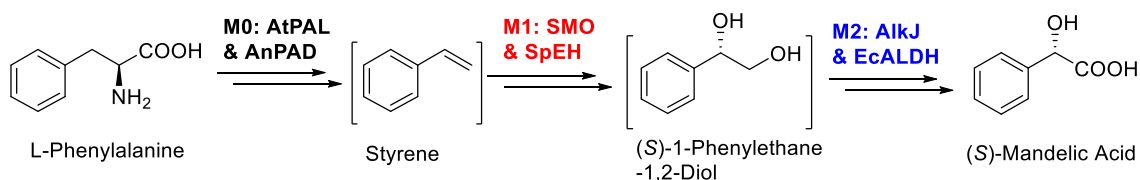
Scheme 5.8. Cascade transformation of L-phenylalanine to chiral (*S*)-mandelic acid with recombinant *E. coli* coexpressing multiple enzymes on Module 0, Module 1, and Module 2.

Now, the transformation of L-phenylalanine to styrene could be coupled with the following oxy- and amino-functionalization of styrene by assembling the Module 0 with appropriate Module 1-4 in one *E. coli* strain. To produce (*S*)-mandelic acid from L-phenylalanine, Module 0, Module 1, and Module 2 need to be combined together. We selected four best strains, *E. coli* strains 2, 3, 5, 12, containing both Module 1 and Module 2 as parental strains for further assembly with Module 0. Module 0 on four different plasmids (A-M0, C-M0, E-M0, & R-M0) was transformed into *E. coli* strains 2, 3, 5, 12 to give *E. coli* strains 33-40, each containing Module 0, Module 1, and Module 2 on different plasmids. The *E. coli* strains 33-40 were studied for cascade transformation of 100 mM L-phenylalanine to (*S*)-mandelic acid in a two-liquid-phase system. To our delight, four out of eight strains efficiently produced >80 mM (*S*)-mandelic acid (Figure 5.23), representing >80% yield over six steps from L-phenylalanine. We further tested the best four strains for converting 150 mM L-

145

phenylalanine in a similar setup. As a result, the strain 33 and strain 40 produced 138-140 mM (21 g/L) (*S*)-mandelic acid in 24 h (Figure 5.25), giving a very high yield of 92-93%. The protein expressing profile was examined by SDS-PAGE analysis, which showed the relative balanced expression of the six enzymes in the best strain 33 and 40 (Figure 5.24). Without a doubt, such a highly efficient multistep reaction clearly demonstrated the potential of cascade biocatalysis, deserving further research and future industrial implementation. During the culturing of strains 33-40, we observed the production of (*S*)-mandelic acid (12-110 mg/L) in the cell culture broth, which evidenced the synthesis from endogenous L-phenylalanine, providing a novel and potential synthetic pathway for fermentative production of (*S*)-mandelic acid from glucose in the future.[398]
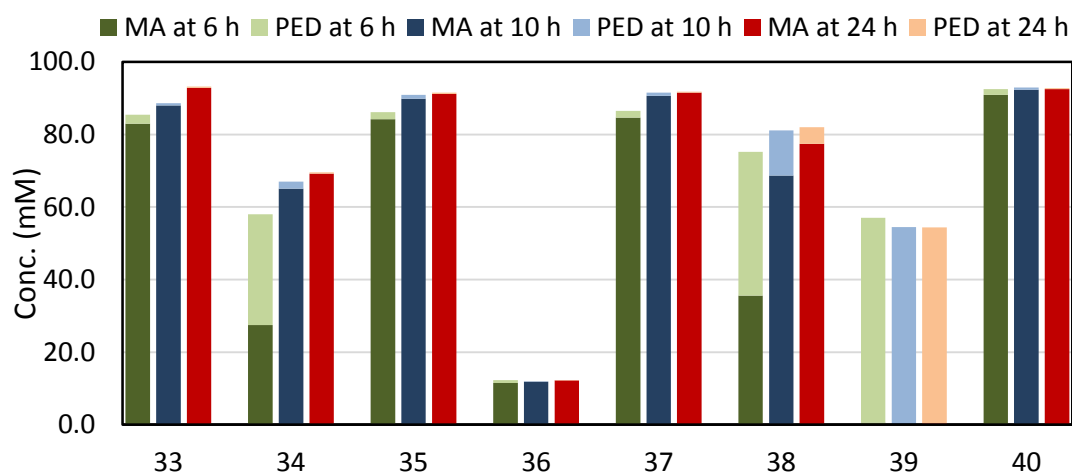
Figure 5.23. Cascade transformation of 100 mM L-phenylalanine to (*S*)-mandelic acid (MA) with different *E. coli* strains 33-40 containing Module 0, 1, and 2, coexpressing AtPAL, AnPAD, SMO, SpEH, AlkJ, and EcALDH. Values are average of three independent results.
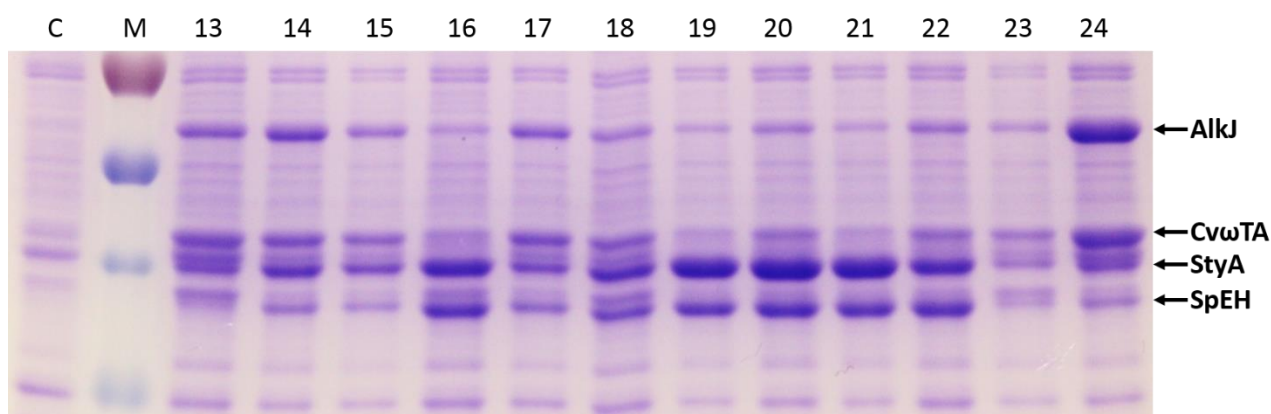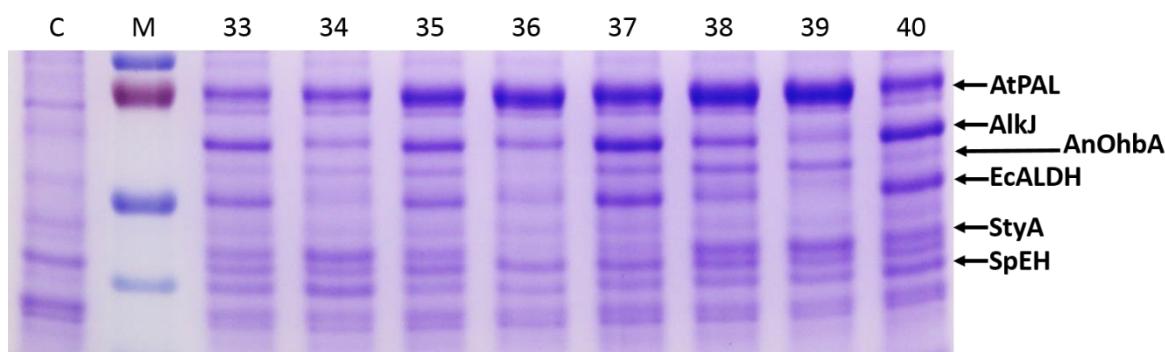

Figure 5.24. SDS-PAGE analysis of whole-cell protein of *E. coli* strains 33-40 containing Module 0, 1, and 2, coexpressing AtPAL, AnPAD, SMO, SpEH, AlkJ, and EcALDH.
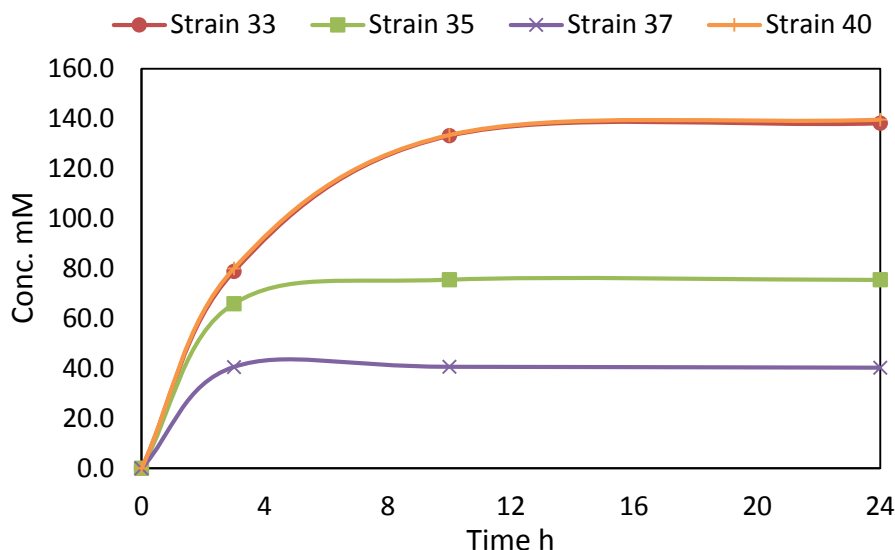
Figure 5.25. Production of (*S*)-mandelic acid from 150 mM L-phenylalanine with *E. coli* strains 33, 35, 37, 40 (15 g cdw/L), each containing Module 0, 1, and 2.

5.3.11 Assembly and Optimization of Module 0, Module 1, and Module 3 for Cascade Transformation of L-Phenylalanine to (*S*)-Phenylethanol Amine
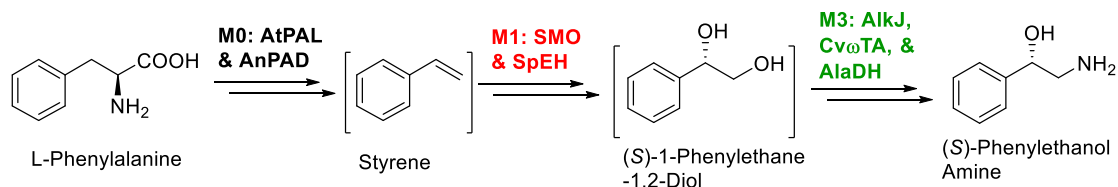
Scheme 5.9. Cascade transformation of L-phenylalanine to chiral (*S*)-phenylethanol amine with recombinant *E. coli* coexpressing multiple enzymes on Module 0, Module 1, and Module 3.

To produce (*S*)-phenylethanol amine from L-phenylalanine, Module 0 needs to be assembled with Module 1 and Module 3. Similarly to the above, the three best strains, strains 13, 17, 24, containing Module 1 and Module 3, were chosen as parental strains for combining with Module 0 on four different plasmids (A-M0, C-M0, E-M0, & R-M0). As a result, six different strains, strains 41-46, were obtained for coexpressing enzymes on the three modules. Initial screening found that strain 43 produced 7 mM (*S*)-phenylethanol amine from 50 mM L-phenylalanine in 24 h without optimization of reaction conditions. We are currently investigating the possible reasons for the low yield. Nevertheless, it still proved the feasibility of the cascade biocatalysis

and suggested the first *de novo* biosynthetic pathway from glucose via phenylalanine to this useful biogenic amine in enantiopure form.

5.3.12 Assembly and Optimization of Module 0, Module 1, Module 2, and Module 4 for Cascade Transformation of L-Phenylalanine to (*S*)-Phenylglycine
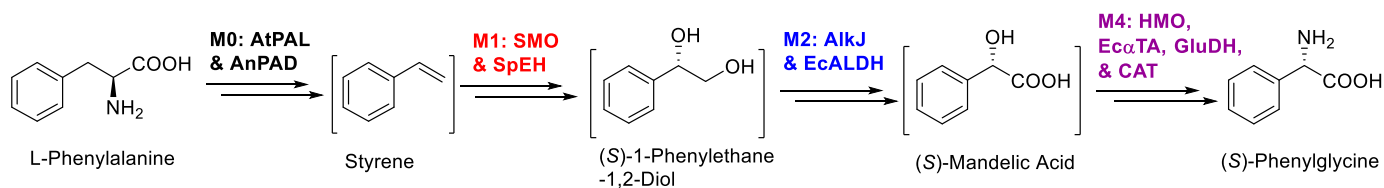
Scheme 5.10. Cascade transformation of L-phenylalanine to chiral (*S*)-phenylglycine with recombinant *E. coli* coexpressing multiple enzymes on Module 0, Module 1, Module 2, and Module 4.

The assembly of Module 0, Module 1, Module 2, and Module 4, could achieve production of (*S*)-phenylglycine from L-phenylalanine (Scheme 5.10). Module 0 on two plasmids (C-M0, E-M0) were transformed into the two best strains (strain 26, 27) containing Module 1, 2, and 4, to give strains 48, 49, respectively. On the other hand, Module 4 on two plasmids (R-M4, A-M4) were transformed into the two best strains (strains 33, 40) containing Module 0, 1, and 2, to offer strains 47, 50, respectively. Each of these four strains (strains 47-50) holds the four modules on four different plasmids and could be induced to coexpress ten enzymes, AtPAL, AnPAD, SMO, SpEH, AlkJ, EcALDH, HMO, EcIlvE, GluDH, and CAT. A set of experiment was performed to test them for converting 50 mM L-phenylalanine in the two-liquid phase system. Preliminary results showed that strain 48 and strain 49 produced 22 mM and 17 mM (*S*)-phenylglycine, respectively, in 24 h. The cascade biocatalysis successful demonstrated the production of non-proteinogenic (*S*)-phenylglycine from L-phenylalanine by assembly of four different modules in *E. coli*, and it also suggested a new *de nove* biosynthetic pathway to produce chiral phenylglycine from simple renewable bioresource, *e.g.* glucose.[399, 400]

5.4 Conclusion

Novel and efficient one-pot multi-step cascade biocatalysis for asymmetric oxy- and amino-functionalization of terminal aryl alkene to produce chiral α-hydroxy acid, 1,2-amino alcohol, and α-amino acid was developed by using a modular approach. The following modules were designed, constructed, and verified to give the desired transformation: (1) monooxygenase-epoxide hydrolase for asymmetric dihydroxylation of alkene to chiral 1,2-diol; (2) alcohol dehydrogenase-aldehyde dehydrogenase for terminal oxidation of chiral diol to chiral α-hydroxy acid; (3) alcohol dehydrogenase-ω-transaminase for terminal amination of 1,2-diol to 1,2-amino alcohol; (4) hydroxy acid oxidase-α-transaminase for sub-terminal amination of α-hydroxy acid to α-amino acid. Assembly of different modules in *E. coli* enabled cascade transformation of styrene to (*S*)-mandelic acid (Module 1 + 2), (*S*)-phenylethanolamine (Module 1 + 3), and (*S*)-phenylglycine (Module 1 + 2 + 4), respectively, with single whole-cell biocatalyst. Importantly, the expression level of multiple enzymes was adjustable by changing the plasmid backbone of different modules, and the expression was optimized to achieve efficient cascade catalysis. As a result of strain and reaction optimization, (*S*)-mandelic acid, (*S*)-phenylethanolamine, and (*S*)-phenylglycine were produced in high yield and excellent enantiopurity from styrene, respectively. In this work, we harnessed cascade biocatalysis to achieve asymmetric one-pot multi-step oxy- and amino-functionalization of hydrocarbons, which is useful but challenging in chemistry: the transformation of styrene to (*S*)-phenylethanolamine represents the first biocatalytic method for asymmetric aminohydroxylation, and the one-pot transformation of styrene to (*S*)-mandelic acid and (*S*)-phenylglycine is reported for the first time, without any known chemical counterparts. From a biochemical point of view, the cascade transformation is also a new artificial pathway, with no known natural equivalents. Other terminal alkenes could also be converted to other chiral α-hydroxy acids, 1,2-amino alcohols, and α-amino acids via the same biocatalytic cascade by

149

using these or other similar enzymes. The modular approach could be generally applied to other biocatalytic cascades to improve efficiency. Furthermore, we extended the cascade biocatalysis to start from L-phenylalanine with one additional module 0 (ammonia lyase-decarboxylase). By combining different modules in *E. coli*, bio-based L-phenylalanine was converted to enantiopure (*S*)-mandelic acid (Module 0 + 1 + 2), (*S*)-phenylethanolamine (Module 0 + 1 + 3), and (*S*)-phenylglycine (Module 0 + 1 + 2 + 4), respectively. This provides the opportunity to produce these useful and valuable enantiopure chemicals from renewable feedstock.

6 CONCLUSIONS AND RECOMMENDATIONS

6.1 Overall Conclusions

Biocatalysis is an emerging tool for production of high value added enantiopure fine chemicals and pharmaceutical intermediates in a green and efficient way. However, many biocatalytic reactions are still not efficient enough for practical application, due to the lack of highly active enzymes. Novel enzymes need to be discovered/engineered, and productive and cost-effective biotransformation needs to be developed. Another current limitation in biocatalysis is that most of industrial biotransformations are mainly based on one-step biocatalysis, which requires tedious intermediate recovery and purification for traditional multistep synthesis. Several types of cascade biocatalysis have been recently reported to overcome the limitation, yet most of them are still suffering from low productivity, limited substrate scope, and no access to multiple enantiomers. Furthermore, new type of cascades are demanded to achieve green and efficient one-pot multistep synthesis of various chiral fine chemicals.

One potential but currently inefficient biotransformation is enantioselective hydrolysis of epoxide with epoxide hydrolase (EH). To address this gap, we successfully identified and cloned a unique SpEH from *Sphingomonas* sp. HXN-200 based on genome sequencing for enantioselective hydrolysis of racemic and *meso*-epoxides to prepare the corresponding (*S*)-epoxides and (*R*, *R*)-vicinal diols, respectively. The engineered *E. coli* (SpEH) highly expressed SpEH and gave 172 folds higher cell-based activity for the hydrolysis of styrene oxide than that of *Sphingomonas* sp. HXN-200. Kinetic resolution of several selected racemic styrene oxides with the resting cells of *E. coli* (SpEH) produced the corresponding (*S*)-styrene oxides in 98.0-99.5% *ee* and 35.1-46.5% yield, representing the highest *R*-enantioselectivity for some styrene oxides among all the known EHs. Hydrolysis of three cyclic *meso*-epoxides afforded the corresponding (*R*, *R*)-vicinal diols in 86-93% *ee* and 90-99% yield. These

biotransformations showed high cell-based specific activities (0.28–4.3 U/mg cdw), product concentration, product/cells ratio, and cell-based productivity. Biotransformation at even higher substrate concentration produced (*S*)-styrene oxide in 430 mM (51 g/L$_{org}$) and (1*R*, 2*R*)-cyclohexene diol in 500 mM (58 g/L). The production of 500 mM (1*R*, 2*R*)-cyclohexene diol stands for the first report of EH-catalyzed hydrolysis of *meso*-epoxide in elevated concentration (>30 g/L). We also performed gram-scale preparation of three enantiopure epoxides and three vicinal diols in high *ee*. In comparison with the industrial standard, Jacobsen's Co(salen) catalyst, for hydrolysis of styrene oxide, *E. coli* (SpEH) showed similar product/catalyst ratio, but higher catalyst-based specific productivity. Clearly, the *E. coli* (SpEH) cells are highly active and easily available biocatalysts for the practical production of these useful and valuable enantiopure epoxides and vicinal diols.

To address the second gap of cascade biocatalysis, we developed an intracellular epoxidation-hydrolysis cascade for efficient asymmetric *trans*-dihydroxylation of aryl olefins to produce chiral vicinal diols by combining styrene monooxygenase (SMO) and epoxide hydrolase. *E. coli* (SSP1) was engineered to coexpress SMO and SpEH for efficient *S*-enantioselective dihydroxylation. Biotransformation of 15 terminal aryl olefins with *E. coli* (SSP1) produced the corresponding 15 (*S*)-vicinal diols in high *ee* (most *ee* 92-99%) and high yield (most yield > 67%). On the other hand, to achieve *R*-enantioselective dihydroxylation, *E. coli* (SST1) was engineered to coexpress SMO and the epoxide hydrolase from *Solanum tuberosum* (StEH, regioselective-complementary to SpEH). Transformations of 15 terminal aryl olefins with *E. coli* (SST1) gave corresponding 15 (*R*)-vicinal diols, in high *ee* (most *ee* 84-99%) and good yield (most yield > 65%). In addition, *E. coli* (SSP1) and *E. coli* (SST1) catalyzed the *trans*-dihydroxylation of *cis* and *trans* β-methyl styrenes with excellent and complementary stereoselectivity, giving each of the four stereoisomers of 1-phenyl-1,2-propanediol in high *ee* and *de*, respectively. Clearly, *E.*

coli (SSP1) and *E. coli* (SST1) are a unique pair of biocatalysts with complementary enantioselectivity, providing access to multiple enantiomers of products in high enantiopurity. The reversing of overall enantioselectivity by changing one-step regioselectivity could be a general strategy for elegant control of stereochemistry in cascade catalysis. Preparation of five (1*S*)-diols and five (1*R*)-diols was also demonstrated, and the process was easily scaled up by using growing cells in a bioreactor. The cascade biocatalysis utilizes molecular oxygen, water, and glucose as inexpensive stoichiometric reagents without involving any toxic metals. Thus it provides a green and useful synthetic tool to produce chiral vicinal diols, complementary to Sharpless *cis*-dihydroxylation.

With the above dihydroxylation, we developed very novel one-pot multi-step cascade biocatalysis for asymmetric oxy- and amino-functionalization of aryl alkenes to produce useful chiral hydroxy acids, amino alcohols, and amino acids. To achieve these challenging transformations, several enzymatic modules were designed, constructed, and validated to give the desired reactions: (1) SMO-SpEH for converting alkene to chiral 1,2-diol; (2) alcohol dehydrogenase-aldehyde dehydrogenase for converting 1,2-diol to chiral α-hydroxy acid; (3) alcohol dehydrogenase-ω-transaminase for converting 1,2-diol to 1,2-amino alcohol; (4) hydroxy acid oxidase-α-transaminase for converting α-hydroxy acid to chiral α-amino acid. Assembly of different modules in *E. coli* enabled cascade transformation of styrene to (*S*)-mandelic acid (Module 1 + 2), (*S*)-phenylethanolamine (Module 1 + 3), and (*S*)-phenylglycine (Module 1 + 2 + 4), respectively, with single whole-cell biocatalyst. As a result of strain and reaction optimization, (*S*)-mandelic acid, (*S*)-phenylethanolamine, and (*S*)-phenylglycine were produced in high yield and excellent enantiopurity from styrene, respectively. In this work, we harnessed cascade biocatalysis to achieve asymmetric one-pot multi-step oxy- and amino-functionalization of hydrocarbons, which is useful but challenging in chemistry: the transformation of styrene to (*S*)-phenylethanolamine

represents the first biocatalytic method for asymmetric aminohydroxylation, and the one-pot transformation of styrene to (*S*)-mandelic acid and (*S*)-phenylglycine is reported for the first time, without any known chemical counterparts. From a biochemical point of view, the cascade transformation is also a new artificial pathway, with no known natural equivalents. It demonstrated the power of retrosynthetic analysis and modular approach in designing and building of non-natural biocatalytic cascades (synthetic pathways). Furthermore, we extended the cascade biocatalysis to start from L-phenylalanine with one additional module 0 (ammonia lyase-decarboxylase). By combining different modules in *E. coli*, bio-based L-phenylalanine was converted to enantiopure (*S*)-mandelic acid (Module 0 + 1 + 2), (*S*)-phenylethanolamine (Module 0 + 1 + 3), and (*S*)-phenylglycine (Module 0 + 1 + 2 + 4), respectively. This provides the opportunity to produce these useful and valuable enantiopure chemicals from renewable feedstock.

To sum up the three parts, we developed several novel recombinant whole-cell biocatalysts and the corresponding processes for green and efficient production of various important chiral chemicals, including epoxide, diol, hydroxyl acid, amino alcohol, and amino acid, in high enantiopurity, from cheap and easily available racemic and *meso*-epoxide, prochiral alkene, or bio-based amino acid.

6.2 Recommendations for Future Work

The further developments would focus on the following directions.

6.2.1 Solving the Structure of SpEH and Protein Engineering

The newly identified SpEH has shown high enantioselectivity and high activity in hydrolysis of several racemic and *meso*-epoxides. To find out the reason for the enantioselectivity and activity at a molecular level, the 3-D structure of SpEH should be obtained to study the molecular interaction between substrate and enzymes. We had

applied homology modeling to get the structure of SpEH based on the most related structure of AnEH (PDB: 3g02A),[116] yet the resulting structure is unreliable (data not shown here), mainly because of the low similarity of 30% between SpEH and AnEH (refer to Figure 3.2). Thus, it is demanded to crystalize the SpEH and solve the 3-D structure to study the structure-function relationship. Furthermore, structure-guided protein engineering will be performed to improve SpEH properties. Although protein engineering of other EHs has been published to enhance the enantioselectivity[115, 116, 122] and activity[401, 402] in hydrolysis of racemic epoxides, there is no report on engineering of EH towards hydrolysis of *meso*-epoxides. Thus, it will be interesting to engineer SpEH for even more practical hydrolysis of many *meso*-epoxides.

6.2.2 Extending Substrate and Product Scope of the Cascade Biocatalysis
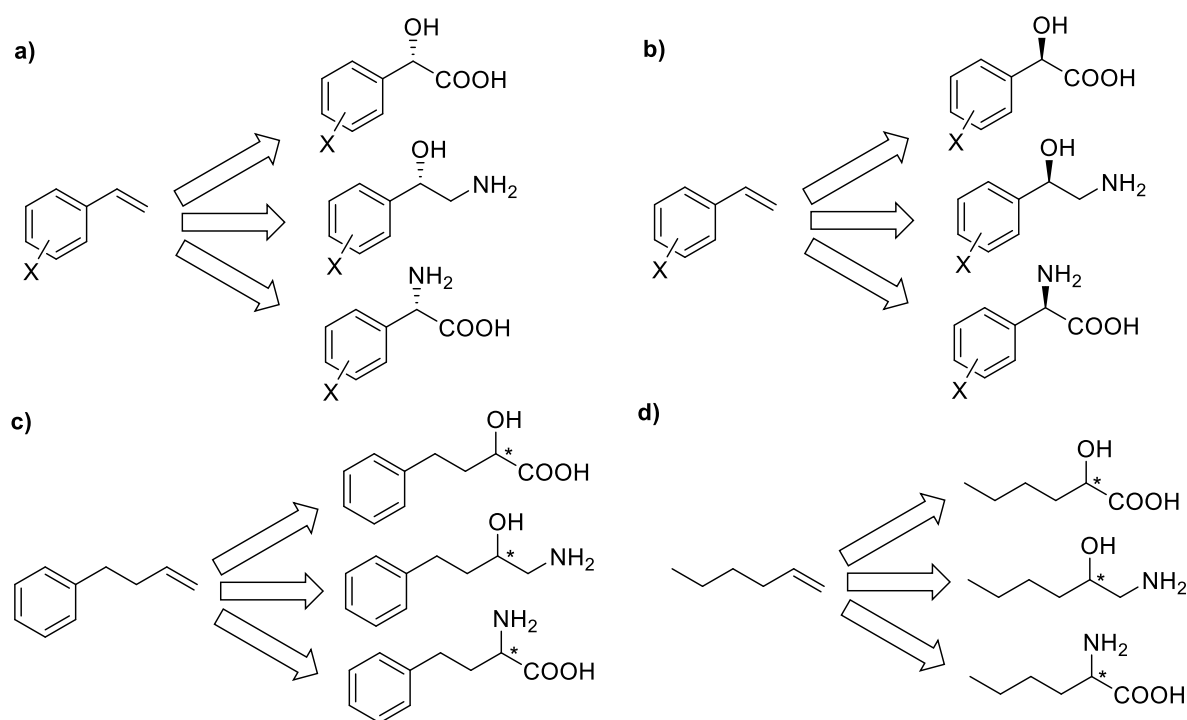
Scheme 6.1. Expended scope of the cascade biocatalysis for terminal alkenes to chiral α-hydroxy acids, 1,2-amino alcohols, and α-amino acids.

In the cascade biocatalysis for asymmetric oxy- and amino-functionalization of aryl alkenes, we had demonstrated the conversion of styrene to (*S*)-mandelic acid, (*S*)-phenylethanolamine, and (*S*)-phenylglycine. Obviously, some substituted styrenes could also be transformed into the corresponding substituted (*S*)-mandelic acids, (*S*)-

phenylethanolamines, and (*S*)-phenylglycines (Scheme 6.1a). Due to the time limitation, only the production of several substituted (*S*)-mandelic acids was reported in this thesis. On the other hand, the other enantiomer of the products, (*R*)-mandelic acids, (*R*)-phenylethanolamines, and (*R*)-phenylglycines, are very useful chiral chemicals as well (Scheme 6.1b). For example, (*R*)-phenylglycine is the key intermediate for manufacturing widely-used Ampicillin and Cefalexin.[238] The transformation of styrenes to these (*R*)-chemicals requires several (*R*)-selective enzymes (ADH, α-TA), and we have obtained some preliminary results on these enzymes. Besides the styrene type of substrates, the cascade biocatalysis could also convert other aromatic or even aliphatic alkenes (Scheme 6.1c, 6.1d) into the corresponding chiral α-hydroxy acids, 1,2-amino alcohols, and α-amino acids by using the same or other enzymes with similar functions. Some of these products are key chiral building blocks for pharmaceuticals, *e.g.* (*R*)-2-amino-4-phenylbutyric acid (L-homophenylalanine) for several angiotensin-converting enzyme (ACE) inhibitors[403] and anti-cancer drug Carfilzomib.[404]

6.2.3 Protein Engineering of Individual Enzymes to Improve Cascade Biocatalysis

During the development of cascade biocatalysis to produce (*S*)-mandelic acid, (*S*)-phenylethanolamine, and (*S*)-phenylglycine, we had identified the possible bottleneck enzymes. For example, the amination of (*S*)-mandelaldehyde to (*S*)-phenylethanolamine with CvωTA is not efficient, resulting in significant amount of (*S*)-mandelaldehyde and (*S*)-mandelic acid remained (refer to section 5.3.7). We suspected that CvωTA is either not stable or not active enough under the reaction condition. Since the structure of CvωTA has been solved recently,[405] protein engineering could be possible to solve this problem. On the other hand, HMO-catalyzed oxidation of (*S*)-mandelic acid is probably the bottleneck of producing (*S*)-phenylglycine. We noticed that the native substrate for HMO is hydroxymandelic acid, and this hydroxy group on the benzene ring might contribute to substrate binding to

HMO. If the amino acid residue for this binding can be identified and mutated, the mutated HMO could exhibit higher activity towards (*S*)-mandelic acid. There are other targets for protein engineering in the cascade biocatalysis, such as AlkJ, and enzymes for production of other products in section 6.2.2. Clearly, protein engineering has become a versatile tool in biocatalysis, and combining of protein engineering with cascade biocatalysis, metabolic engineering, and synthetic biology will enable efficient bio-production of various chemicals.

6.2.4 Development of Efficient Bioprocesses for Oxy- and Amino-Functionalization of Alkenes

Most of the biotransformations in this thesis were performed in shaking flasks with resting cells. In order to further improve the productivity and demonstrate the feasibility for future industrial implementation, the biotransformation should be scaled up in bioreactor (≥ 1 L) and catalyzed with growing cells. Furthermore, downstream processes should be developed as well. In this thesis, we had achieved some initial results for dihydroxylation using bioreactor and growing cells (section 4.3.10), but the more commercially potential transformation of styrene to (*S*)-mandelic acid and (*S*)-phenylglycine has not been performed in bioreactor. In the desired scenario, the recombinant *E. coli* strain is first grown in fermentor with the well-developed high-cell-density cultivation technology.[220-222] The protein expression is induced at a certain time during the growth. When the cells reach high density (*e.g.* 30-50 g cdw/L), styrene will be directly fed into the fermentor to start the biotransformation. Obviously, the feeding strategy of styrene is crucial for a highly productive process: the accumulation of styrene (*e.g.* > 1 mM) will be very toxic to the growing cells, while under-supply of styrene will lead to unsatisfied volumetric productivity. Furthermore, *in situ* product recovery/removal technology[406, 407] could be applied to reduce product inhibition. With all these efforts, we expect to produce (*S*)-mandelic acid and (*S*)-phenylglycine in 30-50 g/L in fermentor with high density of growing cells (representing a 2-5 folds

improvement of the results in shaking flask with less cells, section 5.3.6). This is essential for future commercialization.

6.2.5 Metabolic Engineering to Produce Chiral Chemicals from Glucose
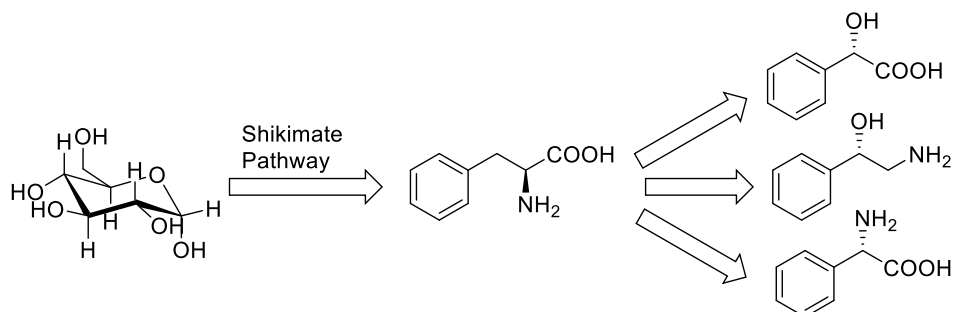
Scheme 6.2. Novel pathway from glucose to (*S*)-mandelic acid, (*S*)-phenylethanolamine, and (*S*)-phenylglycine.

We had demonstrated the conversion of L-phenylalanine to (*S*)-mandelic acid, (*S*)-phenylethanolamine, and (*S*)-phenylglycine, respectively, with multiple modular transformations in *E. coli* (sections 5.3.10-12). Phenylalanine was one of the most popular targets of metabolic engineering during the last decade, and it could be produced at the concentration of > 50 g/L using recombinant strains (*Corynebacterium glutamicum* or *E. coli*) in optimized fermentation.[408-411] Thus, the downstream transformation of phenylalanine could be introduced into the phenylalanine producer to achieve directly fermentative production of (*S*)-mandelic acid, (*S*)-phenylethanolamine, and (*S*)-phenylglycine from glucose. Even though bio-production of mandelic acid and phenylglycine in small concentration (≤1 g/L) has been reported with another pathway,[398-400] it depends on a difficult hydroxymandelate synthase.[194] In comparison, our pathway would probably be more efficient, since (*S*)-mandelic acid has been produced at 21 g/L from phenylalanine (sections 5.3.10). Therefore, it is an opportunity to develop new strains and efficient bioprocesses to produce these valuable chiral chemicals from renewable glucose via a novel pathway.

6.2.6 Cascade Biocatalysis for Formal anti-Markovnikov Hydration and Hydroamination of Aryl Alkenes

Anti-Markovnikov additions are one group of regioselective reactions for direct functionalization of alkenes to various useful chemicals, with huge potential for industrial applications.[412, 413] Two of the most important additions are anti-Markovnikov adding water to produce terminal alcohols (hydration) and adding ammonia to produce terminal amines (hydroamination), which together was named as one of 10 challenges for industrial catalysis.[414] Formal anti-Markovnikov hydration was traditionally achieved by two-step hydroboration-oxidation reaction,[415] and recently realized by oxidation-hydrolysis-reduction using Pd-Acid-Ru triple relay catalysis.[352] Regioselective hydroamination of alkenes was reported by mainly transition-metal-mediated and organocatalytic photoredox approaches.[416-418] However, many of these methods are still problematic: transitional metals, borane reagents, chiral ligands are expensive and toxic in general. And it is very challenging for hydroamination directly using ammonia. On the other hand, nature provides hydratases for hydration of C=C double bonds,[348-351] yet there is no enzyme for hydration of non-activated C=C double bonds with distinct anti-Markovnikov selectivity. Hydroamination of C=C bonds could be achieved with ammonia lyases and aminomutases,[387, 388] but none of them could convert non-activated C=C double bonds.
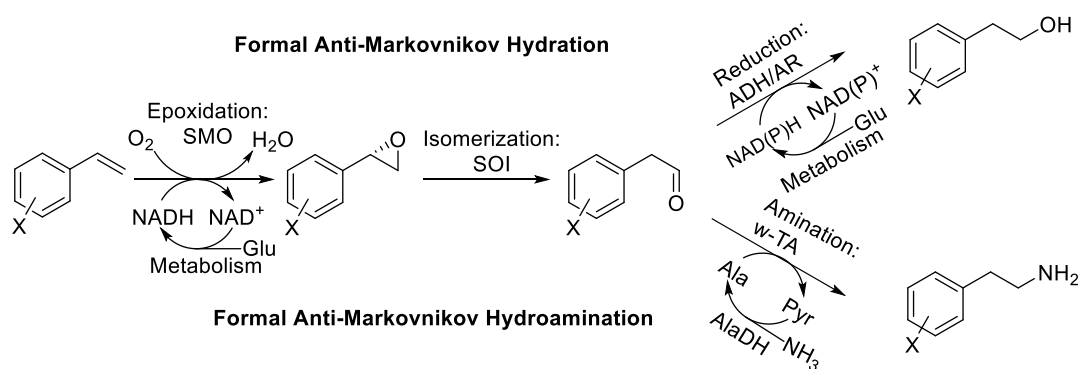
Scheme 6.3. Novel cascade biocatalysis to achieve formal anti-Markovnikov hydration and hydroamination of styrenes.

To address this significant gap, we are developing novel biocatalytic epoxidation-isomerization-reduction and epoxidation-isomerization-amination for formal anti-Markovnikov hydration and hydroamination of non-activated alkenes,

respectively (Scheme 6.3). The key step is isomerization of epoxide into aldehyde by styrene oxide isomerase (SOI). The transformations are very green, only consuming stoichiometric amount of oxygen, glucose, and ammonia. We have obtained very promising preliminary results recently, and more experiments are on-going.

6.2.7 Structure-based *in silico* Analysis and Synthetic Biology Tools for Design and Engineer Biocatalysis Systems

For future development of biocatalysis field, I believe two very important technologies could play a very important role: 1) Structure-based in silico analysis for development of biocatalysis with a single enzyme; and 2) Synthetic biology tools for engineering of biocatalysis system with multiple enzymes.

Enzyme function is determined by its 3-D structure. Thus *in silico* analysis of enzyme structures could provide much valuable insights for engineering enzymes with various improved features, such as high chemo-, regio-, and enantioselectivity, good stability, and expanded substrate scopes. Furthermore, *in silico* analysis of structure could also shed light on understanding of enzyme catalytic mechanisms, which will facilitate the development of new types of reactions.

Recently, many synthetic biology tools have been developed for quick and precise engineering of complex biological systems, and they are also applicable for engineering of novel and efficient cascade biocatalysis systems. Examples of these tools includes: advanced genetic cloning with Gibson's method[419] and DNA assembler[420]; advanced genomic engineering with multiplex automated genome engineering (MAGE)[421] and CRISPR/Cas technology[422]; and balancing multiple protein expression with promoter engineering[423] and engineering of other non-coding sequences[424, 425]. With these powerful tools, more novel and efficient whole-cell biocatalysts will be developed in the near future.

Bibliography

1. http://en.wikipedia.org/wiki/Chirality_(chemistry)

2. Noyori, R. Asymmetric catalysis: science and opportunities (Nobel lecture). *Angew. Chem. Int. Ed.* **2002**, *41*, 2008-2022.

3. Ager, D., Ed. *Handbook of Chiral Chemicals*, 2nd ed.; CRC Press, **2006**.

4. Rouhi, A. M. Chiral chemistry. *Chem. Eng. News*, **2004**, *82*, 47-62.

5. Lin, G. Q.; You, Q. D.; Cheng, J. F., Eds. *Chiral Drugs: Chemistry and Biological Action*; John Wiley & Sons, **2011**.

6. McGrath, N. A.; Brichacek, M.; Njardarson, J. T. A graphical journey of innovative organic architectures that have improved our lives. *J. Chem. Ed.*, **2010**, *87*, 1348-1349. (Top 200 drug poster by Njardarson group at University of Arizona)

7. Williams, A. Opportunities for chiral agrochemicals. *Pest. Sci.*, **1996**, *46*, 3-9.

8. Liu, W.; Gan, J.; Schlenk, D.; Jury, W. A. Enantioselectivity in environmental safety of current chiral insecticides. *Proc. Natl. Acad. Sci. U. S. A.*, **2005**, *102*, 701-706.

9. http://www.leffingwell.com/chirality/chirality.htm

10. Farina, V.; Reeves, J. T.; Senanayake, C. H.; Song, J. J. Asymmetric synthesis of active pharmaceutical ingredients. *Chem. Rev.* **2006**, *106*, 2734-2793.

11. Breuer, M.; Ditrich, K.; Habicher, T.; Hauer, B.; Kesseler, M.; Stürmer, R.; Zelinski, T. Industrial methods for the production of optically active intermediates. *Angew. Chem. Int. Ed.* **2004**, *43*, 788-824.

12. Ojima, I., Ed. *Catalytic Asymmetric Synthesis*, 3rd ed.; John Wiley & Sons, **2010**.

13. Berkessel, A., Gröger, H. *Asymmetric Organocatalysis: from Biomimetic Concepts to Applications in Asymmetric Synthesis*. John Wiley & Sons, **2006**.

14. MacMillan, D. W. The advent and development of organocatalysis. *Nature* **2008**, *455*, 304-308.

15. http://en.wikipedia.org/wiki/Biocatalysis

16. Faber, K. *Biotransformations in Organic Chemistry: a textbook*, 6th ed.; Springer, **2011**.

17. Liese, A.; Seelbach, K.; Wandrey, C., Eds. *Industrial Biotransformations*, 2nd ed.; John Wiley & Sons, **2006**.

18. Drauz, K.; Gröger, H.; May, O., Eds. *Enzyme Catalysis in Organic Synthesis: A Comprehensive Handbook*, 3rd ed.; John Wiley & Sons, **2012**.

19. Schmid, A.; Dordick, J. S.; Hauer, B.; Kiener, A.; Wubbolts, M.; Witholt, B. Industrial biocatalysis today and tomorrow. *Nature* **2001**, *409*, 258-268.

20. Koeller, K. M.; Wong, C. H. Enzymes for chemical synthesis. *Nature* **2001**, *409*, 232-240.

21. Schoemaker, H. E.; Mink, D.; Wubbolts, M. G. Dispelling the myths--biocatalysis in industrial synthesis. *Science* **2003**, *299*, 1694-1697.

22. Patel, R. N. Synthesis of chiral pharmaceutical intermediates by biocatalysis. *Coord. Chem. Rev.* **2008**, *252*, 659-701.

23. Hall, M.; Bommarius, A. S. Enantioenriched compounds via enzyme-catalyzed redox reactions. *Chem. Rev.* **2011**, *111*, 4088-4110.

24. Clouthier, C. M.; Pelletier, J. N. Expanding the organic toolbox: a guide to integrating biocatalysis in synthesis. *Chem. Soc. Rev.* **2012**, *41*, 1585-1605.

25. Bornscheuer, U. T.; Huisman, G. W.; Kazlauskas, R. J.; Lutz, S.; Moore, J. C.; Robins, K. Engineering the third wave of biocatalysis. *Nature* **2012**, *485*, 185-194.

26. Reetz, M. T. Biocatalysis in organic chemistry and biotechnology: past, present, and future. *J. Am. Chem. Soc.* **2013**, *135*, 12480-12496.

27. Nestl, B. M.; Hammer, S. C.; Nebel, B. A.; Hauer, B. New Generation of Biocatalysts for Organic Synthesis. *Angew. Chem. Int. Ed.* **2014**, *53*, 3070-3095.

28. Duetz, W. A.; Van Beilen, J. B.; Witholt, B. Using proteins in their natural environment: potential and limitations of microbial whole-cell hydroxylations in applied biocatalysis. *Curr. Opin. Biotechnol.* **2001**, *12*, 419-425.

29. Ishige, T.; Honda, K.; Shimizu, S. Whole organism biocatalysis. *Curr. Opin. Chem. Biol.* **2005**, *9*, 174-180.

30. Becker, U.; Doderer, K.; Osswald, S.; Verseck, S.; Wienand, W. Industrial applications of whole-cell biocatalysis. **2008**.

31. Carballeira, J. D.; Quezada, M. A.; Hoyos, P.; Simeó, Y.; Hernaiz, M. J.; Alcantara, A. R.; Sinisterra, J. V. Microbial cells as catalysts for stereoselective red–ox reactions. *Biotechnol. Adv.* **2009**, *27*, 686-714.

32. Schrewe, M.; Julsing, M. K.; Bühler, B.; Schmid, A. Whole-cell biocatalysis for selective and productive C–O functional group introduction and modification. *Chem. Soc. Rev.* **2013**, *42*, 6346-6377.

33. Ladkau, N.; Schmid, A.; Bühler, B. The microbial cell - functional unit for energy-dependent multistep biocatalysis. *Curr. Opin. Biotechnol.* **2014**, *30*, 178-189.

34. Riva, S.; Fessner, W.-D., Eds. *Cascade Biocatalysis Integrating Stereoselective and Environmentally Friendly Reactions*, John Wiley & Sons, **2014**.

35. Schrittwieser, J. H.; Sattler, J.; Resch, V.; Mutti, F. G.; Kroutil, W. Recent biocatalytic oxidation–reduction cascades. *Curr. Opin. Chem. Biol.* **2011**, *15*, 249-256.

36. Ricca, E.; Brucher, B.; Schrittwieser, J. H. Multi-Enzymatic Cascade Reactions: Overview and Perspectives. *Adv. Synth. Catal.* **2011**, *353*, 2239-2262.

37. Xue, R.; Woodley, J. M. Process technology for multi-enzymatic reaction systems. *Bioresour. Technol.* **2012**, *115*, 183-195.

38. Oroz-Guinea, I.; García-Junceda, E. Enzyme catalysed tandem reactions. *Curr. Opin. Chem. Biol.* **2013**, *17*, 236-249.

39. Simon, R. C.; Richter, N.; Busto, E.; Kroutil, W. Recent developments of cascade reactions involving ω-transaminases. *ACS Catal.* **2014**, *4*, 129-143.

40. Köhler, V.; Turner, N. J. Artificial concurrent catalytic processes involving enzymes. *Chemical Communications*. **2015**, DOI: 10.1039/C4CC07277D.

41. http://en.wikipedia.org/wiki/Biotechnology

42. Vaeck, M.; Reynaerts, A.; Höfte, H.; Jansens, S.; De Beuckeleer, M.; Dean, C.; Zabeau, M.; Montagu, M. V.; Leemans, J. Transgenic plants protected from insect attack. *Nature* **1987**, *328*, 33-37.

43. Ye, X.; Al-Babili, S.; Klöti, A.; Zhang, J.; Lucca, P.; Beyer, P.; Potrykus, I. Engineering the provitamin A (β-carotene) biosynthetic pathway into (carotenoid-free) rice endosperm. *Science* **2000**, *287*, 303-305.

44. Rob, A. S. What's fueling the biotech engine-2012 to 2013. *Nat. Biotechnol.* **2014**, *32*, 32-39.

45. Takahashi, K.; Yamanaka, S. Induction of pluripotent stem cells from mouse embryonic and adult fibroblast cultures by defined factors. *Cell* **2006**, *126*, 663-676.

46. http://www.dsm.com/content/dam/dsm/cworld/en_US/documents/white-biotech-mckinsey-feb-2009.pdf

47. http://www.europabio.org/sites/default/files/report/industrial_or_white_biotechnology_-_a_driver_of_sustainable_growth_in_europe.pdf

48. http://www.europabio.org/sites/default/files/report/industrial_or_white_biotechnology_-_research_for_europe.pdf

49. Kirk, O.; Borchert, T. V.; Fuglsang, C. C. Industrial enzyme applications. *Curr. Opin. Biotechnol.* **2002**, *13*, 345-351.

50. http://en.wikipedia.org/wiki/Industrial_fermentation

51. Wang, D. I. C.; Cooney, C. L.; Demain, A. L.; Dunnill, P.; Humphrey, A. E.; Lilly, M. D. *Fermentation and Enzyme Technology*; John Wiley & Sons, **1979**.

52. Grady Jr, C. L.; Daigger, G. T.; Love, N. G.; Filipe, C. D.; Leslie Grady, C. P. *Biological wastewater treatment*, 3rd ed.; IWA Publishing, **2011**.

53. http://en.wikipedia.org/wiki/Microbial_fuel_cell

54. https://en.wikipedia.org/wiki/W%C3%B6hler_synthesis

55. Stephanopoulos, G.; Aristidou, A. A.; Nielsen, J. *Metabolic engineering: principles and methodologies*; Academic press, **1998**.

56. Keasling, J. D. Manufacturing molecules through metabolic engineering. *Science* **2010**, *330*, 1355-1358.

57. Lee, J. W.; Na, D.; Park, J. M.; Lee, J.; Choi, S.; Lee, S. Y. Systems metabolic engineering of microorganisms for natural and non-natural chemicals. *Nat. Chem. Biol.* **2012**, *8*, 536-546.

58. Zhao, H., Eds. *Synthetic Biology: Tools and Applications*; Academic press, **2013**.

59. Kalscheuer, R.; Stölting, T.; Steinbüchel, A. Microdiesel: Escherichia coli engineered for fuel production. *Microbiology* **2006**, *152*, 2529-2536.

60. Martin, C. H.; Dhamankar, H.; Tseng, H. C.; Sheppard, M. J.; Reisch, C. R.; Prather, K. L. A platform pathway for production of 3-hydroxyacids provides a biosynthetic route to 3-hydroxy-γ-butyrolactone. *Nat. Commun.* **2013**, *4*, 1414.

61. Dong, C.; Huang, F.; Deng, H.; Schaffrath, C.; Spencer, J. B.; O'Hagan, D.; Naismith, J. H. Crystal structure and mechanism of a bacterial fluorinating enzyme. *Nature* **2004**, *427*, 561-565.

62. http://en.wikipedia.org/wiki/Human_Genome_Project

63. Shendure, J.; Ji, H. Next-generation DNA sequencing. *Nat. Biotechnol.* **2008**, *26*, 1135-1145.

64. Metzker, M. L. Sequencing technologies—the next generation. *Nat. Rev. Genet.* **2009**, *11*, 31-46.

65. Lorenz, P.; Eck, J. Metagenomics and industrial applications. *Nat. Rev. Microbiol.* **2005**, *3*, 510-516.

66. Ferrer, M.; Martínez-Abarca, F.; Golyshin, P. N. Mining genomes and 'metagenomes' for novel catalysts. *Curr. Opin. Biotechnol.* **2005**, *16*, 588-593.

67. Kim, H. J.; Ruszczycky, M. W.; Choi, S. H.; Liu, Y. N.; Liu, H. W. Enzyme-catalysed [4+2] cycloaddition is a key step in the biosynthesis of spinosyn A. *Nature* **2011**, *473*, 109-112.

68. Geu-Flores, F.; Sherden, N. H.; Courdavault, V.; Burlat, V.; Glenn, W. S.; Wu, C.; Nims, E.; Cui, Y.; O'Connor, S. E. An alternative route to cyclic terpenes by reductive cyclization in iridoid biosynthesis. *Nature* **2012**, *492*, 138-142.

69. Schirmer, A.; Rude, M. A.; Li, X.; Popova, E.; Del Cardayre, S. B. Microbial biosynthesis of alkanes. *Science* **2010**, *329*, 559-562.

70. Arnold, F. H. Combinatorial and computational challenges for biocatalyst design. *Nature* **2001**, *409*, 253-257.

71. Zhao, H.; Chockalingam, K.; Chen, Z. Directed evolution of enzymes and pathways for industrial biocatalysis. *Curr. Opin. Biotechnol.* **2002**, *13*, 104-110.

72. Turner, N. J. Directed evolution drives the next generation of biocatalysts. *Nat. Chem. Biol.* **2009**, *5*, 567-573.

73. Reetz, M. T. Laboratory evolution of stereoselective enzymes: a prolific source of catalysts for asymmetric reactions. *Angew. Chem. Int. Ed.* **2011**, *50*, 138-174.

74. Strohmeier, G. A.; Pichler, H.; May, O.; Gruber-Khadjawi, M. Application of designed enzymes in organic synthesis. *Chem. Rev.* **2011**, *111*, 4141-4164.

75. Cobb, R. E.; Si, T.; Zhao, H. Directed evolution: an evolving and enabling synthetic biology tool. *Curr. Opin. Chem. Biol.* **2012**, *16*, 285-291.

76. Reetz, M. T.; Wang, L. W.; Bocola, M. Directed Evolution of Enantioselective Enzymes: Iterative Cycles of CASTing for Probing Protein-Sequence Space. *Angew. Chem. Int. Ed.* **2006**, *45*, 1236-1241.

77. Reetz, M. T.; Carballeira, J. D. Iterative saturation mutagenesis (ISM) for rapid directed evolution of functional enzymes. *Nat. Protoc.* **2007**, *2*, 891-903.

78. Kille, S.; Zilly, F. E.; Acevedo, J. P.; Reetz, M. T. Regio-and stereoselectivity of P450-catalysed hydroxylation of steroids controlled by laboratory evolution. *Nat. Chem.* **2011**, *3*, 738-743.

79. Savile, C. K.; Janey, J. M.; Mundorff, E. C.; Moore, J. C.; Tam, S.; Jarvis, W. R.; Colbeck, J. C.; Krebber, A.; Fleitz, F. J.; Brands, J.; Devine, P. N.; Huisman, G. W.; Hughes, G. J. Biocatalytic asymmetric synthesis of chiral amines from ketones applied to sitagliptin manufacture. *Science* **2010**, *329*, 305-309.

80. Höhne, M.; Schätzle, S.; Jochens, H.; Robins, K.; Bornscheuer, U. T. Rational assignment of key motifs for function guides in silico enzyme identification. *Nat. Chem. Biol.* **2010**, *6*, 807-813.

81. Bornscheuer, U. T.; Kazlauskas, R. J. Catalytic promiscuity in biocatalysis: using old enzymes to form new bonds and follow new pathways. *Angew. Chem. Int. Ed.* **2004**, *43*, 6032-6040.

82. Hult, K.; Berglund, P. Enzyme promiscuity: mechanism and applications. *Trends Biotechnol.* **2007**, *25*, 231-238.

83. Tawfik, O. K. A. D. S. Enzyme promiscuity: a mechanistic and evolutionary perspective. *Annu. Rev. Biochem.* **2010**, *79*, 471-505.

84. Busto, E.; Gotor-Fernández, V.; Gotor, V. Hydrolases: catalytically promiscuous enzymes for non-conventional reactions in organic synthesis. *Chem. Soc. Rev.* **2010**, *39*, 4504-4523.

85. Kapoor, M.; Gupta, M. N. Lipase promiscuity and its biochemical applications. *Process Biochem.* **2012**, *47*, 555-569.

86. Branneby, C.; Carlqvist, P.; Magnusson, A.; Hult, K.; Brinck, T.; Berglund, P. Carbon-carbon bonds by hydrolytic enzymes. *J. Am. Chem. Soc.* **2003**, *125*, 874-875.

87. Coelho, P. S.; Brustad, E. M.; Kannan, A.; Arnold, F. H. Olefin cyclopropanation via carbene transfer catalyzed by engineered cytochrome P450 enzymes. *Science* **2013**, *339*, 307-310.

88. Coelho, P. S.; Wang, Z. J.; Ener, M. E.; Baril, S. A.; Kannan, A.; Arnold, F. H.; Brustad, E. M. A serine-substituted P450 catalyzes highly efficient carbene transfer to olefins in vivo. *Nat. Chem. Biol.* **2013**, *9*, 485-487.

89. Nanda, V.; Koder, R. L. Designing artificial enzymes by intuition and computation. *Nat. Chem.* **2010**, *2*, 15-24.

90. Kiss, G.; Çelebi-Ölçüm, N.; Moretti, R.; Baker, D.; Houk, K. N. Computational enzyme design. *Angew. Chem. Int. Ed.* **2013**, *52*, 5700-5725.

91. Röthlisberger, D.; Khersonsky, O.; Wollacott, A. M.; Jiang, L.; DeChancie, J.; Betker, J.; Gallaher, J. L.; Althoff, E. A.; Zanghellini, A.; Dym, O.; Albeck, S.; Houk, K. N.; Tawfik, D. S.; Baker, D. Kemp elimination catalysts by computational enzyme design. *Nature* **2008**, *453*, 190-195.

92. Siegel, J. B.; Zanghellini, A.; Lovick, H. M.; Kiss, G.; Lambert, A. R.; Clair, J. L. S.; Gallaher, J. L.; Hilvert, D.; Gelb, M. H.; Stoddard, B. L.; Houk, K. N.; Michael, F. E.; Baker, D. Computational design of an enzyme catalyst for a stereoselective bimolecular Diels-Alder reaction. *Science* **2010**, *329*, 309-313.

93. Blomberg, R.; Kries, H.; Pinkas, D. M.; Mittl, P. R.; Grütter, M. G.; Privett, H. K.; Mayo, S. L.; Hilvert, D. Precision is essential for efficient catalysis in an evolved Kemp eliminase. *Nature* **2013**, *503*, 418-421.

94. http://en.wikipedia.org/wiki/Enzyme_Commission_number

95. http://en.wikipedia.org/wiki/List_of_enzymes

96. Morisseau, C.; Hammock, B. D. Epoxide hydrolases: mechanisms, inhibitor designs, and biological roles. *Annu. Rev. Pharmacol. Toxicol.* **2005**, *45*, 311-333.

97. Archelas, A.; Furstoss, R. Synthetic applications of epoxide hydrolases. *Curr. Opin. Chem. Biol.* **2001**, *5*, 112-119.

98. Steinreiber, A.; Faber, K. Microbial epoxide hydrolases for preparative biotransformations. *Curr. Opin. Biotechnol.* **2001**, *12*, 552-558.

99. Smit, M. S.; Labuschagné, M. Diversity of epoxide hydrolase biocatalysts. *Curr. Org. Chem.* **2006**, *10*, 1145-1161.

100. Lee, E. Y.; Shuler, M. L. Molecular engineering of epoxide hydrolase and its application to asymmetric and enantioconvergent hydrolysis. *Biotechnol. Bioeng.* **2007**, *98*, 318-327.

101.   Choi, W. J. Biotechnological production of enantiopure epoxides by enzymatic kinetic resolution. *Appl. Microbiol. Biotechnol.* **2009**, *84*, 239-247.

102.   Widersten, M.; Gurell, A.; Lindberg, D. Structure–function relationships of epoxide hydrolases and their potential use in biocatalysis. *Biochim. Biophys. Acta* **2010**, *1800*, 316-326.

103.   Bala, N.; Chimni, S. S. Recent developments in the asymmetric hydrolytic ring opening of epoxides catalysed by microbial epoxide hydrolase. *Tetrahedron: Asymmetry* **2010**, *21*, 2879-2898.

104.   Kotik, M.; Archelas, A.; Wohlgemuth, R. Epoxide hydrolases and their application in organic synthesis. *Curr. Org. Chem.* **2012**, *16*, 451-482.

105.   Archelas, A.; Furstoss, A. R. Synthesis of enantiopure epoxides through biocatalytic approaches. *Annu. Rev. Microbiol.* **1997**, *51*, 491-525.

106.   Chen, X. J.; Archelas, A.; Furstoss, R. Microbiological transformations. 27. The first examples for preparative-scale enantioselective or diastereoselective epoxide hydrolyses using microorganisms. An unequivocal access to all four bisabolol stereoisomers. *J. Org. Chem.* **1993**, *58*, 5528-5532.

107.   Pedragosa-Moreau, S.; Archelas, A.; Furstoss, R. Microbiological transformations. 28. Enantiocomplementary epoxide hydrolyses as a preparative access to both enantiomers of styrene oxide. *J. Org. Chem.* **1993**, *58*, 5533-5536.

108.   Pedragosa-Moreau, S.; Morisseau, C.; Zylber, J.; Archelas, A.; Baratti, J.; Furstoss, R. Microbiological transformations. 33. Fungal epoxide hydrolases applied to the synthesis of enantiopure para-substituted styrene oxides. A mechanistic approach. *J. Org. Chem.* **1996**, *61*, 7402-7407.

109.   Jin, H.; Li, Z. Y.; Dong, X. W. Enantioselective hydrolysis of various substituted styrene oxides with Aspergillus Niger CGMCC 0496. *Org. Biomol. Chem.* **2004**, *2*, 408-414.

110.   Manoj, K. M.; Archelas, A.; Baratti, J.; Furstoss, R. Microbiological transformations. Part 45: A green chemistry preparative scale synthesis of enantiopure building blocks of Eliprodil: elaboration of a high substrate concentration epoxide hydrolase-catalyzed hydrolytic kinetic resolution process. *Tetrahedron* **2001**, *57*, 695-701.

111.   Monfort, N.; Archelas, A.; Furstoss, R. Enzymatic transformations. Part 55: Highly productive epoxide hydrolase catalysed resolution of an azole antifungal key synthon. *Tetrahedron* **2004**, *60*, 601-605.

112.   Doumèche, B.; Archelas, A.; Furstoss, R. Enzymatic Transformations 62. Preparative Scale Synthesis of Enantiopure Glycidyl Acetals using an Aspergillus

niger Epoxide Hydrolase-Catalysed Kinetic Resolution. *Adv. Synth. Catal.* **2006**, *348*, 1948-1957.

113.   Deregnaucourt, J.; Archelas, A.; Barbirato, F.; Paris, J. M.; Furstoss, R. Enzymatic Transformations 63. High-Concentration Two Liquid-Liquid Phase Aspergillus niger Epoxide Hydrolase-Catalysed Resolution: Application to Trifluoromethyl-Substituted Aromatic Epoxides. *Adv. Synth. Catal.* **2007**, *349*, 1405-1417.

114.   Zou, J.; Hallberg, B. M.; Bergfors, T.; Oesch, F.; Arand, M.; Mowbray, S. L.; Jones, T. A. Structure of Aspergillus niger epoxide hydrolase at 1.8 Å resolution: implications for the structure and function of the mammalian microsomal class of epoxide hydrolases. *Structure* **2000**, *8*, 111-122.

115.   Reetz, M. T.; Torre, C.; Eipper, A.; Lohmer, R.; Hermes, M.; Brunner, B.; Furstoss, R. Enhancing the enantioselectivity of an epoxide hydrolase by directed evolution. *Org. Lett.* **2004**, *6*, 177-180.

116.   Reetz, M. T.; Bocola, M.; Wang, L. W.; Sanchis, J.; Cronin, A.; Arand, M.; Zou, J.; Archelas, A.; Bottalla, A-L.; Naworyta, A.; Mowbray, S. L. Directed evolution of an enantioselective epoxide hydrolase: uncovering the source of enantioselectivity at each evolutionary stage. *J. Am. Chem. Soc.* **2009**, *131*, 7334-7343.

117.   Jacobs, M. H.; Wijngaard, A. J.; Pentenga, M.; Janssen, D. B. Characterization of the epoxide hydrolase from an epichlorohydrin-degrading Pseudomonas sp. *Eur. J. Biochem.* **1991**, *202*, 1217-1222.

118.   Rink, R.; Fennema, M.; Smids, M.; Dehmel, U.; Janssen, D. B. Primary structure and catalytic mechanism of the epoxide hydrolase from Agrobacterium radiobacter AD1. *J. Biol. Chem.* **1997**, *272*, 14650-14657.

119.   Spelberg, J. H. L.; Rink, R.; Kellogg, R. M.; Janssen, D. B. Enantioselectivity of a recombinant epoxide hydrolase from Agrobacterium radiobacter. *Tetrahedron: Asymmetry* **1998**, *9*, 459-466.

120.   van Loo, B.; Kingma, J.; Heyman, G.; Wittenaar, A.; Lutje Spelberg, J. H.; Sonke, T.; Janssen, D. B. Improved enantioselective conversion of styrene epoxides and meso-epoxides through epoxide hydrolases with a mutated nucleophile-flanking residue. *Enzyme Microb. Technol.* **2009**, *44*, 145-153.

121.   Nardini, M.; Ridder, I. S.; Rozeboom, H. J.; Kalk, K. H.; Rink, R.; Janssen, D. B.; Dijkstra, B. W. The X-ray Structure of Epoxide Hydrolase from Agrobacterium radiobacter AD1 An enzyme to detoxify harmful epoxides. *J. Biol. Chem.* **1999**, *274*, 14579-14586.

122.   Rink, R.; Lutje Spelberg, J. H.; Pieters, R. J.; Kingma, J.; Nardini, M.; Kellogg, R. M.; Dijkstra, B. W.; Janssen, D. B. Mutation of tyrosine residues involved in the alkylation half reaction of epoxide hydrolase from Agrobacterium radiobacter AD1 results in improved enantioselectivity. *J. Am. Chem. Soc.* **1999**, *121*, 7417-7418.

123.   van Loo, B.; Spelberg, J. H. L.; Kingma, J.; Sonke, T.; Wubbolts, M. G.; Janssen, D. B. Directed Evolution of Epoxide Hydrolase from A. radiobacter toward Higher Enantioselectivity by Error-Prone PCR and DNA Shuffling. *Chem. Biol.* **2004**, *11*, 981-990.

124.   Rui, L.; Cao, L.; Chen, W.; Reardon, K. F.; Wood, T. K. Protein engineering of epoxide hydrolase from Agrobacterium radiobacter AD1 for enhanced activity and enantioselective production of (R)-1-phenylethane-1, 2-diol. *Appl. Environ. Microbiol.* **2005**, *71*, 3995-4003.

125.   Chang, D.; Wang, Z.; Heringa, M. F.; Wirthner, R.; Witholt, B.; Li, Z. Highly enantioselective hydrolysis of alicyclic meso-epoxides with a bacterial epoxide hydrolase from Sphingomonas sp. HXN-200: simple syntheses of alicyclic vicinal trans-diols. *Chem. Commun.* **2003**, 960-961.

126.   Chang, D.; Heringa, M. F.; Witholt, B.; Li, Z. Enantioselective Trans Dihydroxylation of Nonactivated CC Double Bonds of Aliphatic Heterocycles with Sphingomonas sp. HXN-200. *J. Org. Chem.* **2003**, *68*, 8599-8606.

127.   Liu, Z.; Michel, J.; Wang, Z.; Witholt, B.; Li, Z. Enantioselective hydrolysis of styrene oxide with the epoxide hydrolase of Sphingomonas sp. HXN-200. *Tetrahedron: Asymmetry* **2006**, *17*, 47-52.

128.   Jia, X.; Wang, Z.; Li, Z. Preparation of (S)-2-, 3-, and 4-chlorostyrene oxides with the epoxide hydrolase from Sphingomonas sp. HXN-200. *Tetrahedron: Asymmetry* **2008**, *19*, 407-415.

129.   Lin, H.; Liu, J. Y.; Wang, H. B.; Ahmed, A. A. Q.; Wu, Z. L. Biocatalysis as an alternative for the production of chiral epoxides: a comparative review. *J. Mol. Catal. B: Enzym.* **2011**, *72*, 77-89.

130.   Allain, E. J.; Hager, L. P.; Deng, L.; Jacobsen, E. N. Highly enantioselective epoxidation of disubstituted alkenes with hydrogen peroxide catalyzed by chloroperoxidase. *J. Am. Chem. Soc.* **1993**, *115*, 4415-4416.

131.   Dexter, A. F.; Lakner, F. J.; Campbell, R. A.; Hager, L. P. Highly enantioselective epoxidation of 1, 1-disubstituted alkenes catalyzed by chloroperoxidase. *J. Am. Chem. Soc.* **1995**, *117*, 6412-6413.

132.   Colonna, S.; Gaggero, N.; Casella, L.; Carrea, G.; Pasta, P. Enantioselective epoxidation of styrene derivatives by chloroperoxidase catalysis. *Tetrahedron: Asymmetry* **1993**, *4*, 1325-1330.

133.   Holtmann, D.; Fraaije, M. W.; Arends, I. W.; Opperman, D. J.; Hollmann, F. The taming of oxygen: biocatalytic oxyfunctionalisations. *Chem. Commun.* **2014**, *50*, 13180-13200.

134.   Torres Pazmino, D. E.; Winkler, M.; Glieder, A.; Fraaije, M. W. Monooxygenases as biocatalysts: classification, mechanistic aspects and biotechnological applications. *J. Biotechnol.* **2010**, *146*, 9-24.

135.   Van Berkel, W. J. H.; Kamerbeek, N. M.; Fraaije, M. W. Flavoprotein monooxygenases, a diverse class of oxidative biocatalysts. *J. Biotechnol.* **2006**, *124*, 670-689.

136.   Montersino, S.; Tischler, D.; Gassner, G. T.; van Berkel, W. J. Catalytic and structural features of flavoprotein hydroxylases and epoxidases. *Adv. Synth. Catal.* **2011**, *353*, 2301-2319.

137.   Mooney, A.; Ward, P. G.; O'Connor, K. E. Microbial degradation of styrene: biochemistry, molecular genetics, and perspectives for biotechnological applications. *Appl. Microbiol. Biotechnol.* **2006**, *72*, 1-10.

138.   Panke, S.; Witholt, B.; Schmid, A.; Wubbolts, M. G. Towards a biocatalyst for (S)-styrene oxide production: characterization of the styrene degradation pathway of Pseudomonas sp. strain VLB120. *Appl. Environ. Microbiol.* **1998**, *64*, 2032-2043.

139.   Beltrametti, F.; Marconi, A. M.; Bestetti, G.; Colombo, C.; Galli, E.; Ruzzi, M.; Zennaro, E. Sequencing and functional analysis of styrene catabolism genes from Pseudomonas fluorescens ST. *Appl. Environ. Microbiol.* **1997**, *63*, 2232-2239.

140.   Velasco, A.; Alonso, S.; García, J. L.; Perera, J.; Díaz, E. Genetic and functional analysis of the styrene catabolic cluster of Pseudomonas sp. strain Y2. *J. Bacteriol.* **1998**, *180*, 1063-1071.

141.   Otto, K.; Hofstetter, K.; Röthlisberger, M.; Witholt, B.; Schmid, A. Biochemical characterization of StyAB from Pseudomonas sp. strain VLB120 as a two-component flavin-diffusible monooxygenase. *J. Bacteriol.* **2004**, *186*, 5292-5302.

142.   Tischler, D.; Eulberg, D.; Lakner, S.; Kaschabek, S. R.; van Berkel, W. J.; Schlömann, M. Identification of a novel self-sufficient styrene monooxygenase from Rhodococcus opacus 1CP. *J. Bacteriol.* **2009**, *191*, 4996-5009.

143.   Schmid, A.; Hofstetter, K.; Feiten, H. J.; Hollmann, F.; Witholt, B. Integrated biocatalytic synthesis on gram scale: the highly enantioselective preparation of

chiral oxiranes with styrene monooxygenase. *Adv. Synth. Catal.* **2001**, *343*, 732-737.

144.   Bernasconi, S.; Orsini, F.; Sello, G.; Di Gennaro, P. Bacterial monooxygenase mediated preparation of nonracemic chiral oxiranes: study of the effects of substituent nature and position. *Tetrahedron: asymmetry* **2004**, *15*, 1603-1606.

145.   Toda, H.; Imae, R.; Itoh, N. Efficient biocatalysis for the production of enantiopure (S)-epoxides using a styrene monooxygenase (SMO) and Leifsonia alcohol dehydrogenase (LSADH) system. *Tetrahedron: Asymmetry* **2012**, *23*, 1542-1549.

146.   Hofstetter, K.; Lutz, J.; Lang, I.; Witholt, B.; Schmid, A. Coupling of biocatalytic asymmetric epoxidation with NADH regeneration in organic–aqueous emulsions. *Angew. Chem. Int. Ed.* **2004**, *43*, 2163-2166.

147.   Hollmann, F.; Lin, P. C.; Witholt, B.; Schmid, A. Stereospecific biocatalytic epoxidation: the first example of direct regeneration of a FAD-dependent monooxygenase for catalysis. *J. Am. Chem. Soc.* **2003**, *125*, 8209-8217.

148.   Hollmann, F.; Hofstetter, K.; Habicher, T.; Hauer, B.; Schmid, A. Direct electrochemical regeneration of monooxygenase subunits for biocatalytic asymmetric epoxidation. *J. Am. Chem. Soc.* **2005**, *127*, 6540-6541.

149.   Panke, S.; Wubbolts, M. G.; Schmid, A.; Witholt, B. Production of enantiopure styrene oxide by recombinant Escherichia coli synthesizing a two-component styrene monooxygenase. *Biotechnol. Bioeng.* **2000**, *69*, 91-100.

150.   Panke, S.; Held, M.; Wubbolts, M. G.; Witholt, B.; Schmid, A. Pilot-scale production of (S)-styrene oxide from styrene by recombinant Escherichia coli synthesizing styrene monooxygenase. *Biotechnol. Bioeng.* **2002**, *80*(1), 33-41.

151.   Park, J. B.; Bühler, B.; Habicher, T.; Hauer, B.; Panke, S.; Witholt, B.; Schmid, A. The efficiency of recombinant Escherichia coli as biocatalyst for stereospecific epoxidation. *Biotechnol. Bioeng.* **2006**, *95*, 501-512.

152.   Kuhn, D.; Kholiq, M. A.; Heinzle, E.; Bühler, B.; Schmid, A. Intensification and economic and ecological assessment of a biocatalytic oxyfunctionalization process. *Green Chem.* **2010**, *12*, 815-827.

153.   Ukaegbu, U. E.; Kantz, A.; Beaton, M.; Gassner, G. T.; Rosenzweig, A. C. Structure and ligand binding properties of the epoxidase component of styrene monooxygenase. *Biochemistry* **2010**, *49*, 1678-1688.

154.   Morrison, E.; Kantz, A.; Gassner, G. T.; Sazinsky, M. H. Structure and Mechanism of Styrene Monooxygenase Reductase: New Insight into the FAD-Transfer Reaction. *Biochemistry* **2013**, *52*, 6063-6075.

155.   Lin, H.; Tang, D. F.; Ahmed, A. A. Q.; Liu, Y.; Wu, Z. L. Mutations at the putative active cavity of styrene monooxygenase: enhanced activity and reversed enantioselectivity. *J. Biotechnol.* **2012**, *161*, 235-241.

156.   Bernhardt, R. Cytochromes P450 as versatile biocatalysts. *J. Biotechnol.* **2006**, *124*, 128-145.

157.   O'Reilly, E.; Köhler, V.; Flitsch, S. L.; Turner, N. J. Cytochromes P450 as useful biocatalysts: addressing the limitations. *Chem. Commun.* **2011**, *47*, 2490-2501.

158.   Urlacher, V. B.; Girhard, M. Cytochrome P450 monooxygenases: an update on perspectives for synthetic application. *Trends Biotechnol.* **2012**, *30*, 26-36.

159.   Fasan, R. Tuning P450 enzymes as oxidation catalysts. *ACS Catal.* **2012**, *2*, 647-666.

160.   Thibodeaux, C. J.; Chang, W. C.; Liu, H. W. Enzymatic chemistry of cyclopropane, epoxide, and aziridine biosynthesis. *Chem. Rev.* **2012**, *112*, 1681-1709.

161.   Martinez, C. A.; Stewart, J. D. Cytochrome P450s potential catalysts for asymmetric olefin epoxidations. *Curr. Org. Chem.* **2000**, *4*, 263-282.

162.   Whitehouse, C. J.; Bell, S. G.; Wong, L. L. P450BM3 (CYP102A1): connecting the dots. *Chem. Soc. Rev.* **2012**, *41*, 1218-1260.

163.   Fruetel, J. A.; Mackman, R. L.; Peterson, J. A.; de Montellano, P. O. Relationship of active site topology to substrate specificity for cytochrome P450terp (CYP108). *J. Biol. Chem.* **1994**, *269*, 28815-28821.

164.   Tee, K. L.; Schwaneberg, U. A screening system for the directed evolution of epoxygenases: importance of position 184 in P450 BM3 for stereoselective styrene epoxidation. *Angew. Chem. Int. Ed.* **2006**, *45*, 5380-5383.

165.   Zhang, W.; Tang, W. L.; Wang, Z.; Li, Z. Regio-and Stereoselective Biohydroxylations with a Recombinant Escherichia coli Expressing P450pyr Monooxygenase of Sphingomonas Sp. HXN-200. *Adv. Synth. Catal.* **2010**, *352*, 3380-3390.

166.   Tang, W. L.; Li, Z.; Zhao, H. Inverting the enantioselectivity of P450pyr monooxygenase by directed evolution. *Chem. Commun.* **2010**, *46*, 5461-5463.

167.   Pham, S. Q.; Pompidor, G.; Liu, J.; Li, X. D.; Li, Z. Evolving P450pyr hydroxylase for highly enantioselective hydroxylation at non-activated carbon atom. *Chem. Commun.* **2012**, *48*, 4618-4620.

168.   Yang, Y.; Liu, J.; Li, Z. Engineering of P450pyr Hydroxylase for the Highly Regio-and Enantioselective Subterminal Hydroxylation of Alkanes. *Angew. Chem. Int. Ed.* **2014**, *53*, 3120-3124.

169.   Li, A.; Liu, J.; Pham, S. Q.; Li, Z. Engineered P450pyr monooxygenase for asymmetric epoxidation of alkenes with unique and high enantioselectivity. *Chem. Commun.* **2013**, *49*, 11572-11574.

170.   Li, A.; Wu, S.; Adams, J. P.; Snajdrova, R.; Li, Z. Asymmetric epoxidation of alkenes and benzylic hydroxylation with P450tol monooxygenase from Rhodococcus coprophilus TC-2. *Chem. Commun.* **2014**, *50*, 8771-8774.

171.   Kroutil, W.; Mang, H.; Edegger, K.; Faber, K. Biocatalytic oxidation of primary and secondary alcohols. *Adv. Synth. Catal.* **2004**, *346*, 125-142.

172.   Hollmann, F.; Arends, I. W.; Buehler, K.; Schallmey, A.; Bühler, B. Enzyme-mediated oxidations for the chemist. *Green Chem.* **2011**, *13*, 226-265.

173.   Turner, N. J. Enantioselective oxidation of C–O and C–N bonds using oxidases. *Chem. Rev.* **2011**, *111*, 4073-4087.

174.   Romano, D.; Villa, R.; Molinari, F. Preparative biotransformations: oxidation of alcohols. *ChemCatChem* **2012**, *4*, 739-749.

175.   Kroutil, W.; Mang, H.; Edegger, K.; Faber, K. Recent advances in the biocatalytic reduction of ketones and oxidation of sec-alcohols. *Curr. Opin. Chem. Biol.* **2004**, *8*, 120-126.

176.   Jörnvall, H. Horse liver alcohol dehydrogenase. *Eur. J. Biochem.* **1970**, *16*, 25-40.

177.   Eklund, H.; Plapp, B. V.; Samama, J. P.; Brändén, C. I. Binding of substrate in a ternary complex of horse liver alcohol dehydrogenase. *J. Biol. Chem.* **1982**, *257*, 14349-14358.

178.   Wong, C. H.; Matos, J. R. Enantioselective oxidation of 1, 2-diols to L-alpha-hydroxy acids using co-immobilized alcohol and aldehyde dehydrogenases as catalysts. *J. Org. Chem.* **1985**, *50*, 1992-1994.

179.   Cannio, R.; Rossi, M.; Bartolucci, S. A few amino acid substitutions are responsible for the higher thermostability of a novel NAD+-dependent bacillar alcohol dehydrogenase. *Eur. J. Biochem.* **1994**, *222*, 345-352.

180.   Zhang, X.; Bruice, T. C. Temperature-Dependent Structure of the ES Complex of Bacillus stearothermophilus Alcohol Dehydrogenase. *Biochemistry* **2007**, *46*, 837-843.

181.   Yakushi, T.; Matsushita, K. Alcohol dehydrogenase of acetic acid bacteria: structure, mode of action, and applications in biotechnology. *Appl. Microbiol. Biotechnol.* **2010**, *86*, 1257-1265.

182.   Wei, L. J.; Zhou, J. L.; Zhu, D. N.; Cai, B. Y.; Lin, J. P.; Hua, Q.; Wei, D. Z. Functions of Membrane-bound Alcohol Dehydrogenase and Aldehyde

Dehydrogenase in the Bio-oxidation of Alcohols in Gluconobacter oxydans DSM 2003. *Biotechnol. Bioproc. Eng.* **2012**, *17*, 1156-1164.

183.   Peters, B.; Mientus, M.; Kostner, D.; Junker, A.; Liebl, W.; Ehrenreich, A. Characterization of membrane-bound dehydrogenases from Gluconobacter oxydans 621H via whole-cell activity assays using multideletion strains. *Appl. Microbiol. Biotechnol.* **2013**, *97*, 6397-6412.

184.   Gupta, A.; Singh, V. K.; Qazi, G. N.; Kumar, A. Gluconobacter oxydans: its biotechnological applications. *J. Mol. Microbiol. Biotechnol.* **2001**, *3*, 445-456.

185.   Prust, C.; Hoffmeister, M.; Liesegang, H.; Wiezer, A.; Fricke, W. F.; Ehrenreich, A.; Gottschalk, G.; Deppenmeier, U. Complete genome sequence of the acetic acid bacterium Gluconobacter oxydans. *Nat. Biotechnol.* **2005**, *23*, 195-200.

186.   van Beilen, J. B.; Wubbolts, M. G.; Witholt, B. Genetics of alkane oxidation by Pseudomonas oleovorans. *Biodegradation* **1994**, *5*, 161-174.

187.   van Beilen, J. B.; Panke, S.; Lucchini, S.; Franchini, A. G.; Röthlisberger, M.; Witholt, B. Analysis of Pseudomonas putida alkane-degradation gene clusters and flanking insertion sequences: evolution and regulation of the alk genes. *Microbiology* **2001**, *147*, 1621-1630.

188.   Cavener, D. R. GMC oxidoreductases: a newly defined family of homologous proteins with diverse catalytic activities. *J. Mol. Biol.* **1992**, *223*, 811-814.

189.   Kirmair, L.; Skerra, A. Biochemical Analysis of Recombinant AlkJ from Pseudomonas putida Reveals a Membrane-Associated, Flavin Adenine Dinucleotide-Dependent Dehydrogenase Suitable for the Biosynthetic Production of Aliphatic Aldehydes. *Appl. Environ. Microbiol.* **2014**, *80*, 2468-2477.

190.   Winter, R. T.; Fraaije, M. W. Applications of flavoprotein oxidases in organic synthesis: novel reactivities that go beyond amine and alcohol oxidation. *Curr. Org. Chem.* **2012**, *16*, 2542-2550.

191.   Dijkman, W. P.; de Gonzalo, G.; Mattevi, A.; Fraaije, M. W. Flavoprotein oxidases: classification and applications. *Appl. Microbiol. Biotechnol.* **2013**, *97*, 5177-5188.

192.   Umena, Y.; Yorita, K.; Matsuoka, T.; Kita, A.; Fukui, K.; Morimoto, Y. The crystal structure of l-lactate oxidase from Aerococcus viridans at 2.1 Å resolution reveals the mechanism of strict substrate recognition. *Biochem. Biophys. Res. Commun.* **2006**, *350*, 249-256.

193.   Adam, W.; Lazarus, M.; Boss, B.; Saha-Möller, C. R.; Humpf, H. U.; Schreier, P. Enzymatic resolution of chiral 2-hydroxy carboxylic acids by enantioselective

oxidation with molecular oxygen catalyzed by the glycolate oxidase from spinach (Spinacia oleracea). *J. Org. Chem.* **1997**, *62*, 7841-7843.

194.　　Hubbard, B. K.; Thomas, M. G.; Walsh, C. T. Biosynthesis of L-p-hydroxyphenylglycine, a non-proteinogenic amino acid constituent of peptide antibiotics. *Chem. Biol.* **2000**, *7*, 931-942.

195.　　Li, T. L.; Choroba, O. W.; Charles, E. H.; Sandercock, A. M.; Williams, D. H.; Spencer, J. B. Characterisation of a hydroxymandelate oxidase involved in the biosynthesis of two unusual amino acids occurring in the vancomycin group of antibiotics. *Chem. Commun.* **2001**, 1752-1753.

196.　　Zhu, D.; Hua, L. Biocatalytic asymmetric amination of carbonyl functional groups–a synthetic biology approach to organic chemistry. *Biotechnol. J.* **2009**, *4*, 1420-1431.

197.　　Ward, J.; Wohlgemuth, R. High-yield biocatalytic amination reactions in organic synthesis. *Curr. Org. Chem.* **2010**, *14*, 1914-1927.

198.　　Taylor, P. P.; Pantaleone, D. P.; Senkpeil, R. F.; Fotheringham, I. G. Novel biosynthetic approaches to the production of unnatural amino acids using transaminases. *Trends Biotechnol.* **1998**, *16*, 412-418.

199.　　Galkin, A.; Kulakova, L.; Yoshimura, T.; Soda, K.; Esaki, N. Synthesis of optically active amino acids from alpha-keto acids with Escherichia coli cells expressing heterologous genes. *Appl. Environ. Microbiol.* **1997**, *63*, 4651-4656.

200.　　Park, E. S.; Dong, J. Y.; Shin, J. S. Biocatalytic Asymmetric Synthesis of Unnatural Amino Acids through the Cascade Transfer of Amino Groups from Primary Amines onto Keto Acids. *ChemCatChem* **2013**, *5*, 3538-3542.

201.　　Nugent, T. C., Ed. *Chiral amine synthesis: methods, developments and applications*; John Wiley & Sons, **2010**.

202.　　Koszelewski, D.; Tauber, K.; Faber, K.; Kroutil, W. ω-Transaminases for the synthesis of non-racemic α-chiral primary amines. *Trends Biotechnol.* **2010**, *28*, 324-332.

203.　　Tufvesson, P.; Lima-Ramos, J.; Jensen, J. S.; Al-Haque, N.; Neto, W.; Woodley, J. M. Process considerations for the asymmetric synthesis of chiral amines using transaminases. *Biotechnol. Bioeng.* **2011**, *108*, 1479-1493.

204.　　Malik, M. S.; Park, E. S.; Shin, J. S. Features and technical applications of ω-transaminases. *Appl. Microbiol. Biotechnol.* **2012**, *94*, 1163-1171.

205.　　Mathew, S.; Yun, H. ω-Transaminases for the production of optically pure amines and unnatural amino acids. *ACS Catal.* **2012**, *2*, 993-1001.

206. Kohls, H.; Steffen-Munsberg, F.; Höhne, M. Recent achievements in developing the biocatalytic toolbox for chiral amine synthesis. *Curr. Opin. Chem. Biol*. **2014**, *19*, 180-192.

207. Shin, J. S.; Kim, B. G. Asymmetric synthesis of chiral amines with ω-transaminase. *Biotechnol. Bioeng.* **1999**, *65*, 206-211.

208. Kaulmann, U.; Smithies, K.; Smith, M. E.; Hailes, H. C.; Ward, J. M. Substrate spectrum of ω-transaminase from Chromobacterium violaceum DSM30191 and its potential for biocatalysis. *Enzyme Microb. Technol.* **2007**, *41*, 628-637.

209. Schätzle, S.; Steffen-Munsberg, F.; Thontowi, A.; Höhne, M.; Robins, K.; Bornscheuer, U. T. Enzymatic Asymmetric Synthesis of Enantiomerically Pure Aliphatic, Aromatic and Arylaliphatic Amines with (R)-Selective Amine Transaminases. *Adv. Synth. Catal.* **2011**, *353*, 2439-2445.

210. Koszelewski, D., Lavandera, I., Clay, D., Guebitz, G. M., Rozzell, D., Kroutil, W. Formal asymmetric biocatalytic reductive amination. *Angew. Chem. Int. Ed.* **2008**, *47*, 9337-9340.

211. van der Donk, W. A.; Zhao, H. Recent developments in pyridine nucleotide regeneration. *Curr. Opin. Biotechnol.* **2003**, *14*, 421-426.

212. Zhao, H.; van der Donk, W. A. Regeneration of cofactors for use in biocatalysis. *Curr. Opin. Biotechnol.* **2003**, *14*, 583-589.

213. Liu, W.; Wang, P. Cofactor regeneration for sustainable enzymatic biosynthesis. *Biotechnol. Adv.* **2007**, *25*, 369-384.

214. Favre-Bulle, O.; Schouten, T.; Kingma, J.; Witholt, B. Bioconversion of n-octane to octanoic acid by a recombinant Escherichia coli cultured in a two-liquid phase bioreactor. *Nat. Biotechnol.* **1991**, *9*, 367-371.

215. Suzuki, M.; Hayakawa, T.; Shaw, J. P.; Rekik, M.; Harayama, S. Primary structure of xylene monooxygenase: similarities to and differences from the alkane hydroxylation system. *J. Bacteriol.* **1991**, *173*, 1690-1695.

216. Leon, R.; Fernandes, P.; Pinheiro, H. M.; Cabral, J. M. S. Whole-cell biocatalysis in organic media. *Enzyme Microb. Technol.* **1998**, *23*, 483-500.

217. Heipieper, H. J.; Neumann, G.; Cornelissen, S.; Meinhardt, F. Solvent-tolerant bacteria for biotransformations in two-phase fermentation systems. *Appl. Microbiol. Biotechnol.* **2007**, *74*, 961-973.

218. Pfruender, H.; Amidjojo, M.; Kragl, U.; Weuster-Botz, D. Efficient Whole-Cell Biotransformation in a Biphasic Ionic Liquid/Water System. *Angew. Chem. Int. Ed.* **2004**, *43*, 4529-4531.

219. Pfruender, H.; Jones, R.; Weuster-Botz, D. Water immiscible ionic liquids as solvents for whole cell biocatalysis. *J. Biotechnol.* **2006**, *124*, 182-190.

220.   Riesenberg, D.; Schulz, V.; Knorre, W. A.; Pohl, H. D.; Korz, D.; Sanders, E. A.; Roβ, A.; Deckwer, W. D. High cell density cultivation of Escherichia coli at controlled specific growth rate. *J. Biotechnol.* **1991**, *20*, 17-27.

221.   Lee, S. Y. High cell-density culture of Escherichia coli. *Trends Biotechnol.* **1996**, *14*, 98-105.

222.   Riesenberg, D.; Guthke, R. High-cell-density cultivation of microorganisms. *Appl. Microbiol. Biotechnol.* **1999**, *51*, 422-430.

223.   Blank, L. M.; Ebert, B. E.; Bühler, B.; Schmid, A. Metabolic capacity estimation of Escherichia coli as a platform for redox biocatalysis: constraint-based modeling and experimental verification. *Biotechnol. Bioeng.* **2008**, *100*, 1050-1065.

224.   Julsing, M. K.; Kuhn, D.; Schmid, A.; Bühler, B. Resting cells of recombinant E. coli show high epoxidation yields on energy source and high sensitivity to product inhibition. *Biotechnol. Bioeng.* **2012**, *109*, 1109-1119.

225.   Ni, Y.; Li, C. X.; Zhang, J.; Shen, N. D.; Bornscheuer, U. T.; Xu, J. H. Efficient Reduction of Ethyl 2-Oxo-4-phenylbutyrate at $620 g \cdot L-1$ by a Bacterial Reductase with Broad Substrate Spectrum. *Adv. Synth. Catal.* **2011**, *353*, 1213-1217.

226.   Chen, R. R. Permeability issues in whole-cell bioprocesses and cellular membrane engineering. *Appl. Microbiol. Biotechnol.* **2007**, *74*, 730-738.

227.   Zhang, J.; Witholt, B.; Li, Z. Coupling of permeabilized microorganisms for efficient enantioselective reduction of ketone with cofactor recycling. *Chem. Commun.* **2006**, 398-400.

228.   Zhang, W.; O'Connor, K.; Wang, D. I.; Li, Z. Bioreduction with efficient recycling of NADPH by coupled permeabilized microorganisms. *Appl. Environ. Microbiol.* **2009**, *75*, 687-694.

229.   Ni, Y.; Chen, R. R. Accelerating whole-cell biocatalysis by reducing outer membrane permeability barrier. *Biotechnol. Bioeng.* **2004**, *87*, 804-811.

230.   Julsing, M. K.; Schrewe, M.; Cornelissen, S.; Hermann, I.; Schmid, A.; Bühler, B. Outer membrane protein AlkL boosts biocatalytic oxyfunctionalization of hydrophobic substrates in Escherichia coli. *Appl. Environ. Microbiol.* **2012**, *78*, 5724-5733.

231.   Cornelissen, S.; Julsing, M. K.; Volmer, J.; Riechert, O.; Schmid, A.; Bühler, B. Whole-cell-based CYP153A6-catalyzed (S)-limonene hydroxylation efficiency depends on host background and profits from monoterpene uptake via AlkL. *Biotechnol. Bioeng.* **2013**, *110*, 1282-1292.

232.   Bruggink, A.; Schoevaart, R.; Kieboom, T. Concepts of nature in organic synthesis: cascade catalysis and multistep conversions in concert. *Org. Process Res. Dev.* **2003**, *7*, 622-640.

233. Fogg, D. E.; dos Santos, E. N. Tandem catalysis: a taxonomy and illustrative review. *Coord. Chem. Rev.* **2004**, *248*, 2365-2379.

234. Wasilke, J. C.; Obrey, S. J.; Baker, R. T.; Bazan, G. C. Concurrent tandem catalysis. *Chem. Rev.* **2005**, *105*, 1001-1020.

235. Altenbuchner, J.; Siemann-Herzberg, M.; Syldatk, C. Hydantoinases and related enzymes as biocatalysts for the synthesis of unnatural chiral amino acids. *Curr. Opin. Biotechnol.* **2001**, *12*, 559-563.

236. Heras-Vazquez, F. J.; Clemente-Jimenez, J. M.; Martinez-Rodriguez, S.; Rodriguez-Vico, F. Optically pure α-amino acids production by the "Hydantoinase Process". *Recent Pat. Biotechnol.* **2008**, *2*, 35-46.

237. Martínez-Rodríguez, S.; Martínez-Gómez, A. I.; Rodríguez-Vico, F.; Clemente-Jiménez, J. M.; Las Heras-Vázquez, F. J. Carbamoylases: characteristics and applications in biotechnological processes. *Appl. Microbiol. Biotechnol.* **2010**, *85*, 441-458.

238. Wegman, M. A.; Janssen, M. H.; van Rantwijk, F.; Sheldon, R. A. Towards biocatalytic synthesis of β-lactam antibiotics. *Adv. Synth. Catal.* **2001**, *343*, 559-576.

239. Martínez-Gómez, A. I.; Martínez-Rodríguez, S.; Clemente-Jiménez, J. M.; Pozo-Dengra, J.; Rodríguez-Vico, F.; Las Heras-Vázquez, F. J. Recombinant polycistronic structure of hydantoinase process genes in Escherichia coli for the production of optically pure D-amino acids. *Appl. Environ. Microbiol.* **2007**, *73*, 1525-1531.

240. Mateo, C.; Chmura, A.; Rustler, S.; van Rantwijk, F.; Stolz, A.; Sheldon, R. A. Synthesis of enantiomerically pure (S)-mandelic acid using an oxynitrilase–nitrilase bienzymatic cascade: a nitrilase surprisingly shows nitrile hydratase activity. *Tetrahedron: Asymmetry* **2006**, *17*, 320-323.

241. van Pelt, S.; van Rantwijk, F.; Sheldon, R. A. Synthesis of Aliphatic (S)-α-Hydroxycarboxylic Amides using a One-Pot Bienzymatic Cascade of Immobilised Oxynitrilase and Nitrile Hydratase. *Adv. Synth. Catal.* **2009**, *351*, 397-404.

242. Sosedov, O.; Matzer, K.; Bürger, S.; Kiziak, C.; Baum, S.; Altenbuchner, J.; Chmura, A.; van Rantwijk, F.; Stolz, A. Construction of Recombinant Escherichia coli Catalysts which Simultaneously Express an (S)-Oxynitrilase and Different Nitrilase Variants for the Synthesis of (S)-Mandelic Acid and (S)-Mandelic Amide from Benzaldehyde and Cyanide. *Adv. Synth. Catal.* **2009**, *351*, 1531-1538.

243. Baum, S.; van Rantwijk, F.; Stolz, A. Application of a Recombinant Escherichia coli Whole-Cell Catalyst Expressing Hydroxynitrile Lyase and

Nitrilase Activities in Ionic Liquids for the Production of (S)-Mandelic Acid and (S)-Mandeloamide. *Adv. Synth. Catal.* **2012**, *354*, 113-122.

244.   Abraham, W. R.; Stumpf, B.; Kieslich, K. Microbial transformations of terpenoids with 1-p-menthene skeleton. *Appl. Microbiol. Biotechnol.* **1986**, *24*, 24-30.

245.   Demyttenaere, J. C.; Van Belleghem, K.; De Kimpe, N. Biotransformation of (R)-(+)-and (S)-(−)-limonene by fungi and the use of solid phase microextraction for screening. *Phytochemistry* **2001**, *57*, 199-208.

246.   Chang, D.; Zhang, J.; Witholt, B.; Li, Z. Chemical and enzymatic synthetic methods for asymmetric oxidation of the CC double bond. *Biocatal. Biotransform.* **2004**, *22*, 113-131.

247.   Xu, Y.; Jia, X.; Panke, S.; Li, Z. Asymmetric dihydroxylation of aryl olefins by sequential enantioselective epoxidation and regioselective hydrolysis with tandem biocatalysts. *Chem. Commun.* **2009**, 1481-1483.

248.   Xu, Y.; Li, A.; Jia, X.; Li, Z. Asymmetric trans-dihydroxylation of cyclic olefins by enzymatic or chemo-enzymatic sequential epoxidation and hydrolysis in one-pot. *Green Chem.* **2011**, *13*, 2452-2458.

249.   Wentzel, A.; Ellingsen, T. E.; Kotlar, H. K.; Zotchev, S. B.; Throne-Holst, M. Bacterial metabolism of long-chain n-alkanes. *Appl. Microbiol. Biotechnol.* **2007**, *76*, 1209-1221.

250.   Rojo, F. Degradation of alkanes by bacteria. *Environ. Microbiol.* **2009**, *11*, 2477-2490.

251.   Zhang, W.; Tang, W. L.; Wang, D. I. C.; Li, Z. Concurrent oxidations with tandem biocatalysts in one pot: green, selective and clean oxidations of methylene groups to ketones. *Chem. Commun.* **2011**, *47*, 3284.

252.   Staudt, S.; Burda, E.; Giese, C.; Müller, C. A.; Marienhagen, J.; Schwaneberg, U.; Hummel, W.; Drauz, K.; Gröger, H. Direct oxidation of cycloalkanes to cycloalkanones with oxygen in water. *Angew. Chem. Int. Ed.* **2013**, *52*, 2359-2363.

253.   Müller, C. A.; Akkapurathu, B; Winkler, T.; Staudt, S.; Hummel, W.; Gröger, H.; Schwaneberg, U. In Vitro Double Oxidation of n-Heptane with Direct Cofactor Regeneration. *Adv. Synth. Catal.* **2013**, *355*, 1787-1798.

254.   Müller, C. A.; Dennig, A.; Welters, T.; Winkler, T.; Ruff, A. J.; Hummel, W., Gröger, H.; Schwaneberg, U. Whole-cell double oxidation of n-heptane. *J. Biotechnol.* **2014**, *191*, 196-204.

255.   Seisser, B.; Lavandera, I.; Faber, K.; Spelberg, J. H. L.; Kroutil, W. Stereo-Complementary Two-Step Cascades Using a Two-Enzyme System Leading to Enantiopure Epoxides. *Adv. Synth. Catal.* **2007**, *349*, 1399-1404.

256.   Hasnaoui-Dijoux, G.; Majerić Elenkov, M.; Lutje Spelberg, J. H.; Hauer, B.; Janssen, D. B. Catalytic promiscuity of halohydrin dehalogenase and its application in enantioselective epoxide ring opening. *ChemBioChem* **2008**, *9*, 1048-1051.

257.   You, Z. Y.; Liu, Z. Q.; Zheng, Y. G. Properties and biotechnological applications of halohydrin dehalogenases: current state and future perspectives. *Appl. Microbiol. Biotechnol.* **2013**, *97*, 9-21.

258.   Schrittwieser, J. H.; Lavandera, I.; Seisser, B.; Mautner, B.; Kroutil, W. Biocatalytic Cascade for the Synthesis of Enantiopure β-Azidoalcohols and β-Hydroxynitriles. *Eur. J. Org. Chem.* **2009**, 2293-2298.

259.   Chen, S. Y.; Yang, C. X.; Wu, J. P.; Xu, G.; Yang, L. R. Multi-Enzymatic Biosynthesis of Chiral β-Hydroxy Nitriles through Co-Expression of Oxidoreductase and Halohydrin Dehalogenase. *Adv. Synth. Catal.* **2013**, *355*, 3179-3190.

260.   Ma, S. K.; Gruber, J.; Davis, C.; Newman, L.; Gray, D.; Wang, A.; Grate, J.; Huisman, G. W.; Sheldon, R. A. A green-by-design biocatalytic process for atorvastatin intermediate. *Green Chem.* **2010**, *12*, 81-86.

261.   Brovetto, M.; Gamenara, D.; Saenz Mendez, P.; Seoane, G. A. C−C Bond-Forming Lyases in Organic Synthesis. *Chem. Rev.* **2011**, *111*, 4346-4403.

262.   Müller, M.; Sprenger, G. A.; Pohl, M. CC bond formation using ThDP-dependent lyases. *Curr. Opin. Chem. Biol.* **2013**, *17*, 261-270.

263.   Kihumbu, D.; Stillger, T.; Hummel, W.; Liese, A. Enzymatic synthesis of all stereoisomers of 1-phenylpropane-1, 2-diol. *Tetrahedron: Asymmetry* **2002**, *13*, 1069-1072.

264.   Jakoblinnert, A.; Rother, D. A two-step biocatalytic cascade in micro-aqueous medium: using whole cells to obtain high concentrations of a vicinal diol. *Green Chem.* **2014**, *16*, 3472-3482.

265.   Wachtmeister, J.; Jakoblinnert, A.; Kulig, J.; Offermann, H.; Rother, D. Whole-Cell Teabag Catalysis for the Modularisation of Synthetic Enzyme Cascades in Micro-Aqueous Systems. *ChemCatChem* **2014**, *6*, 1051-1058.

266.   Sehl, T.; Hailes, H. C.; Ward, J. M.; Wardenga, R.; von Lieres, E.; Offermann, H.; Westphal, R.; Pohl, M.; Rother, D. Two steps in one pot: enzyme cascade for the synthesis of nor (pseudo) ephedrine from inexpensive starting materials. *Angew. Chem. Int. Ed.* **2013**, *52*, 6772-6775.

267.   Sehl, T.; Hailes, H. C.; Ward, J. M.; Menyes, U.; Pohl, M.; Rother, D. Efficient 2-step biocatalytic strategies for the synthesis of all nor (pseudo) ephedrine isomers. *Green Chem.* **2014**, *16*, 3341-3348.

268. Voss, C. V.; Gruber, C. C.; Kroutil, W. Deracemization of secondary alcohols through a concurrent tandem biocatalytic oxidation and reduction. *Angew. Chem. Int. Ed.* **2008**, *47*, 741-745.

269. Voss, C. V.; Gruber, C. C.; Faber, K.; Knaus, T.; Macheroux, P.; Kroutil, W. Orchestration of concurrent oxidation and reduction cycles for stereoinversion and deracemisation of sec-alcohols. *J. Am. Chem. Soc.* **2008**, *130*, 13969-13972.

270. Xue, Y. P.; Zheng, Y. G.; Zhang, Y. Q.; Sun, J. L.; Liu, Z. Q.; Shen, Y. C. One-pot, single-step deracemization of 2-hydroxyacids by tandem biocatalytic oxidation and reduction. *Chem. Commun.* **2013**, *49*, 10706-10708.

271. Sattler, J. H.; Fuchs, M.; Tauber, K.; Mutti, F. G.; Faber, K.; Pfeffer, J.; Haas, T.; Kroutil, W. Redox Self-Sufficient Biocatalyst Network for the Amination of Primary Alcohols. *Angew. Chem. Int. Ed.* **2012**, *51*, 9156-9159.

272. Fuchs, M.; Tauber, K.; Sattler, J.; Lechner, H.; Pfeffer, J.; Kroutil, W.; Faber, K. Amination of benzylic and cinnamic alcohols via a biocatalytic, aerobic, oxidation–transamination cascade. *RSC Adv.* **2012**, *2*, 6262-6265.

273. Tauber, K.; Fuchs, M.; Sattler, J. H.; Pitzer, J.; Pressnitz, D.; Koszelewski, D.; Faber, K.; Pfeffer, J.; Haas, T.; Kroutil, W. Artificial Multi-Enzyme Networks for the Asymmetric Amination of sec-Alcohols. *Chem. Eur. J.* **2013**, *19*, 4030-4035.

274. Schrewe, M.; Ladkau, N.; Bühler, B.; Schmid, A. Direct Terminal Alkylamino-Functionalization via Multistep Biocatalysis in One Recombinant Whole-Cell Catalyst. *Adv. Synth. Catal.* **2013**, *355*, 1693-1697.

275. Liu, J.; Li, Z. Cascade Biotransformations via Enantioselective Reduction, Oxidation, and Hydrolysis: Preparation of (R)-δ-Lactones from 2-Alkylidenecyclopentanones. *ACS Catal.* **2013**, *3*, 908-911.

276. Liu, J.; Wu, J.; Li, Z. Enoyl acyl carrier protein reductase (FabI) catalyzed asymmetric reduction of CC double bond of α, β-unsaturated ketones: preparation of (R)-2-alkyl-cyclopentanones. *Chem. Commun.* **2014**.

277. Oberleitner, N.; Peters, C.; Muschiol, J.; Kadow, M.; Saß, S.; Bayer, T.; Schaaf, P.; Iqbal, N.; Rudroff, F.; Mihovilovic, M. D.; Bornscheuer, U. T. An enzymatic toolbox for cascade reactions: a showcase for an in vivo redox sequence in asymmetric synthesis. *ChemCatChem*, **2013**, *5*, 3524-3528.

278. Agudo, R.; Reetz, M. T. Designer cells for stereocomplementary de novo enzymatic cascade reactions based on laboratory evolution. *Chem. Commun.* **2013**, *49*, 10914-10916.

279. Song, J. W.; Jeon, E. Y.; Song, D. H.; Jang, H. Y.; Bornscheuer, U. T.; Oh, D. K.; Park, J. B. Multistep Enzymatic Synthesis of Long-Chain α, ω-Dicarboxylic

and ω-Hydroxycarboxylic Acids from Renewable Fatty Acids and Plant Oils. *Angew. Chem. Int. Ed.* **2013**, *52*, 2534-2537.

280.   Song, J. W.; Lee, J. H.; Bornscheuer, U. T.; Park, J. B. Microbial Synthesis of Medium-Chain α, ω-Dicarboxylic Acids and ω-Aminocarboxylic Acids from Renewable Long-Chain Fatty Acids. *Adv. Synth. Catal.* **2014**, *356*, 1782-1788.

281.   Sattler, J. H.; Fuchs, M.; Mutti, F. G.; Grischek, B.; Engel, P.; Pfeffer, J.; Woodley, J. M.; Kroutil, W. Introducing an In Situ Capping Strategy in Systems Biocatalysis To Access 6-Aminohexanoic acid. *Angew. Chem. Int. Ed.* **2014**, DOI: 10.1002/ange.201409227.

282.   Tokunaga, M.; Larrow, J. F.; Kakiuchi, F.; Jacobsen, E. N. Asymmetric catalysis with water: efficient kinetic resolution of terminal epoxides by means of catalytic hydrolysis. *Science* **1997**, *277*, 936-938.

283.   Schaus, S. E.; Brandes, B. D.; Larrow, J. F.; Tokunaga, M.; Hansen, K. B.; Gould, A. E.; Furrow, M. E.; Jacobsen, E. N. Highly selective hydrolytic kinetic resolution of terminal epoxides catalyzed by chiral (salen) CoIII complexes. Practical synthesis of enantioenriched terminal epoxides and 1, 2-diols. *J. Am. Chem. Soc.* **2002**, *124*, 1307-1315.

284.   Symoens, J.; Cree, D. E.; Vanbeer, W. F. M.; Janssen, P. A. J. In *Pharmacological and Biochemical Properties of Drug Substances*; Goldberg M. E., Eds.; American Pharmaceutical Association: Washington, **1979**; Vol. 2, p 407.

285.   Moertel, C. G.; Fleming, T. R.; Macdonald, J. S.; Haller, D. G.; Laurie, J. A.; Goodman, P. J.; Ungerleider, J. S.; Emerson, W. A.; Tormey, D. C.; Glick, J. H. Levamisole and fluorouracil for adjuvant therapy of resected colon carcinoma. *N. Engl. J. Med.* **1990**, *322*, 352-358.

286.   Hodgson, D. M.; Man, S. Synthesis of the Anti-HIV Agent (−)-Hyperolactone C by Using Oxonium Ylide Formation–Rearrangement. *Chem. Eur. J.* **2011**, *17*, 9731-9737.

287.   Schnute, M. E.; Anderson D. J.; (Pharmacia & Upjohn Co LLC, USA), WO Patent 2005003140, **2005**.

288.   Wittman, M.; Carboni, J.; Attar, R.; Balasubramanian, B.; Balimane, P.; Brassil, P.; Beaulieu, F.; Chang, C.; Clarke, W.; Dell, J.; Eummer, J.; Frennesson, D.; Gottardis, M.; Greer, A.; Hansel, S.; Hurlburt, W.; Jacobson, B.; Krishnananthan, S.; Lee, F. Y.; Li, A.; Lin, T.-A.; Liu, P.; Ouellet, C.; Sang, X.; Saulnier, M. G.; Stoffan, K.; Sun, Y.; Velaparthi, U.; Wong, H.; Yang, Z.; Zimmermann, K.; Zoeckler, M.; Vyas, D. Discovery of a 1 H-Benzoimidazol-2-yl)-1 H-pyridin-2-one (BMS-536924) inhibitor of insulin-like growth factor I receptor kinase with in vivo antitumor activity. *J. Med. Chem.* **2005**, *48*, 5639-5643.

289.   Kharkar, P. S.; Batman, A. M.; Zhen, J.; Beardsley, P. M.; Reith, M. E. A.; Dutta, A. K. Synthesis and Biological Characterization of (3R, 4R)-4-(2-(Benzhydryloxy) ethyl)-1-((R)-2-hydroxy-2-phenylethyl)-piperidin-3-ol and Its Stereoisomers for Activity toward Monoamine Transporters. *ChemMedChem* **2009**, *4*, 1075-1085.

290.   Scott, I. L.; Kuksa, V. A.; Orme, M. W.; Hong, F.; Little, T. L.; Kubota, R. (Acucela, Inc., USA), WO Patent 2009058216 A1, **2009**.

291.   Waldmeier, P. C.; Maitre, L.; Baumann, P. A.; Hauser, K.; Bischoff, S.; Bittiger, H.; Paioni, R. Ifoxetine, a compound with atypical effects on serotonin uptake. *Eur. J. Pharmacol.* **1986**, *130*, 1-10.

292.   Serradell, M. N.; Castaner, J.; Neuman, M.; *Drugs Future* **1984**, 9, 497.

293.   Or, Y. S.; Ma, J.; Wang, G.; Long, J.; Wang, B. (Enanta Pharmaceuticals, Inc., USA) . US Patent 20120070416 A1, **2012**.

294.   Cunningham, A. F.; Kuendig, E. P. An efficient synthesis of both enantiomers of trans-1, 2-cyclopentanediol and their conversion to two novel bidentate phosphite and fluorophosphinite ligands. *J. Org. Chem.* **1988**, *53*, 1823-1825.

295.   Puig, T.; Turrado, C.; Benhamu, B.; Aguilar, H.; Relat, J.; Ortega-Gutierrez, S.; Casals, G.; Marrero, P. F.; Urruticoechea, A.; Haro, D.; Lopez-Rodriguez, M. L.; Colomer, R. Novel inhibitors of fatty acid synthase with anticancer activity. *Clin. Cancer Res.* **2009**, *15*, 7608-7615.

296.   Lamoral-Theys, D.; Pottier, L.; Kerff, F.; Dufrasne, F.; Proutière, F.; Wauthoz, N.; Neven, P.; Ingrassia, L.; Antwerpen, P. V.; Lefranc, F. Simple di-and trivanillates exhibit cytostatic properties toward cancer cells resistant to pro-apoptotic stimuli. *Bioorg. Med. Chem.* **2010**, *18*, 3823-3833.

297.   Laumen, K.; Breitgoff, D.; Seemayer, R.; Schneider, M. P. Enantiomerically pure cyclohexanols and cyclohexane-1, 2-diol derivatives; chiral auxiliaries and substitutes for (–)-8-phenylmenthol. A facile enzymatic route. *J. Chem. Soc., Chem. Commun.* **1989**, 148-150.

298.   Huang, H.; Wong, C. H. Synthesis of Biologically Active Sialyl Lewis X Mimetics. *J. Org. Chem.* **1995**, *60*, 3100-3106.

299.   Davis, B. G.; Maughan, M. A. T.; Chapman, T. M.; Villard, R.; Courtney, S. Novel cyclic sugar imines: Carbohydrate mimics and easily elaborated scaffolds for aza-sugars. *Org. Lett.* **2001**, *4*, 103-106.

300.   Kang, Y. K.; Shin, K. J.; Yoo, K. H.; Seo, K. J.; Park, S. Y.; Kim, D. J.; Park, S. W. Synthesis and biological evaluation of novel 1β-methylcarbapenems having a new moiety at C-2. *Bioorg. Med. Chem. Lett.* **1999**, *9*, 2385-2390.

301. Lee, E. Y.; Yoo, S.-S.; Kim, H. S.; Lee, S. J.; Oh, Y.-K.; Park, S. Production of (S)-styrene oxide by recombinant Pichia pastoris containing epoxide hydrolase from Rhodotorula glutinis. *Enzyme Microb. Technol.* **2004**, *35*, 624-631.

302. Weijers, C. A. G. M. Enantioselective hydrolysis of aryl, alicyclic and aliphatic epoxides by Rhodotorula glutinis. *Tetrahedron: Asymmetry* **1997**, *8*, 639-647.

303. Zhao, L.; Han, B.; Huang, Z.; Miller, M.; Huang, H.; Malashock, D. S.; Zhu, Z.; Milan, A.; Robertson, D. E.; Weiner, D. P.; Burk, M. J. Epoxide Hydrolase-Catalyzed Enantioselective Synthesis of Chiral 1, 2-Diols via Desymmetrization of meso-Epoxides. *J. Am. Chem. Soc.* **2004**, *126*, 11156-11157.

304. Yildirim, D.; Tükel, S. S.; Alagöz, D.; Alptekin, Ö. Preparative-scale kinetic resolution of racemic styrene oxide by immobilized epoxide hydrolase. *Enzyme Microb. Technol.* **2011**, *49*, 555-559.

305. Yoo, S. S.; Park, S.; Lee, E. Y. Enantioselective resolution of racemic styrene oxide at high concentration using recombinant Pichia pastoris expressing epoxide hydrolase of Rhodotorula glutinis in the presence of surfactant and glycerol. *Biotechnol. Lett.* **2008**, *30*, 1807-1810.

306. Baldascini, H.; Ganzeveld, K. J.; Janssen, D. B.; Beenackers, A. A. C. M. Effect of mass transfer limitations on the enzymatic kinetic resolution of epoxides in a two-liquid-phase system. *Biotechnol. Bioeng.* **2001**, *73*, 44-54.

307. Kotik, M.; Štěpánek, V.; Grulich, M.; Kyslík, P.; Archelas, A. Access to enantiopure aromatic epoxides and diols using epoxide hydrolases derived from total biofilter DNA. *J. Mol. Catal. B: Enzym.* **2010**, *65*, 41-48.

308. Kim, H. S.; Lee, O. K.; Lee, S. J.; Hwang, S.; Kim, S. J.; Yang, S.-H.; Park, S.; Lee, E. Y. Enantioselective epoxide hydrolase activity of a newly isolated microorganism, Sphingomonas echinoides EH-983, from seawater. *J. Mol. Catal. B: Enzym.* **2006**, *41*, 130-135.

309. Kotik, M.; Kyslík, P. Purification and characterisation of a novel enantioselective epoxide hydrolase from Aspergillus niger M200. *Biochim. Biophys. Acta, Gen. Subj.* **2006**, 1760, 245-252.

310. Forbes, D. C.; Bettigeri, S. V.; Patrawala, S. A.; Pischek, S. C.; Standen, M. C. S-Methylidene agents: preparation of chiral non-racemic heterocycles. *Tetrahedron* **2009**, *65*, 70-76.

311. Matsumoto, K.; Oguma, T.; Katsuki, T. Highly Enantioselective Epoxidation of Styrenes Catalyzed by Proline-Derived C1-Symmetric Titanium (Salan) Complexes. *Angew. Chem. Int. Ed.* **2009**, *48*, 7432–7435.

312.   Bellucci, G.; Capitani, I.; Chiappe, C.; Marioni, F. Product enantioselectivity of the microsomal and cytosolic epoxide hydrolase catalysed hydrolysis of meso epoxides. *J. Chem. Soc., Chem. Comm.* **1989**, 1170-1171.

313.   Hayashi, Y.; Yamaguchi, J.; Sumiya, T.; Hibino, K.; Shoji, M. Direct proline-catalyzed asymmetric α-aminoxylation of aldehydes and ketones. *J. Org. Chem.* **2004**, *69*, 5966-5973.

314.   Sharpless, K. B. Searching for new reactivity (Nobel lecture). *Angew. Chem. Int. Ed.* **2002**, *41*, 2024-2032.

315.   Kolb, H. C.; VanNieuwenhze, M. S.; Sharpless, K. B. Catalytic asymmetric dihydroxylation. *Chem. Rev.* **1994**, *94*, 2483-2547.

316.   Boyd, D. R.; Sharma, N. D.; Allen, C. C. Aromatic dioxygenases: molecular biocatalysis and applications. *Curr. Opin. Biotechnol.* **2001**, *12*, 564-573.

317.   Boyd, D. R.; Sharma, N. D.; Bowers, N. I.; Brannigan, I. N.; Groocock, M. R.; Malone, J. F.; McConville, G.; Allen, C. C. Biocatalytic Asymmetric Dihydroxylation of Conjugated Mono- and Poly-alkenes to Yield Enantiopure Cyclic cis-Diols. *Adv. Synth. Catal.* **2005**, *347*, 1081-1089.

318.   Zhang, W.; Loebach, J. L.; Wilson, S. R.; Jacobsen, E. N. Enantioselective epoxidation of unfunctionalized olefins catalyzed by salen manganese complexes. *J. Am. Chem. Soc.* **1990**, *112*, 2801-2803.

319.   Nicolaou, K. C.; Huang, X.; Snyder, S. A.; Bheema Rao, P.; Bella, M.; Reddy, M. V. A Novel Regio-and Stereoselective Synthesis of Sulfamidates from 1, 2-Diols Using Burgess and Related Reagents: A Facile Entry into β-Amino Alcohols. *Angew. Chem. Int. Ed.* **2002**, *41*, 834-838.

320.   Pandey, R. K.; Fernandes, R. A.; Kumar, P. An asymmetric dihydroxylation route to enantiomerically pure norfluoxetine and fluoxetine. *Tetrahedron Lett.* **2002**, *43*, 4425-4426.

321.   Gavrilov, K. N.; Zheglov, S. V.; Gavrilova, M. N.; Chuchelkin, I. V.; Groshkin, N. N.; Rastorguev, E. A.; Davankov, V. A. Phosphoramidites based on phenyl-substituted 1, 2-diols as ligands in palladium-catalyzed asymmetric allylations: the contribution of steric demand and chiral centers to the enantioselectivity. *Tetrahedron Lett.* **2011**, *52*, 5706-5710.

322.   Kim, J.-H.; Yang, H.; Park, J.; Boons, G.-J. A general strategy for stereoselective glycosylations. *J. Am. Chem. Soc.* **2005**, *127*, 12090-12097.

323.   Zhao, D.; Song, S.; Li, Y.; Xiong, X.; Sun, L.; Miao, J. (Shenyang Pharmaceutical University), CN Patent 102477008A, **2012**.

324. Hattori, K.; Nagano, M.; Kato, T.; Nakanishi, I.; Imai, K.; Kinoshita, T.; Sakane, K. Asymmetric synthesis of FR165914: A novel β3-adrenergic agonist with a benzocycloheptene structure. *Bioorg. Med. Chem. Lett.* **1995**, *5*, 2821-2824.

325. Jones, G. B.; Guzel, M. S.; Heaton, B. Enantioselective catalysis using planar chiral η6-arene chromium complexes: 1, 2-diols as cycloaddition catalysts. *Tetrahedron: Asymmetry* **2000**, *11*, 4303-4320.

326. Choi, Y. M.; Lee, F. (Bio-Pharm Solutions Co., Inc., KR), US Patent 20130005801A1, **2013**.

327. Sayyed, I. A.; Sudalai, A. Asymmetric synthesis of l-DOPA and (R)-selegiline via, OsO4-catalyzed asymmetric dihydroxylation. *Tetrahedron: Asymmetry* **2004**, *15*, 3111-3116.

328. Chartrain, M.; Jackey, B. A.; Heimbuch, B.; Taylor, C. S. (Merck & Co., Inc., USA), US Patent 5871981A, **1999**.

329. Zhang, J.; Xu, T.; Li, Z. Enantioselective Biooxidation of Racemic trans-Cyclic Vicinal Diols: One-Pot Synthesis of Both Enantiopure (S, S)-Cyclic Vicinal Diols and (R)-α-Hydroxy Ketones. *Adv. Synth. Catal.* **2013**, *355*, 3147-3153.

330. Fringuelli, F.; Germani, R.; Pizzo, F.; Savelli, G. One-pot two-steps synthesis of 1, 2-diol. *Synth. Commun.* **1989**, *19*, 1939–1943.

331. Moreno-Dorado, F. J.; Guerra, F. M.; Ortega, M. J.; Zubía, E.; Massanet, G. M. Enantioselective synthesis of arylmethoxyacetic acid derivatives. *Tetrahedron: Asymmetry* **2003** *14*, 503-510.

332. Riesenberg, D.; Schulz, V.; Knorre, W. A.; Pohl, H. D.; Korz, D.; Sanders, E. A.; Ross, A.; Deckwer, W. D. High cell density cultivation of Escherichia coli at controlled specific growth rate. *J. Biotechnol.* **1991**, *20*, 17-28.

333. Stapleton, A.; Beetham, J. K.; Pinot, F.; Garbarino, J. E.; Rockhold, D. R.; Friedman, M.; Hammock, B. D.; Belknap, W. R. Cloning and expression of soluble epoxide hydrolase from potato. *Plant J.* **1994**, *6*, 251-258.

334. Morisseau, C.; Beetham, J. K.; Pinot, F.; Debernard, S.; Newman, J. W.; Hammock, B. D. Cress and potato soluble epoxide hydrolases: purification, biochemical characterization, and comparison to mammalian enzymes. *Arch. Biochem. Biophys.* **2000**, *378*, 321-332.

335. Monterde, M. I.; Lombard, M.; Archelas, A.; Cronin, A.; Arand, M.; Furstoss, R. Enzymatic transformations. Part 58: Enantioconvergent biohydrolysis of styrene oxide derivatives catalysed by the Solanum tuberosum epoxide hydrolase. *Tetrahedron: Asymmetry* **2004**, *15*, 2801-2805.

336. Lindberg, D.; Gogoll, A.; Widersten, M. Substrate-dependent hysteretic behavior in StEH1-catalyzed hydrolysis of styrene oxide derivatives. *FEBS J.* **2008**, *275*, 6309-6320.

337. Mugford, P. F.; Wagner, U. G.; Jiang, Y.; Faber, K.; Kazlauskas, R. J. Enantiocomplementary Enzymes: Classification, Molecular Basis for Their Enantiopreference, and Prospects for Mirror-Image Biotransformations. *Angew. Chem. Int. Ed.* **2008**, *47*, 8782-8793.

338. Ohkuma, T.; Utsumi, N.; Watanabe, M.; Tsutsumi, K.; Arai, N.; Murata, K. Asymmetric hydrogenation of α-hydroxy ketones catalyzed by MsDPEN-Cp* Ir (III) complex. *Org. lett.* **2007**, *9*, 2565-2567.

339. Mahajabeen, P.; Chadha, A. One-pot synthesis of enantiomerically pure 1, 2-diols: asymmetric reduction of aromatic α-oxoaldehydes catalysed by Candida parapsilosis ATCC 7330. *Tetrahedron: Asymmetry* **2011**, *22*, 2156-2160.

340. Li, X.; Tanasova, M.; Vasileiou, C.; Borhan, B. Fluorinated porphyrin tweezer: a powerful reporter of absolute configuration for erythro and threo diols, amino alcohols, and diamines. *J. Am. Chem. Soc.* **2008**, *130*, 1885-1893.

341. McDonald, R. I.; Liu, G.; Stahl, S. S. Palladium (II)-catalyzed alkene functionalization via nucleopalladation: stereochemical pathways and enantioselective catalytic applications. *Chem. Rev.* **2011**, *111*, 2981-3019.

342. Dong, J. J.; Browne, W. R.; Feringa, B. L. Palladium-Catalyzed anti-Markovnikov Oxidation of Terminal Alkenes. *Angew. Chem. Int. Ed.* **2014**, doi: 10.1002/anie.201404856.

343. Tondreau, A. M.; Atienza, C. C. H.; Weller, K. J.; Nye, S. A.; Lewis, K. M., Delis, J. G.; Chirik, P. J. Iron catalysts for selective anti-markovnikov alkene hydrosilylation using tertiary silanes. *Science* **2012**, *335*, 567-570.

344. Jat, J. L.; Paudyal, M. P.; Gao, H.; Xu, Q. L.; Yousufuddin, M.; Devarajan, D.; Ess, D. H.; Kürti, L.; Falck, J. R. Direct Stereospecific Synthesis of Unprotected NH and N-Me Aziridines from Olefins. *Science* **2014**, *343*, 61-65.

345. Wu, L.; Liu, Q.; Fleischer, I.; Jackstell, R.; Beller, M. Ruthenium-catalysed alkoxycarbonylation of alkenes with carbon dioxide. *Nat. Commun.* **2014**, *5*, 3091.

346. Wilger, D. J.; Grandjean, J. M. M.; Lammert, T. R.; Nicewicz, D. A. The direct anti-Markovnikov addition of mineral acids to styrenes. *Nat. Chem.* **2014**, *6*, 720-726.

347. Bühler, B.; Bühler, K.; Hollmann, F. in *Enzyme Catalysis in Organic Synthesis: A Comprehensive Handbook*, 3rd ed. Drauz, K.; Gröger, H.; May, O., Eds.; John Wiley & Sons, **2012**, pp1278-1301.

348.   Jin, J.; Hanefeld, U. The selective addition of water to C=C bonds; enzymes are the best chemists. *Chem. Commun.* **2011**, *47*, 2502-2510.

349.   Hiseni, A.; Arends, I. W.; Otten, L. G. New Cofactor-Independent Hydration Biocatalysts: Structural, Biochemical, and Biocatalytic Characteristics of Carotenoid and Oleate Hydratases. *ChemCatChem* **2014**, doi: 10.1002/cctc.201402511.

350.   Resch, V.; Hanefeld, U. The selective addition of water. *Catal. Sci. Technol.* **2015**, DOI: 10.1039/C4CY00692E.

351.   Wuensch, C.; Gross, J.; Steinkellner, G.; Gruber, K.; Glueck, S. M.; Faber, K. Asymmetric Enzymatic Hydration of Hydroxystyrene Derivatives. *Angew. Chem. Int. Ed.* **2013**, *52*, 2293-2297.

352.   Dong, G.; Teo, P.; Wickens, Z. K.; Grubbs, R. H. Primary alcohols from terminal olefins: formal anti-Markovnikov hydration via triple relay catalysis. *Science* **2011**, *333*, 1609-1612.

353.   Mlynarski, S. N.; Schuster, C. H.; Morken, J. P. Asymmetric synthesis from terminal alkenes by cascades of diboration and cross-coupling. *Nature* **2014**, *505*, 386-390.

354.   Denard, C. A.; Huang, H.; Bartlett, M. J.; Lu, L.; Tan, Y.; Zhao, H.; Hartwig, J. F. Cooperative Tandem Catalysis by an Organometallic Complex and a Metalloenzyme. *Angew. Chem. Int. Ed.* **2014**, *53*, 465-469.

355.   Wang, Z. J.; Clary, K. N.; Bergman, R. G.; Raymond, K. N.; Toste, F. D. A supramolecular approach to combining enzymatic and transition metal catalysis. *Nat. Chem.* **2013**, *5*, 100-103.

356.   Köhler, V.; Wilson, Y. M.; Dürrenberger, M.; Ghislieri, D.; Churakova, E.; Quinto, T.; Knörr, L.; Häussinger, D.; Hollmann, F.; Turner N. J.; Ward, T. R. Synthetic cascades are enabled by combining biocatalysts with artificial metalloenzymes. *Nat. Chem.* **2013**, *5*, 93-99.

357.   Coppola, G. M.; Schuster, H. F. *α-Hydroxy Acids in Enantioselective Syntheses*; John Wiley & Sons, **2011**.

358.   Ager, D. J.; Prakash, I.; Schaad, D. R. 1, 2-Amino alcohols and their heterocyclic derivatives as chiral auxiliaries in asymmetric synthesis. *Chem Rev.* **1996**, *96*, 835-876.

359.   Soloshonok, V. A.; Izawa, K., Eds. *Asymmetric Synthesis and Application of α-Amino Acids*; American Chemical Society, **2009**.

360.   Najera, C.; Sansano, J. M. Catalytic asymmetric synthesis of α-amino acids. *Chem. Rev.* **2007**, *107*, 4584-4671.

361.   Carey, F. A.; Sundberg, R. J. *Advanced Organic Chemistry: Part B: Reactions and Synthesis*; Springer, **2007**.

362.   Li, G.; Chang, H. T.; Sharpless, K. B. Catalytic asymmetric aminohydroxylation (AA) of olefins. *Angew. Chem. Int. Ed.* **1996**, *35*, 451-454.

363.   O'Brien, P. Sharpless asymmetric aminohydroxylation: scope, limitations, and use in synthesis. *Angew. Chem. Int. Ed.* **1999**,*38*, 326-329.

364.   Donohoe, T. J.; Callens, C. K.; Flores, A.; Lacy, A. R.; Rathi, A. H. Recent developments in methodology for the direct oxyamination of olefins. *Chem. Eur. J.* **2011**, *17*, 58-76.

365.   Turner, N. J.; O'Reilly, E. Biocatalytic retrosynthesis. *Nat. Chem. Biol.* **2013**, *9*, 285-288.

366.   Purnick, P. E.; Weiss, R. The second wave of synthetic biology: from modules to systems. *Nat. Rev. Mol. Cell Biol.* **2009**, *10*, 410-422.

367.   Wang, B.; Kitney, R. I.; Joly, N.; Buck, M. Engineering modular and orthogonal genetic logic gates for robust digital-like synthetic biology. *Nat. Commun.* **2011**, *2*, 508.

368.   Zhang, H.; Lin, M.; Shi, H.; Ji, W.; Huang, L.; Zhang, X.; Shen, S.; Gao, R.; Wu, S.; Tian, C.; Yang, Z.; Zhang, G.; He, S.; Wang, H.; Saw, T.; Chen, Y.; Ouyang, Q. Programming a Pavlovian-like conditioning circuit in Escherichia coli. *Nat. Commun.* **2014**, *5*, 3102.

369.   Ajikumar, P. K.; Xiao, W. H.; Tyo, K. E.; Wang, Y.; Simeon, F.; Leonard, E.; Mucha, O.; Too, H. P.; Pfeifer, B.; Stephanopoulos, G. Isoprenoid pathway optimization for Taxol precursor overproduction in Escherichia coli. *Science* **2010**, *330*, 70-74.

370.   Xu, P.; Gu, Q.; Wang, W.; Wong, L.; Bower, A. G.; Collins, C. H.; Koffas, M. A. Modular optimization of multi-gene pathways for fatty acids production in E. coli. *Nat. Commun.* **2013**, *4*, 1409.

371.   Sheppard, M. J.; Kunjapur, A. M.; Wenck, S. J.; Prather, K. L. Retro-biosynthetic screening of a modular pathway design achieves selective route for microbial synthesis of 4-methyl-pentanol. *Nat. Commun.* **2014**, *5*, 6031.

372.   Zhang, J.; Wu, S.; Wu, J.; Li, Z. Enantioselective Cascade Biocatalysis via Epoxide Hydrolysis and Alcohol Oxidation: One-Pot Synthesis of (R)-α-Hydroxy Ketones from Meso-or Racemic Epoxides. *ACS Catal*. **2015**, *5*, 51-58.

373.   Ferrández, A.; Prieto, M. A.; García, J. L.; Díaz, E. Molecular characterization of PadA, a phenylacetaldehyde dehydrogenase from Escherichia coli. *FEBS Lett.* **1997**, *406*, 23-27.

374. Tsou, A. Y.; Ransom, S. C.; Gerlt, J. A.; Buechter, D. D.; Babbitt, P. C.; Kenyon, G. L. Mandelate pathway of Pseudomonas putida: sequence relationships involving mandelate racemase, (S)-mandelate dehydrogenase, and benzoylformate decarboxylase and expression of benzoylformate decarboxylase in Escherichia coli. *Biochemistry* **1990**, *29*, 9856-9862.

375. Sukumar, N.; Xu, Y.; Gatti, D. L.; Mitra, B.; Mathews, F. S. Structure of an active soluble mutant of the membrane-associated (S)-mandelate dehydrogenase. *Biochemistry* **2001**, *40*, 9870-9878.

376. Resch, V.; Fabian, W. M.; Kroutil, W. Deracemisation of Mandelic Acid to Optically Pure Non-Natural L-Phenylglycine via a Redox-Neutral Biocatalytic Cascade. *Adv. Synth. Catal.* **2010**, *352*, 993-997.

377. Hummel, W.; Schütte, H.; Schmidt, E.; Wandrey, C.; Kula, M. R. Isolation of L-phenylalanine dehydrogenase from Rhodococcus sp. M4 and its application for the production of L-phenylalanine. *Appl. Microbiol. Biotechnol.* **1987**, *26*, 409-416.

378. Vanhooke, J. L.; Thoden, J. B.; Brunhuber, N. M.; Blanchard, J. S.; Holden, H. M. Phenylalanine dehydrogenase from Rhodococcus sp. M4: high-resolution X-ray analyses of inhibitory ternary complexes reveal key features in the oxidative deamination mechanism. *Biochemistry* **1999**, *38*, 2326-2339.

379. Mast, Y. J.; Wohlleben, W.; Schinko, E. Identification and functional characterization of phenylglycine biosynthetic genes involved in pristinamycin biosynthesis in Streptomyces pristinaespiralis. *J. Biotechnol.* **2011**, *155*, 63-67.

380. Kuramitsu, S.; Ogawa, T.; Ogawa, H.; Kagamiyama, H. Branched-chain amino acid aminotransferase of Escherichia coli: nucleotide sequence of the ilvE gene and the deduced amino acid sequence. *J. Biochem.* **1985**, *97*, 993-999.

381. Kuramitsu, S.; Inoue, K.; Ogawa, T.; Ogawa, H.; Kagamiyama, H. Aromatic amino acid aminotransferase of Escherichiacoli: Nucleotide sequence of the tyrB gene. *Biochem. Biophys. Res. Commun.* **1985**, *133*, 134-139.

382. Iraqui, I.; Vissers, S.; Cartiaux, M.; Urrestarazu, A. Characterisation of Saccharomyces cerevisiae ARO8 and ARO9 genes encoding aromatic aminotransferases I and II reveals a new aminotransferase subfamily. *Mol. Gen. Genet.* **1998**, *257*, 238-248.

383. von Ossowski, I.; Mulvey, M. R.; Leco, P. A.; Borys, A.; Loewen, P. C. Nucleotide sequence of Escherichia coli katE, which encodes catalase HPII. *J. Bacteriol.* **1991**, *173*, 514-520.

384. Alper, H.; Fischer, C.; Nevoigt, E.; Stephanopoulos, G. Tuning genetic control through promoter engineering. *Proc. Natl. Acad. Sci. U. S. A.* **2006**, *102*, 12678-12683.

385.   Pfleger, B. F.; Pitera, D. J.; Smolke, C. D.; Keasling, J. D. Combinatorial engineering of intergenic regions in operons tunes expression of multiple genes. *Nat. Biotechnol.* **2006**, *24*, 1027-1032

386.   Salis, H. M.; Mirsky, E. A.; Voigt, C. A. Automated design of synthetic ribosome binding sites to control protein expression. *Nat. Biotechnol.* **2009**, *27*, 946-950.

387.   Turner, N. J. Ammonia lyases and aminomutases as biocatalysts for the synthesis of α-amino and β-amino acids. *Curr. Opin. Chem. Biol.* **2011**, *15*, 234-240.

388.   Heberling, M. M.; Wu, B.; Bartsch, S.; Janssen, D. B. Priming ammonia lyases and aminomutases for industrial and therapeutic applications. *Curr. Opin. Chem. Biol.* **2013**, *17*, 250-260.

389.   MacDonald, M. J.; D'Cunha, G. B. A modern view of phenylalanine ammonia lyase. *Biochem. Cell Biol.* **2007**, *85*, 273-282.

390.   Cochrane, F. C.; Davin, L. B.; Lewis, N. G. The Arabidopsis phenylalanine ammonia lyase gene family: kinetic characterization of the four PAL isoforms. *Phytochemistry* **2004**, *65*, 1557-1564.

391.   Moffitt, M. C.; Louie, G. V.; Bowman, M. E.; Pence, J.; Noel, J. P.; Moore, B. S. Discovery of two cyanobacterial phenylalanine ammonia lyases: kinetic and structural characterization. *Biochemistry* **2007**, *46*, 1004-1012.

392.   Anson, J. G.; Gilbert, H. J.; Oram, J. D.; Minton, N. P. Complete nucleotide sequence of the Rhodosporidium toruloides gene coding for phenylalanine ammonia-lyase. *Gene* **1987**, *58*, 189-199.

393.   Clausen, M.; Lamb, C. J.; Megnet, R.; Doerner, P. W. PAD1 encodes phenylacrylic acid decarboxylase which confers resistance to cinnamic acid in Saccharomyces cerevisiae. *Gene* **1994**, *142*, 107-112.

394.   Plumridge, A.; Stratford, M.; Lowe, K. C.; Archer, D. B. The weak-acid preservative sorbic acid is decarboxylated and detoxified by a phenylacrylic acid decarboxylase, PadA1, in the spoilage mold Aspergillus niger. *Appl. Environ. Microbiol.* **2008**, *74*, 550-552.

395.   Mukai, N.; Masaki, K.; Fujii, T.; Kawamukai, M.; Iefuji, H. PAD1 and FDC1 are essential for the decarboxylation of phenylacrylic acids in Saccharomyces cerevisiae. *J. Biosci. Bioeng.* **2010**, *109*, 564-569.

396.   Plumridge, A.; Melin, P.; Stratford, M.; Novodvorska, M.; Shunburne, L.; Dyer, P. S.; Archer, D. B. The decarboxylation of the weak-acid preservative, sorbic acid, is encoded by linked genes in Aspergillus spp. *Fungal Genet. Biol.* **2010**, *47*, 683-692.

397.   McKenna, R.; Nielsen, D. R. Styrene biosynthesis from glucose by engineered E. coli. *Metab. Eng.* **2011**, *13*, 544-554.

398.   Sun, Z.; Ning, Y.; Liu, L.; Liu, Y.; Sun, B.; Jiang, W.; Yang, C.; Yang, S. Metabolic engineering of the L-phenylalanine pathway in Escherichia coli for the production of S-or R-mandelic acid. *Microb. Cell Fact.* **2011**, *10*, 71.

399.   Müller, U.; Van Assema, F.; Gunsior, M.; Orf, S.; Kremer, S.; Schipper, D.; Wagemans, A.; Townsend, C. A.; Sonke, T.; Bovenberg, R.; Wubbolts, M. Metabolic engineering of the E. coli l-phenylalanine pathway for the production of d-phenylglycine (d-Phg). *Metab. Eng.* **2006**, *8*, 196-208.

400.   Liu, S. P.; Liu, R. X.; El-Rotail, A. A.; Ding, Z. Y.; Gu, Z. H.; Zhang, L.; Shi, G. Y. Heterologous pathway for the production of l-phenylglycine from glucose by E. coli. *J. Biotechnol.* **2014**, *186*, 91-97.

401.   Kong, X. D.; Ma, Q.; Zhou, J.; Zeng, B. B.; Xu, J. H. A Smart Library of Epoxide Hydrolase Variants and the Top Hits for Synthesis of (S)-β-Blocker Precursors. *Angew. Chem. Int. Ed.* **2014**, *53*, 6641-6644.

402.   Kong, X. D.; Yuan, S.; Li, L.; Chen, S.; Xu, J. H.; Zhou, J. Engineering of an epoxide hydrolase for efficient bioresolution of bulky pharmaco substrates. *Proc. Nat. Acad. Sci. U. S. A.* **2014**, *111*, 15717-15722.

403.   Brown, N. J.; Vaughan, D. E. Angiotensin-converting enzyme inhibitors. *Circulation* **1998**, *97*, 1411-1420.

404.   Kuhn, D. J.; Chen, Q.; Voorhees, P. M.; Strader, J. S.; Shenk, K. D.; Sun, C. M.; Demo, S.D.; Bennett, M. K.; van Leeuwen, F. W. B.; Chanan-Khan, A. A.; Orlowski, R. Z. Potent activity of carfilzomib, a novel, irreversible inhibitor of the ubiquitin-proteasome pathway, against preclinical models of multiple myeloma. *Blood* **2007**, *110*, 3281-3290.

405.   Humble, M. S.; Cassimjee, K. E.; Håkansson, M.; Kimbung, Y. R.; Walse, B.; Abedi, V.; Federsel, H.-J.; Berglund, P.; Logan, D. T. Crystal structures of the Chromobacterium violaceum ω-transaminase reveal major structural rearrangements upon binding of coenzyme PLP. *FEBS J.* **2012**, *279*, 779-792.

406.   Lye, G. J.; Woodley, J. M. Application of in situ product-removal techniques to biocatalytic processes. *Trends Biotechnol.* **1999**, *17*, 395-402.

407.   Stark, D.; von Stockar, U. In situ product removal (ISPR) in whole cell biotechnology during the last twenty years. In *Process Integration in Biochemical Engineering* pp. 149-175. Springer **2003**.

408.   Bongaerts, J.; Krämer, M.; Müller, U.; Raeven, L.; Wubbolts, M. Metabolic engineering for microbial production of aromatic amino acids and derived compounds. *Metab. Eng.* **2001**, *3*, 289-300.

409.   Ikeda, M. Towards bacterial strains overproducing L-tryptophan and other aromatics by metabolic engineering. *Appl. Microbiol. Biotechnol.* **2006**, *69*, 615-626.

410.   Gosset, G. Production of aromatic compounds in bacteria. *Curr. Opin. Biotechnol.* **2009**, *20*, 651-658.

411.   Rodriguez, A.; Martínez, J. A.; Flores, N.; Escalante, A.; Gosset, G.; Bolivar, F. Engineering Escherichia coli to overproduce aromatic amino acids and derived compounds. *Microb. Cell Fact.* **2014**, *13*, 126.

412.   Beller, M.; Seayad, J.; Tillack, A.; Jiao, H. Catalytic Markovnikov and anti-Markovnikov Functionalization of Alkenes and Alkynes: Recent Developments and Trends. *Angew. Chem. Int. Ed.* **2004**, *43*, 3368-3398

413.   Dong, J. J.; Browne, W. R.; Feringa, B. L. Palladium-Catalyzed anti-Markovnikov Oxidation of Terminal Alkenes. *Angew. Chem. Int. Ed.* **2014**, doi:10.1002/anie.201404856.

414.   Haggin, J. Chemists seek greater recognition for catalysis. *Chem. Eng. News* **1993**, *71*, 23-27.

415.   Smith, M. B.; March, J. *March's Advanced Organic Chemistry*, John Wiley & Sons, **2007**.

416.   Nobis, M.; Drießen-Hölscher, B. Recent Developments in Transition Metal Catalyzed Intermolecular Hydroamination Reactions—A Breakthrough? *Angew. Chem. Int. Ed.* **2001**, *40*, 3983-3985.

417.   Müller, T. E.; Hultzsch, K. C.; Yus, M.; Foubelo, F.; Tada, M. Hydroamination: direct addition of amines to alkenes and alkynes. *Chem. Rev.* **2008**, *108*, 3795-3892.

418.   Nguyen, T. M.; Manohar, N.; Nicewicz, D. A. anti-Markovnikov Hydroamination of Alkenes Catalyzed by a Two-Component Organic Photoredox System: Direct Access to Phenethylamine Derivatives. *Angew. Chem. Int. Ed.* **2014**, *53*, 6198-6201.

419.   Gibson, D. G.; Young, L.; Chuang, R. Y.; Venter, J. C.; Hutchison, C. A.; Smith, H. O. Enzymatic assembly of DNA molecules up to several hundred kilobases. *Nat. Methods* **2009**, *6*, 343-345.

420.   Shao, Z.; Zhao, H.; Zhao, H. DNA assembler, an in vivo genetic method for rapid construction of biochemical pathways. *Nucleic acids Res.* **2009**, *37*, e16-e16.

421.   Wang, H. H.; Isaacs, F. J.; Carr, P. A.; Sun, Z. Z.; Xu, G.; Forest, C. R.; Church, G. M. Programming cells by multiplex genome engineering and accelerated evolution. *Nature* **2009**, *460*, 894-898.

422.   Cong, L.; Ran, F. A.; Cox, D.; Lin, S.; Barretto, R.; Habib, N.; Hsu, P. D. Wu, X.; Jiang, W.; Marraffini, L. A.; Zhang, F. Multiplex genome engineering using CRISPR/Cas systems. *Science* **2013**, *339*, 819-823.

423.   Alper, H.; Fischer, C.; Nevoigt, E.; Stephanopoulos, G. Tuning genetic control through promoter engineering. *Proc. Natl. Acad. Sci. USA* **2005**, *102*, 12678-12683.

424.   Pfleger, B. F.; Pitera, D. J.; Smolke, C. D.; Keasling, J. D. Combinatorial engineering of intergenic regions in operons tunes expression of multiple genes. *Nat. Biotechnol.* **2006**, *24*, 1027-1032.

425.   Salis, H. M.; Mirsky, E. A.; Voigt, C. A. Automated design of synthetic ribosome binding sites to control protein expression. *Nat. Biotechnol.* **2009**, *27*, 946-950.

Appendix I: Supporting Information for Chapter 3

>**DNA Sequence of SpEH**

ATGATGAACGTCGAACATATCCGCCCGTTCCGCGTCGAGGTGCCGCAGGACGCGCTCGA
CGATCTTCGCGACCGGCTGGCGCGCACTCGCTGGCCCGAGAAGGAAACGGTCGACGACT
GGGATCAGGGCATCCCGCTCGCCTATGCCCGCGAACTCGCCATCTACTGGCGCGACGAGT
ACGACTGGCGGCGGATCGAGGCGCGGCTCAACACCTGGCCCAACTTTCTGGCCACAGTC
GACGGGCTCGATATCCATTTCCTCCATATCCGCTCGGACAATCCTGCCGCGCGGCCGCTG
GTGTTGACGCACGGCTGGCCGGGATCGGTCCTCGAATTTCTCGACGTCATCGAACCGCTG
TCGGCCGACTATCACCTCGTCATCCCGTCGCTTCCCGGTTTCGGTTTCTCGGGCAAGCCCA
CCCGCCCCGGCTGGGATGTCGAGCATATCGCCGCCGCGTGGGACGCGCTGATGCGCGCG
CTCGGCTATGACCGCTATTTTGCGCAGGGCGGCGACTGGGGCAGCGCGGTAACCTCGGC
GATCGGCATGCACCACGCCGGCCATTGCGCGGGCATCCACGTCAACATGGTCGTCGGCG
CGCCGCCGCCCGAGTTGATGAACGACCTCACCGACGAAGAGAAGCTCTATCTCGCGCGC
TTCGGCTGGTATCAGGCGAAGGACAATGGCTATTCGACGCAGCAGGCGACGCGGCCGCA
GACGATCGGCTATGCGCTCACCGATTCCCGGCCGGACAGATGGCGTGGATCGCGGAGA
AATTCCACGGCTGGACCGATTGCGGGCACCAGCCCGGCGGCCAGTCGGTCGGCGGCCAC
CCCGAACAGGCGGTCTCGAAGGATGCGATGCTCGACACGATCAGCCTCTATTGGCTGAC
CGCCAGCGCCGCTTCGTCGGCGCGGCTATACTGGCACAGCTTCCGTCAGTTCGCGGCGGG
CGAGATCGACGTGCCGACGGGATGCAGCCTGTTCCCGAACGAGATCATGCGCCTGTCGC
GGCGCTGGGCCGAACGGCGGTATCGCAACATCGTCTATTGGAGCGAAGCGGCTCGCGGC
GGCCATTTCGCCGCCTGGGAACAACCCGAGCTGTTTGCCGCCGAGGTCCGCGCGGCCTTT
GCACAGATGGATCTTTGA

>**Protein Sequence of SpEH**

MMNVEHIRPFRVEVPQDALDDLRDRLARTRWPEKETVDDWDQGIPLAYARELAIYWRDEY
DWRRIEARLNTWPNFLATVDGLDIHFLHIRSDNPAARPLVLTHGWPGSVLEFLDVIEPLSADY
HLVIPSLPGFGFSGKPTRPGWDVEHIAAAWDALMRALGYDRYFAQGGDWGSAVTSAIGMH
HAGHCAGIHVNMVVGAPPPELMNDLTDEEKLYLARFGWYQAKDNGYSTQQATRPQTIGYA
LTDSPAGQMAWIAEKFHGWTDCGHQPGGQSVGGHPEQAVSKDAMLDTISLYWLTASAASS
ARLYWHSFRQFAAGEIDVPTGCSLFPNEIMRLSRRWAERRYRNIVYWSEAARGGHFAAWEQ
PELFAAEVRAAFAQMDL-

Figure S1.1-S1.9. Chiral HPLC chromatograms
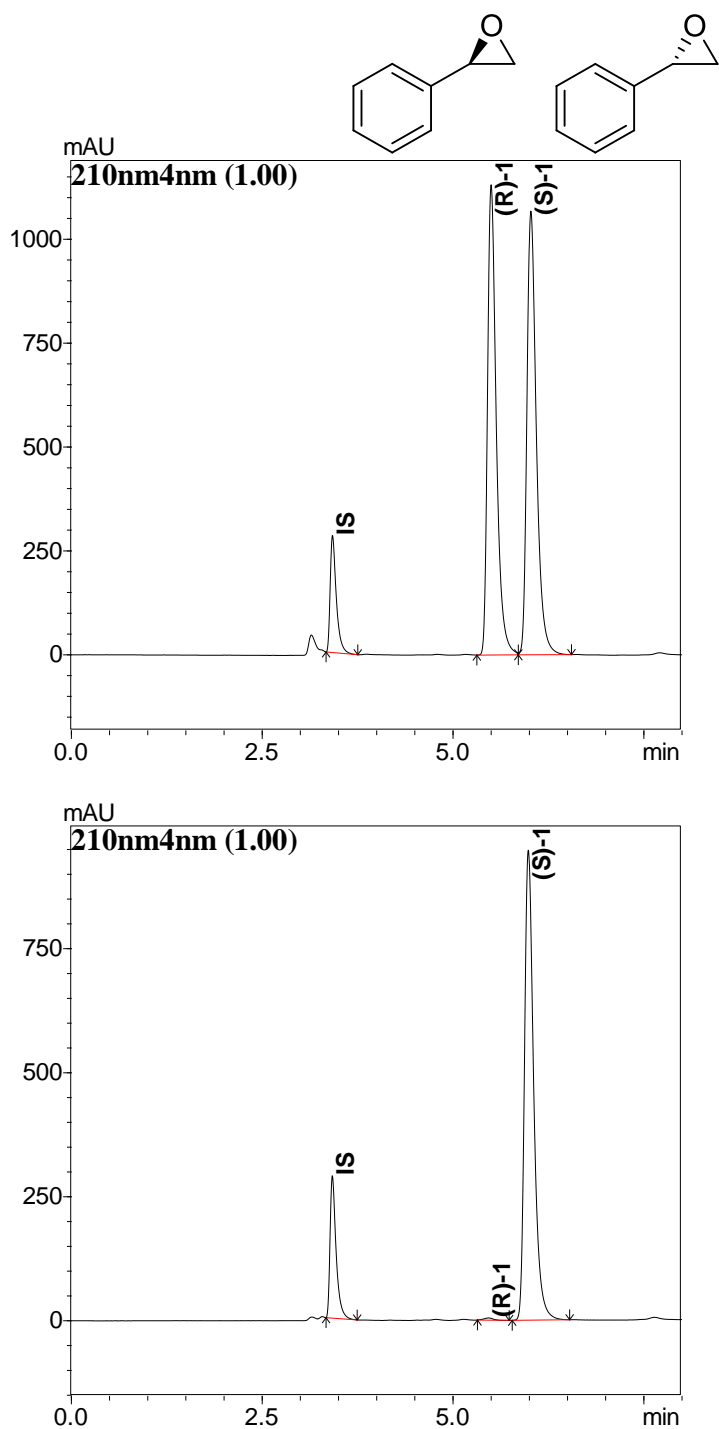
Figure S1.1. Chiral HPLC chromatogram of racemic **1** and product (*S*)-**1** (Column: Daicel AS-H (250 × 4.6 mm, 5µm); eluent: 10% IPA: 90% *n*-hexane; flow rate: 1.0 mL min^{-1}).
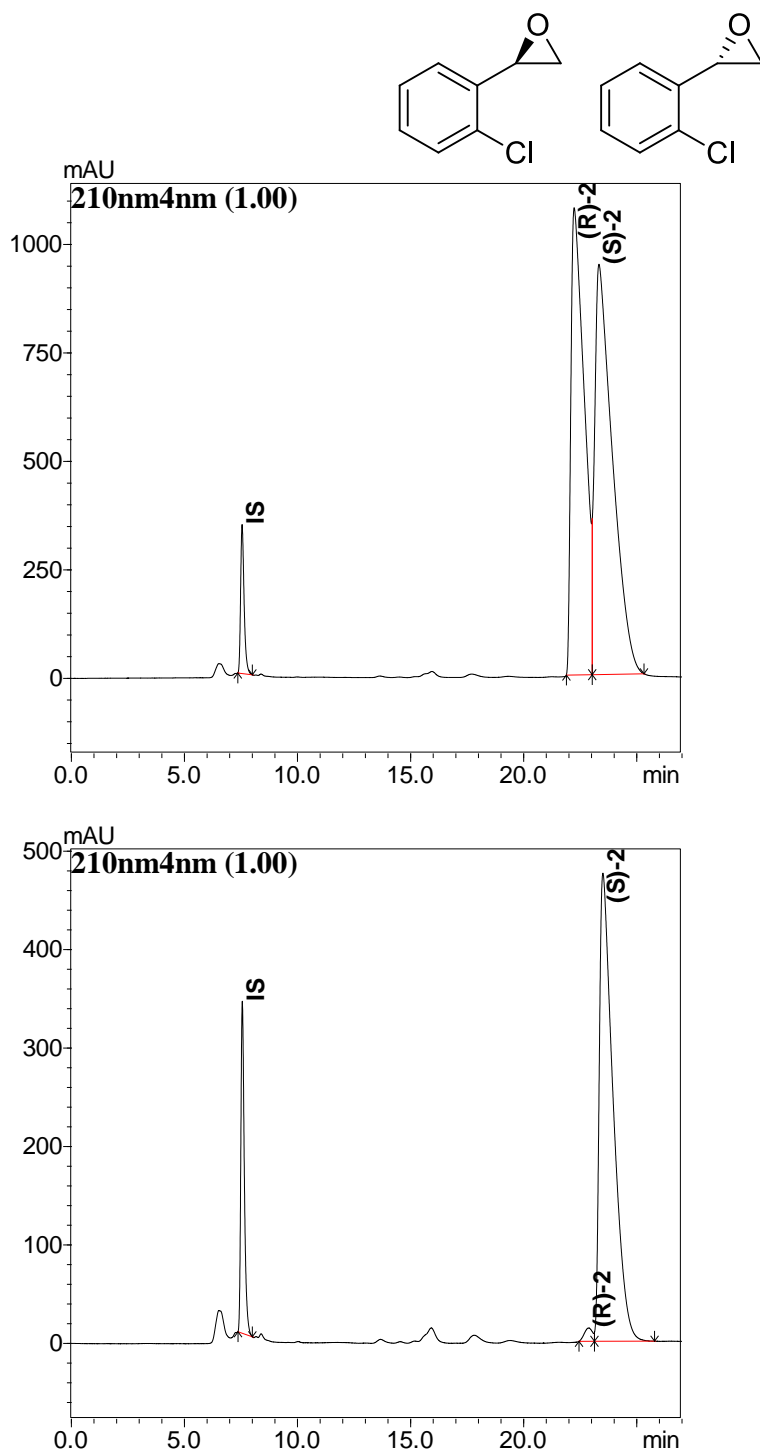
Figure S1.2. Chiral HPLC chromatogram of racemic **2** and product (*S*)-**2** (Column: Daicel AS-H (250 × 4.6 mm, 5µm); eluent: 0% IPA: 100% *n*-hexane; flow rate: 0.5 mL min^{-1}).
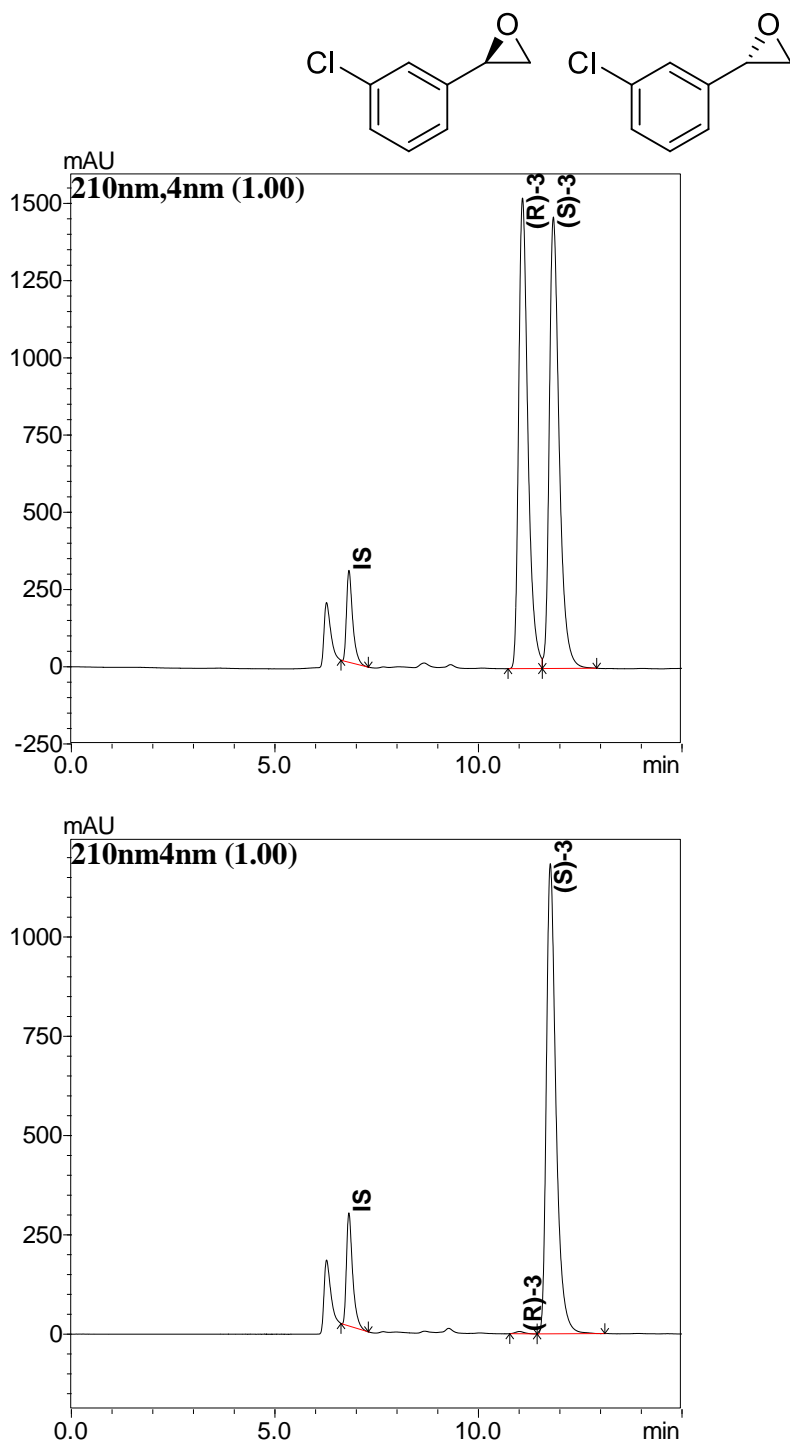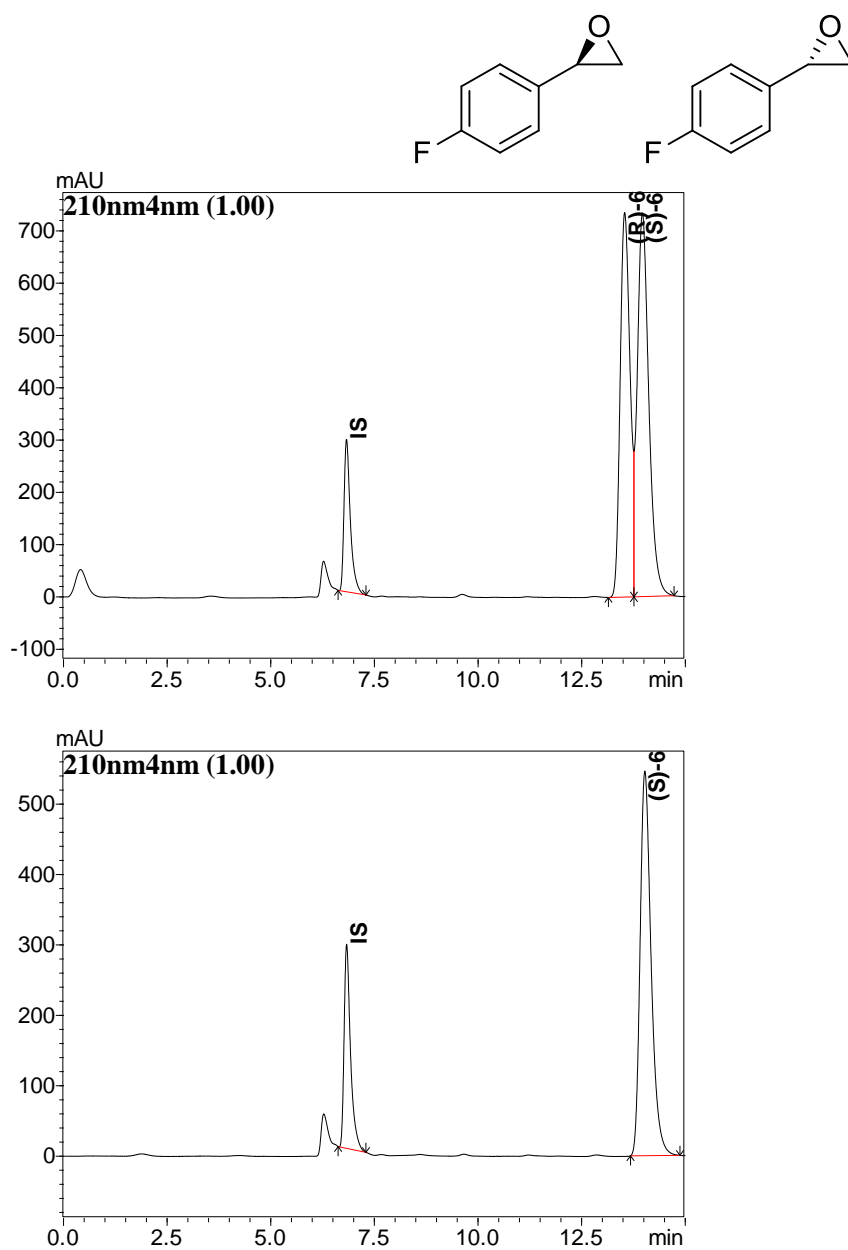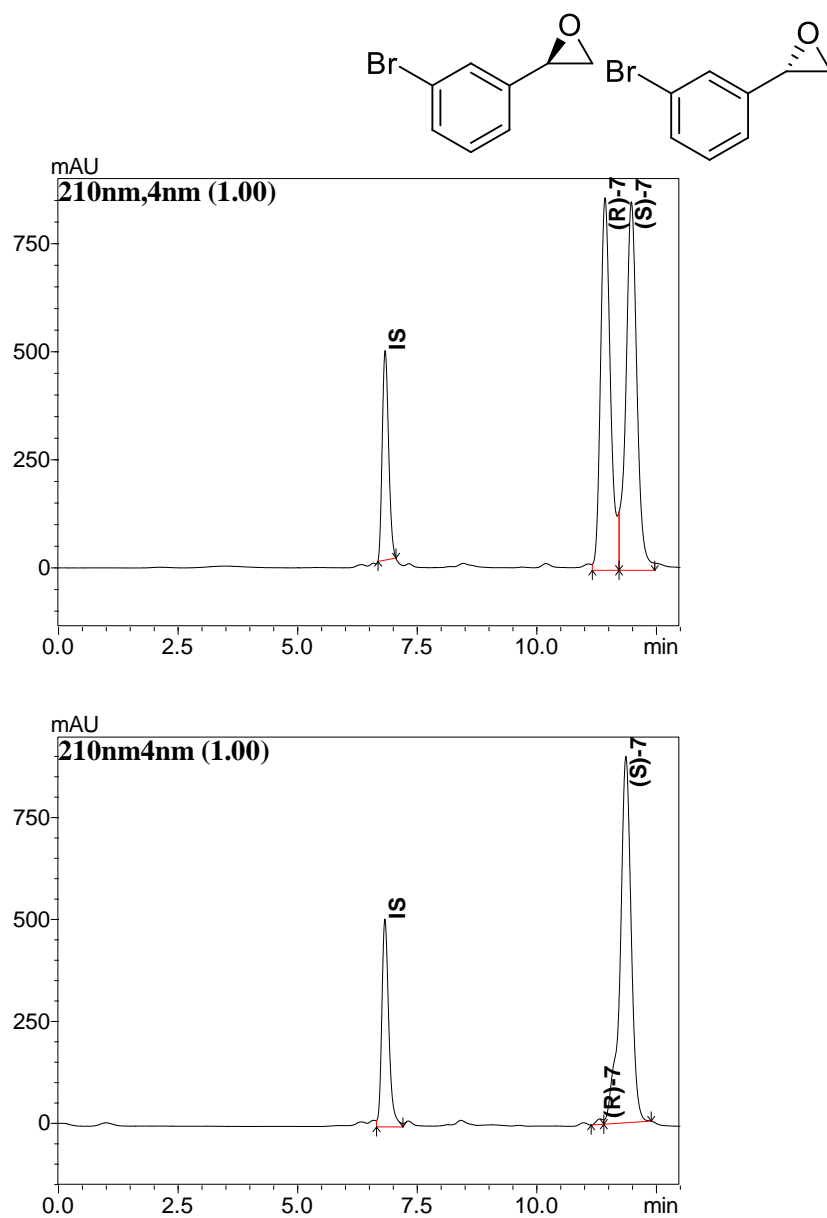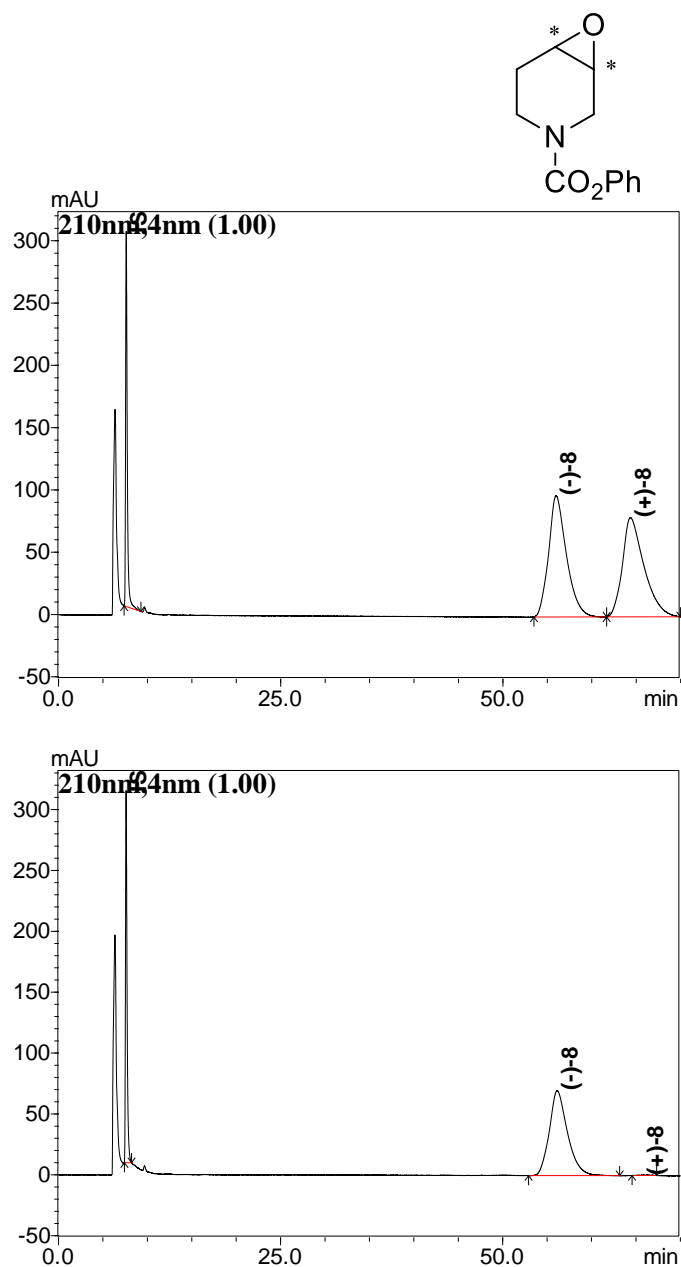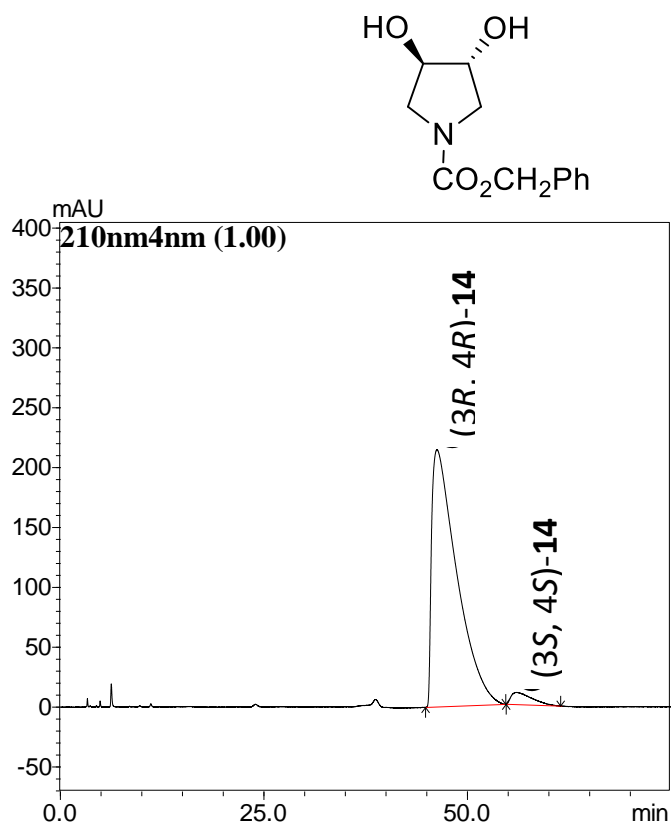
Figure S1.3. Chiral HPLC chromatogram of racemic **3** and product (*S*)-**3** (Column: Daicel AS-H (250 × 4.6 mm, 5µm); eluent: 10% IPA: 90% *n*-hexane; flow rate: 0.5 mL min^{-1}).
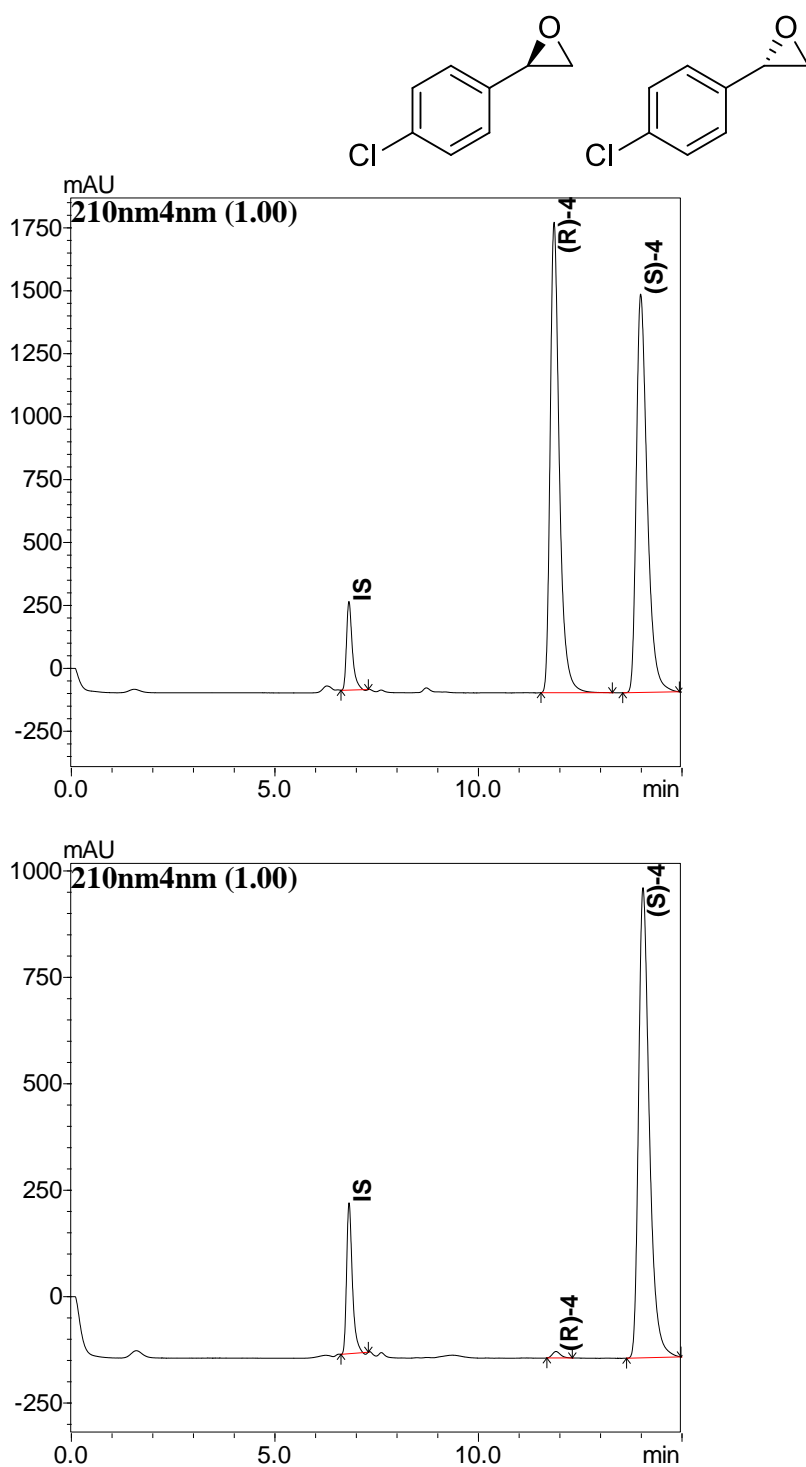
Figure S1.4. Chiral HPLC chromatogram of racemic **4** and product (*S*)-**4** (Column: Daicel AS-H (250 × 4.6 mm, 5µm); eluent: 10% IPA: 90% *n*-hexane; flow rate: 0.5 mL min^{-1}).
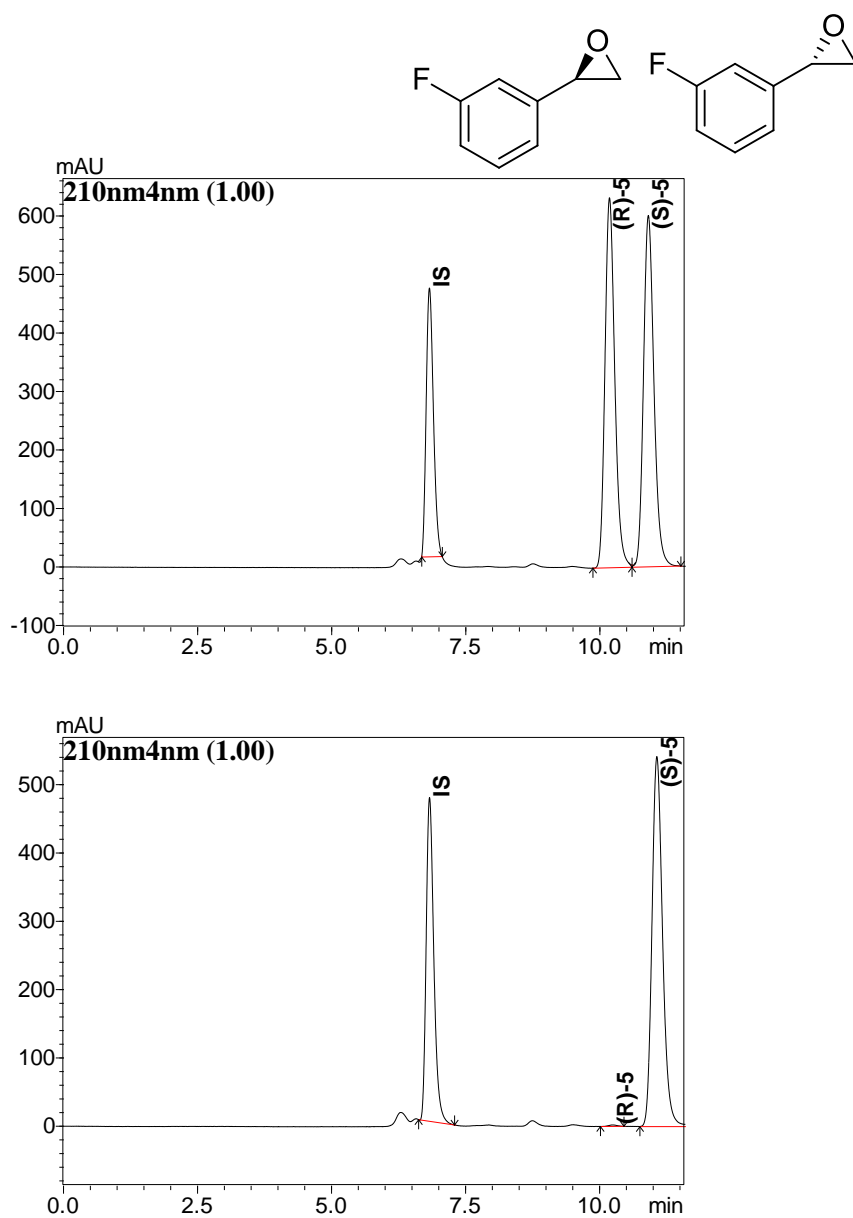
Figure S1.5. Chiral HPLC chromatogram of racemic **5** and product (*S*)-**5** (Column: Daicel AS-H (250 × 4.6 mm, 5μm); eluent: 10% IPA: 90% *n*-hexane; flow rate: 0.5 mL min^{-1}).

Figure S1.6. Chiral HPLC chromatogram of racemic **6** and product (*S*)-**6** (Column: Daicel AS-H (250 × 4.6 mm, 5µm); eluent: 10% IPA: 90% *n*-hexane; flow rate: 0.5 mL min^{-1}).

Figure S1.7. Chiral HPLC chromatogram of racemic **7** and product (*S*)-**7** (Column: Daicel AS-H (250 × 4.6 mm, 5µm); eluent: 10% IPA: 90% *n*-hexane; flow rate: 0.5 mL min^{-1}).

Figure S1.8. Chiral HPLC chromatogram of racemic **8** and product (−)-**8** (Column: Daicel OB-H

(250 × 4.6 mm, 5μm); eluent: 40% IPA: 60% *n*-hexane; flow rate: 0.5 mL min⁻¹).

Figure S1.9. Chiral HPLC chromatogram of product (3*R*, 4*R*)-**14** (Column: Daicel AS-H (250 × 4.6 mm, 5µm); eluent: 5% IPA: 95% *n*-hexane; flow rate: 1.0 mL min^{-1}).

Figure S1.10-S1.11: Chiral GC chromatograms
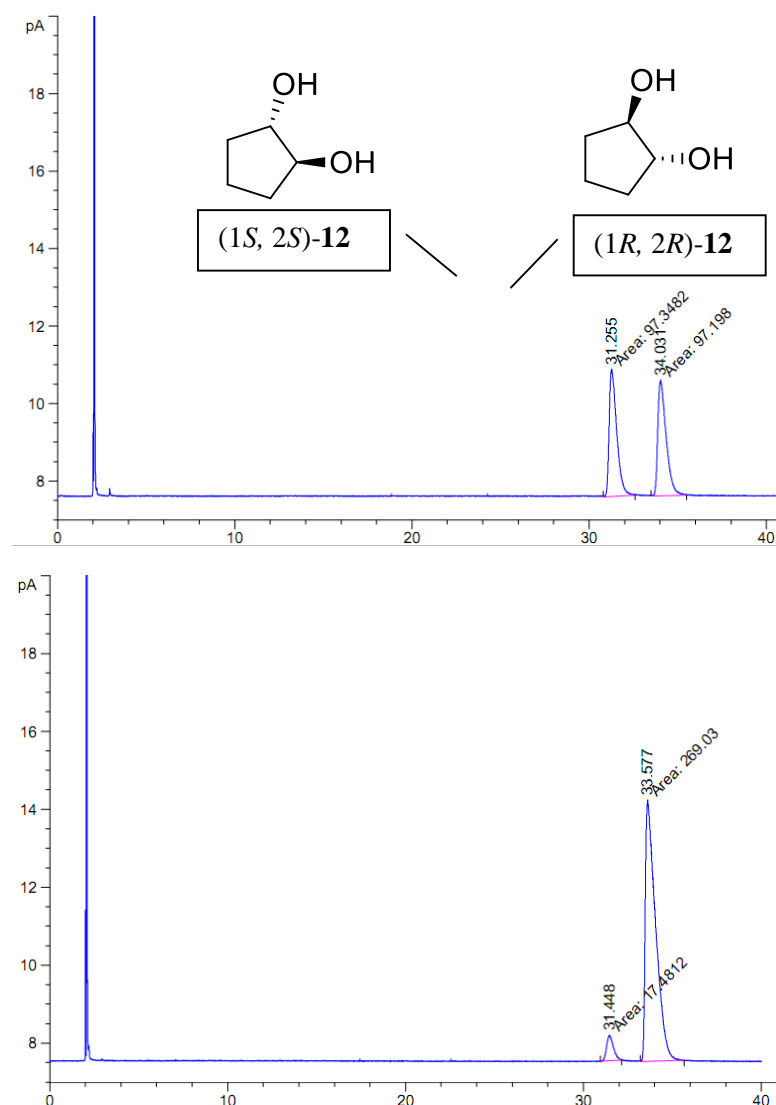
Figure S1.10. Chiral GC chromatogram of *trans*-**12** and product (1*R*, 2*R*)-**12** (Column: Macherey-Nagel Lipodex-E (25 m × 0.25 mm); temperature: 100 °C constant; pressure: 11.093 psi).
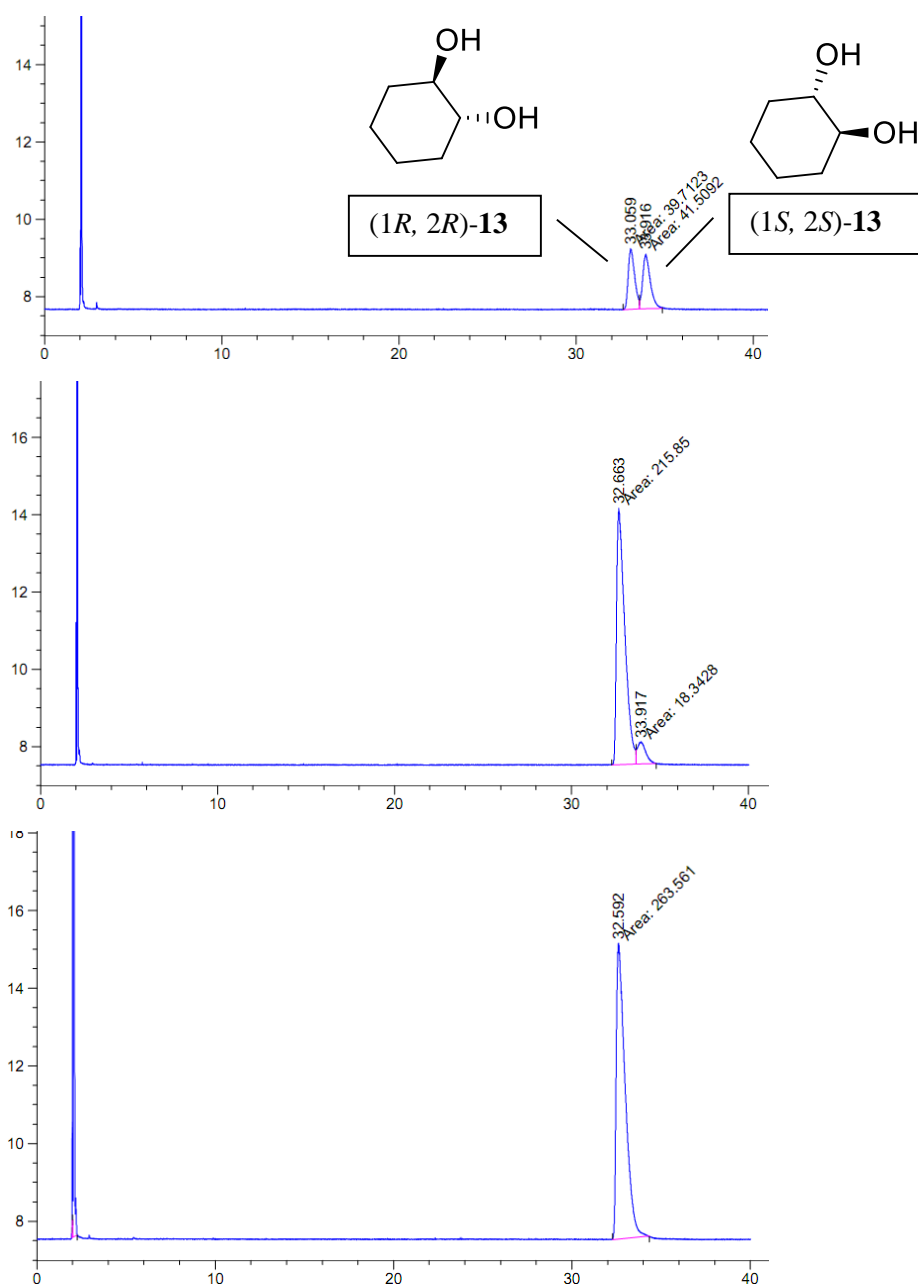
Figure S1.11. Chiral GC chromatogram of *trans*-**13**, product (1*R*, 2*R*)-**13**, and product (1*R*, 2*R*)-**13**

after crystallization (Column: Macherey-Nagel Lipodex-E (25 m × 0.25 mm); temperature: 100 ºC

constant; pressure: 11.093 psi).

Figure S1.12-S1.17. ^{1}H NMR spectra
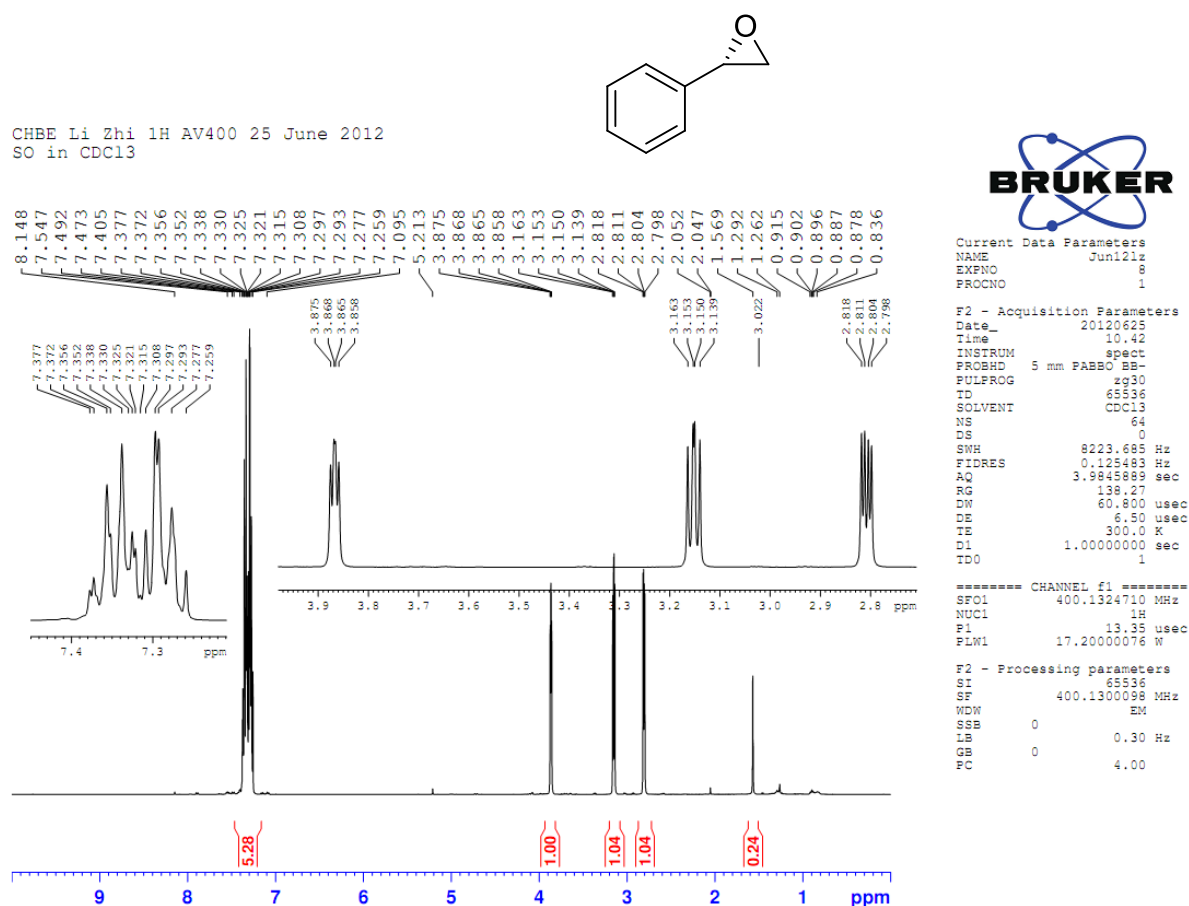
Figure S1.12. ^{1}H NMR spectrum of biotransformation product (*S*)-**1** (400 MHz, CDCl$_3$, TMS).
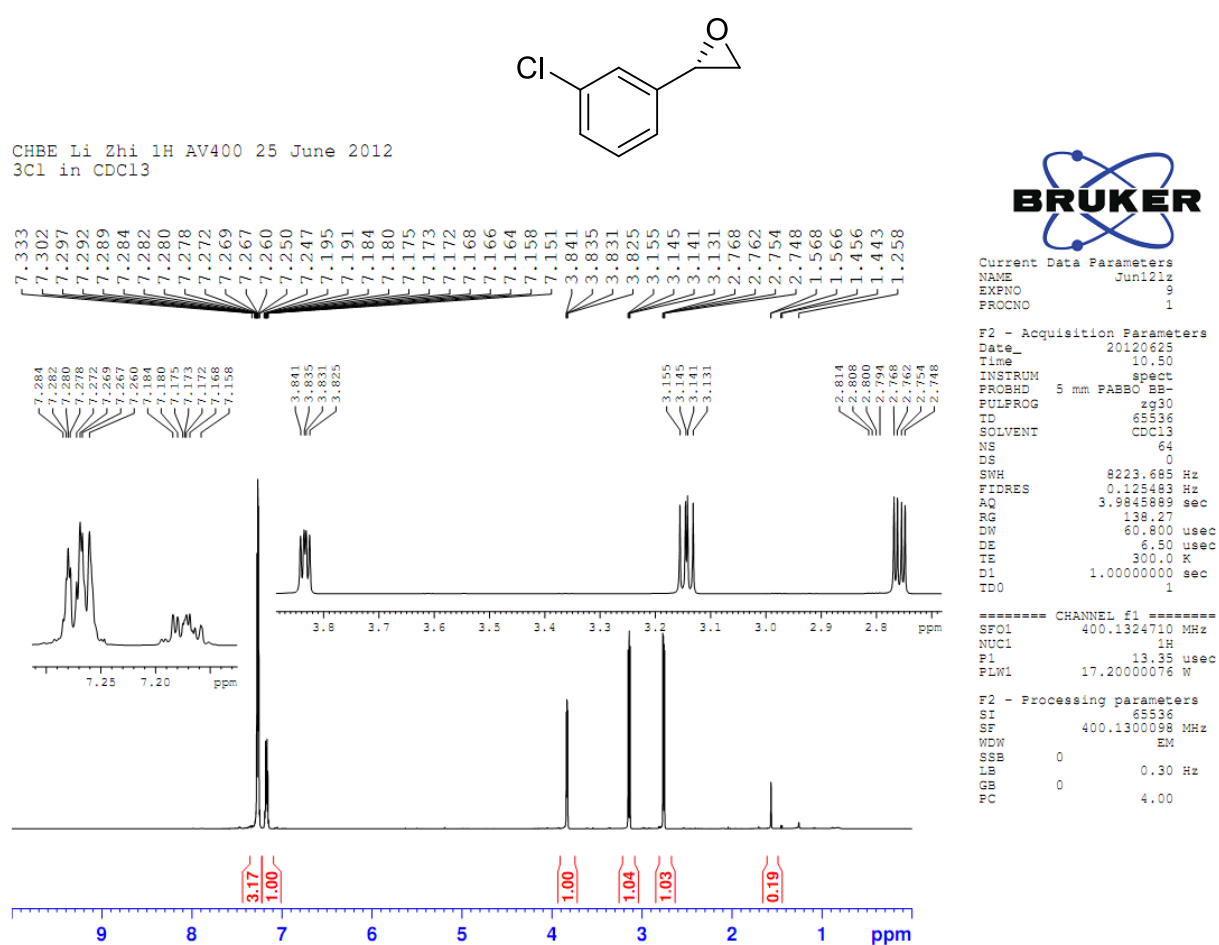
Figure S1.13. ^{1}H NMR spectrum of biotransformation product (*S*)-**3** (400 MHz, CDCl$_3$, TMS).
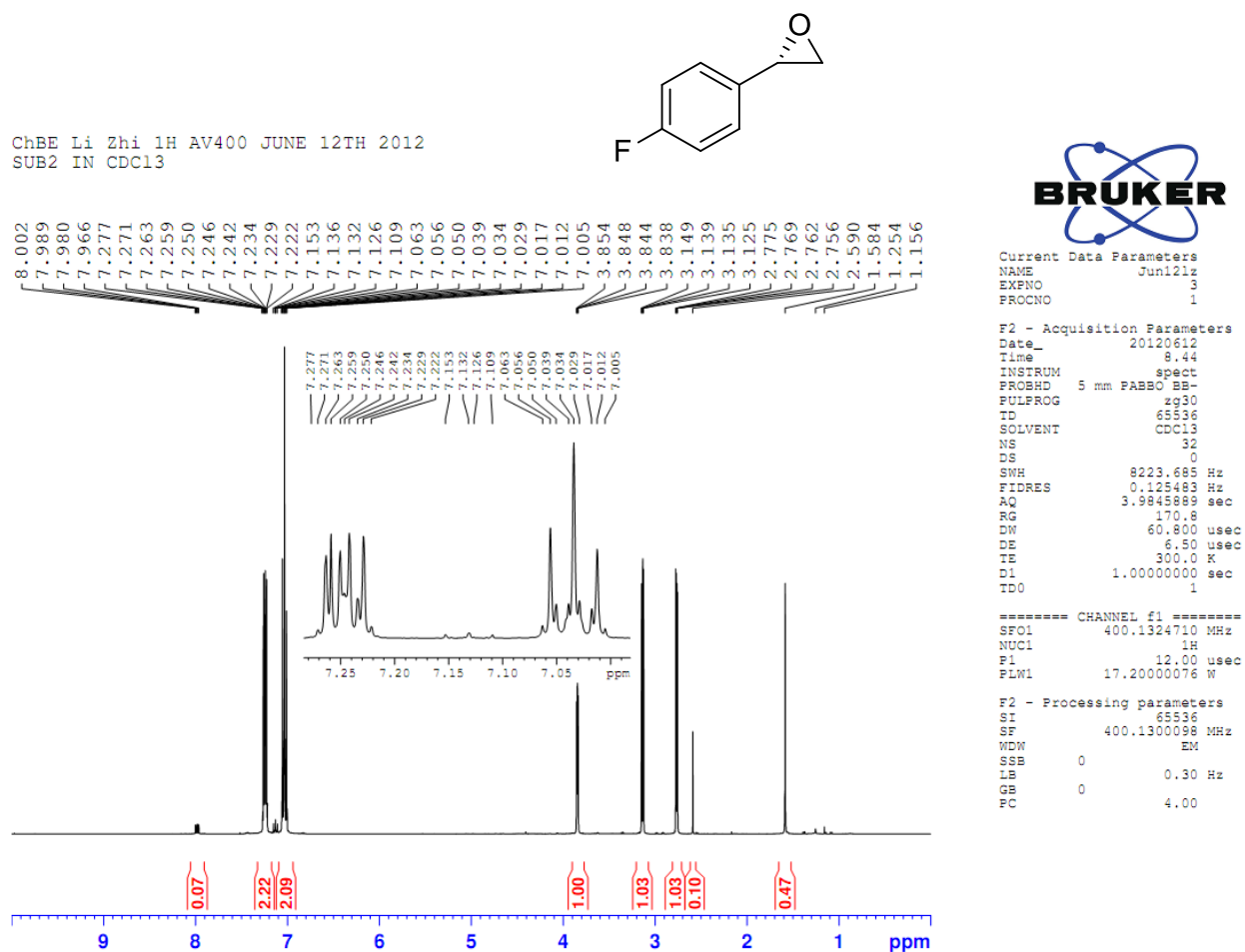
Figure S1.14. ^{1}H NMR spectrum of biotransformation product (*S*)-**6** (400 MHz, CDCl$_3$, TMS).
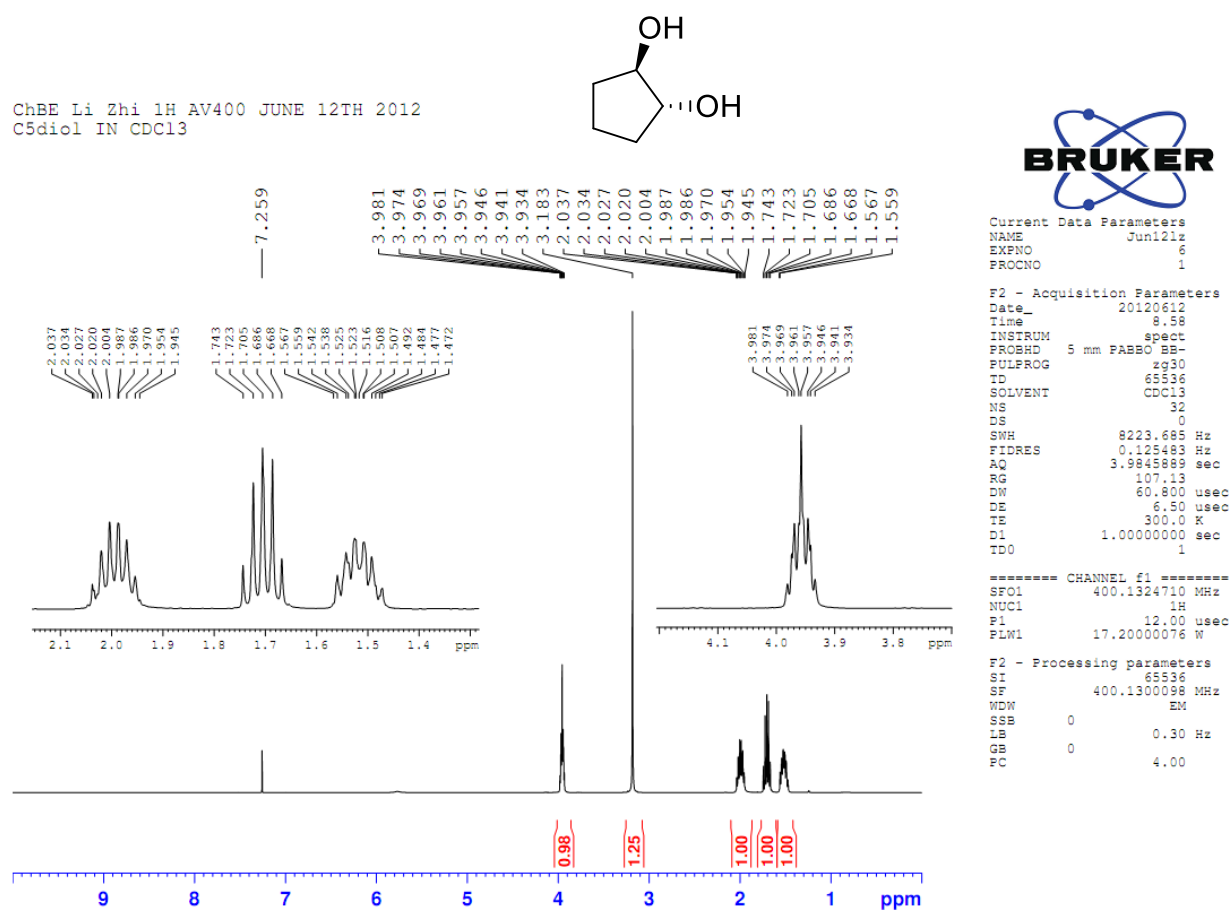
Figure S1.15. ^{1}H NMR spectrum of biotransformation product (1*R*, 2*R*)-**12** (400 MHz, CDCl$_3$, TMS).
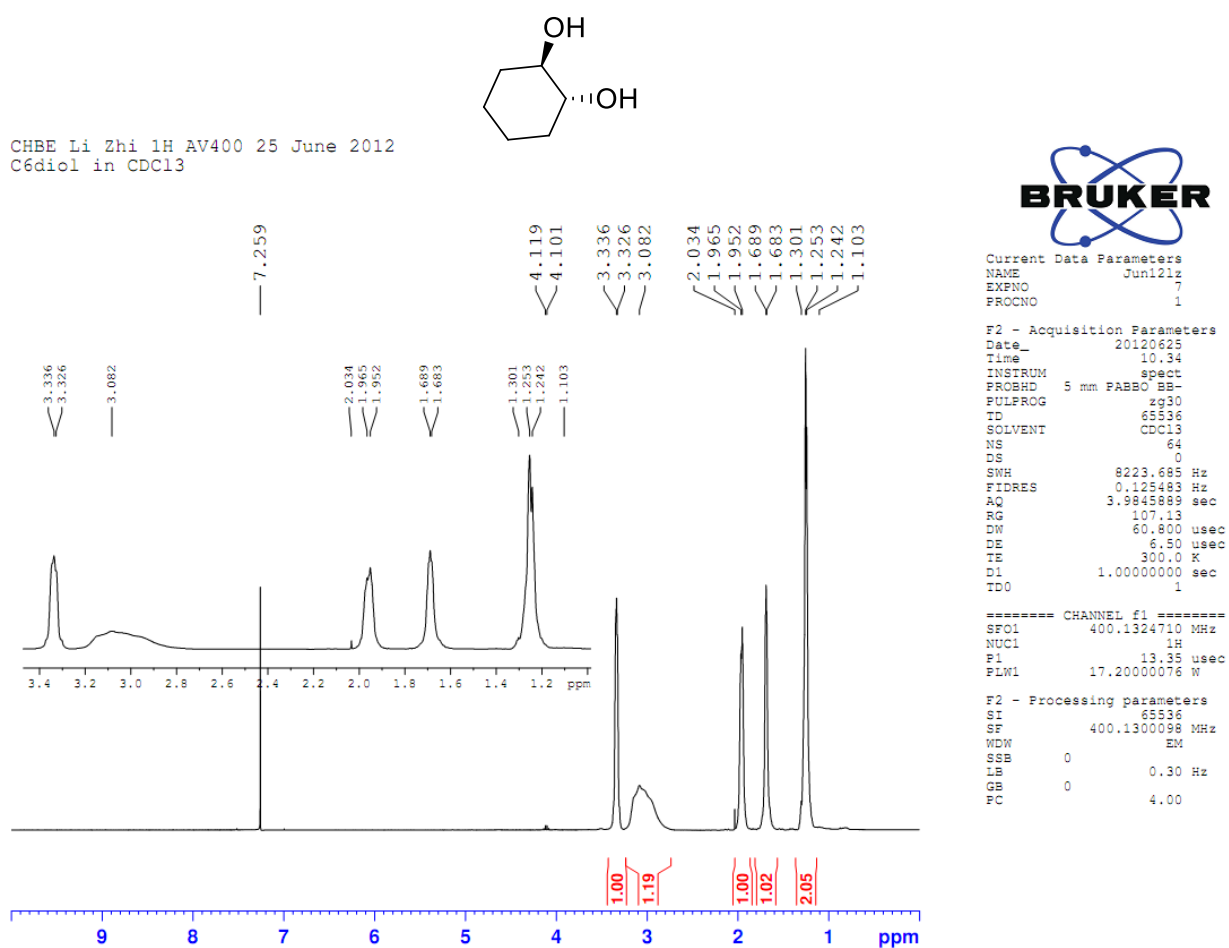
Figure S1.16. ^{1}H NMR spectrum of biotransformation product (1*R,* 2*R*)-**13** (400 MHz, CDCl$_3$, TMS).
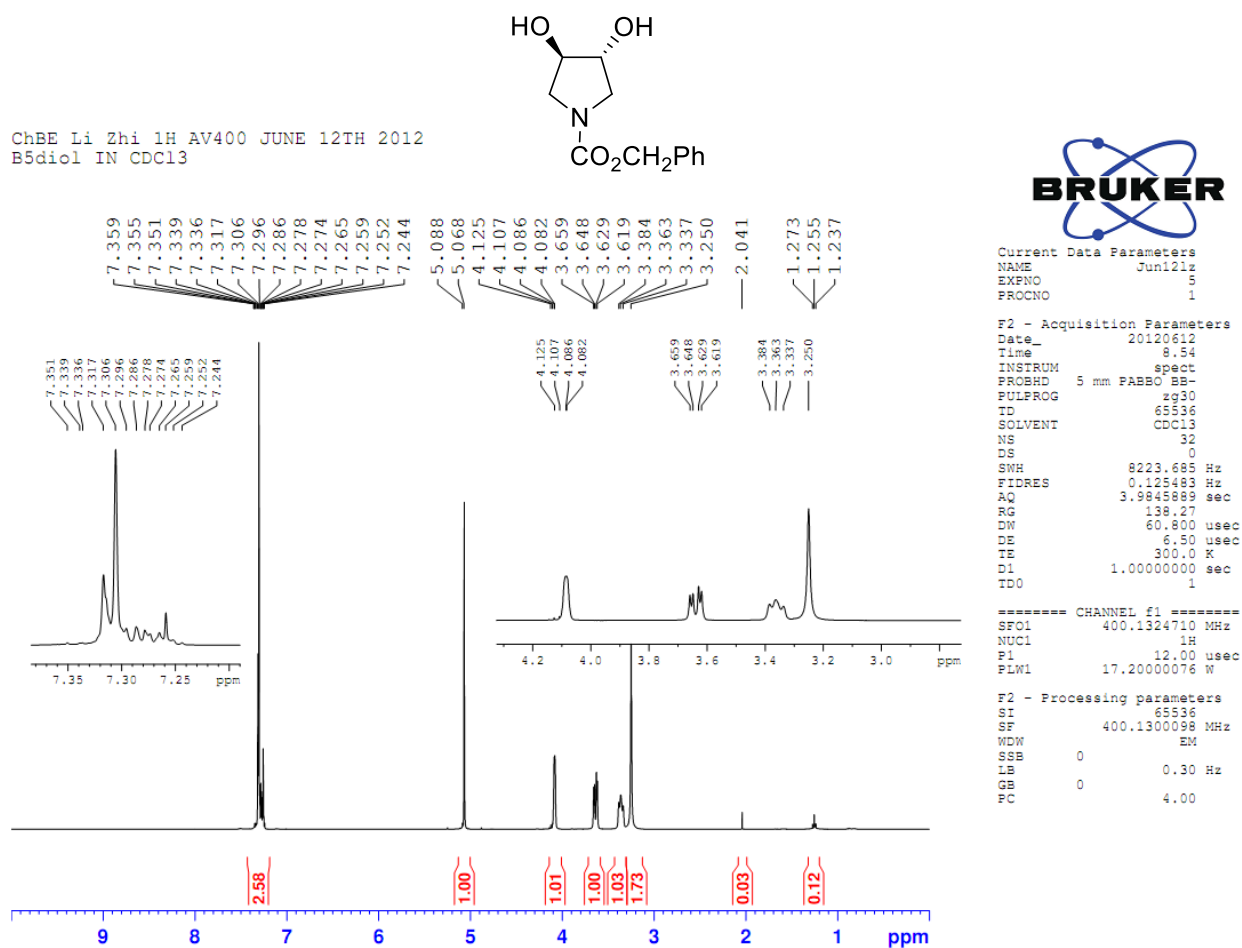
Figure S1.17. ^{1}H NMR spectrum of biotransformation product (3*R,* 4*R*)-**14** (400 MHz, CDCl$_3$, TMS).

Appendix II: Supporting Information for Chapter 4

>DNA Sequence of Synthesized StEH (codon optimized for *E. coli*)

ATGGAGAAAATCGAACACAAGATGGTTGCTGTAAATGGCCTGAATATGCATCTGGCAGAGCTGG
GCGAAGGTCCGACCATTCTGTTTATTCATGGCTTCCCGGAACTGTGGTATAGCTGGCGTCACCA
GATGGTTTATCTGGCAGAACGTGGTTACCGTGCAGTCGCTCCGGATCTGCGTGGTTACGGTGAC
ACCACGGGTGCACCGCTGAACGATCCGAGTAAATTTTCCATCCTGCATCTGGTGGGCGACGTGG
TTGCACTGCTGGAAGCGATTGCCCCGAATGAAGAAAAGTTTTTGTCGTGGCGCATGATTGGGG
CGCACTGATTGCTTGGCACCTGTGCCTGTTTCGTCCGGACAAAGTCAAAGCCCTGGTGAACCTG
TCAGTTCATTTCTCGAAACGCAACCCGAAAATGAATGTTGTCGAAGGCCTGAAAGCAATCTATGG
TGAAGATCACTACATTAGTCGTTTTCAAGTGCCGGGCGAAATCGAAGCGGAATTTGCCCCGATTG
GTGCGAAATCAGTTCTGAAGAAAATTCTGACCTATCGCGATCCGGCGCCGTTTTACTTCCCGAAA
GGCAAAGGTCTGGAAGCCATTCCGGATGCACCGGTGGCTCTGAGCTCTTGGCTGTCCGAAGAA
GAACTGGACTATTACGCCAACAAATTTGAACAGACCGGCTTCACGGGTGCAGTGAACTATTACCG
TGCTCTGCCGATCAATTGGGAACTGACCGCACCGTGGACGGGTGCACAAGTGAAAGTTCCGAC
GAAATTTATTGTCGGCGAATTTGATCTGGTGTATCATATCCCGGGTGCGAAAGAATACATTCACA
ATGGCGGTTTTAAAAAAGACGTCCCGCTGCTGGAAGAAGTGGTTGTCCTGGAAGGCGCGGCCC
ACTTCGTTAGCCAGGAACGCCCGCATGAAATTTCTAAACACATCTATGATTTTATTCAAAAATTCT
AA

>Protein Sequence of Synthesized StEH

MEKIEHKMVAVNGLNMHLAELGEGPTILFIHGFPELWYSWRHQMVYLAERGYRAVAPDLR
GYGDTTGAPLNDPSKFSILHLVGDVVALLEAIAPNEEKVFVVAHDWGALIAWHLCLFRPDKV
KALVNLSVHFSKRNPKMNVVEGLKAIYGEDHYISRFQVPGEIEAEFAPIGAKSVLKKILTYRD
PAPFYFPKGKGLEAIPDAPVALSSWLSEEELDYYANKFEQTGFTGAVNYYRALPINWELTAP
WTGAQVKVPTKFIVGEFDLVYHIPGAKEYIHNGGFKKDVPLLEEVVVLEGAAHFVSQERPHE
ISKHIYDFIQKF-

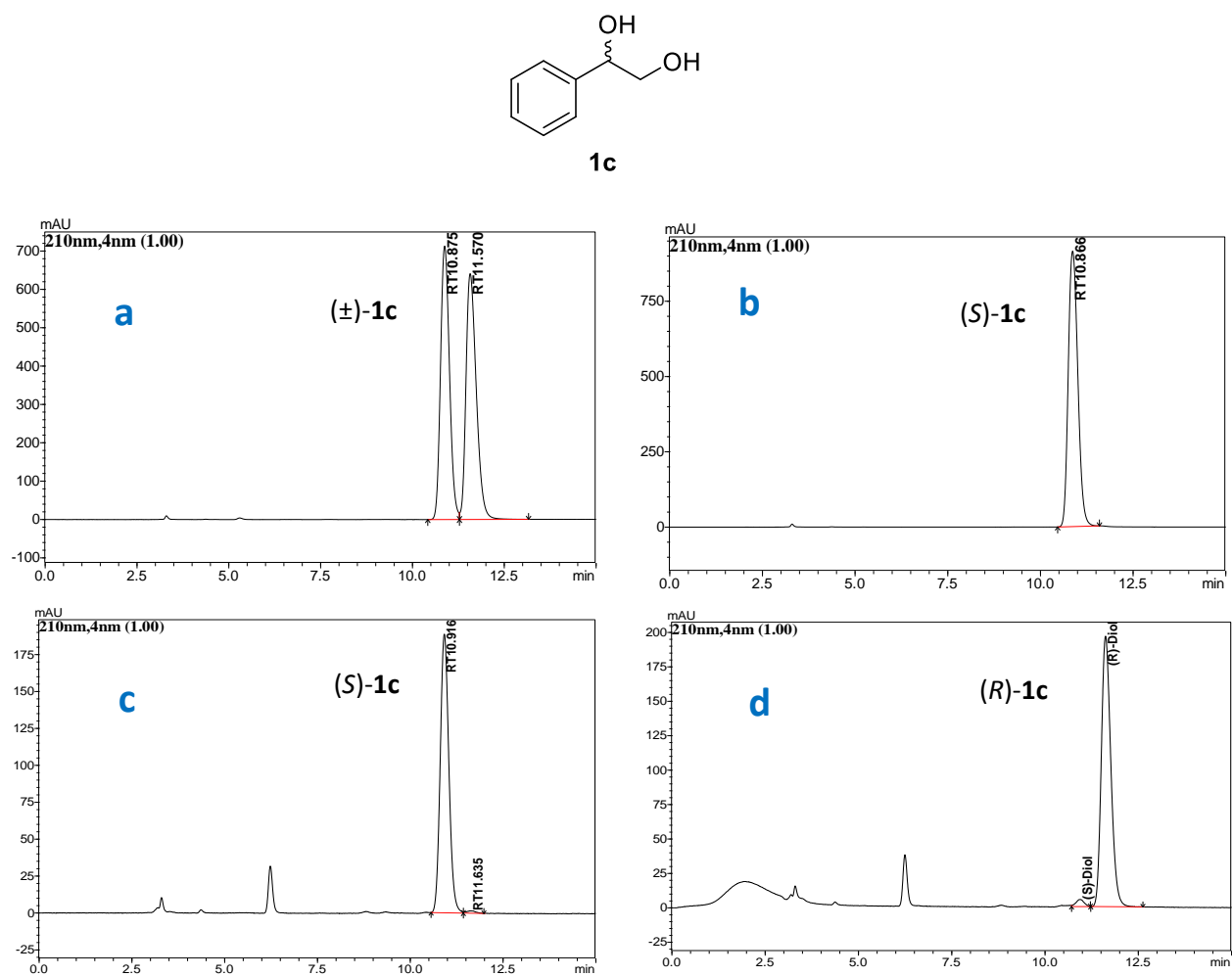**Figure S2.1-S2.22. Chiral HPLC Chromatograms**

1c

Figure S2.1. Chiral HPLC chromatograms of diol **1c**. a) racemic **1c**; b) (*S*)-**1c** standard; c) (*S*)-**1c** produced by *E. coli* (SSP1); d) (*R*)-**1c** produced by *E. coli* (SST1). (Daicel Chiralpak AS-H (250 × 4.6 mm, 5μm) column, mobile phase 10% IPA: 90% *n*-hexane, flow rate 1.0 mL min^{-1}, oven temperature 25 ℃, UV detection at 210 nm)
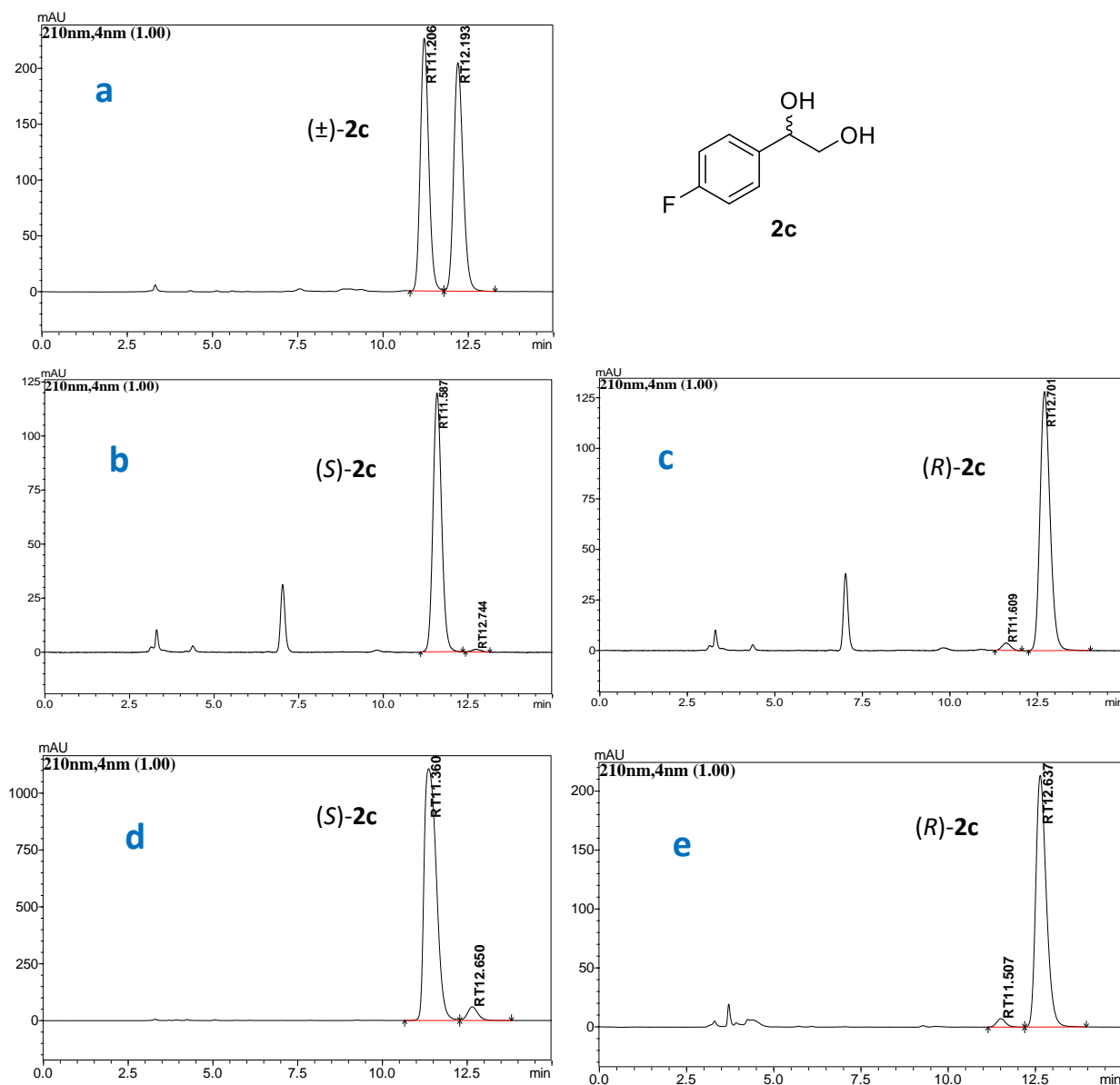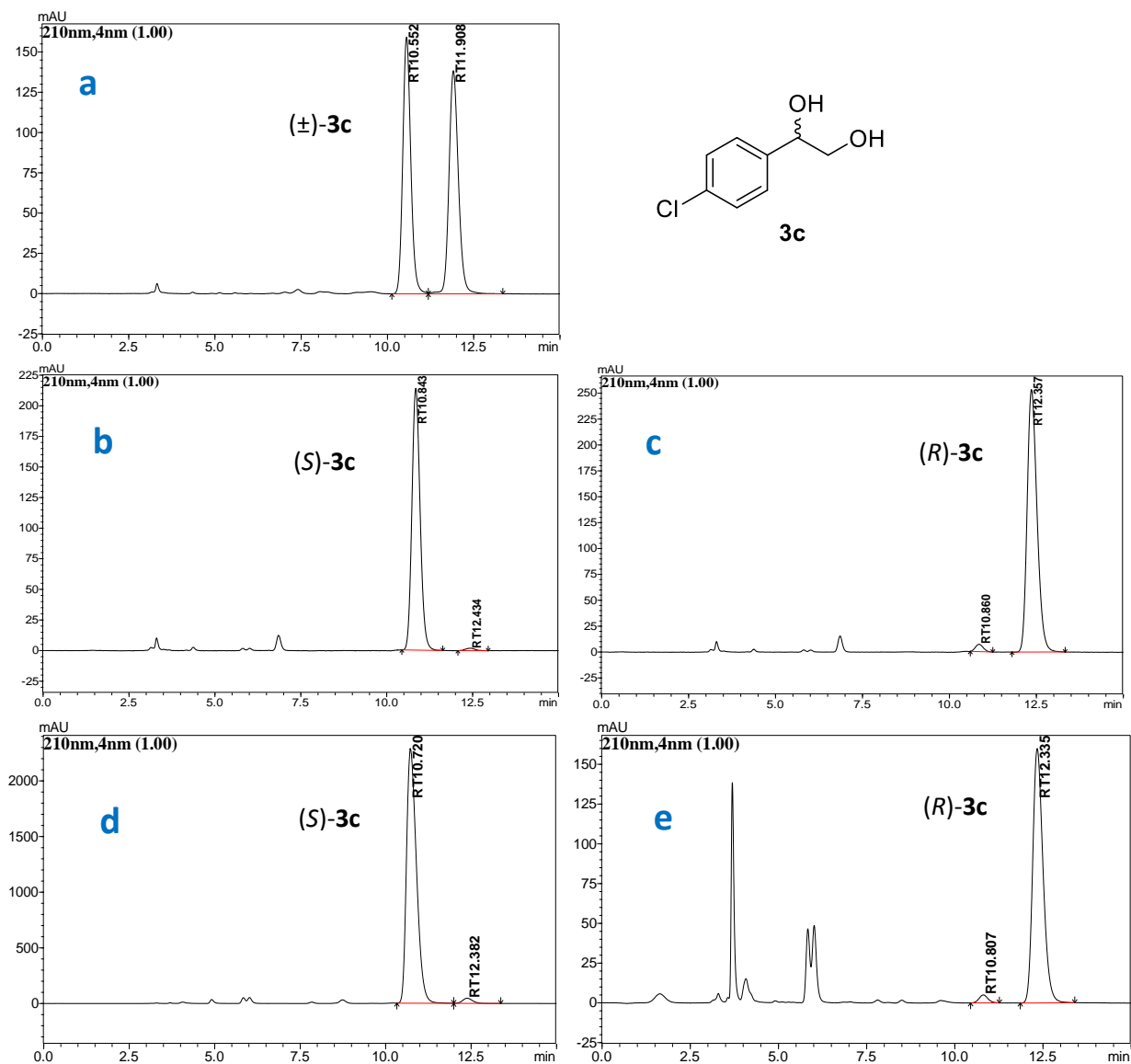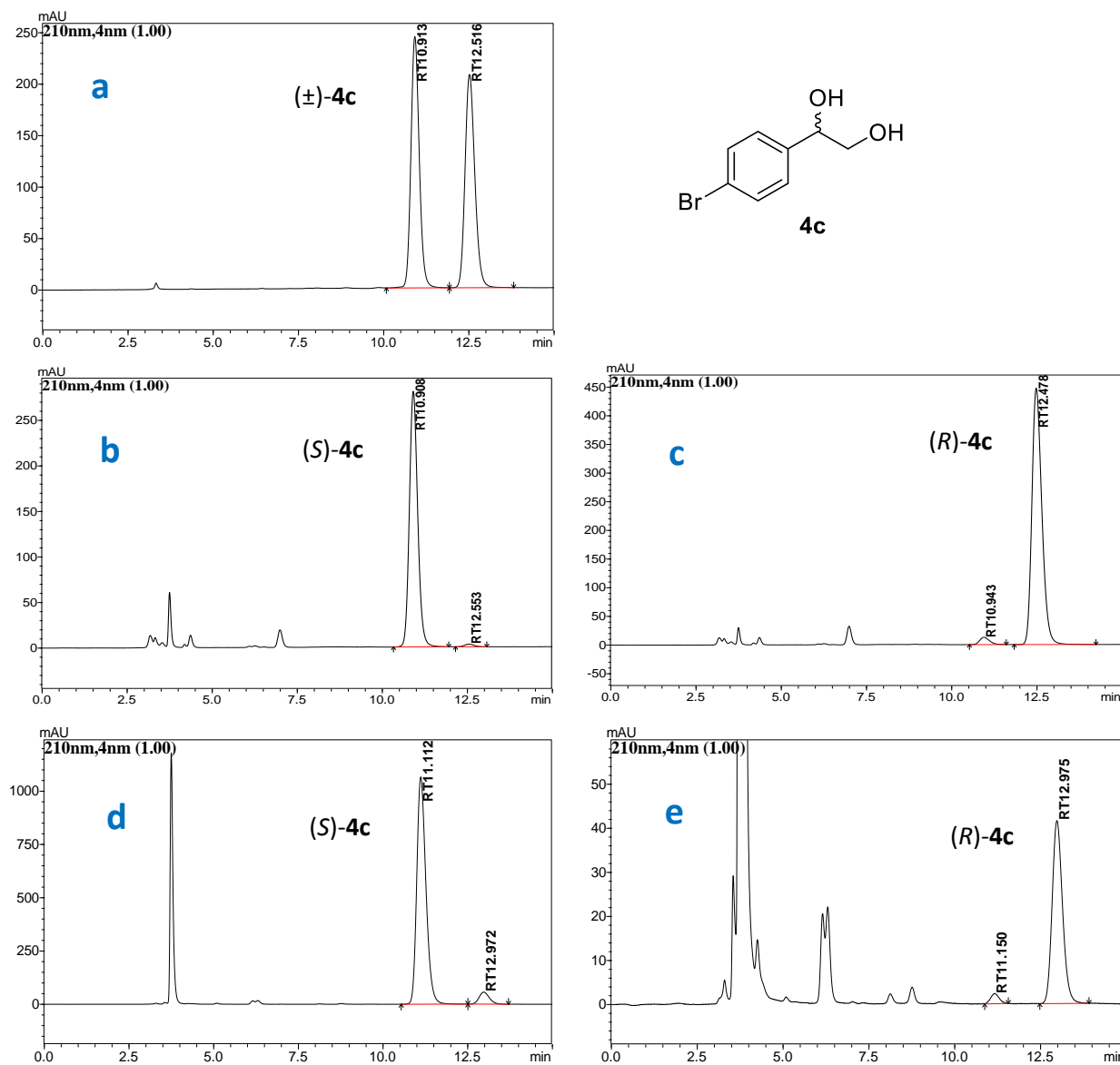
Figure S2.2. Chiral HPLC chromatograms of diol **2c**. a) racemic **2c**; b) (*S*)-**2c** produced by *E. coli* (SSP1); c) (*R*)-**2c** produced by *E. coli* (SST1); d) (*S*)-**2c** produced by AD-mix-α; e) (*R*)-**2c** produced by AD-mix-β. (Daicel Chiralpak AS-H (250 × 4.6 mm, 5μm) column, mobile phase 10% IPA: 90% *n*-hexane, flow rate 1.0 mL min^{-1}, oven temperature 25 °C, UV detection at 210 nm)
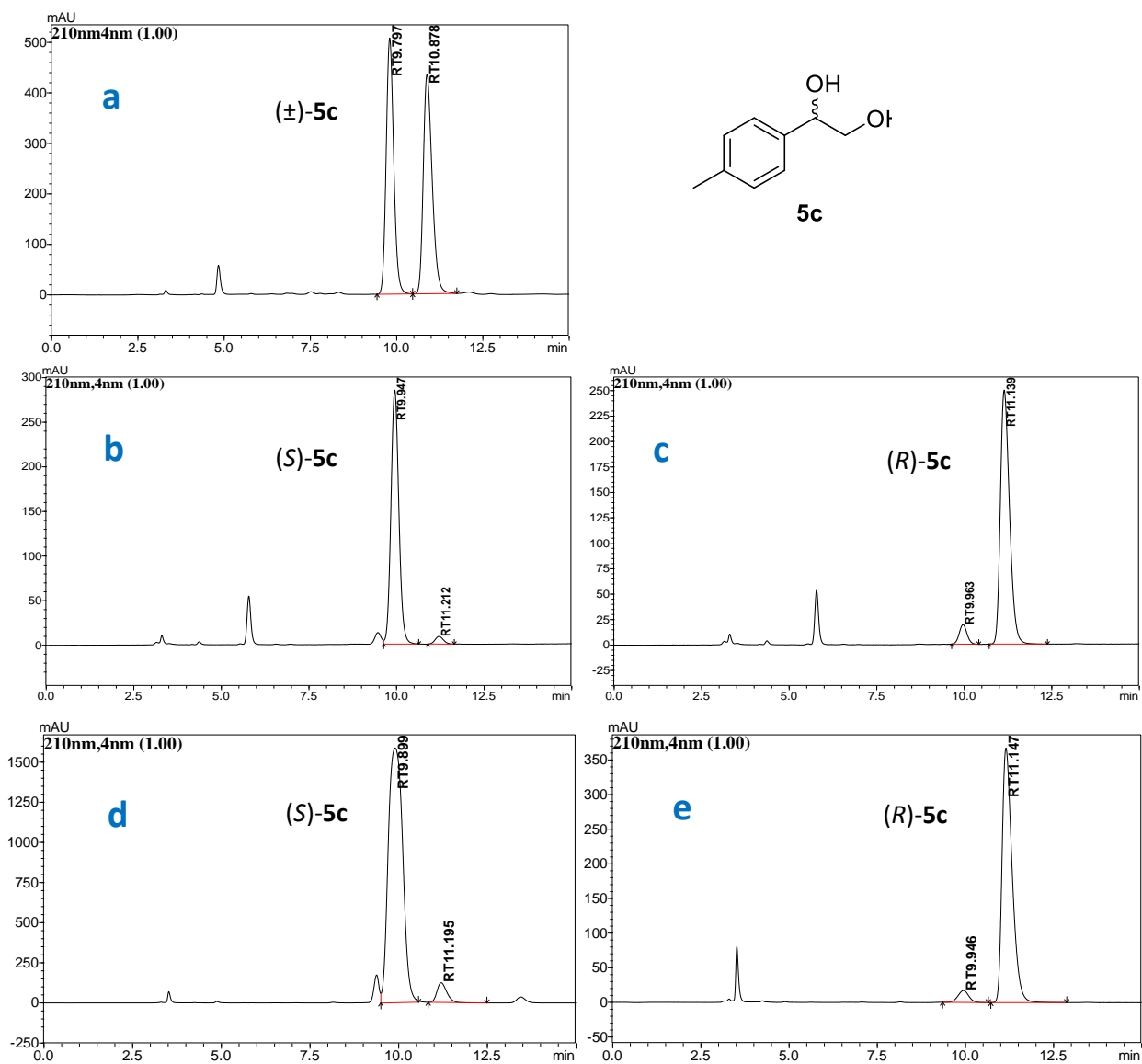
Figure S2.3. Chiral HPLC chromatograms of diol **3c**. a) racemic **3c**; b) (*S*)-**3c** produced by *E. coli* (SSP1); c) (*R*)-**3c** produced by *E. coli* (SST1); d) (*S*)-**3c** produced by AD-mix-α; e) (*R*)-**3c** produced by AD-mix-β. (Daicel Chiralpak AS-H (250 × 4.6 mm, 5μm) column, mobile phase 10% IPA: 90% *n*-hexane, flow rate 1.0 mL min⁻¹, oven temperature 25 °C, UV detection at 210 nm)
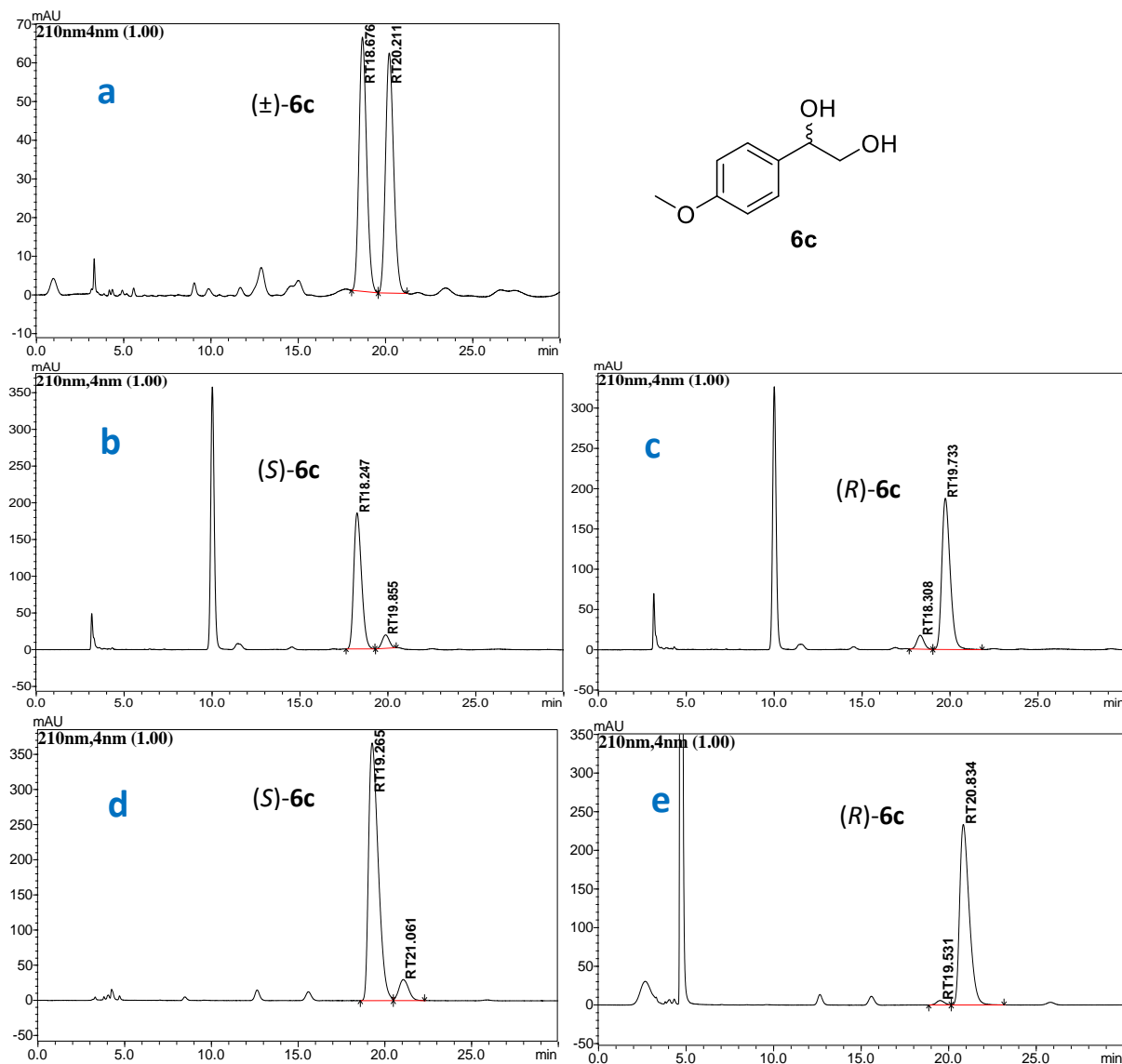
Figure S2.4. Chiral HPLC chromatograms of diol **4c**. a) racemic **4c**; b) (*S*)-**4c** produced by *E. coli* (SSP1); c) (*R*)-**4c** produced by *E. coli* (SST1); d) (*S*)-**4c** produced by AD-mix-α; e) (*R*)-**4c** produced by AD-mix-β. (Daicel Chiralpak AS-H (250 × 4.6 mm, 5μm) column, mobile phase 10% IPA: 90% *n*-hexane, flow rate 1.0 mL min⁻¹, oven temperature 25 °C, UV detection at 210 nm)

Figure S2.5. Chiral HPLC chromatograms of diol **5c**. a) racemic **5c**; b) (*S*)-**5c** produced by *E. coli* (SSP1); c) (*R*)-**5c** produced by *E. coli* (SST1); d) (*S*)-**5c** produced by AD-mix-α; e) (*R*)-**5c** produced by AD-mix-β. (Daicel Chiralpak AS-H (250 × 4.6 mm, 5μm) column, mobile phase 10% IPA: 90% *n*-hexane, flow rate 1.0 mL min⁻¹, oven temperature 25 °C, UV detection at 210 nm)
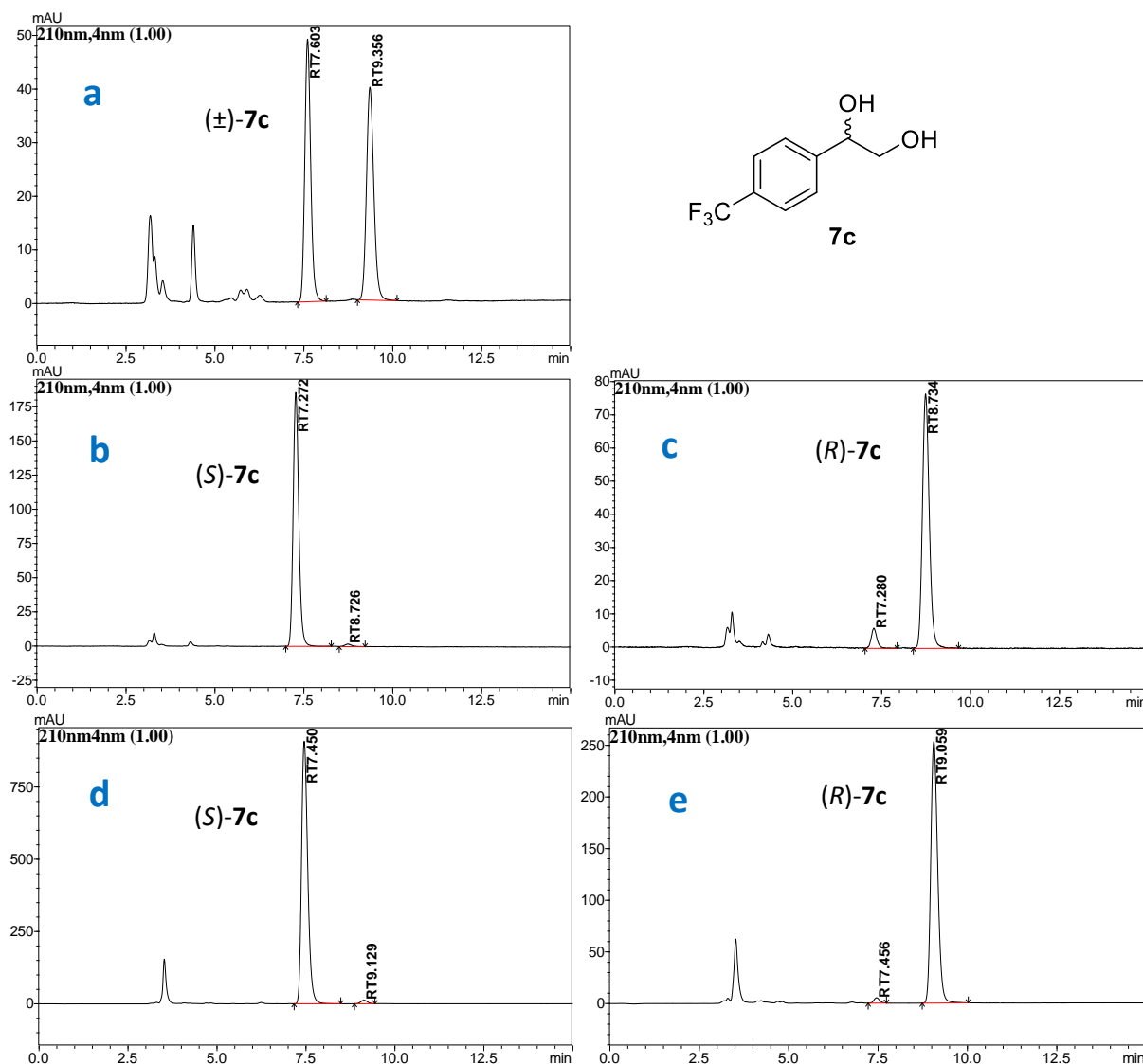
Figure S2.6. Chiral HPLC chromatograms of diol **6c**. a) racemic **6c**; b) (*S*)-**6c** produced by *E. coli* (SSP1); c) (*R*)-**6c** produced by *E. coli* (SST1); d) (*S*)-**6c** produced by AD-mix-α; e) (*R*)-**6c** produced by AD-mix-β. (Daicel Chiralpak AS-H (250 × 4.6 mm, 5μm) column, mobile phase 10% IPA: 90% *n*-hexane, flow rate 1.0 mL min⁻¹, oven temperature 25 ᵒC, UV detection at 210 nm)
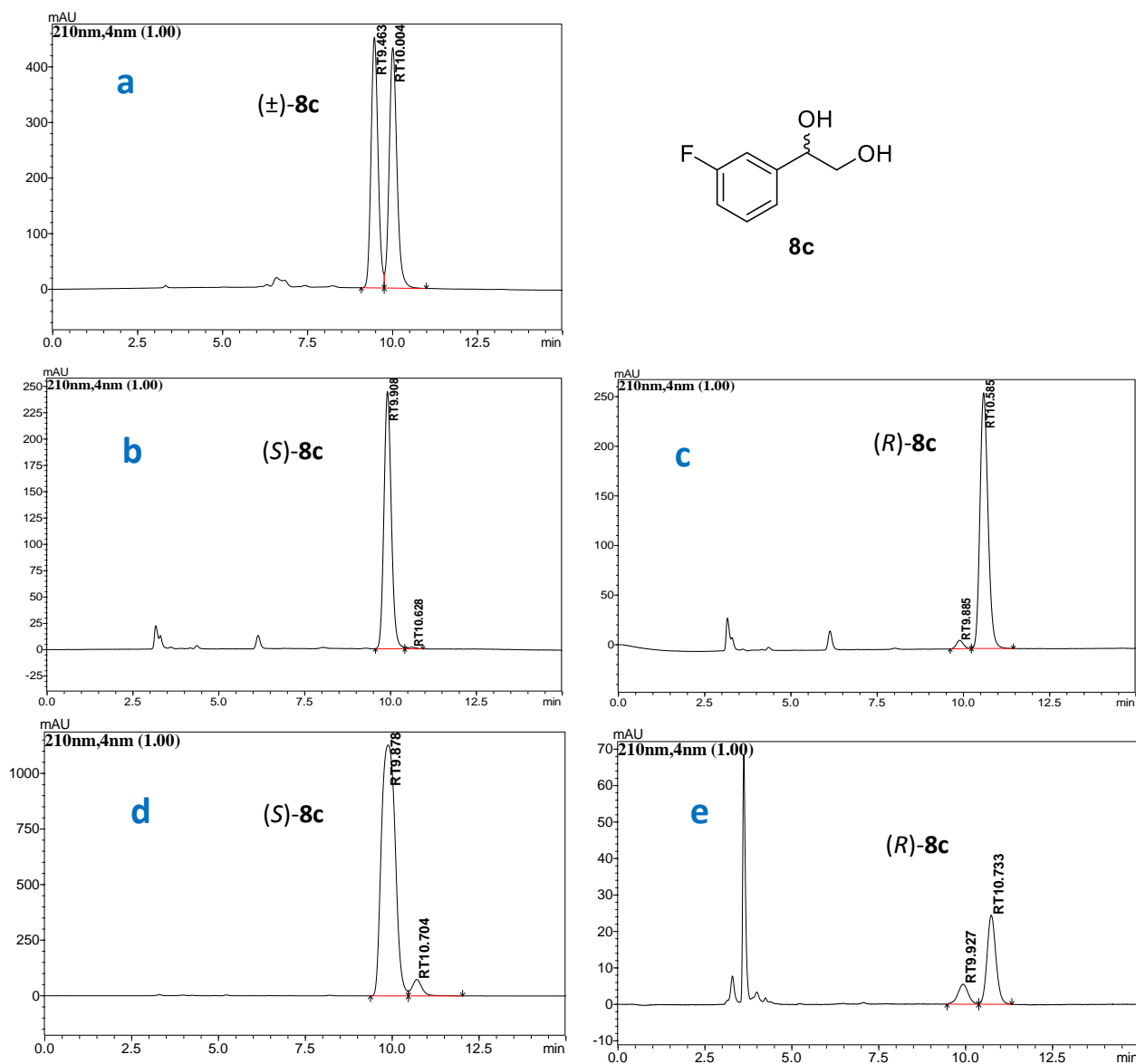
Figure S2.7. Chiral HPLC chromatograms of diol **7c**. a) racemic **7c**; b) (*S*)-**7c** produced by *E. coli* (SSP1); c) (*R*)-**7c** produced by *E. coli* (SST1); d) (*S*)-**7c** produced by AD-mix-α; e) (*R*)-**7c** produced by AD-mix-β. (Daicel Chiralpak AS-H (250 × 4.6 mm, 5μm) column, mobile phase 10% IPA: 90% *n*-hexane, flow rate 1.0 mL min^{-1}, oven temperature 25 ºC, UV detection at 210 nm)
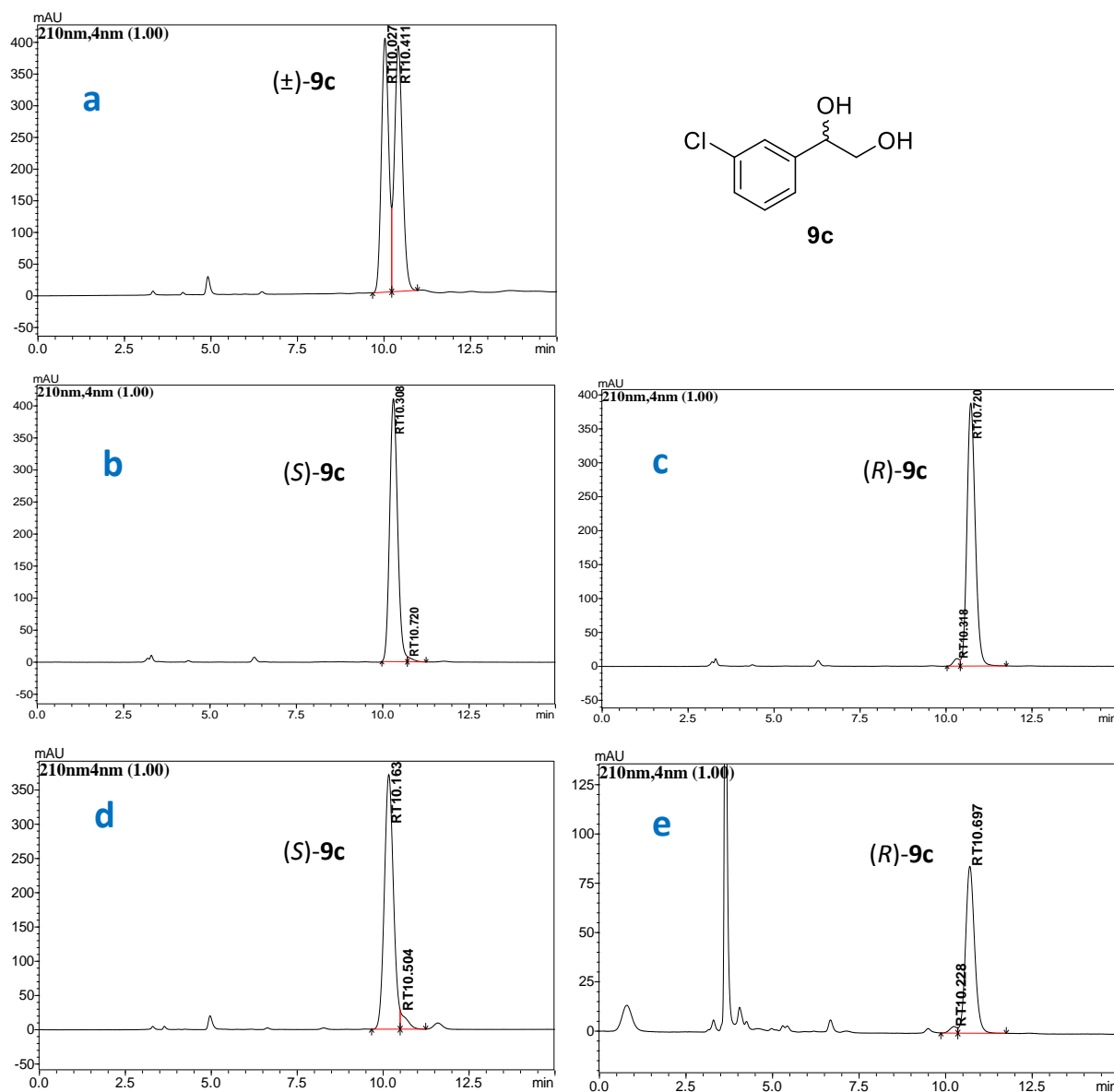
Figure S2.8. Chiral HPLC chromatograms of diol **8c**. a) racemic **8c**; b) (*S*)-**8c** produced by *E. coli* (SSP1); c) (*R*)-**8c** produced by *E. coli* (SST1); d) (*S*)-**8c** produced by AD-mix-α; e) (*R*)-**8c** produced by AD-mix-β. (Daicel Chiralpak AS-H (250 × 4.6 mm, 5µm) column, mobile phase 10% IPA: 90% *n*-hexane, flow rate 1.0 mL min^{-1}, oven temperature 25 ºC, UV detection at 210 nm)

Figure S2.9. Chiral HPLC chromatograms of diol **9c**. a) racemic **9c**; b) (*S*)-**9c** produced by *E. coli* (SSP1); c) (*R*)-**9c** produced by *E. coli* (SST1); d) (*S*)-**9c** produced by AD-mix-α; e) (*R*)-**9c** produced by AD-mix-β. (Daicel Chiralpak AS-H (250 × 4.6 mm, 5μm) column, mobile phase 10% IPA: 90% *n*-hexane, flow rate 1.0 mL min^{-1}, oven temperature 25 °C, UV detection at 210 nm)
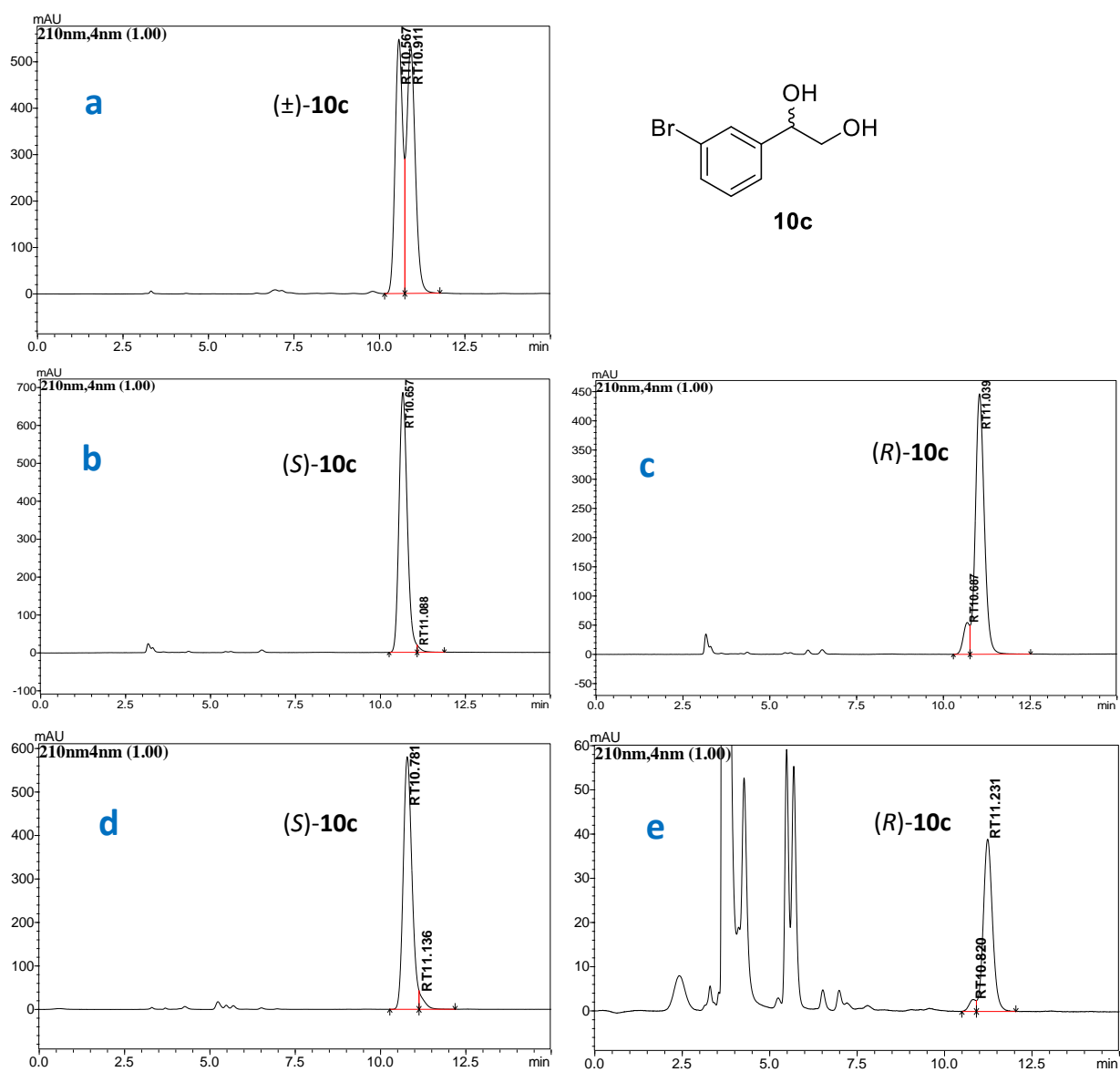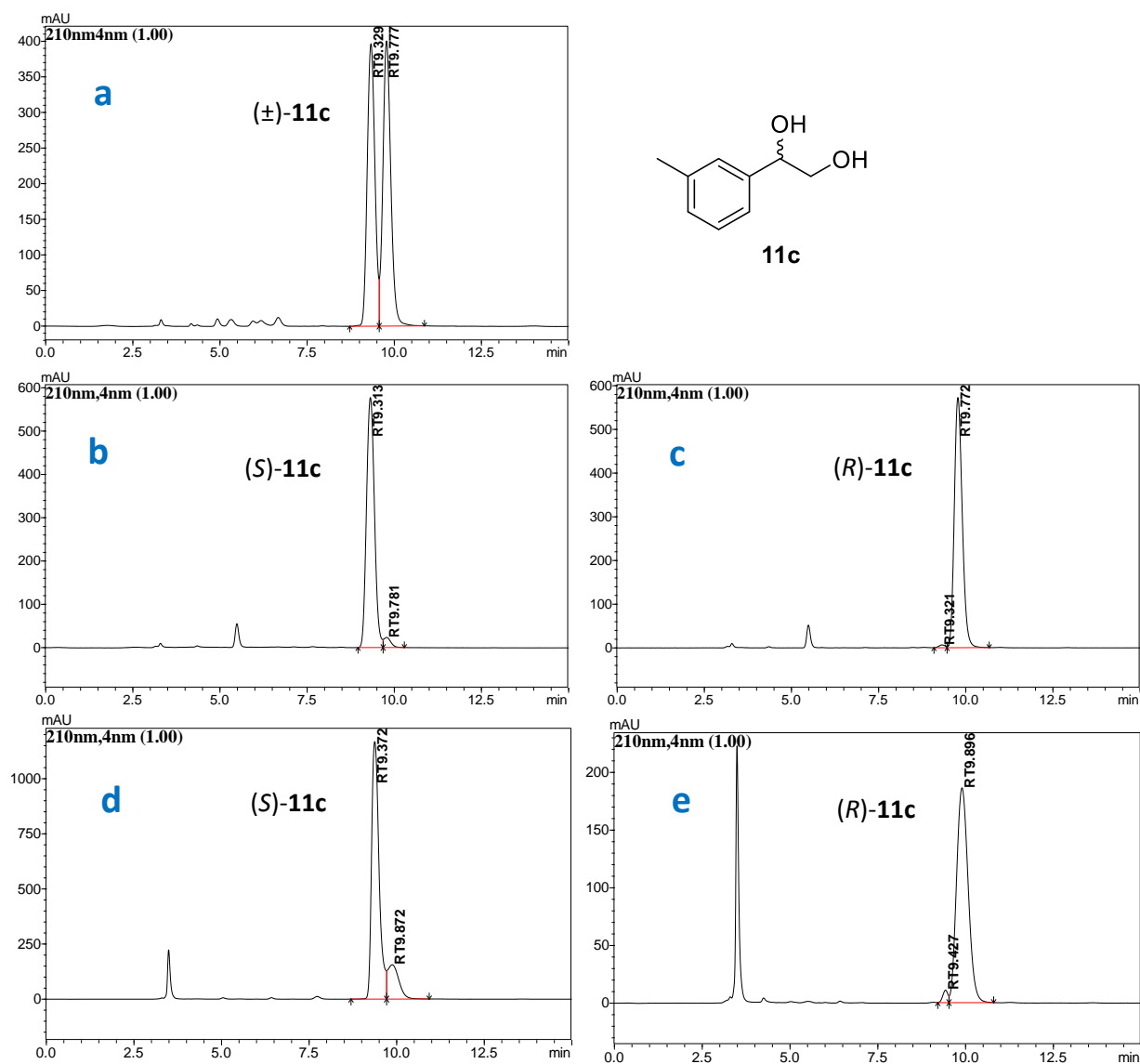
Figure S2.10. Chiral HPLC chromatograms of diol **10c**. a) racemic **10c**; b) (*S*)-**10c** produced by *E. coli* (SSP1); c) (*R*)-**10c** produced by *E. coli* (SST1); d) (*S*)-**10c** produced by AD-mix-α; e) (*R*)-**10c** produced by AD-mix-β. (Daicel Chiralpak AS-H (250 × 4.6 mm, 5μm) column, mobile phase 10% IPA: 90% *n*-hexane, flow rate 1.0 mL min⁻¹, oven temperature 25 ºC, UV detection at 210 nm)

Figure S2.11. Chiral HPLC chromatograms of diol **11c**. a) racemic **11c**; b) (*S*)-**11c** produced by *E. coli* (SSP1); c) (*R*)-**11c** produced by *E. coli* (SST1); d) (*S*)-**11c** produced by AD-mix-α; e) (*R*)-**11c** produced by AD-mix-β. (Daicel Chiralpak AS-H (250 × 4.6 mm, 5μm) column, mobile phase 10% IPA: 90% *n*-hexane, flow rate 1.0 mL min⁻¹, oven temperature 25 ᵒC, UV detection at 210 nm)
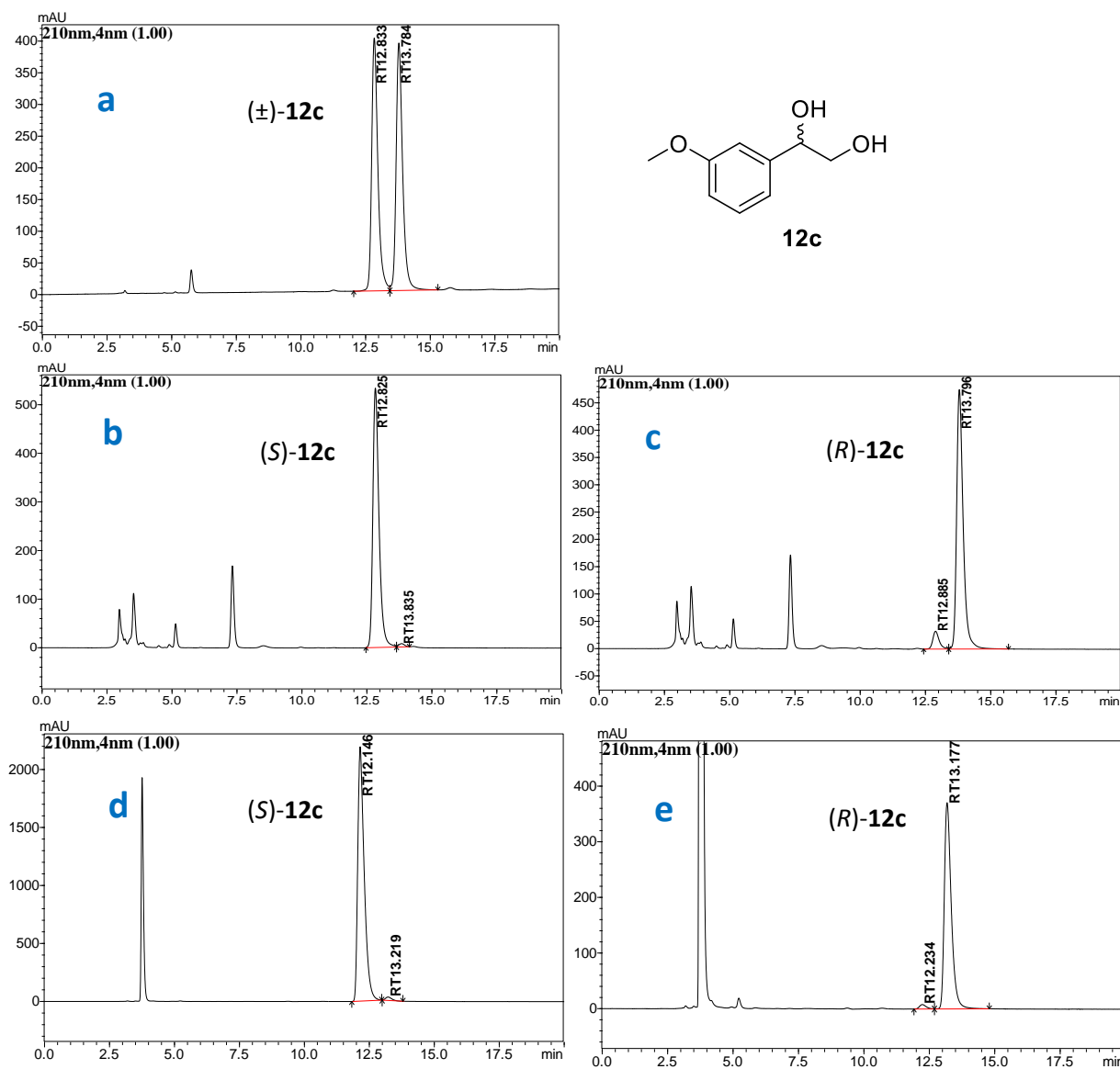
Figure S2.12. Chiral HPLC chromatograms of diol **12c**. a) racemic **12c**; b) (*S*)-**12c** produced by *E. coli* (SSP1); c) (*R*)-**12c** produced by *E. coli* (SST1); d) (*S*)-**12c** produced by AD-mix-α; e) (*R*)-**12c** produced by AD-mix-β. (Daicel Chiralpak IA-3 (250 × 4.6 mm, 3μm) column, mobile phase 10% IPA: 90% *n*-hexane, flow rate 1.0 mL min^{-1}, oven temperature 25 °C, UV detection at 210 nm)
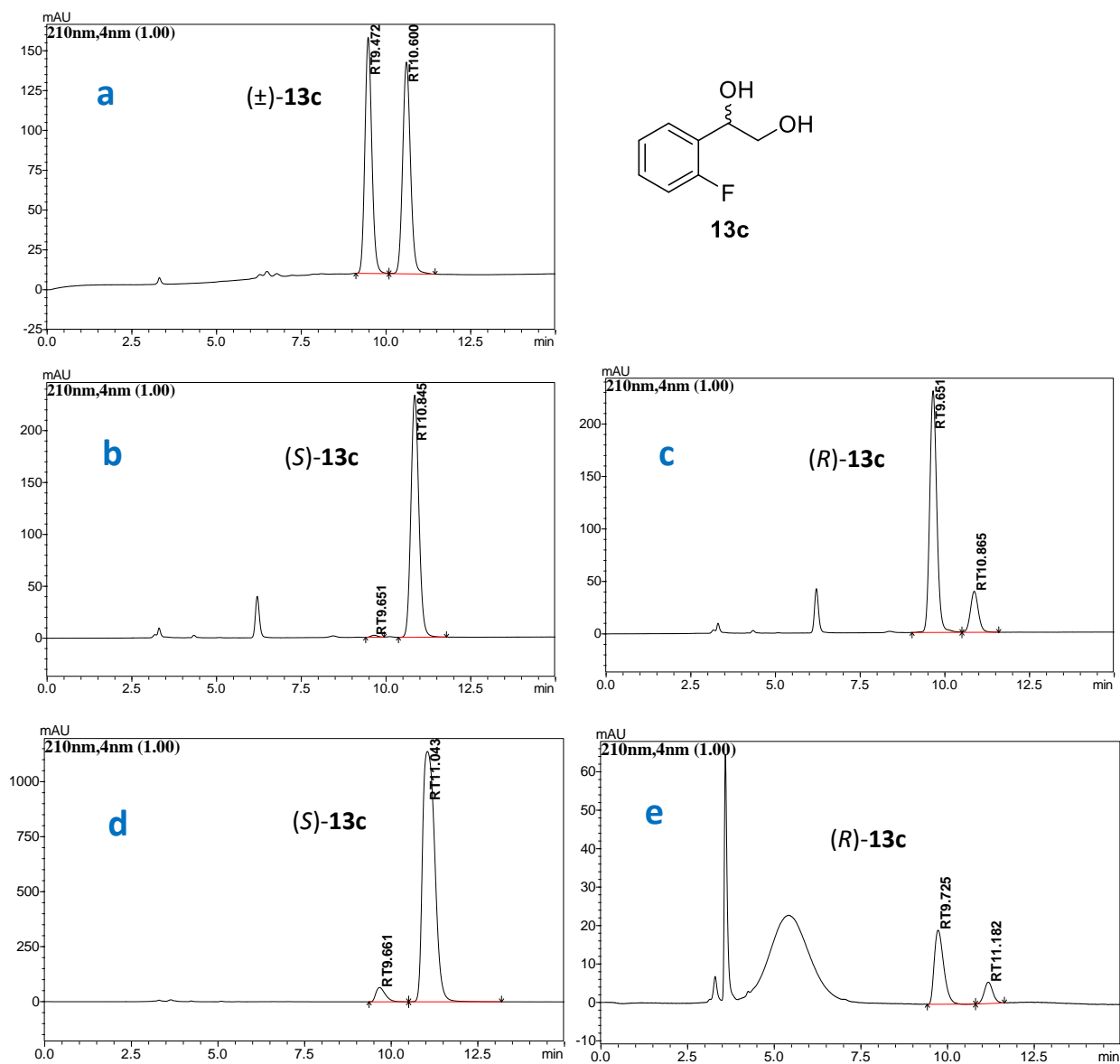
Figure S2.13. Chiral HPLC chromatograms of diol **13c**. a) racemic **13c**; b) (*S*)-**13c** produced by *E. coli* (SSP1); c) (*R*)-**13c** produced by *E. coli* (SST1); d) (*S*)-**13c** produced by AD-mix-α; e) (*R*)-**13c** produced by AD-mix-β. (Daicel Chiralpak AS-H (250 × 4.6 mm, 5µm) column, mobile phase 10% IPA: 90% *n*-hexane, flow rate 1.0 mL min⁻¹, oven temperature 25 °C, UV detection at 210 nm)
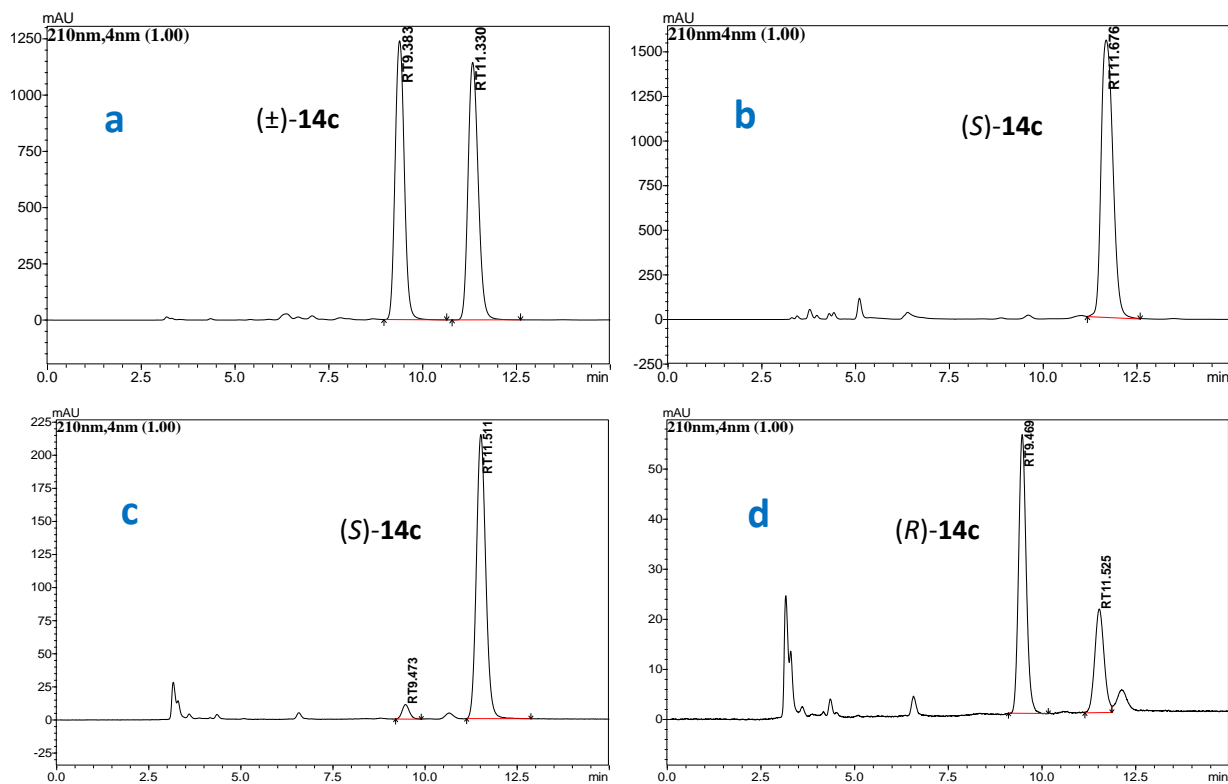
Figure S2.14. Chiral HPLC chromatograms of diol **14c**. a) racemic **14c**; b) (*S*)-**14c** standard; c) (*S*)-**14c** produced by *E. coli* (SSP1); d) (*R*)-**14c** produced by *E. coli* (SST1). (Daicel Chiralpak AS-H (250×4.6 mm, 5μm) column, mobile phase 10% IPA: 90% *n*-hexane, flow rate 1.0 mL min^{-1}, oven temperature 25 °C, UV detection at 210 nm)

Figure S2.15. Chiral HPLC chromatograms of diol **15c**. a) racemic **15c**; b) (*S*)-**15c** produced by *E. coli* (SSP1); c) (*R*)-**15c** produced by *E. coli* (SST1); d) (*S*)-**15c** produced by AD-mix-α; e) (*R*)-**15c** produced by AD-mix-β. (Daicel Chiralpak AS-H (250 × 4.6 mm, 5μm) column, mobile phase 10% IPA: 90% *n*-hexane, flow rate 1.0 mL min⁻¹, oven temperature 25 ºC, UV detection at 210 nm)
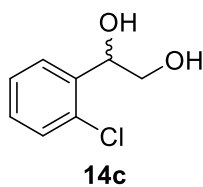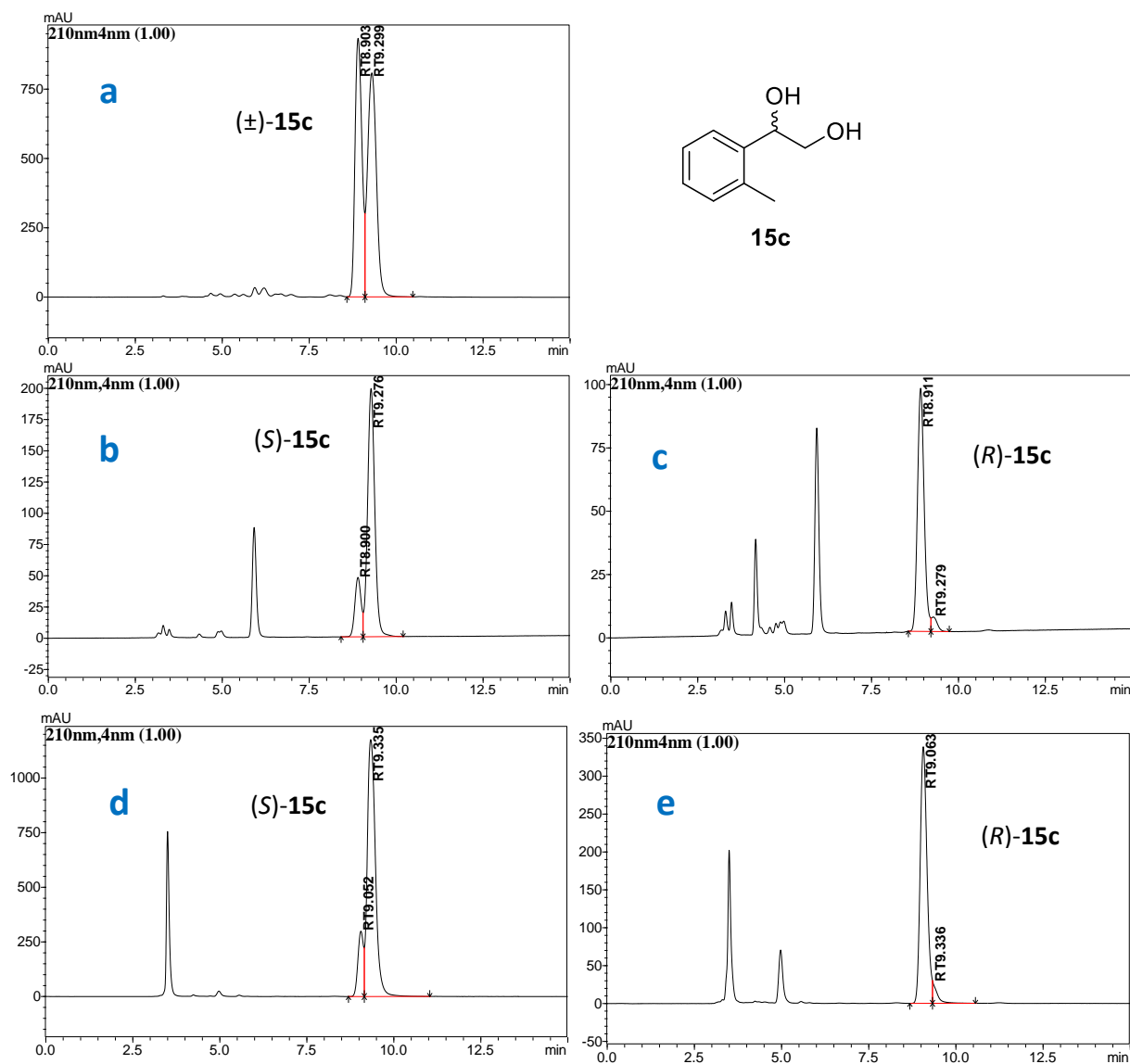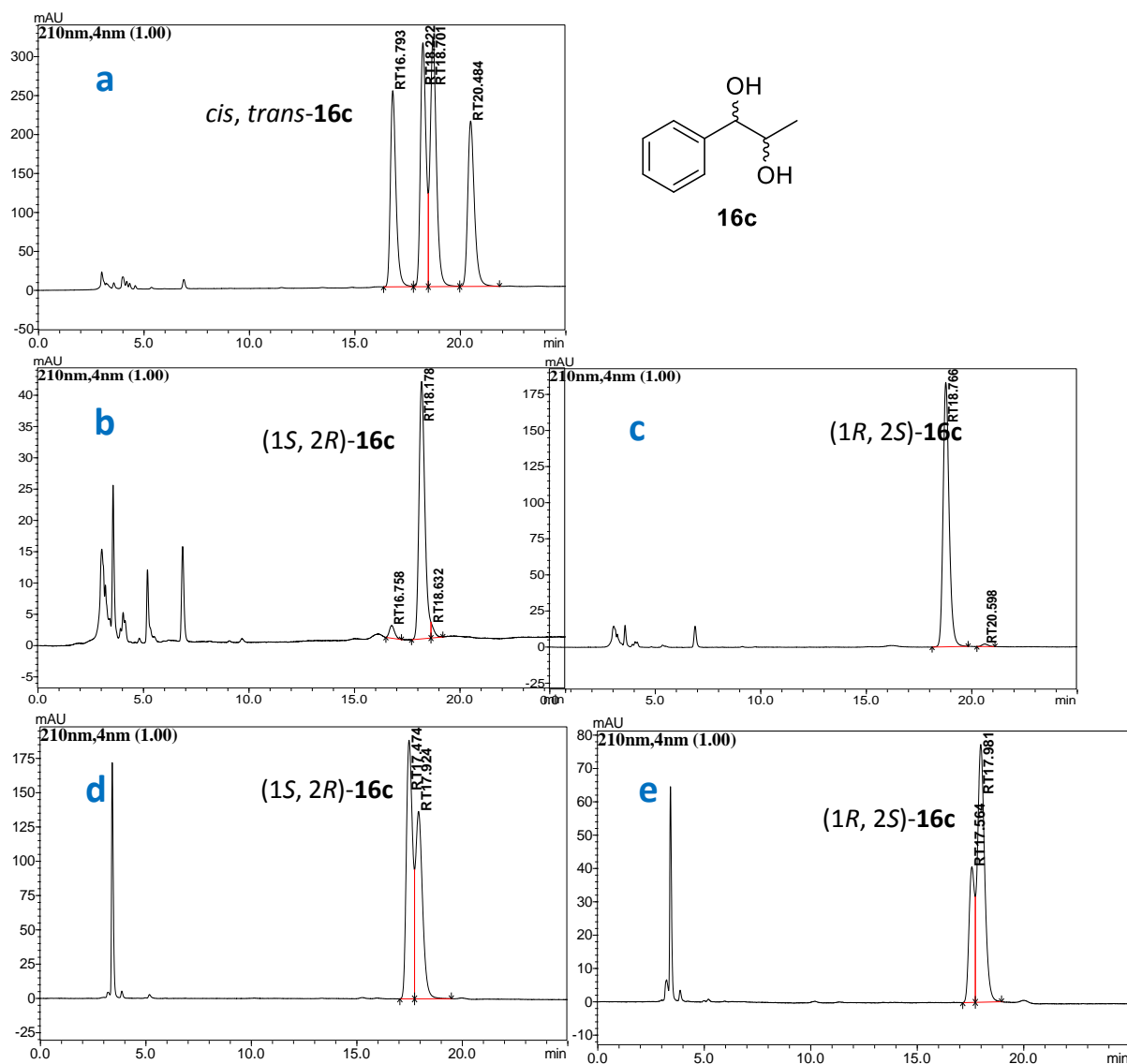
Figure S2.16. Chiral HPLC chromatograms of diol **16c**. a) racemic **16c** (mixture of *trans* and *cis*); b) (1*S*, 2*R*)-**16c** produced by *E. coli* (SSP1) from **16a**; c) (1*R*, 2*S*)-**16c** produced by *E. coli* (SST1) from **16a**; d) (1*S*, 2*R*)-**16c** produced by AD-mix-α from **17a** (low *ee*); e) (1*R*, 2*S*)-**16c** produced by AD-mix-β from **17a** (low *ee*). (Daicel Chiralpak IA-3 (250 × 4.6 mm, 3μm) column, mobile phase 5% IPA: 95% *n*-hexane, flow rate 1.0 mL min⁻¹, oven temperature 25 °C, UV detection at 210 nm)
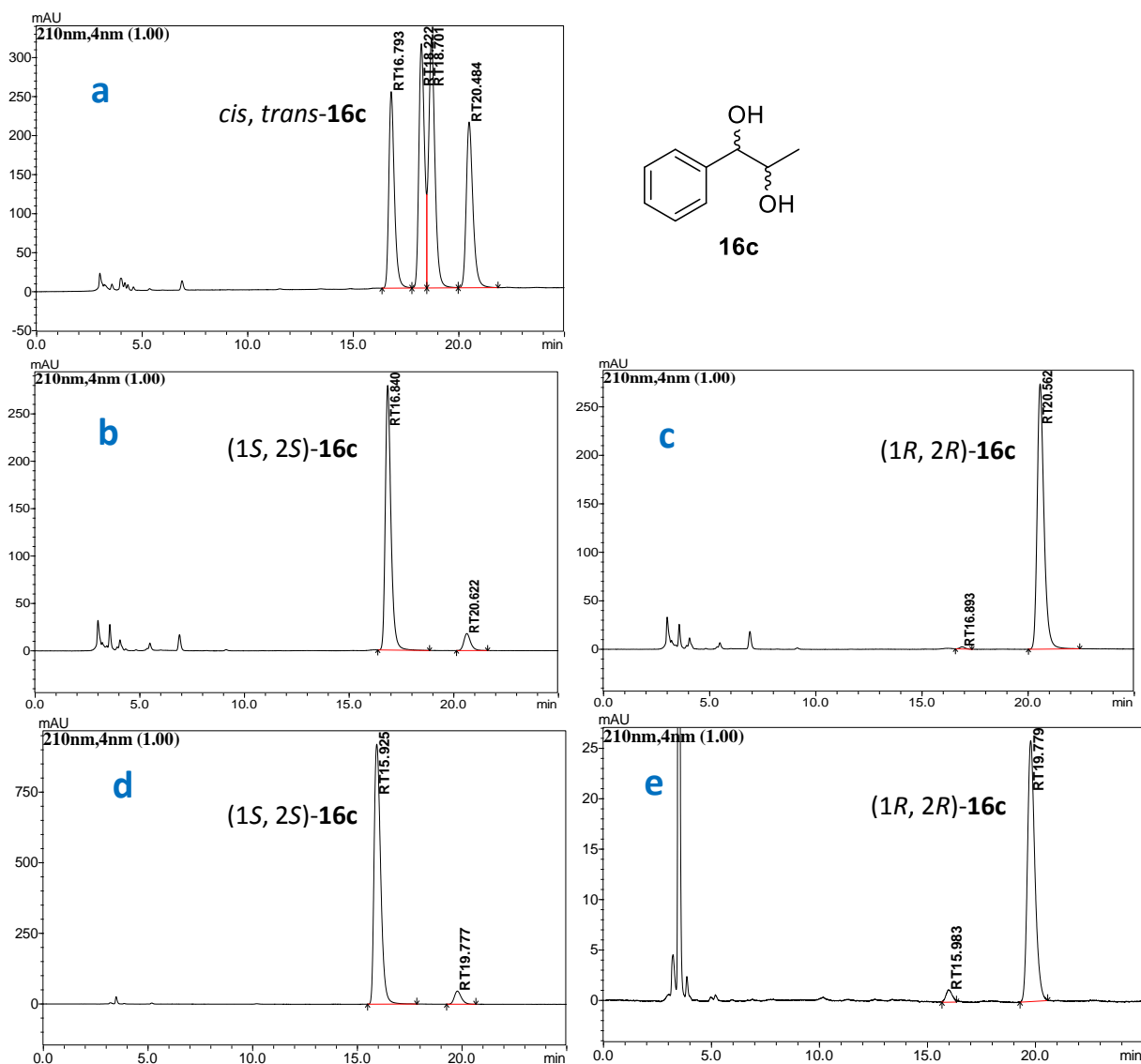
Figure S2.17. Chiral HPLC chromatograms of diol **16c** (continue). a) racemic **16c** (mixture of *trans* and *cis*); b) (1*S*, 2*S*)-**16c** produced by *E. coli* (SSP1) from **17a**; c) (1*R*, 2*R*)-**16c** produced by *E. coli* (SST1) from **17a**; d) (1*S*, 2*S*)-**16c** produced by AD-mix-α from **16a**; e) (1*R*, 2*R*)-**16c** produced by AD-mix-β from **16a**. (Daicel Chiralpak IA-3 (250 × 4.6 mm, 3μm) column, mobile phase 5% IPA: 95% *n*-hexane, flow rate 1.0 mL min^{-1}, oven temperature 25 °C, UV detection at 210 nm)

Figure S2.18. Chiral HPLC chromatograms of diol **18c**. a) racemic **18c** (mixture of *cis* and *trans*); b) *trans*-**18c** strandard; c) (1*R*, 2*R*)-**18c** strandard; d) **18c** (mixture of *cis* and *trans*) produced by styrene monooxygenase and undergo autohydrolysis; e) (1*R*, 2*R*)-**18c** produced by *E. coli* (SSP1); f) (1*R*, 2*R*)-**18c** produced by *E. coli* (SST1). (Daicel Chiralpak OB-H (250 × 4.6 mm, 5µm) column, mobile phase 10% IPA: 90% *n*-hexane, flow rate 0.5 mL min⁻¹, oven temperature 25 ºC, UV detection at 210 nm)

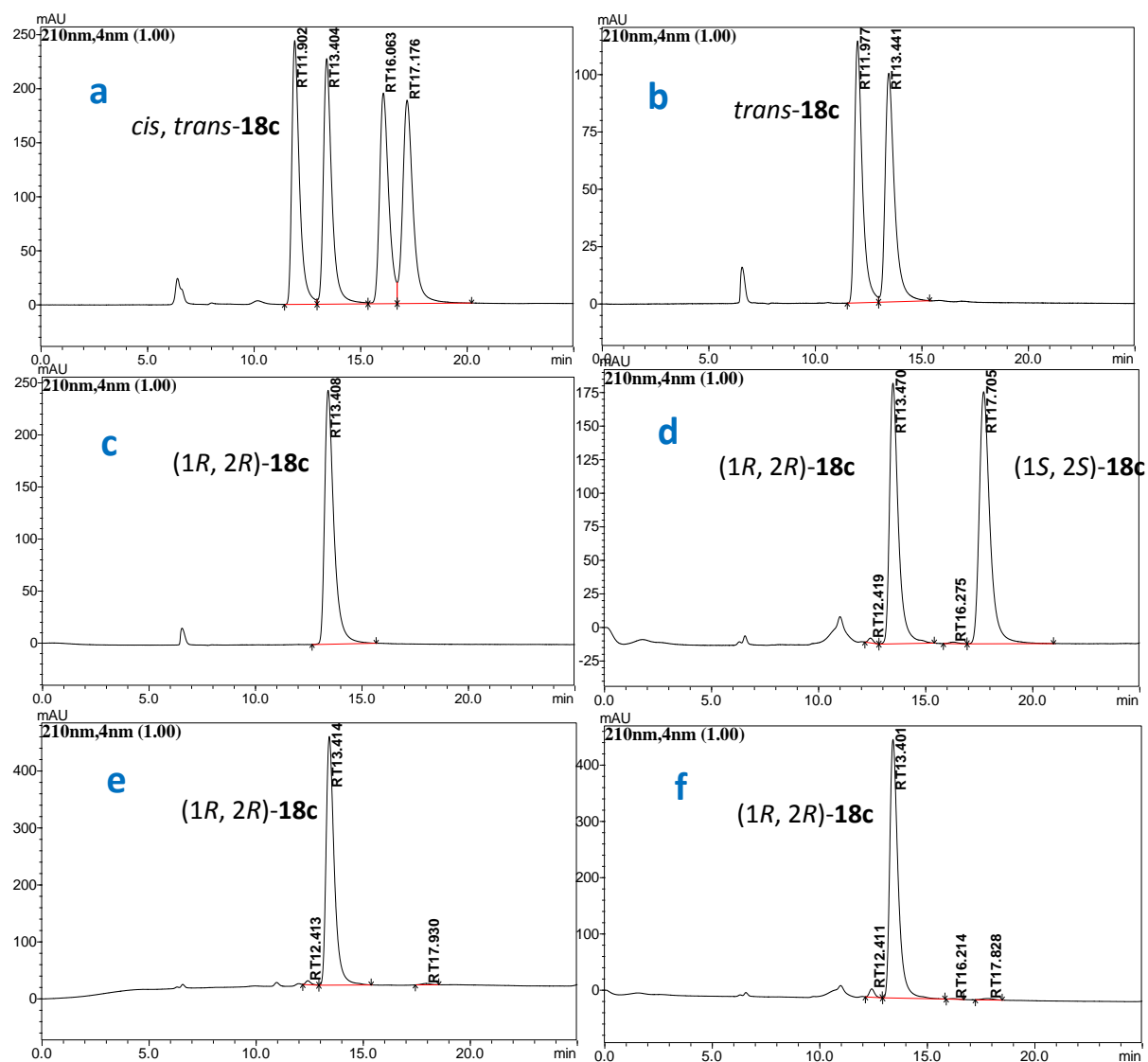**Figure S2.19**. Chiral HPLC chromatograms of diol **19c**. a) racemic **19c** (mainly *trans*, some *cis*); b) (1*R*, 2*R*)-**19c** strandard; c) (1*S*, 2*S*)-**19c** strandard; d) (1*R*, 2*R*)-**19c** produced by *E. coli* (SSP1); e) (1*R*, 2*R*)-**19c** produced by *E. coli* (SST1). (Daicel Chiralpak OB-H (250 × 4.6 mm, 5μm) column, mobile phase 10% IPA: 90% *n*-hexane, flow rate 0.5 mL min^{-1}, oven temperature 25 °C, UV detection at 210 nm)
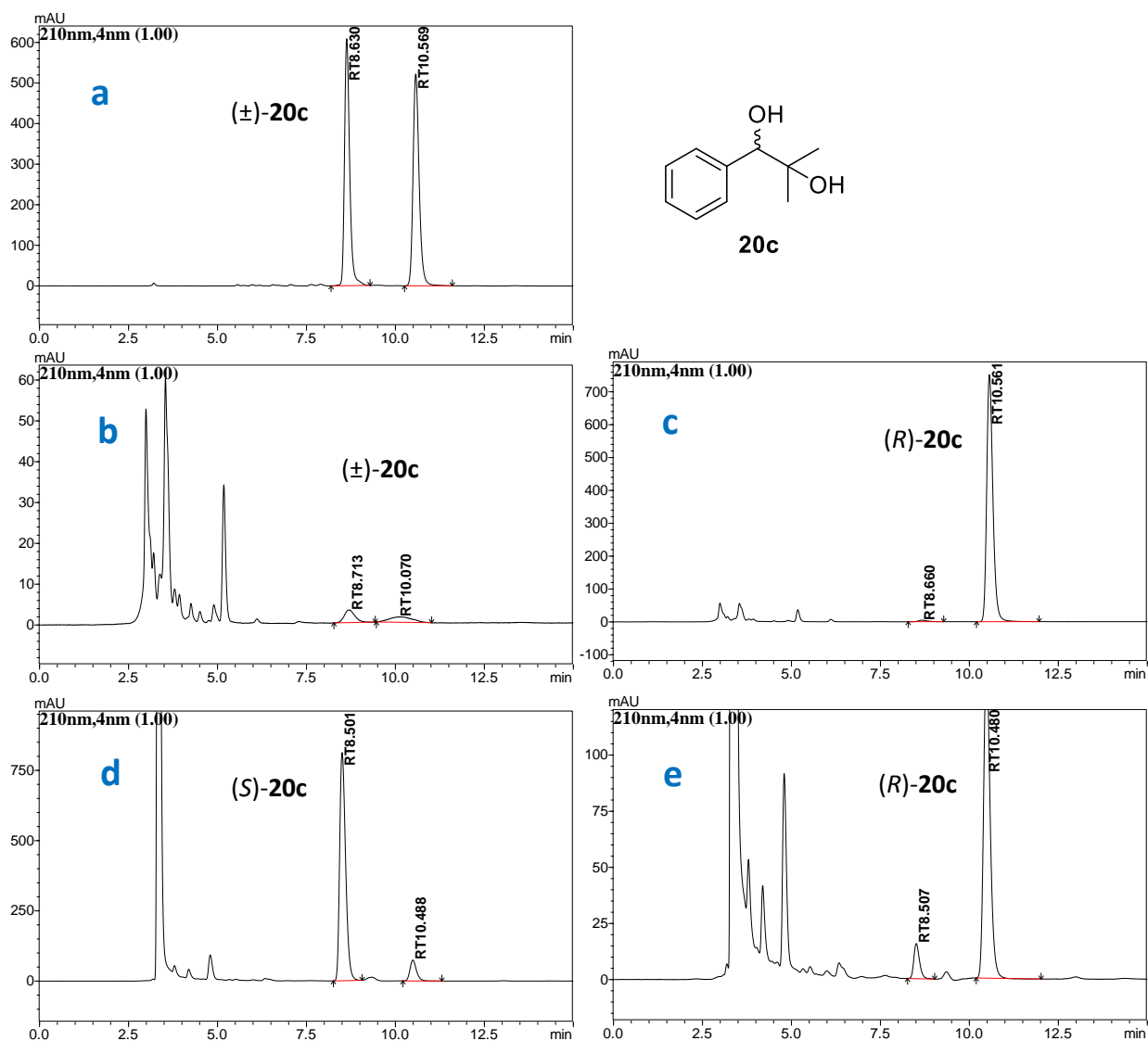
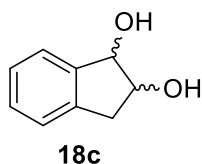**Figure S2.20**. Chiral HPLC chromatograms of diol **20c**. a) racemic **20c**; b) (*S*)-**20c** produced by *E. coli* (SSP1) (low *ee*); c) (*R*)-**20c** produced by *E. coli* (SST1); d) (*S*)-**20c** produced by AD-mix-α; e) (*R*)-**20c** produced by AD-mix-β. (Daicel Chiralpak IA-3 (250 × 4.6 mm, 3μm) column, mobile phase 10% IPA: 90% *n*-hexane, flow rate 1.0 mL min⁻¹, oven temperature 25 ºC, UV detection at 210 nm)
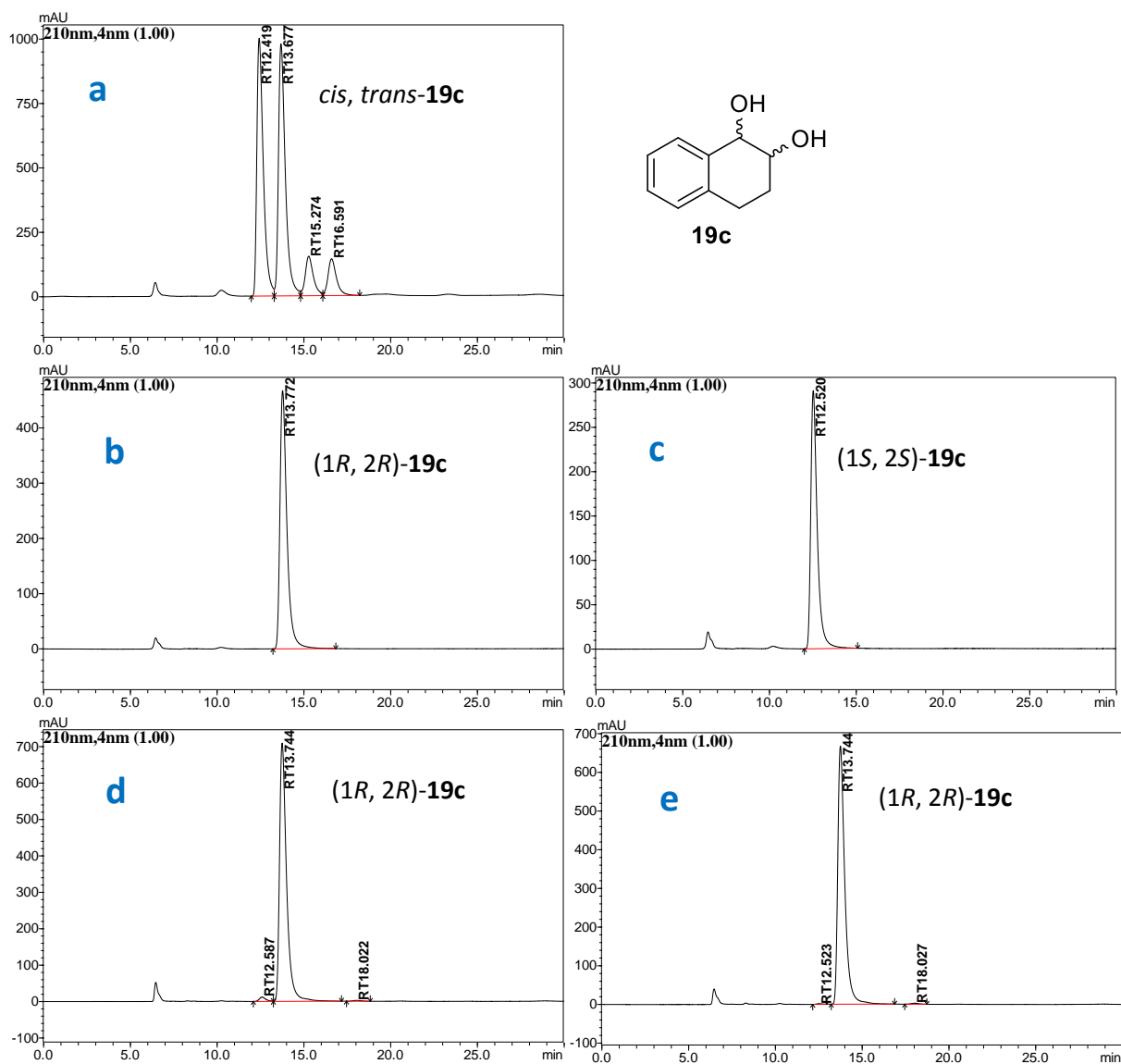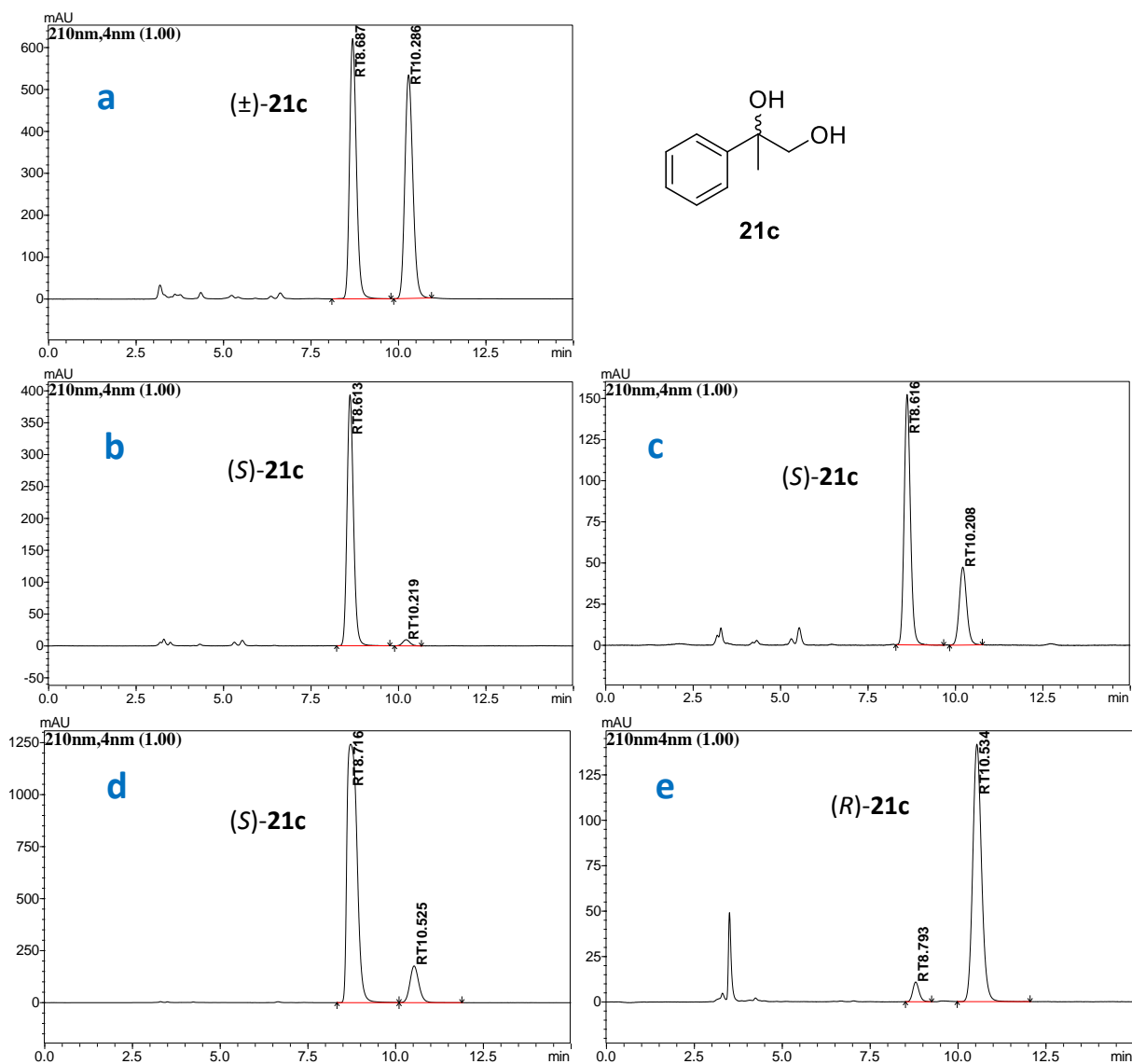
Figure S2.21. Chiral HPLC chromatograms of diol **21c**. a) racemic **21c**; b) (*S*)-**21c** produced by *E. coli* (SSP1); c) (*S*)-**21c** produced by *E. coli* (SST1); d) (*S*)-**21c** produced by AD-mix-α; e) (*R*)-**21c** produced by AD-mix-β. (Daicel Chiralpak AS-H (250 × 4.6 mm, 5μm) column, mobile phase 10% IPA: 90% *n*-hexane, flow rate 1.0 mL min⁻¹, oven temperature 25 ºC, UV detection at 210 nm)
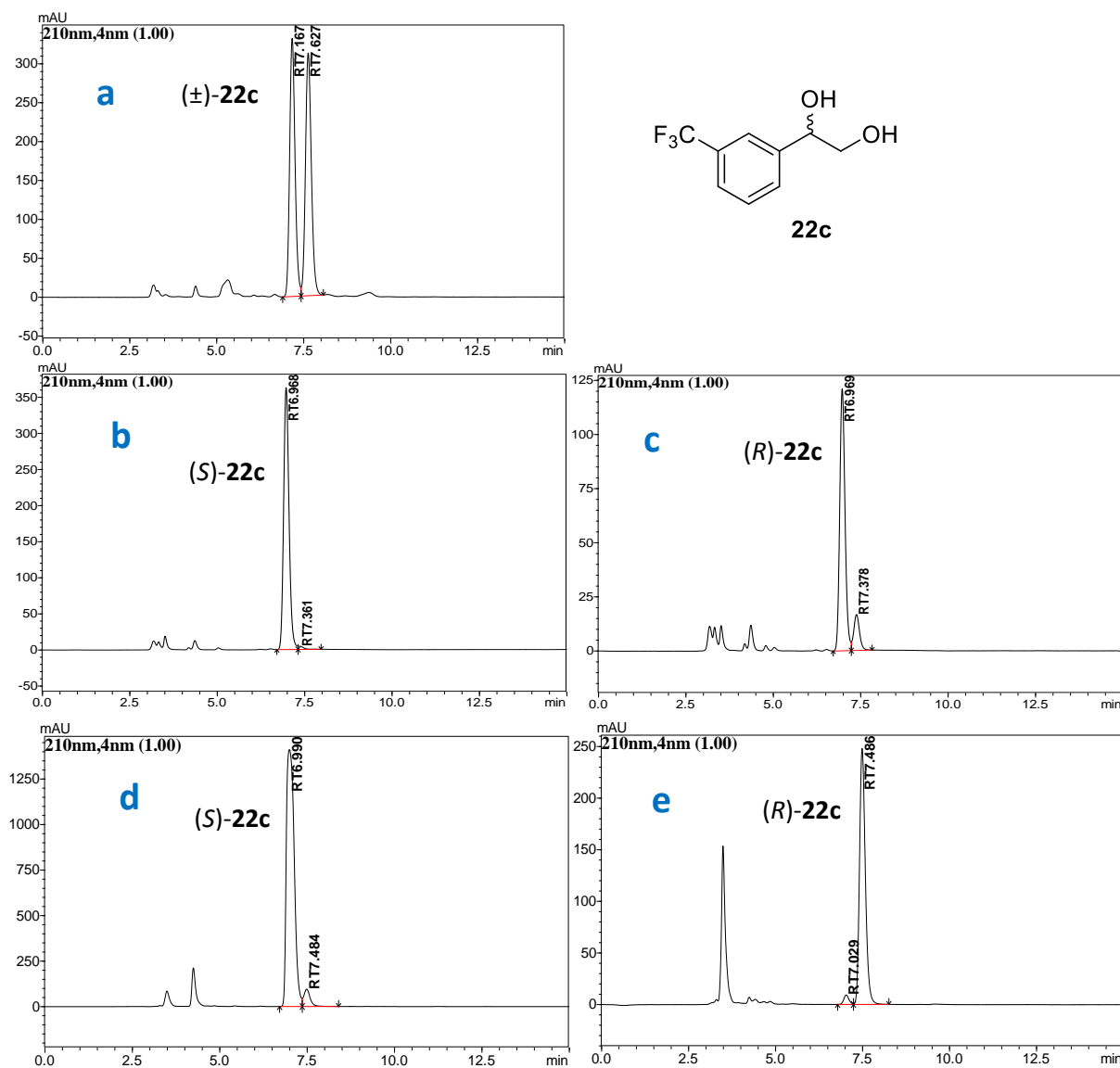
Figure S2.22. Chiral HPLC chromatograms of diol **22c**. a) racemic **22c**; b) (*S*)-**22c** produced by *E. coli* (SSP1); c) (*S*)-**22c** produced by *E. coli* (SST1); d) (*S*)-**22c** produced by AD-mix-α; e) (*R*)-**22c** produced by AD-mix-β. (Daicel Chiralpak AS-H (250 × 4.6 mm, 5µm) column, mobile phase 10% IPA: 90% *n*-hexane, flow rate 1.0 mL min⁻¹, oven temperature 25 ºC, UV detection at 210 nm)

Figure S2.23-S2.32. ¹H NMR Spectra and Chiral HPLC Chromatograms of Prepared Diols

Figure S2.23. ¹H NMR spectrum and Chiral HPLC chromatogram of prepared product (*S*)-**1c**. a) ¹H NMR (400 MHz, CDCl₃, TMS); b) Chiral HPLC (Daicel Chiralpak AS-H (250 × 4.6 mm, 5μm) column, mobile phase 10% IPA: 90% *n*-hexane, flow rate 1.0 mL min⁻¹, oven temperature 25 °C, UV detection at 210 nm).

CHBE Li Zhi 1H AV400 26 Feb 2013
R-D in CDCl3

(R)-**1c**

Current Data Parameters
NAME   Feb26lz
EXPNO   2
PROCNO   1

F2 - Acquisition Parameters
Date_   20130226
Time   10.05
INSTRUM   spect
PROBHD   5 mm PABBO BB-
PULPROG   zg30
TD   65536
SOLVENT   CDCl3
NS   40
DS   0
SWH   8223.685 Hz
FIDRES   0.125483 Hz
AQ   3.9845889 sec
RG   86.87
DW   60.800 usec
DE   6.50 usec
TE   298.7 K
D1   1.00000000 sec
TD0   1

======== CHANNEL f1 ========
SFO1   400.1324710 MHz
NUC1   1H
P1   13.35 usec
PLW1   17.20000076 W

F2 - Processing parameters
SI   65536
SF   400.1300104 MHz
WDW   EM
SSB   0
LB   0.30 Hz
GB   0
PC   4.00
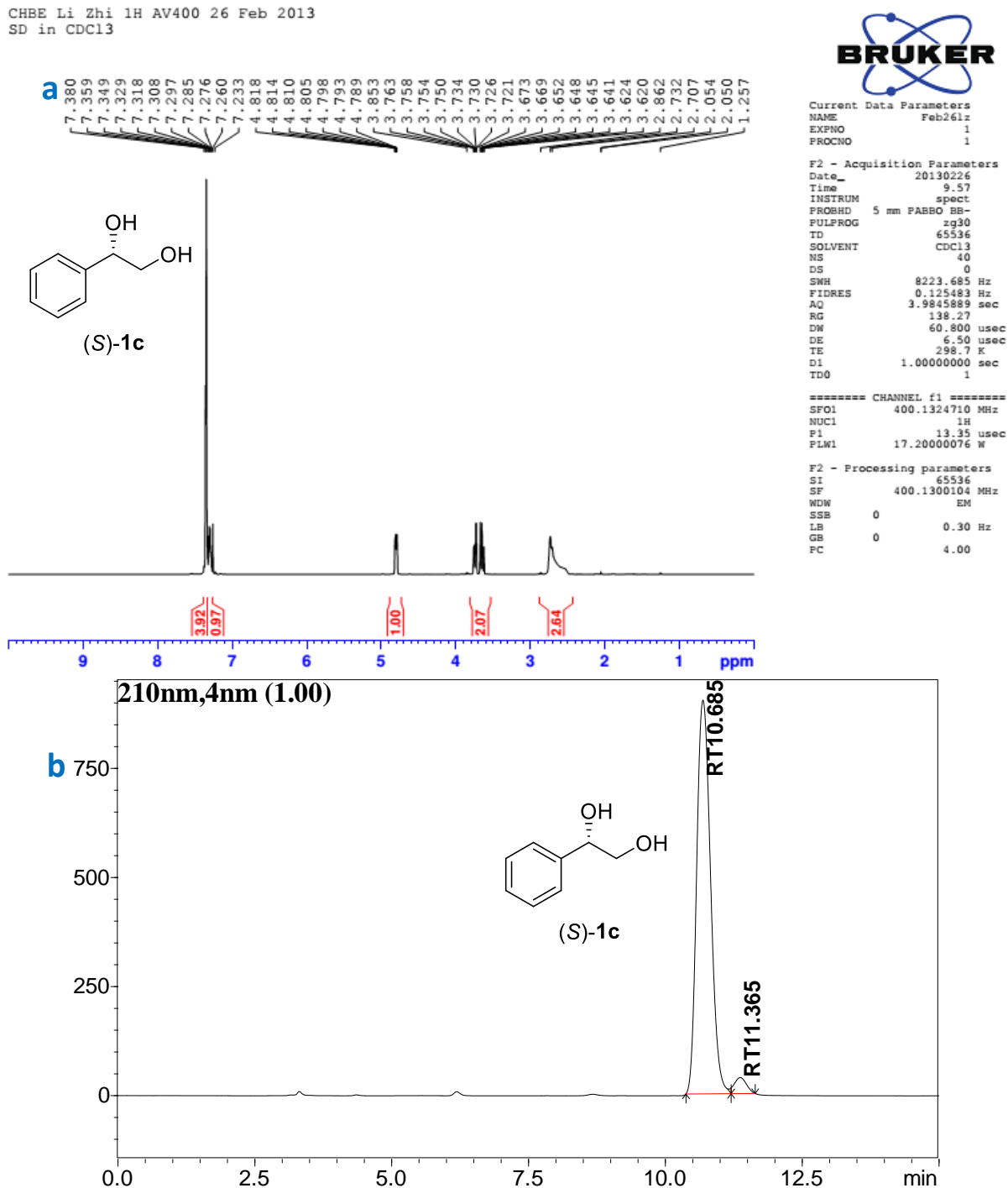
mAU
210nm,4nm (1.00)

(R)-**1c**

Figure S2.24. ^{1}H NMR spectrum and Chiral HPLC chromatogram of prepared product (R)-**1c**. a) [1]H

NMR (400 MHz, CDCl$_3$, TMS); b) Chiral HPLC (Daicel Chiralpak AS-H (250 × 4.6 mm, 5 μm) column,

mobile phase 10% IPA: 90% *n*-hexane, flow rate 1.0 mL min^{-1}, oven temperature 25 °C, UV detection

at 210 nm).

Figure S2.25. ^{1}H NMR spectrum and Chiral HPLC chromatogram of prepared product (*S*)-**2c**. a) [1]H

NMR (400 MHz, CDCl$_3$, TMS); b) Chiral HPLC (Daicel Chiralpak AS-H (250 × 4.6 mm, 5µm) column,

mobile phase 10% IPA: 90% *n*-hexane, flow rate 1.0 mL min^{-1}, oven temperature 25 °C, UV detection
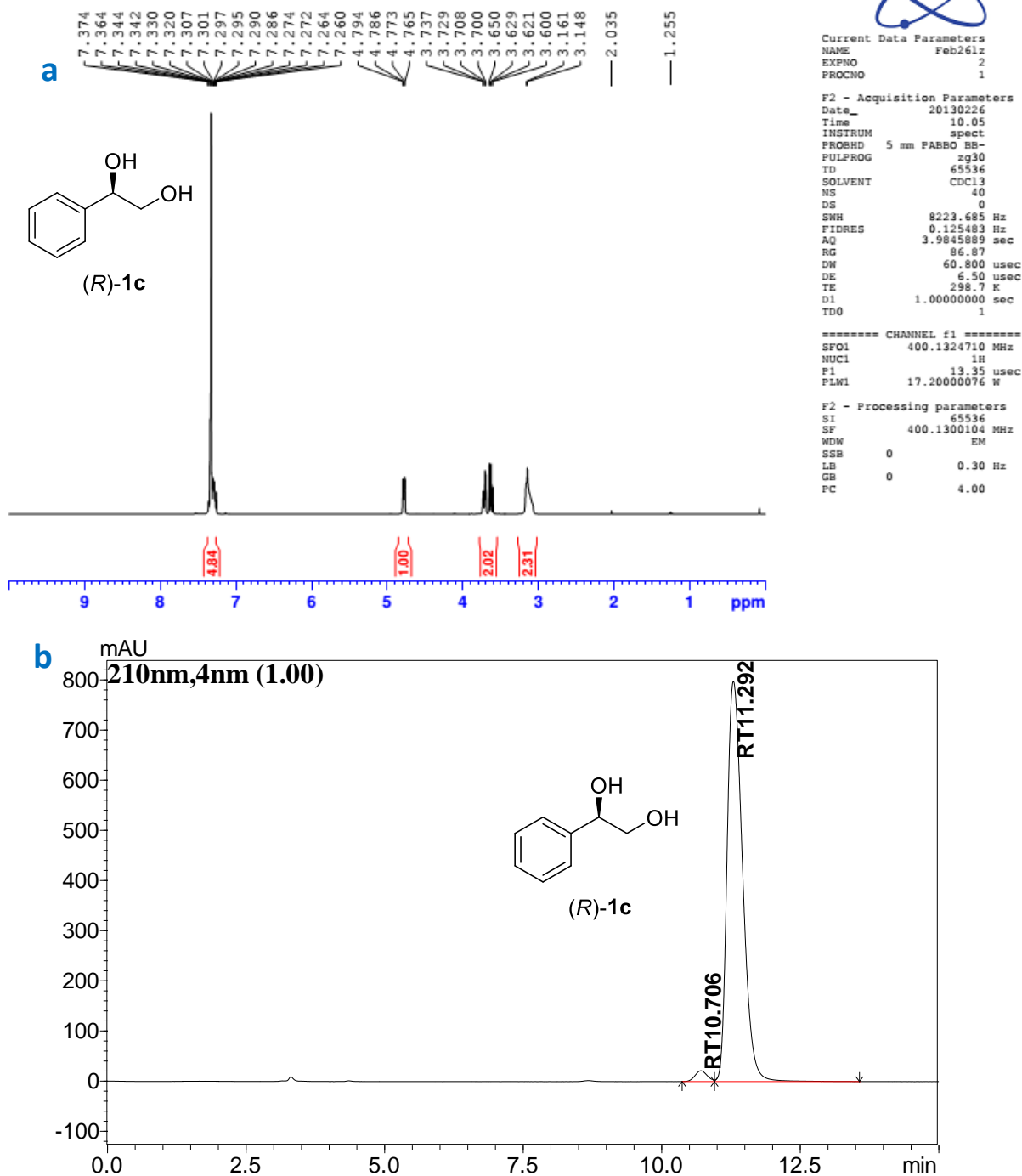
at 210 nm).

Figure S2.26. ^{1}H NMR spectrum and Chiral HPLC chromatogram of prepared product (*R*)-**2c**. a) [1]H

NMR (400 MHz, CDCl₃, TMS); b) Chiral HPLC (Daicel Chiralpak AS-H (250 × 4.6 mm, 5μm) column,

mobile phase 10% IPA: 90% *n*-hexane, flow rate 1.0 mL min⁻¹, oven temperature 25 °C, UV detection
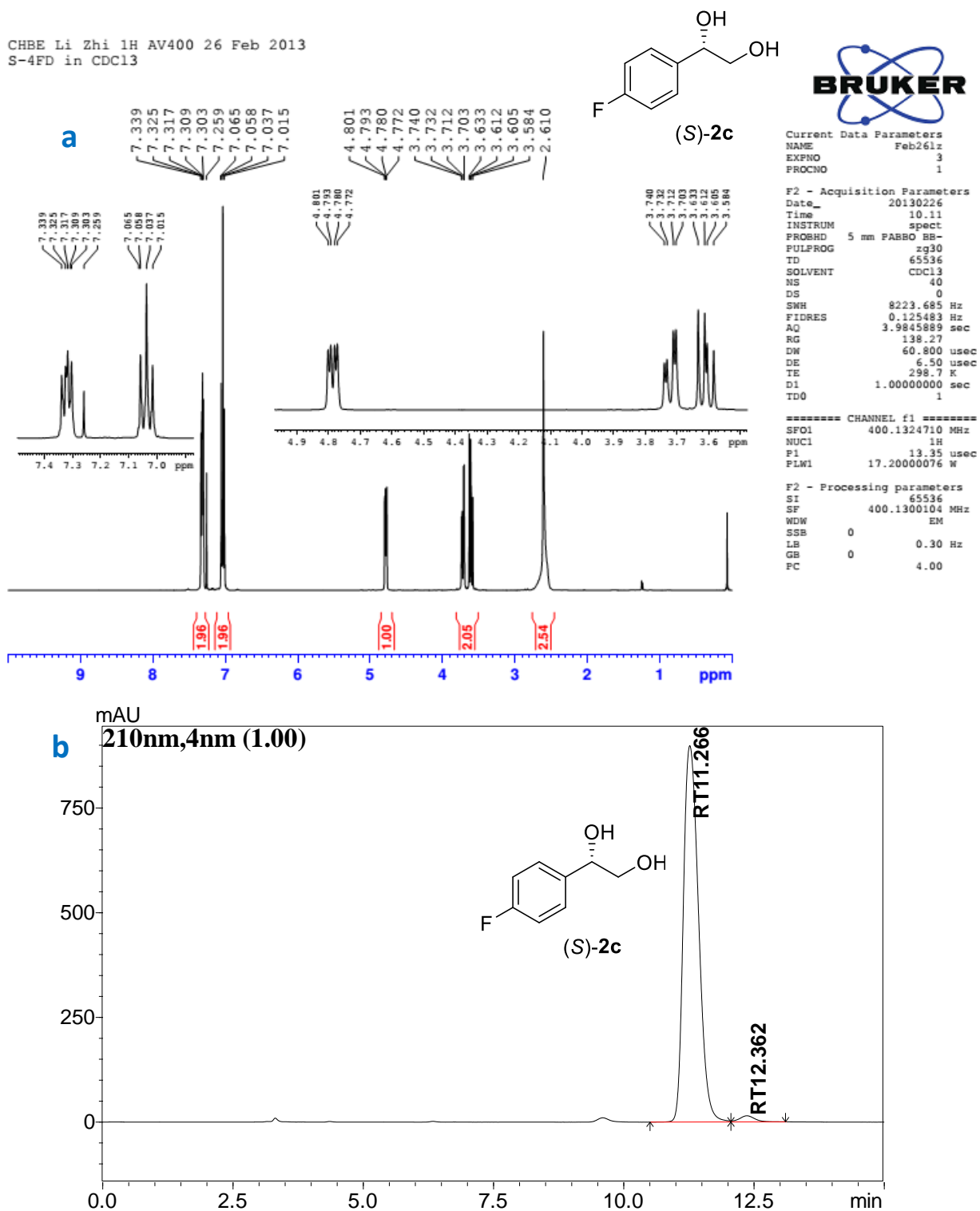
at 210 nm).

Figure S2.27. ^{1}H NMR spectrum and Chiral HPLC chromatogram of prepared product (*S*)-**5c**. a) ^{1}H NMR (400 MHz, CDCl₃, TMS); b) Chiral HPLC (Daicel Chiralpak AS-H (250 × 4.6 mm, 5μm) column, mobile phase 10% IPA: 90% *n*-hexane, flow rate 1.0 mL min⁻¹, oven temperature 25 °C, UV detection at 210 nm).

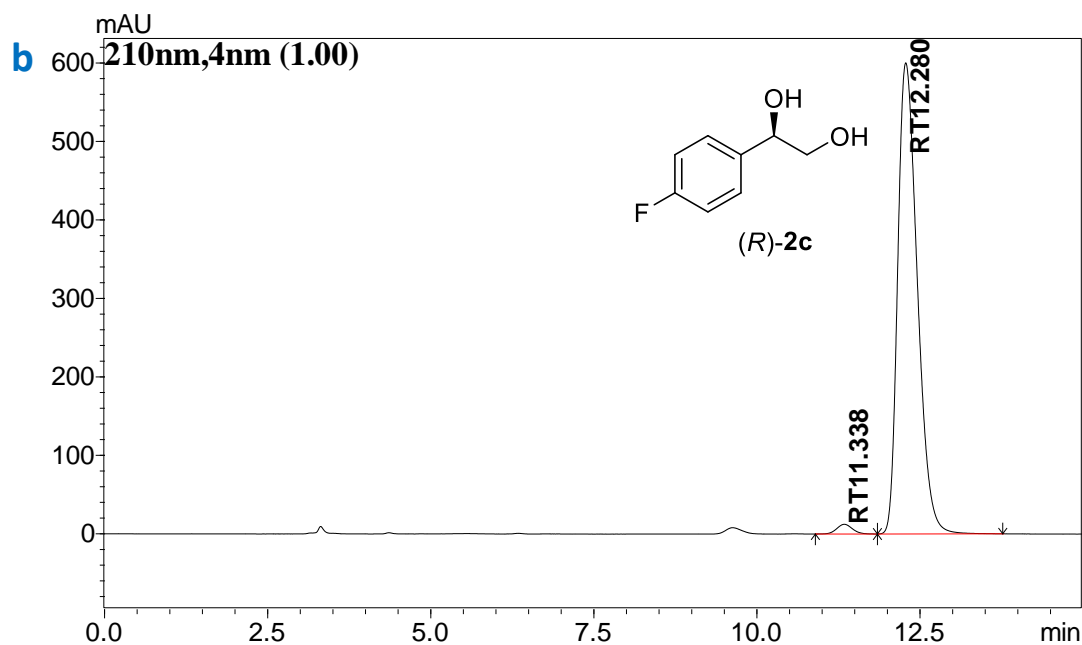**Figure S2.28.** ^{1}H NMR spectrum and Chiral HPLC chromatogram of prepared product (*S*)-**9c**. a) ^{1}H NMR (400 MHz, CDCl$_3$, TMS); b) Chiral HPLC (Daicel Chiralpak AS-H (250 × 4.6 mm, 5 µm) column, mobile phase 10% IPA: 90% *n*-hexane, flow rate 1.0 mL min^{-1}, oven temperature 25 °C, UV detection at 210 nm).
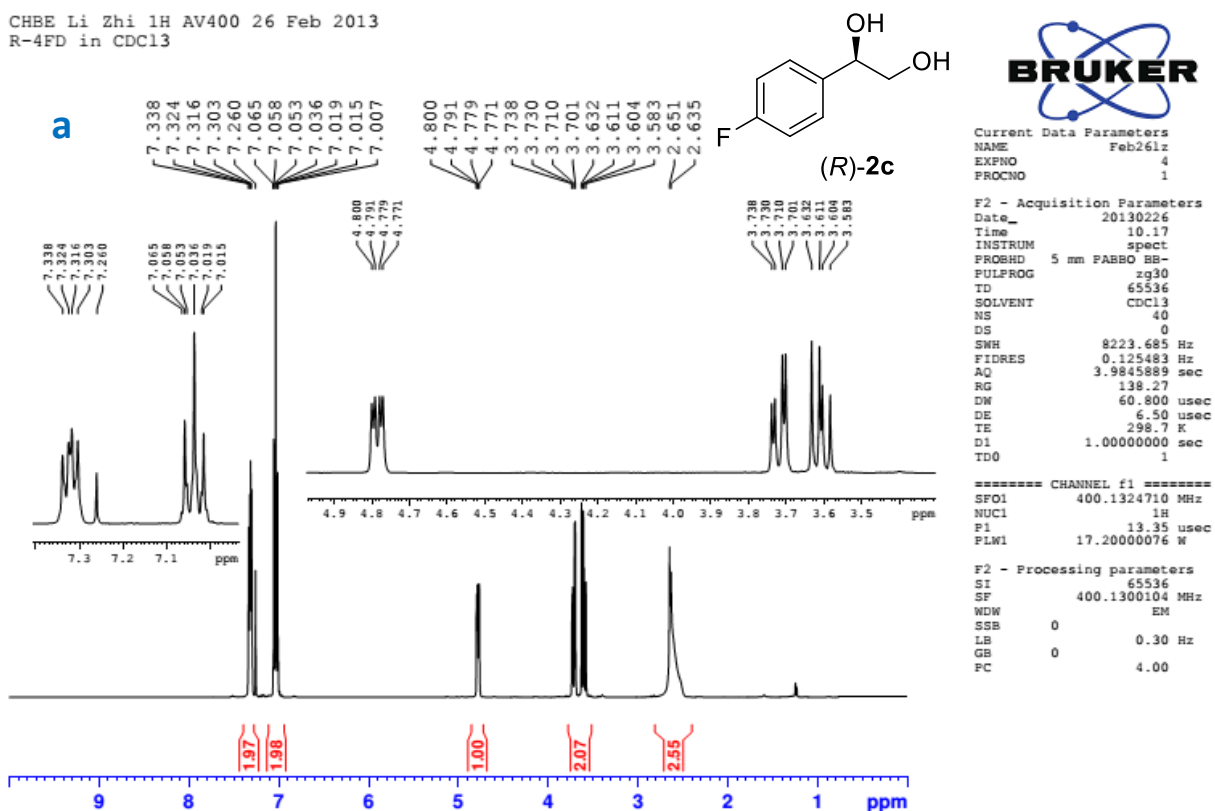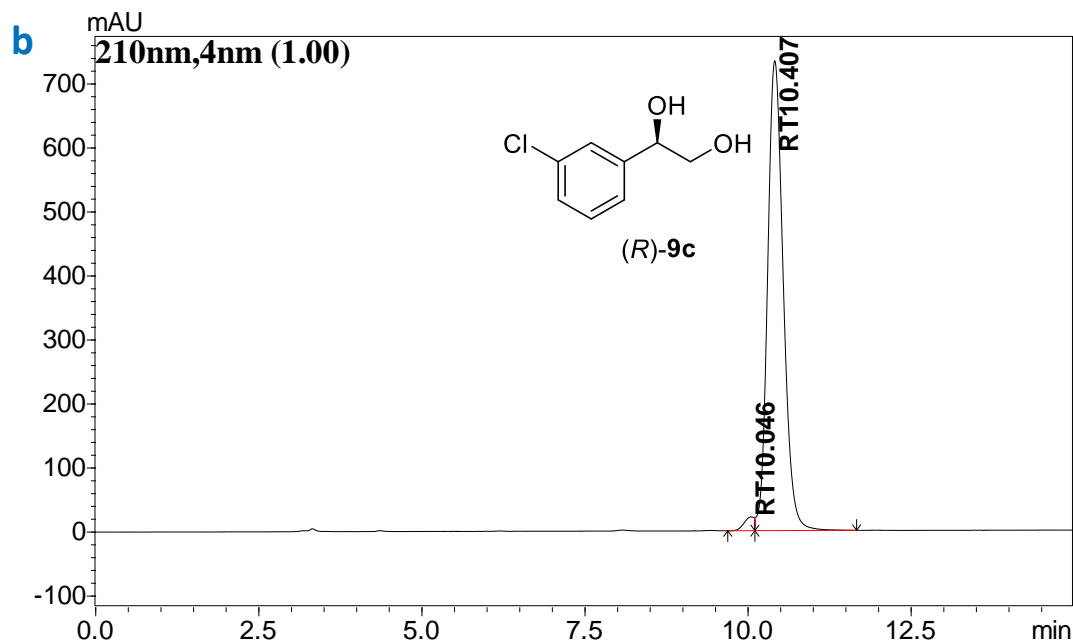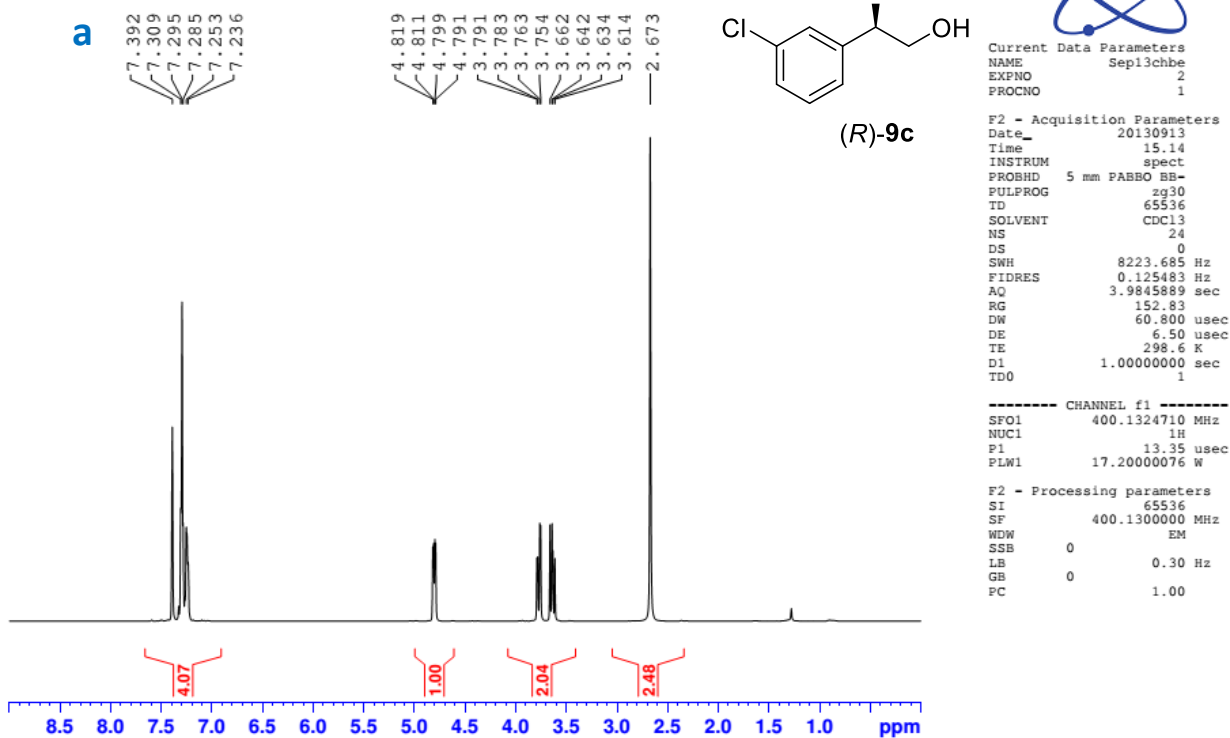
Figure S2.29. ^{1}H NMR spectrum and Chiral HPLC chromatogram of prepared product (*R*)-**9c**. a) [1]H

NMR (400 MHz, CDCl₃, TMS); b) Chiral HPLC (Daicel Chiralpak AS-H (250 × 4.6 mm, 5μm) column,

mobile phase 10% IPA: 90% *n*-hexane, flow rate 1.0 mL min⁻¹, oven temperature 25 °C, UV detection

at 210 nm).

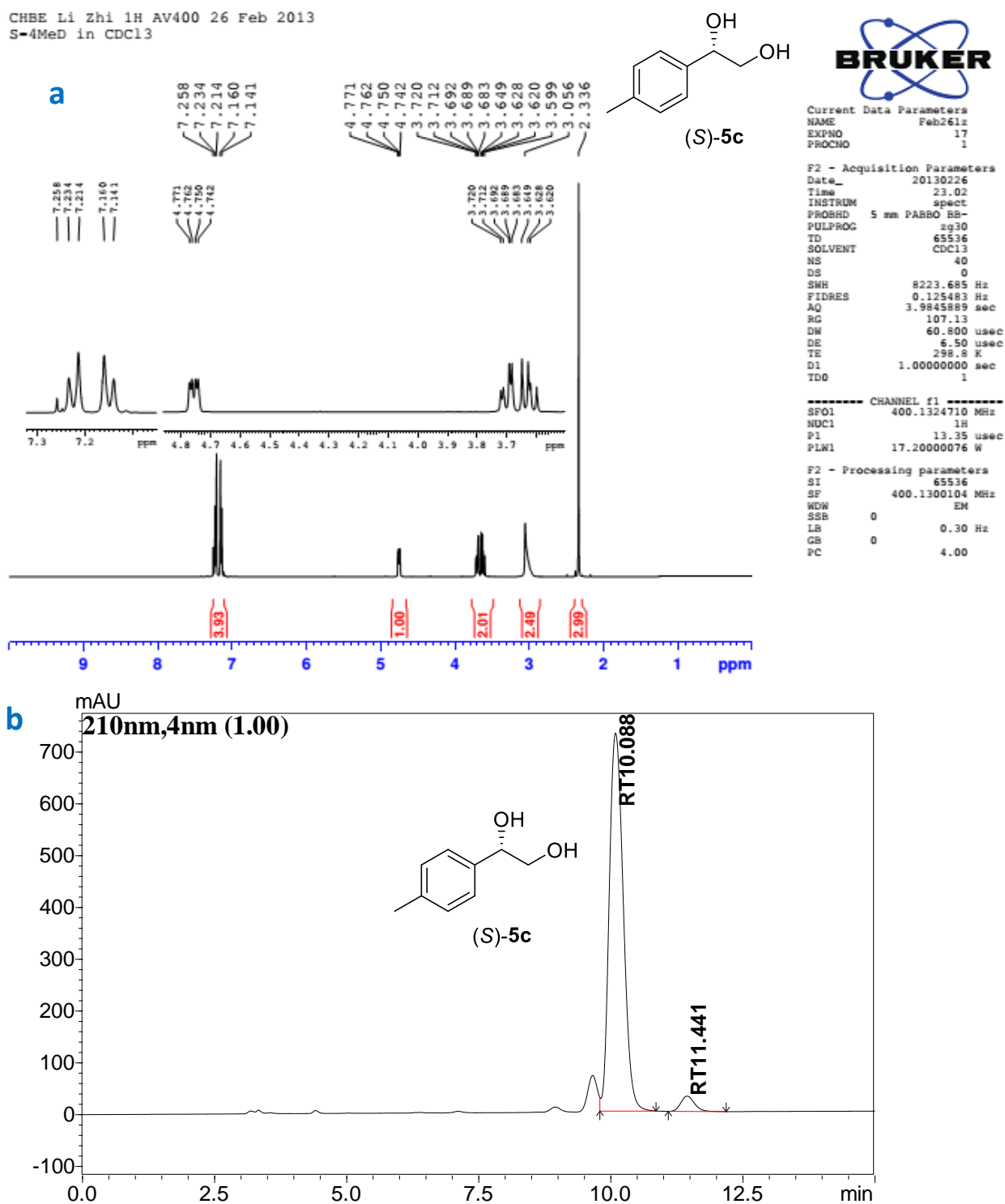**Figure S2.30.** ^{1}H NMR spectrum and Chiral HPLC chromatogram of prepared product (*S*)-**12c**. a) [1]H

NMR (400 MHz, CDCl₃, TMS); b) Chiral HPLC (Daicel Chiralpak IA-3 (250 × 4.6 mm, 3µm) column,

mobile phase 10% IPA: 90% *n*-hexane, flow rate 1.0 mL min⁻¹, oven temperature 25 ℃, UV detection

at 210 nm. thod C).
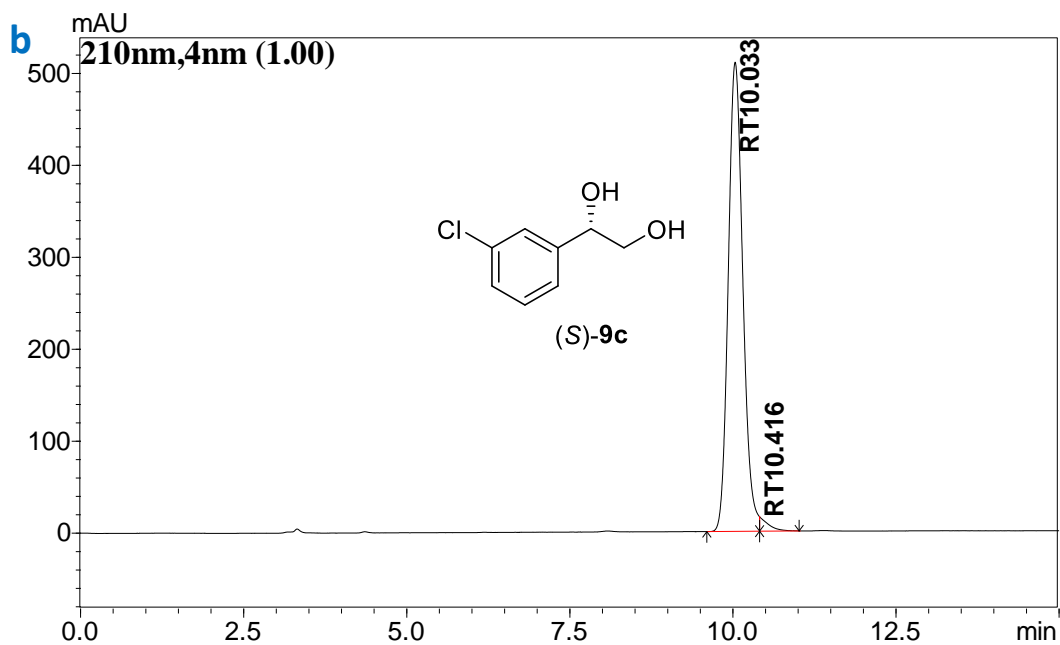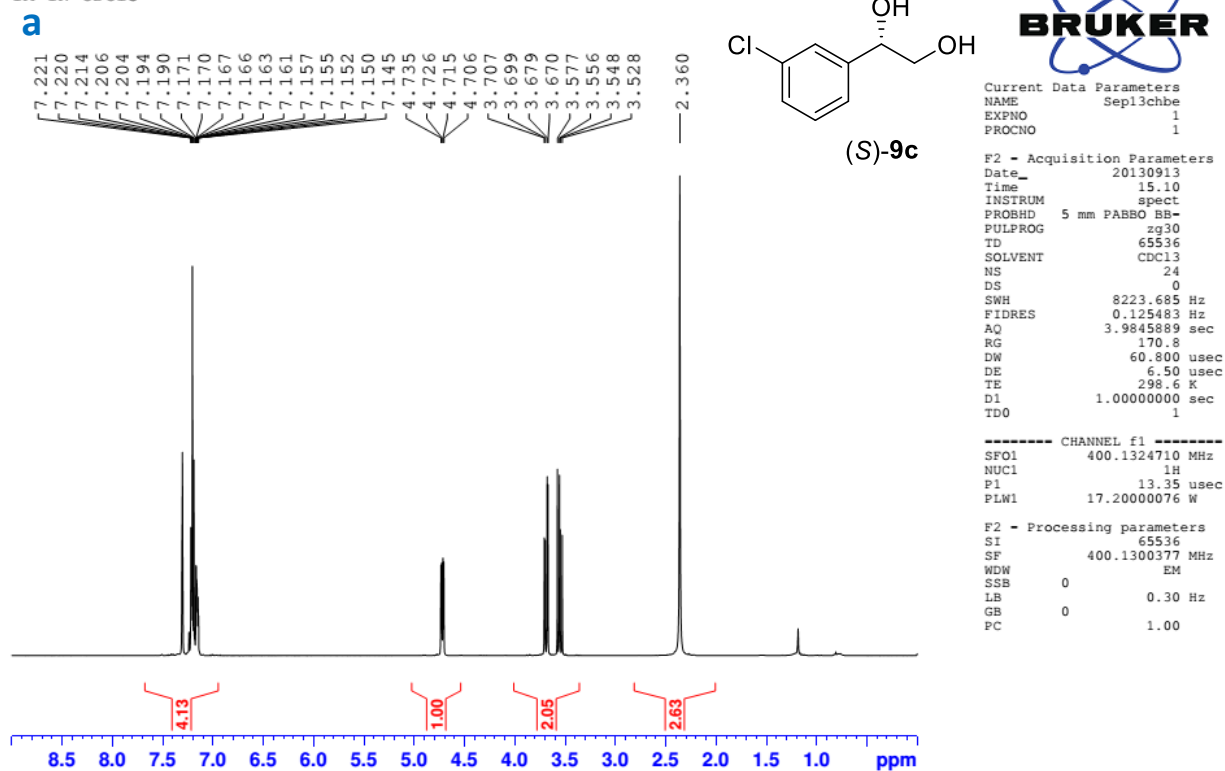
```
CHBE LIZHI 1H AV400
4A IN CDCl3
```

Current Data Parameters
NAME   Sep13chbe
EXPNO   4
PROCNO   1

F2 - Acquisition Parameters
Date_   20130913
Time   18.07
INSTRUM   spect
PROBHD   5 mm PABBO BB-
PULPROG   zg30
TD   65536
SOLVENT   CDCl3
NS   24
DS   0
SWH   8223.685 Hz
FIDRES   0.125483 Hz
AQ   3.9845889 sec
RG   138.27
DW   60.800 usec
DE   6.50 usec
TE   298.7 K
D1   1.00000000 sec
TD0   1

-------- CHANNEL f1 --------
SFO1   400.1324710 MHz
NUC1   1H
P1   13.35 usec
PLW1   17.20000076 W

F2 - Processing parameters
SI   65536
SF   400.1300000 MHz
WDW   EM
SSB   0
LB   0.30 Hz
GB   0
PC   1.00

Figure S2.31. ^{1}H NMR spectrum and Chiral HPLC chromatogram of prepared product (1*R*, 2*S*)-**16c**. a) ^{1}H NMR (400 MHz, CDCl$_3$, TMS); b) Chiral HPLC (Daicel Chiralpak IA-3 (250 × 4.6 mm, 3μm) column, mobile phase 5% IPA: 95% *n*-hexane, flow rate 1.0 mL min^{-1}, oven temperature 25 ºC, UV detection at 210 nm).
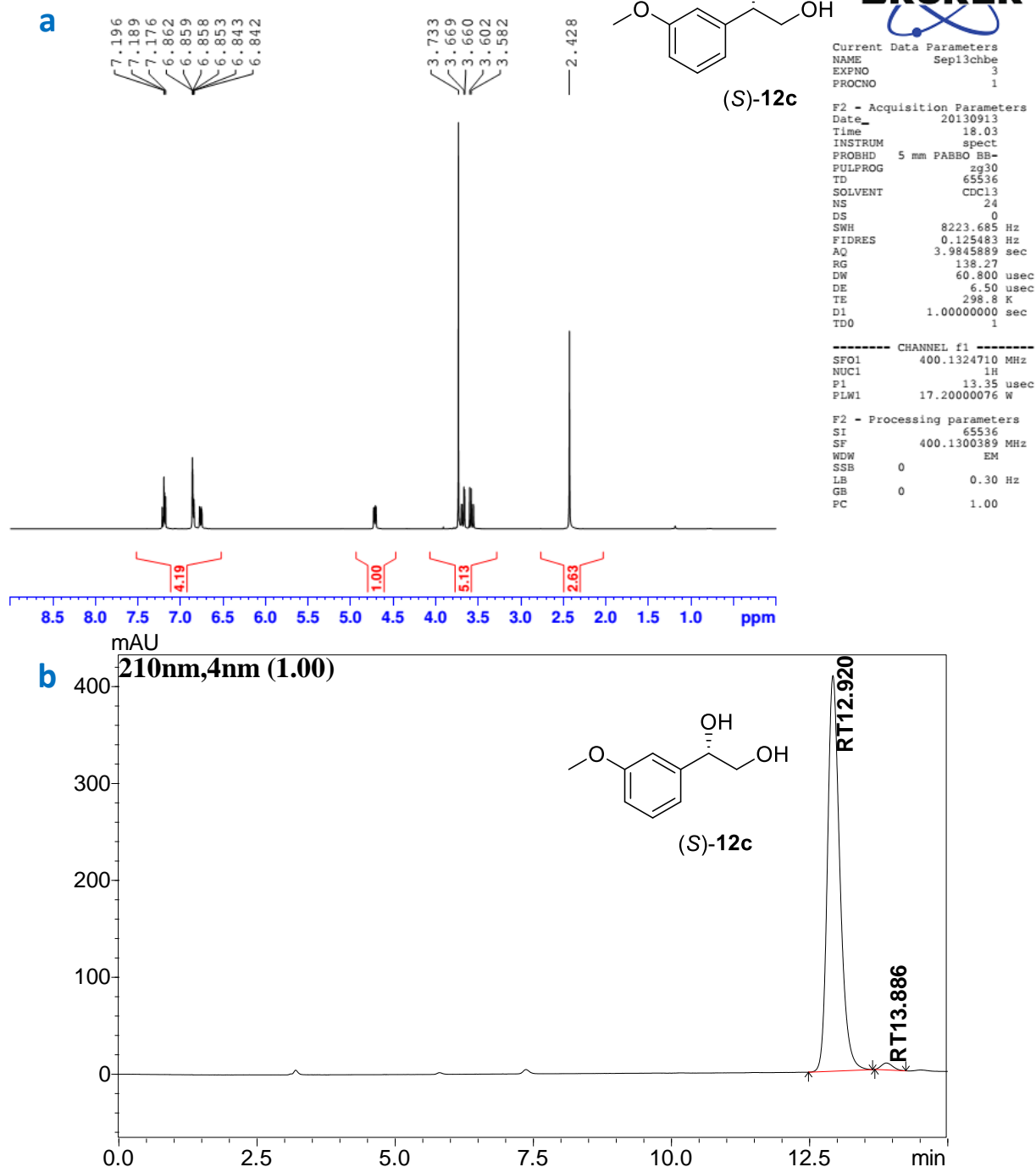
Figure S2.32. ^{1}H NMR spectrum and Chiral HPLC chromatogram of prepared product (1*R*, 2*R*)-**16c**.

a) ^{1}H NMR (400 MHz, CDCl₃, TMS); b) Chiral HPLC (Daicel Chiralpak IA-3 (250 × 4.6 mm, 3μm)

column, mobile phase 5% IPA: 95% *n*-hexane, flow rate 1.0 mL min⁻¹, oven temperature 25 ℃, UV
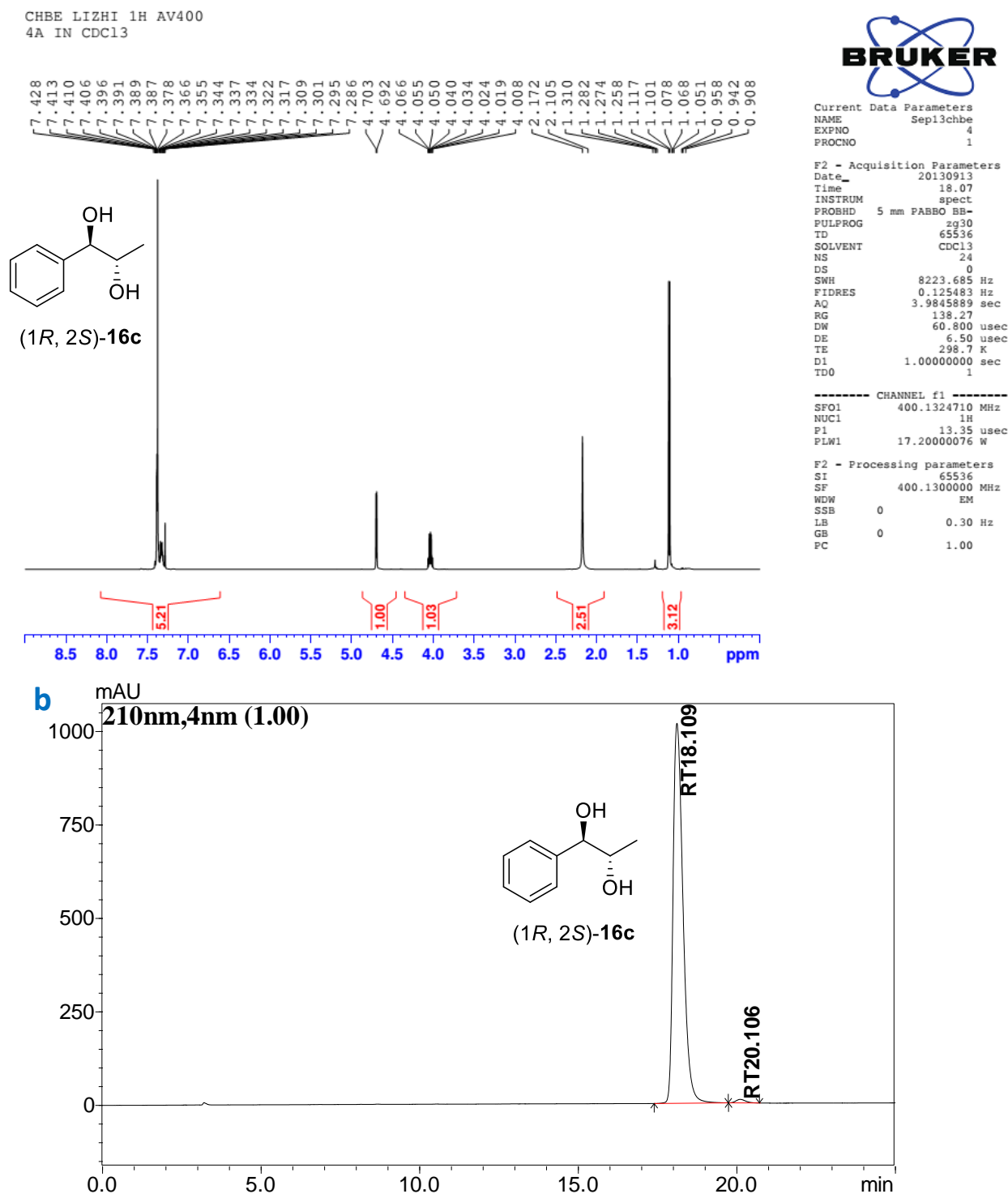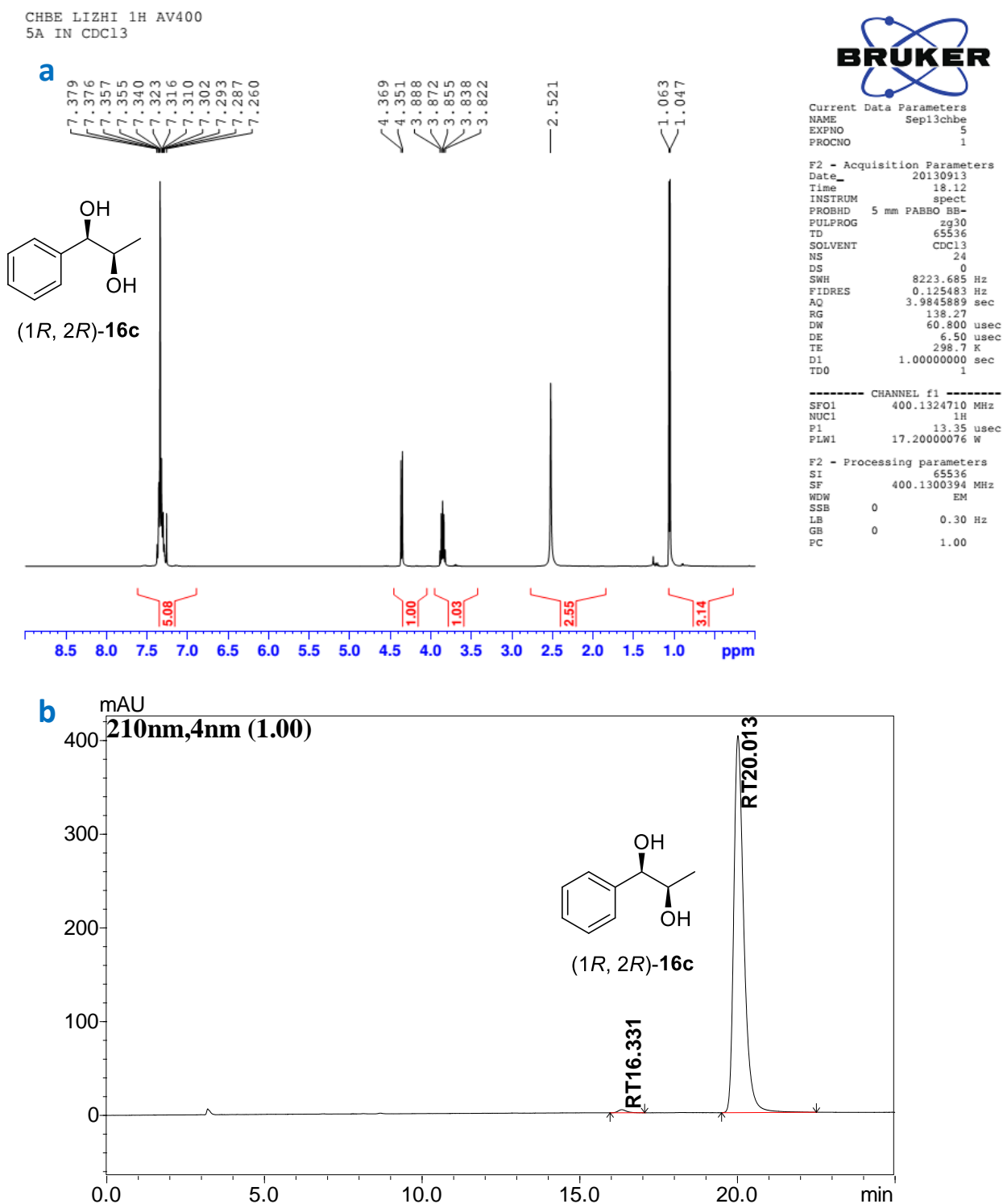
detection at 210 nm).

Appendix III: Supporting Information for Chapter 5

>DNA Sequence of Synthesized CvωTA (codon optimized for *E. coli*)

ATGCAAAAACAACGCACCACCTCACAATGGCGCGAACTGGATGCCGCACACCACCTGCA
CCCGTTTACCGACACCGCAAGCCTGAATCAGGCCGGCGCCCGTGTTATGACCCGCGGCG
AAGGTGTGTATCTGTGGGATTCTGAGGGTAACAAAATTATCGACGGCATGGCTGGTCTGT
GGTGCGTTAATGTCGGCTATGGTCGTAAAGATTTTGCCGAAGCGGCCCGTCGCCAAATGG
AAGAACTGCCGTTCTACAACACCTTTTTCAAAACCACGCATCCGGCGGTGGTTGAACTGA
GCAGCCTGCTGGCGGAAGTTACGCCGGCCGGCTTTGATCGTGTGTTCTATACCAATTCAG
GTTCGGAAAGCGTGGATACGATGATCCGCATGGTTCGTCGCTACTGGGACGTCCAGGGC
AAACCGGAAAAGAAACCCTGATCGGTCGTTGGAACGGCTATCATGGTTCTACGATTGG
CGGTGCAAGTCTGGGCGGTATGAAATACATGCACGAACAGGGCGATCTGCCGATTCCGG
GTATGGCGCATATCGAACAACCGTGGTGGTACAAACACGGCAAGATATGACCCCGGAC
GAATTTGGTGTCGTGGCAGCTCGCTGGCTGGAAGAAAAAATTCTGGAAATCGGCGCCGA
TAAAGTGGCGGCCTTTGTTGGCGAACCGATTCAGGGTGCGGGCGGTGTGATTGTTCCGCC
GGCCACCTATTGGCCGGAAATTGAACGTATCTGCCGCAAATACGATGTTCTGCTGGTCGC
AGACGAAGTTATTTGTGGCTTTGGTCGTACCGGCGAATGGTTCGGTCATCAGCACTTTGG
CTTCCAACCGGACCTGTTTACGGCAGCTAAAGGCCTGAGTTCCGGTTATCTGCCGATCGG
CGCCGTCTTCGTGGGTAAACGCGTTGCAGAAGGTCTGATTGCTGGCGGTGATTTTAATCA
TGGCTTCACCTATAGCGGTCACCCGGTCTGTGCGGCCGTGGCACATGCTAATGTGGCAGC
TCTGCGTGACGAAGGCATCGTGCAGCGCGTTAAAGATGACATTGGTCCGTATATGCAAA
AACGTTGGCGCGAAACGTTTAGCCGTTTCGAACACGTCGATGACGTGCGCGGCGTTGGTA
TGGTCCAGGCATTTACCCTGGTGAAAAATAAAGCTAAACGCGAACTGTTTCCGGATTTCG
GCGAAATTGGTACGCTGTGCCGTGACATCTTTTTCCGCAACAATCTGATTATGCGTGCGT
GTGGTGATCACATTGTTAGCGCCCCGCCGCTGGTTATGACCCGCGCAGAAGTCGACGAA
ATGCTGGCCGTGGCGGAACGCTGCCTGGAAGAATTTGAACAGACCCTGAAAGCTCGTGG
CCTGGCGTAA

>Protein Sequence of Synthesized CvωTA

MQKQRTTSQWRELDAAHHLHPFTDTASLNQAGARVMTRGEGVYLWDSEGNKIIDGMAGL
WCVNVGYGRKDFAEAARRQMEELPFYNTFFKTTHPAVVELSSLLAEVTPAGFDRVFYTNSG
SESVDTMIRMVRRYWDVQGKPEKKTLIGRWNGYHGSTIGGASLGGMKYMHEQGDLPIPGM
AHIEQPWWYKHGKDMTPDEFGVVAARWLEEKILEIGADKVAAFVGEPIQGAGGVIVPPATY
WPEIERICRKYDVLLVADEVICGFGRTGEWFGHQHFGFQPDLFTAAKGLSSGYLPIGAVFVG
KRVAEGLIAGGDFNHGFTYSGHPVCAAVAHANVAALRDEGIVQRVKDDIGPYMQKRWRET
FSRFEHVDDVRGVGMVQAFTLVKNKAKRELFPDFGEIGTLCRDIFFRNNLIMRACGDHIVSAP
PLVMTRAEVDEMLAVAERCLEEFEQTLKARGLA

246

>DNA Sequence of Synthesized HMO (codon optimized for *E. coli*)

ATGCGTGAACCGCTGACGCTGGATGATTTCGCTCGCCTGGCCCGTGGTCAACTGCCGGCA
GCAACCTGGGATTTTATCGCGGGTGGCGCAGGTCGTGAACGTACCCTGGCAGCAAACGA
AGCTGTGTTTGGTGCAGTTCGTCTGCGCCCGCGTGCGCTGCCGGGCATTGAAGAACCGGA
TACCAGCGTGGAAGTTCTGGGTTCTCGCTGGCCGGCACCGGTTGGTATCGCTCCGGTCGC
GTATCATGGTCTGGCACACCCGGATGGTGAACCGGCAACGGCAGCTGCGGCCGGCGCTC
TGGGTCTGCCGCTGGTTGTGAGTACCTTTGCAGGCCGCTCCCTGGAAGAAGTGGCCCGTG
CAGCTTCAGCACCGCTGTGGCTGCAACTGTATTGCTTCCGCGATCACGAAACCACGCTGG
GTCTGGCACGTCGCGCACGTGACTCGGGCTACCAAGCGCTGGTTCTGACCGTCGATACGC
CGTTTACCGGTCGTCGCCTGCGCGACCTGCGTAACGGCTTCGCTGTGCCGGCGCATATTA
CGCCGGCGAATCTGACCGGCACCGCGGCGGCGGGCAGCGCAACCCCGGGCGCACACTCG
CGCCTGGCGTTTGATCGTCGCCTGGACTGGAGCTTCGTTGCACGTCTGGGCGCTGCATCT
GGTCTGCCGGTGCTGGCAAAAGGTGTTCTGACCGCACCGGATGCAGAAGCCGCAGTCGC
TGCGGGCGTGGCAGGTATCGTCGTGAGTAATCATGGCGGTCGCCAGCTGGACGGTGCGC
CGGCAACGCTGGAAGCGCTGCCGGAAGTTGTCTCCGCCGTCCGCGGTCGTTGTCCGGTGC
TGCTGGATGGCGGTGTTCGTACCGGTGCAGACGTCCTGGCAGCACTGGCTCTGGGTGCTC
GCGCGGTCCTGGTGGGCCGTCCGGCACTGTACGCCCTGGCAGTGGGCGGTGCAAGTGGT
GTTCGTCGCATGCTGACGCTGCTGACCGAAGATTTCGCGGACACGATGGTTCTGACCGGT
CACGCTGCAACCGGCACGATTGGTCCGGATACGCTGGCTCCGCCGCATCACGCACCGCC
GCATCACGGTCCGCCGACCGCTCCGCGTCCGGCACCGCATCGCGATCGTTCTCACGGCTA
A

>Protein Sequence of Synthesized HMO

MREPLTLDDFARLARGQLPAATWDFIAGGAGRERTLAANEAVFGAVRLRPRALPGIEEPDTS
VEVLGSRWPAPVGIAPVAYHGLAHPDGEPATAAAAGALGLPLVVSTFAGRSLEEVARAASA
PLWLQLYCFRDHETTLGLARRARDSGYQALVLTVDTPFTGRRLRDLRNGFAVPAHITPANLT
GTAAAGSATPGAHSRLAFDRRLDWSFVARLGAASGLPVLAKGVLTAPDAEAAVAAGVAGI
VVSNHGGRQLDGAPATLEALPEVVSAVRGRCPVLLDGGVRTGADVLAALALGARAVLVGR
PALYALAVGGASGVRRMLTLLTEDFADTMVLTGHAATGTIGPDTLAPPHHAPPHHGPPTAPR
PAPHRDRSHG

>DNA Sequence of Synthesized AnPAD (codon optimized for *E. coli*)

ATGATGTTCAACTCACTTCTGTCCGGCACTACTACACCAAACTCCGGCCGTGCAAGCCCT
CCGGCAAGCGAAATGCCGATTGATAACGACCATGTTGCAGTCGCACGTCCGGCACCGCG
TCGCCGTCGCATCGTGGTTGCAATGACCGGTGCAACGGGTGCAATGCTGGGCATTAAAGT
GCTGATCGCCCTGCGTCGCCTGAACGTCGAAACCCACCTGGTGATGAGTAAATGGGCAG
AAGCTACCATTAAATATGAAACGGATTACCATCCGTCAAATGTGCGCGCGCTGGCCGATT
ATGTTCACAACATTAATGACATGGCGGCCCCGGTTAGCTCTGGCAGCTTTCGTGCGGATG
GTATGATCGTCGTGCCGTGCTCTATGAAAACCCTGGCAGCTATTCATAGTGGCTTCTGTG
ATGACCTGATCTCCCGCACGGCAGATGTCATGCTGAAAGAACGTCGCCGTCTGGTGCTGG
TTGCTCGTGAAACCCCGCTGTCCGAAATCCACCTGCGCAACATGCTGGAAGTTACGCGTG
CAGGTGCTGTTATTTTTCCGCCGGTCCCGGCATTCTACATCAAAGCTGGCTCAATTGAAG
ATCTGATCGACCAGTCGGTGGGTCGCATGCTGGACCTGTTTGATCTGGACACCGGCGACT
TCGAACGTTGGAATGGTTGGGAAAAATAA

>Protein Sequence of Synthesized AnPAD

MFNSLLSGTTTPNSGRASPPASEMPIDNDHVAVARPAPRRRRIVVAMTGATGAMLGIKVLIA
LRRLNVETHLVMSKWAEATIKYETDYHPSNVRALADYVHNINDMAAPVSSGSFRADGMIVV
PCSMKTLAAIHSGFCDDLISRTADVMLKERRRLVLVARETPLSEIHLRNMLEVTRAGAVIFPP
VPAFYIKAGSIEDLIDQSVGRMLDLFDLDTGDFERWNGWEK

>DNA Sequence of Synthesized AnOhbA (codon optimized for *E. coli*)

ATGAGCGCGCAACCTGCGCACCTGTGCTTCCGCAGTTTCGTGGAAGCACTGAAAGTTGAT
AACGATCTGGTGGAAATTAATACCCCGATCGATCCGAACCTGGAAGCGGCGGCAATTAC
CCGTCGCGTGTGCGAAACGAATGATAAAGCCCCGCTGTTTAACAATCTGATTGGCATGAA
AAACGGTCTGTTCCGCATCCTGGGTGCACCGGGCAGTCTGCGTAAAAGCTCTGCGGATCG
TTATGGTCGTCTGGCACGTCATCTGGCACTGCCGCCGACCGCAAGCATGCGTGAAATTCT
GGATAAAATGCTGAGTGCGAGCGATATGCCGCCGATTCCGCCGACCATCGTGCCGACGG
GTCCGTGTAAAGAAAATAGCCTGGATGATTCTGAATTTGATCTGACCGAACTGCCGGTTC
CGCTGATCCATAAAAGCGATGGCGGTAAATATATTCAGACGTACGGTATGCACATCGTG
CAGAGTCCGGATGGCACCTGGACGAATTGGAGCATTGCGCGTGCGATGGTGCATGATAA
AAACCACCTGACCGGTCTGGTGATCCCGCCGCAGCATATTTGGCAGATCCACCAGATGTG
GAAAAAAGAAGGTCGTAGCGATGTTCCGTGGGCACTGGCATTCGGCGTGCCGCCGGCGG
CAATTATGGCGAGTAGCATGCCGATCCCGGATGGTGTTACCGAAGCGGGTTATGTGGGC
GCCATGACGGGCTCTAGTCTGGAACTGGTTAAATGCGATACCAACGATCTGTACGTTCCG
GCGACGTCTGAAATTGTGCTGGAAGGCACCCTGTCTATCAGTGAAACGGGTCCGGAAGG
CCCGTTTGGTGAAATGCATGGCTATATTTTCCCGGGTGATACCCACCTGGGCGCCAAATA
TAAAGTGAATCGCATTACGTACCGTAACAATGCAATCATGCCGATGAGCAGCTGCGGTC
GCCTGACCGATGAAACCCATACGATGATTGGCAGCCTGGCAGCGGCCGAAATCCGTAAA
CTGTGTCAGCAGAACGATCTGCCGATCACGGATGCATTTGCGCCGTTCGAAAGCCAGGTG
ACCTGGGTTGCCCTGCGCGTTGATACGGAAAAACTGCGTGCAATGAAAACCACGTCTGA
AGGTTTTCGTAAACGCGTGGGCGATGTGGTTTTCAATCATAAAGCGGGTTATACCATTCA
CCGCCTGGTGCTGGTTGGTGATGATATCGATGTTTACGAAGGCAAAGATGTGCTGTGGGC
CTTTTCTACCCGTTGTCGCCCGGGTATGGATGAAACGCTGTTTGAAGATGTTCGCGGCTTC
CCGCTGATTCCGTACATGGGTCATGGCAACGGTCCGGCACACCGTGGCGGTAAAGTTGTT
AGTGATGCCCTGATGCCGACCGAATATACCACGGGTCGTAATTGGGAAGCAGCGGATTT
TAACCAGTCTTACCCGGAAGACCTGAAACAGAAAGTGCTGGATAATTGGACCAAAATGG
GCTTCAGTAACTAA

>Protein Sequence of Synthesized AnOhbA

MSAQPAHLCFRSFVEALKVDNDLVEINTPIDPNLEAAAITRRVCETNDKAPLFNNLIGMKNGL
FRILGAPGSLRKSSADRYGRLARHLALPPTASMREILDKMLSASDMPPIPPTIVPTGPCKENSL
DDSEFDLTELPVPLIHKSDGGKYIQTYGMHIVQSPDGTWTNWSIARAMVHDKNHLTGLVIPP
QHIWQIHQMWKKEGRSDVPWALAFGVPPAAIMASSMPIPDGVTEAGYVGAMTGSSLELVKC
DTNDLYVPATSEIVLEGTLSISETGPEGPFGEMHGYIFPGDTHLGAKYKVNRITYRNNAIMPM
SSCGRLTDETHTMIGSLAAAEIRKLCQQNDLPITDAFAPFESQVTWVALRVDTEKLRAMKTT
SEGFRKRVGDVVFNHKAGYTIHRLVLVGDDIDVYEGKDVLWAFSTRCRPGMDETLFEDVRG
FPLIPYMGHGNGPAHRGGKVVSDALMPTEYTTGRNWEAADFNQSYPEDLKQKVLDNWTK
MGFSN

Appendix IV: Publications, Patent Application, and Presentations

List of Publications (manuscripts in preparation or submission are not listed here)

1. <u>Wu, Shuke</u>; Li, Aitao; Chin, Yit Siang; Li, Zhi[*]. Enantioselective Hydrolysis of Racemic and *Meso*-epoxides with Recombinant *Escherichia coli* Expressing Epoxide Hydrolase from *Sphingomonas sp*. HXN-200: Preparation of Epoxides and Vicinal Diols in High *ee* and High Concentration. *ACS Catalysis* **2013**, *3* (4), 752–759.
   http://pubs.acs.org/doi/abs/10.1021/cs300804v

2. <u>Wu, Shuke</u>; Chen, Yongzheng; Xu, Yi; Li, Aitao; Xu, Qisong; Glieder, Anton; Li, Zhi[*]. Enantioselective *trans*-Dihydroxylation of Aryl Olefins by Cascade Biocatalysis with Recombinant *Escherichia coli* Coexpressing Monooxygenase and Epoxide Hydrolase. *ACS Catalysis* **2014**, *4* (2), 409–420. http://pubs.acs.org/doi/abs/10.1021/cs400992z
   Selected as ACS Editors' choice, featured by *C&EN*, **2014**, *92* (2), 8, and also highlighted on *Synfacts*, **2014**; *10* (3), 0316.

3. Huang, Renliang; <u>Wu, Shuke</u>; Li, Aitao; Li, Zhi[*]. Integrating Interfacial Self-assembly and Electrostatic Complexation at an Aqueous Interface for Capsule Synthesis and Enzyme Immobilization. *Journal of Materials Chemistry A* **2014**, *2* (6), 1672–1676.

4. Li, Aitao; <u>Wu, Shuke</u>; Adams, Joe P; Snajdrova, Radka; Li, Zhi[*]. Asymmetric Epoxidation of Alkene and Benzylic Hydroxylation with P450tol Monooxygenase from *Rhodococcus coprophilus* TC-2. *Chemical Communications* **2014**, *50* (63), 8771–8774.

5. Zhang, Jiandong; <u>Wu, Shuke</u>; Wu, Jinchuan; Li, Zhi[*]. Enantioselective Cascade Biocatalysis via Epoxide Hydrolysis and Alcohol Oxidation: One-Pot Synthesis of (R)-α-Hydroxy Ketones from Meso- or Racemic Epoxides. *ACS Catalysis* **2015**, *5* (1), 51–58.

List of Patent Application

1. Li, Zhi; <u>Wu, Shuke</u>. Production of Enantiopure α-Hydroxy Carboxylic Acids from Alkenes by Cascade Biocatalysis. PCT Application No. PCT/SG2014/000221.

List of Presentations

1. <u>Wu, Shuke</u>; Wang, Daniel I. C.; Li, Zhi. Cascade Biocatalysis for Asymmetric Oxyfunctionalization of Alkenes. *247th ACS National Meeting,* Dallas, TX, USA, **2014**. Oral presentation.

2. <u>Wu, Shuke</u>; Wang, Daniel I. C.; Li, Zhi. Enantioselective Cascade Biocatalysis: Oxyfunctionalization of Aryl Alkenes to Chiral Diols and α-Hydroxyl Acids. *7th Singapore Catalysis Forum*, Singapore, **2014**. Oral presentation.

3. <u>Wu, Shuke</u>; Li, Zhi. A Green and Efficient Method for Asymmetric Dihydroxylation of Alkenes: Cascade Biocatalysis with Epoxidase and Hydrolase. *15th Tetrahedron Symposium – Asian Edition*, Singapore, **2014**. Poster presentation (Elsevier Best Poster Prize).

4. <u>Wu, Shuke</u>; Li, Zhi. Engineering of Recombinant Whole-cell Biocatalysts for Efficient Synthesis of Aromatic Diols in High Enantiopurity. *5th Asian Symposium on Innovative Bioproduction and Biorefinery in Tainan (iBio-T)*, Tainan, Taiwan, **2014**. Poster presentation.

5. <u>Wu, Shuke</u>; Li, Zhi. Biotechnology for Asymmetric Dihydroxylation of Alkenes: Cascade Biocatalysis with Epoxidase and Hydrolase. *Biosystems Design 1.0*, Singapore, **2015**. Poster presentation (Poster Award 2nd Prize).

6. <u>Wu, Shuke</u>; Li, Zhi. Cascade Biocatalysis for Green and Efficient Asymmetric Dihydroxylation of Aryl Alkenes. *Southeast Asia Catalysis Conference (SACC) 2015*, Singapore, **2015**. Poster presentation.